Apoptosis & senescence: cell fate determination in inhibitor-treated melanoma cells

Dissertation

zur Erlangung des naturwissenschaftlichen Doktorgrades

der Bayerischen Julius-Maximilians-Universität Würzburg

vorgelegt von

Andreas Borst

Geboren am 20.10.1984 in Würzburg

Würzburg, 2017

Eingereicht am: ……..……..

<u>Mitglieder der Promotionskommission:</u>

Vorsitzender: ……..

1.Gutachter: PD Dr. Roland Houben

2.Gutachter: Prof. Dr. Krohne

Tag des Promotionskolloquiums: ……..…

Doktorurkunde ausgehändigt am: ……..

Table of contents Page

1. Preface

The herein presented thesis consists of a selection of four original articles that are published. Furthermore, this thesis includes a shared summary, introduction, and discussion concerning these four articles, which are attached at the end of the thesis:

Article I (shared first author):
*Haferkamp S, **Borst A**, Adam C, Becker TM, Motschenbacher S, Windhovel S, Hufnagel AL, Houben R, Meierjohann S: Vemurafenib induces senescence features in melanoma cells. J Invest Dermatol 133:1601-1609 (2013).*

Article II:
*Houben R, Dreher C, Angermeyer S, **Borst A**, Utikal J, Haferkamp S, Peitsch WK, Schrama D, Hesbacher S: Mechanisms of p53 restriction in Merkel cell carcinoma cells are independent of the Merkel cell polyoma virus T antigens. J Invest Dermatol 133:2453-2460 (2013).*

Article III:
*Hesbacher S, Pfitzer L, Wiedorfer K, Angermeyer S, **Borst A**, Haferkamp S, Scholz CJ, Wobser M, Schrama D, Houben R: RB1 is the crucial target of the Merkel cell polyomavirus Large T antigen in Merkel cell carcinoma cells. Oncotarget 7:32956-32968 (2016).*

Article IV (first author):
***Borst A**, Haferkamp S, Grimm J, Rosch M, Zhu G, Guo S, Li C, Gao T, Meierjohann S, Schrama D, Houben R: BIK is involved in BRAF/MEK inhibitor induced apoptosis in melanoma cell lines. Cancer Lett 404:70-78 (2017).*

The work presented in this thesis was carried out from June 2012 to May 2016. It was supervised by principal supervisor PD Dr. rer. nat. Roland Houben. Experimental work was performed at the Department of Dermatology of the University Hospital Wuerzburg, Germany.

2. Summary

Neoplasms of the skin represent the most frequent tumors worldwide; fortunately, most of them are benign or semi-malignant and well treatable. However, the two most aggressive and deadly forms of malignant skin-neoplasms are melanoma and Merkel cell carcinoma (MCC), being responsible for more than 90% of skin-cancer related deaths. The last decade has yielded enormous progress in melanoma therapy with the advent of targeted therapies, like BRAF or MEK inhibitors, and immune-stimulating therapies, using checkpoint antibodies targeting CTLA-4, PD-1 or PD-L1. Very recent studies suggest that also MCC patients benefit from a treatment with checkpoint antibodies. Nevertheless, in an advanced metastatic stage, a cure for both of these aggressive malignancies is still hard to achieve: while only a subset of patients experience durable benefit from the immune-based therapies, the widely applicable targeted therapies struggle with development of resistances that inevitably occur in most patients, and finally lead to their death. The four articles included in this thesis addressed current questions concerning therapy and carcinogenesis of melanoma and MCC. Moreover, they are discussed in the light of the up-to-date research regarding targeted and immune-based therapies. In article I we demonstrated that besides apoptosis, MAPK pathway inhibition in BRAF-mutated melanoma cells also induces senescence, a permanent cell cycle arrest. These cells may provide a source for relapse, as even permanently arrested cancer cells can contribute to a pro-tumorigenic milieu. To identify molecular factors determining the differential response, we established M14 melanoma cell line derived single cell clones that either undergo cell death or arrest when treated with BRAF/MEK inhibitors. Using these single cell clones, we demonstrated in article IV that downregulation of the pro-apoptotic BH3-only protein BIK via epigenetic silencing is involved in apoptosis deficiency, which can be overcome by HDAC inhibitors. These observations provide a possible explanation for the lack of a complete and durable response to MAPK inhibitor treatment in melanoma patients, and suggest the application of HDAC inhibitors as a complimentary therapy to MAPK pathway inhibition. Concerning MCC, we scrutinized the interactions between the Merkel cell polyomavirus' (MCV) T antigens (TA) and the tumor suppressors p53 and Rb in article II and III, respectively. In article III, we demonstrated that the cell cycle master regulator Rb is the crucial target of MCV large T (LT), while it - in contrast to

other polyomavirus LTs - exhibits much lower affinity to the related proteins p107 and p130. Knockdown of MCV LT led to proliferation arrest in MCC cells, which can be rescued by knockdown of Rb, but not by knockdown of p107 and p130. Contrary to Rb, restriction of p53 in MCC seems to be independent of the MCV TAs, as we demonstrated in article II. In conclusion, the presented thesis has revealed new molecular details, regarding the response of melanoma cells towards an important treatment modality and the mechanisms of viral carcinogenesis in MCC.

3. Zusammenfassung

Die häufigsten Tumore weltweit sind Neoplasien der Haut; glücklicherweise sind die meisten dieser benigne oder semi-maligne und gut behandelbar. Die beiden aggressivsten und tödlichsten Formen bösartiger Hauttumoren sind das Melanom und das Merkelzell-Karzinom (MCC), welche verantwortlich für über 90% aller durch Hauttumore verursachten Todesfälle sind. Im letzten Jahrzehnt gab es jedoch erstaunliche Fortschritte in der Therapie des malignen Melanoms, was vor allem durch das Aufkommen der zielgerichteten Therapien wie den BRAF oder MEK Inhibitoren und den immunstimulierenden Therapien, welche Checkpoint-Antikörper gegen CTLA-4, PD-1 oder PD-L1 verwenden, bedingt ist. Neueste Studien legen nahe, dass auch MCC Patienten von diesen Checkpoint-Antikörpern profitieren können. In fortgeschrittenen, metastasierten Stadien ist jedoch für beide Malignitäten eine Heilung immer noch sehr schwer erreichbar: nur eine kleine Gruppe der Patienten erreichen einen dauerhaften Nutzen durch die Immuntherapien, während die breit anwendbaren zielgerichteten Therapien mit der Entwicklung von Resistenzen zu kämpfen haben, welche unausweichlich in den meisten Patienten entstehen und letztendlich zu deren Tod führen. Die vier dieser Dissertation beigefügten Publikationen adressierten aktuelle Fragestellungen bezüglich Therapie und Karzinogenese des Melanoms und des MCCs. Des Weiteren werden diese im Licht des heutigen Forschungsstandes diskutiert, im Besonderen mit Blick auf die zielgerichteten und immunbasierten Therapien. In Publikation I zeigten wir, dass Inhibition des MAPK Signalwegs in BRAF-mutierten Melanom-Zellen neben Apoptose auch zu Seneszenz, einem permanenten Zellzyklusarrest, führen kann. Diese Zellen können der Ursprung der Resistenzbildung sein, da auch permanent arretierte Krebszellen zu einem Tumor-fördernden Milieu beitragen können. Um molekulare Faktoren zu identifizieren, die für diese unterschiedliche Behandlungsreaktion ursächlich sind, haben wir Einzelzellklone aus der M14 Melanom-Zelllinie etabliert, welche entweder mit Zelltod oder Arrest auf die BRAF/MEK Inhibitor Behandlung reagieren. Mit Hilfe dieser Klone zeigten wir in Publikation IV, dass die Herunterregulierung des pro-apoptotischen BH3-only Proteins BIK durch einen epigenetischen Mechanismus zur Apoptose-Resistenz dieser Zellen führt, was durch den Einsatz von HDAC-Inhibitoren umgangen werden kann. Diese Beobachtungen bieten eine mögliche Erklärung für das Ausbleiben eines vollständigen und

dauerhaften Ansprechens auf die MAPK-Inhibitor Behandlung der Melanom-Patienten, und legen den Einsatz von HDAC-Inhibitoren als komplementäre Therapieoption nahe. Beim MCC haben wir jeweils die Interaktion zwischen den Merkelzell-Polyomavirus (MCV) T Antigenen (TA) und den Tumor-Suppressoren p53 und Rb in Publikation II und III näher betrachtet. In Publikation III haben wir gezeigt, dass das zentrale, Zellzyklus-regulierende Protein Rb das vorrangige Ziel des MCV large T Antigens (LT) ist, während es - im Gegensatz zu anderen Polyomavirus-LTs - viel weniger Affinität zu den verwandten Proteinen p107 und p 130 aufweist. Der Knockdown des MCV LT führte zu Proliferationsarrest in MCC Zellen, welcher durch Knockdown von Rb aufgehoben werden konnte, nicht jedoch durch Knockdown von p107 und p130. Die Restriktion von p53 scheint im Gegensatz zu Rb im MCC unabhängig von den MCV TAs zu sein, wie wir in Publikation II gezeigt haben. Zusammenfassend gibt diese Dissertation Aufschluss über neue molekulare Zusammenhänge bezüglich der Reaktion von Melanom-Zellen gegenüber einer wichtigen Behandlungsmöglichkeit und den Mechanismen der viralen Karzinogenese des MCC.

4. Introduction

4.1. The epidermis: macroscopic and cellular structure

The skin is the largest organ of the human body and has an important role in immunity, water homeostasis, thermal regulation, sensation, and a multitude of other functions. It is build up in three layers of ectodermal tissue: the epidermis, the dermis, and the hypodermis (subcutaneous tissue). The outer layer of the skin - the epidermis - is the first mechanical and immunological barrier between the body and environmental threats like pathogens, radiation or chemicals, some of which have the potential to cause DNA damage and thereby can be classified as carcinogenic substances (1). It contains no blood vessels and is nourished by diffusion from the underlying dermis. The epidermis is subdivided into five layers: stratum basale, stratum spinosum, stratum granulosum, stratum lucidum, and stratum corneum (see Fig. 1A). The most common cells in the epidermis are keratinocytes (about 95%), which are continuously generated at the basal layer, wander up the strata, while changing their appearance during the process of keratinization and finally die before they reach the corneum. Besides immunologically active Langerhans cells, residing within the stratum spinosum, two additional cell types are found in the basal layer: (I) Merkel cells, which are touch sensitive oval-shaped mechanoreceptors that form synaptic contacts with sensory neurons and are abundant in sensitive skin and (II) melanocytes, melanin producing cells with dendritic arms mainly responsible for skin coloring and UV protection (2, 3).

Highly aggressive neoplastic skin malignancies named after these two cell types are known as Merkel cell carcinoma (MCC) (Fig. 1B) and melanoma (Fig. 1C), respectively. In the four publications this thesis is based on, established cell lines derived from the aforementioned two skin cancers were used to address and elucidate molecular biological questions arising in the context of up-to-date cancer research.

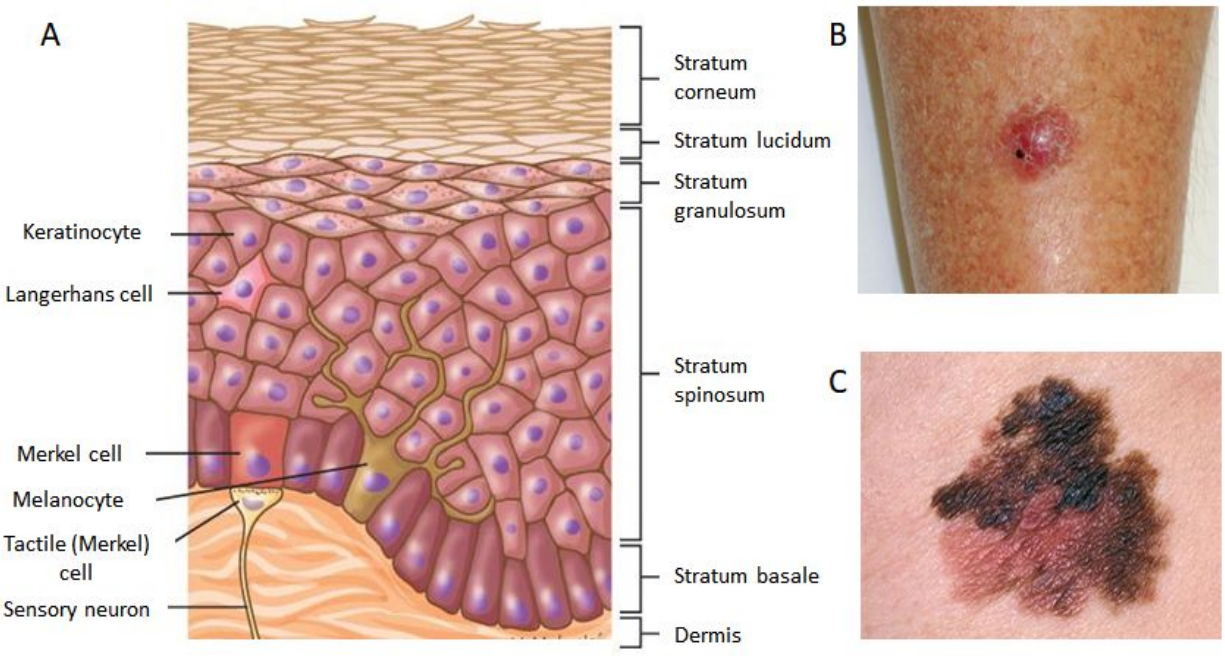

Fig. 1: Structural overview of the epidermis; Merkel cell carcinoma and melanoma lesions.
A: layers and cell types commonly found in the epidermis (image adapted from (4)). **B:** Merkel cell carcinoma; a dome-shaped nodule present on the leg of a patient (image adapted from (5)). **C:** Typical superficial spreading melanoma lesion (image adapted from (6)).

4.2. Merkel cell carcinoma (MCC)

Merkel cell carcinoma is a very aggressive neuroendocrine skin cancer, occurring mostly in elderly and/or immunosuppressed patients. The median age of patients diagnosed with MCC is 76.2 years for women and 73.6 years for men (7). Although MCC is still a rare disease, with approximately 0.6 new cases per 100.000, its incidence is steadily increasing in different countries (7). Most often the tumors arise in sun-exposed areas like the head and neck (8). Clinical characteristics for MCC have been summarized under the acronym AEIOU: asymptomatic/lack of tenderness, expanding rapidly, immunosuppression, older than age 50, and UV exposed site on a fair-skinned person (9). Diagnosis of MCC can be challenging, in particular when based on morphology, as small cell lung cancer displays very similar features (10). An important characteristic to distinguish MCC from other tumors is the presence of peri-nuclear cyto-keratin (CK)-20. Moreover, the lack of thyroid transcription factor-1 (TTF-1) may also serve as a marker (10).

Current treatment therapies are surgical resection of the primary tumor, commonly followed by radiotherapy which grants good loco-regional control. As MCC is associated with occurrence of early nodal and distant metastasis, also chemotherapy can be applied in advanced stages and has a high response rate of 60-75%, which is, however, only of very limited duration and not resulting in significantly increased overall survival (OS) (11, 12). Therefore, chemotherapeutic regimens are often only applied with palliative intention (13). Very recent reports suggest that immune checkpoint blockade may be able to achieve lasting responses in a large proportion of patients with metastatic MCC (14, 15); this aspect will be discussed later.

Transformation of epidermal Merkel cells had been considered to be the source of MCC, originally termed trabecular neuroendocrine carcinoma (16, 17). This view, however, has been challenged recently and epidermal stem cells, other skin derived precursor cells as well as pre-B cells are discussed as possible cells of origin for MCC (18, 19). Although the cell of origin is unclear, understanding of the molecular-biological events involved in development and progression of MCC has made major advances in the last decade: the fact that besides UV-exposure also immunosuppression is a risk factor for MCC has provided a rationale to search for a viral etiology. In 2008, DNA sequence analysis finally revealed the presence of the Merkel cell polyomavirus (MCV) in 80% of MCC tumors (20). In most cases, the viral DNA is clonally integrated into the genome of the MCV-positive tumor cells, suggesting MCV infection as a crucial event in the pathogenesis of MCC.

4.2.1. Merkel cell polyomavirus (MCV)

MCV is a double-stranded DNA virus of the *Polyomaviridae* family consisting of 73 species identified so far; 13 of these are known to infect humans (21). Since the discovery of the simian virus 40 (SV40) decades ago, polyomaviruses have been suspected to bear the potential to induce human cancer, because in experimental animal studies virus infection leads to tumor formation following integration of viral DNA in the genome of the host cells (22-25). Still, MCV is so far the only member of this virus family which could be linked to a human cancer. MCV is an ubiquitary virus which can be detected frequently on human skin and other environmental surfaces (26). Furthermore, about 80% of all people over the age of 50 are sero-positive for

antibodies against the MCV capsid protein VP1 (27, 28). The reasons why MCC is nevertheless a rare cancer are not yet fully understood. The circumstance that specific mutations truncating one of the viral proteins in conjunction with accidental integration of the viral genome into the human genome has to occur, may contribute to its uncommonness. Furthermore, rarity of the cell of origin and/or rarity of its infection by MCV may contribute to the fact that MCC is relatively uncommon, despite the high prevalence of MCV (29).

The MCV genome consists of 5,387 base pairs and encodes, like other polyomaviruses, for two distinct groups of proteins. The T antigens (TA), which bear transforming potential, are expressed early after infection. In case of MCV, a large T antigen (LT), small T antigen (ST), and 57k T antigen (57kT) are derived by alternative splicing of a common precursor mRNA (5, 20). Additionally, in an alternate coding frame ALTO, a protein of unknown function, is encoded by the LT mRNA (30). The second group of viral proteins consists of the capsid proteins (VP1-3), which are expressed in later stages of the viral life cycle and constitute the envelope of newly formed viruses. These transport the viral genome to other cells after host cell lysis (5). For MCV, however, VP3 is inactive or not expressed at all. An overview of the MCV genome organization is summarized in Fig. 2A. Several oncogenic viruses require the cellular DNA replication machinery for their own reproduction and have therefore acquired the ability to activate the host's cell cycle machinery. As a consequence, they presumably acquired transforming potential (31). Transformation induced by polyomaviruses is attributed to the T antigens, which can interfere with different cell cycle regulatory pathways and proliferation cascades and are able to impair tumor suppressor mechanisms (31). The different MCV T antigens share the N-terminal amino-acid sequence containing a DnaJ domain for binding the cellular heat shock protein HSC70 and the so called conserved region 1 (CR1). However, they differ substantially in the C-terminal region, determining the functional variability of the T antigen splice products (20, 32) (Fig. 2B).

The LT antigen is encoded by two exons and has several functions in MCV infection like initiation of viral replication and altering the host cell's cell cycle (5, 33). Besides the above mentioned DnaJ and CR1 domain, several further domains conserved among polyomavirus LTs are present in MCV LT: the retinoblastoma protein (Rb) binding domain, a specific nuclear localization sequence (NLS), the origin-binding domain (OBD) as well as a DNA binding and a helicase domain. The presence of the NLS results in nuclear localization of MCV LT when expressed in

mammalian cells (34). From studies with SV40 polyomavirus LT, it is known that the OBD and helicase region also mediate interactions with a multitude of cellular proteins - the most prominent of them is the tumor suppressor protein p53. Though, MCV LT does not bind to p53 (35-37). In most cases of MCC tumor cells, the integrated MCV genome contains mutations truncating the C-terminus of LT, aborting the virus's ability to replicate and also eliminating growth suppressive properties of the C-terminus (37-39). Generally, however, the Rb-binding site is preserved in the MCC associated truncated versions of the LT protein.

The MCV ST antigen consists of 186 amino acids and plays a role in viral replication and cellular transformation (5). The C-terminal region is produced via transcriptional read-through of the exon splice site used by LT and 57kT. ST can be found in the nucleus as well as in the cytoplasm (40). The typical polyomavirus protein phosphatase 2A (PP2A) Aα subunit binding site is unique for the ST antigen and is important for viral replication and virus-induced transformation in other polyomaviruses (41). A recently discovered MCV ST domain is the LT-stabilization domain, which mediates inactivation of the ubiquitin ligase SCF (Fbw7) and thereby represses proteasomal degradation of LT (42).

In contrast, little is known about the 57k protein that shares a MCV unique region (MUR) with LT, consisting of a sequence located between the first exon and the OBD, which contains the Rb-binding domain. Furthermore, there is some degree of homology between 57kT and SV40 17kT, what plays a role in promoting host cell proliferation (43, 44). In tumor cells nevertheless, a distinction between LT and 57kT is not relevant because the truncating mutations in most cases delete all diverging C-terminal parts of the two proteins. The MCV genome resembles other polyomaviruses not only in its organization and proteins encoded, but also – just like other family members - encodes a microRNA, which is involved in regulating early viral gene expression (45).

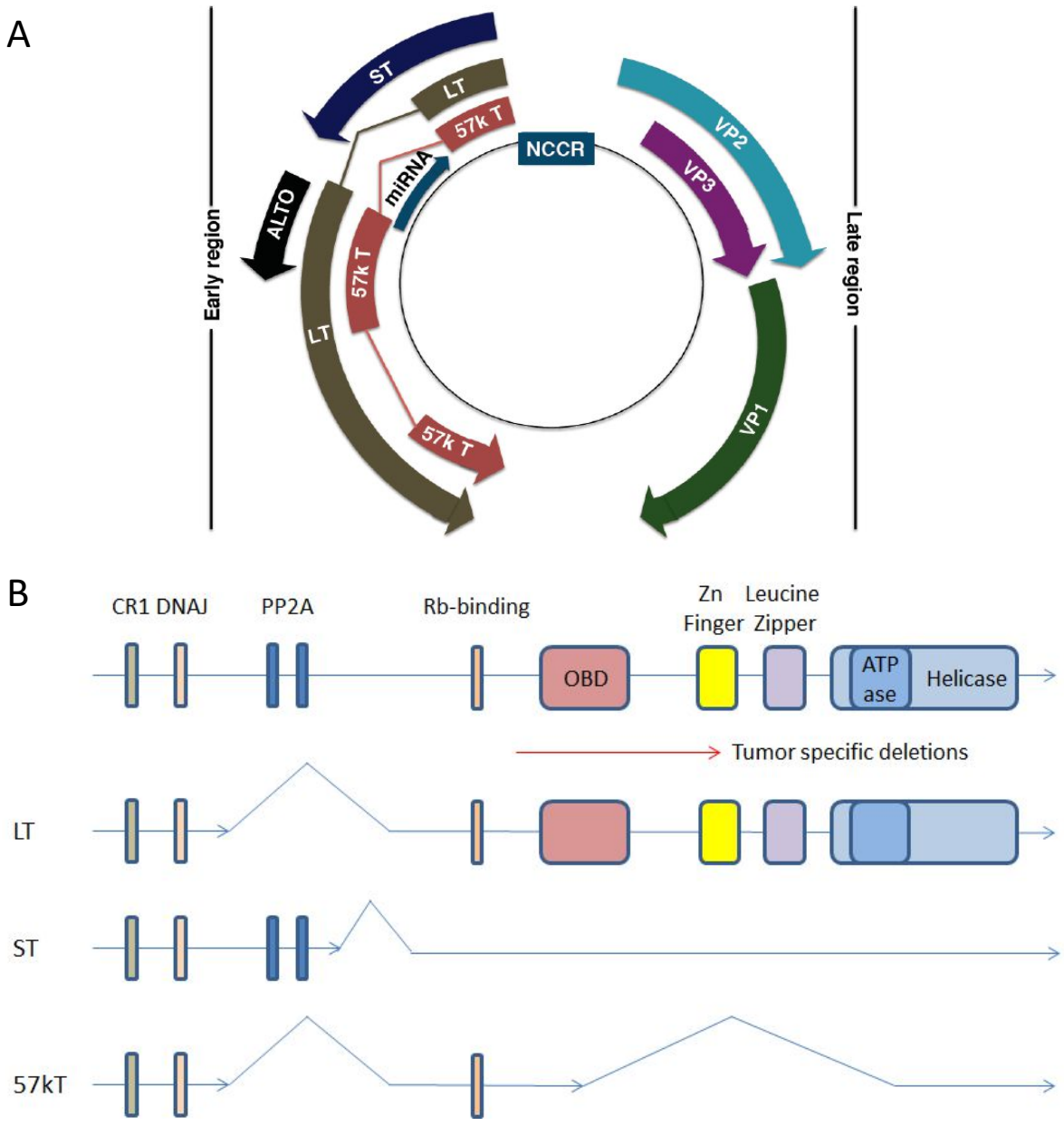

Fig. 2: Mapping of the MCV genome and the alternatively spliced MCV T antigens.
A: The MCV genome consists of a non-coding control region (NCCR) containing promoter elements as well as the origin of replication. An early gene region contains the large T antigen (LT), small T antigen (ST), 57kT antigen (57kT), and an alternative T antigen open reading frame (ALTO). The late gene region is coding for the capsid proteins (VP1-3) and a microRNA (miRNA) regulating early viral transcription levels (image adapted from (5)). **B:** All T antigen isoforms originate in one pre-mRNA and encode the conserved CR1 epitope and DnaJ (HSC70 binding) domain. Unique for the ST antigen are two PP2A binding sites, a PP2A Aβ/PP4C binding site, and a large T-stabilization domain. LT and 57kT share a MCV-unique region in the second exon with a retinoblastoma protein (Rb) binding domain and the origin binding domain (OBD), while LT additionally has C-terminal zinc finger, leucine zipper, ATPase, and helicase domains (5, 46).

4.2.2. MCV T antigens in MCC carcinogenesis

The discovery of MCV and its T antigens has profoundly extended our understanding of the molecular pathogenesis of MCV-positive MCC, which - besides the virus integration - is characterized by a relatively low frequency of somatic mutations and a lack of recurrent genetic alterations (47). For many polyomaviruses, LT is the major transforming protein and its transforming potential is attributed to its capability to impair the major tumor suppressor proteins p53 and Rb (48, 49). In MCC though, the mechanism of tumorigenesis and the exact roles of the two T antigens are not yet fully understood. MCV-positive MCC cell lines *in vitro* and in xeno-transplant mouse models are dependent on the expression of the MCV T antigens and in particular on LT, as short hairpin RNA (shRNA) mediated knockdown leads to cell cycle arrest and/or cell death (50). Whether established MCV-positive MCC cells are also addicted to ST has been reported inconsistently (51, 52). Nevertheless, MCV ST is capable of transforming rodent fibroblasts, whereas MCV LT is not and does also not cooperate with ST in this respect (53). Consequently, the dependency of the tumor cells on the T antigens identified these proteins as potential therapeutic targets. For the development of such new therapeutic strategies, however, a more detailed understanding of the interactions between the T antigens and their cellular partners is required.

4.2.3. MCV and tumor suppressor proteins

The transforming potential of SV40 LT is mainly based on its interaction with tumor suppressor proteins like p53 and members of the pocket protein family (54, 55). The latter consists of three members: Rb, p107, and p130. In concert these 3 proteins restrict the mitotic activity of a cell by affecting the G1 to S-Phase transition mainly through binding and inhibiting members of the E2F transcription factor family, which are involved in cell cycle regulation and synthesis of DNA in mammalian cells (56). E2F proteins form cell cycle promoting complexes with a dimerization partner (DP), while an active Rb protein binds and denies these E2F-DP dimers to induce proliferative signals (57). Prior to entering S-phase, complexes of cyclin-dependent kinases (CDK4/6) and cyclins (cyclin D) phosphorylate Rb that thereby loses the ability to form

complexes with E2F-DP and is deactivated (58, 59). Rb usually remains in a phosphorylated state throughout S, G2, and M phase. The E2F proteins are generally split into two functional groups: transcription activators and repressors. In activators it has been shown that E2F binding with Rb masks the transactivation domain responsible for transcription activation, while in E2F repressors binding of pocket proteins (especially p107 and p130) leads to formation of repressor complexes to silence target genes (60, 61). Historically, it has been supposed that the pocket proteins suppress transcriptional activity by direct interaction with chromatin-bound E2F molecules at their corresponding promoters, what - according to some studies - appears to be true only for p107 and p130 (62-64). Rb however, is undetectable at these promoters in the context of transcriptional repression. Importantly, Rb-mediated and p107/p130-mediated cell cycle control is not redundant; indeed, a lot of E2F-responsive genes are dysregulated in p107/p130-deficient cells (56).

Another important tumor suppressor protein is the aforementioned p53, which is a transcription factor that is found inactivated by mutations or deletions in more than 50% of human tumors (65). P53 is also referred to as the “guardian of the genome”, due to its central role in the response to genotoxic stress and UV radiation. Depending on the context, p53 can induce cell cycle arrest, senescence, DNA repair, and apoptosis and contributes thereby to genomic stability and counteracts tumor formation (66). Various intra- and extracellular stress induced stimuli can activate p53; these include for example: DNA damage, oxidative stress, osmotic shock, ribonucleotide depletion, loss of adhesion or deregulated oncogene expression (67-69). P53 activity is mainly regulated by two mechanisms: (I) phosphorylation of certain N-terminal serine/threonine residues enhances its transcriptional activity. (II) Increasing or decreasing the half-life of the protein. The latter is mediated by murine double minute 2 (MDM2) or in humans human double minute 2 (HDM2), a E3 ubiquitin ligase which tags p53 for proteasomal degradation (70). Because of an auto-regulatory mechanism, p53 levels are kept low in unstressed cells, as HDM2 expression is regulated by p53. Stress induced transcription of phosphatase and tensin homologue (*PTEN*) for example, inhibits HDM2/p53 complex formation and subsequently leads to p53 activation (71). In contrast to SV40 LT, MCV LT was reported not to be able to bind p53 and in the MCC associated LT proteins the C-terminus responsible for direct interaction of SV40 LT with p53 is missing (39, 72). However, the LxCxE motif known to be

essential for binding of the Rb family proteins is preserved in MCV LT expressed in MCC cells and it has been demonstrated that this LxCxE motif is required for MCV LT to promote growth of MCC cells (73). One publication included in this thesis (article III) investigates in detail which of the three Rb family proteins are bound and inactivated by the MCV LT antigen in MCC, while a second paper (article II) describes whether MCV T antigens are involved in restricting the tumor suppressor function of p53 in MCC.

4.3. Melanoma

Melanoma is a highly malignant tumor derived from the melanin producing cells in the epidermis, the melanocytes (Fig. 1C). Established risk factors for the development of melanoma include light skin and UV exposure, in particular excessive sunburns in childhood (74). The American Cancer Society's estimated lifetime risk of Caucasian men being diagnosed with melanoma is 1/35, while for Caucasian women it is 1/54 (75). Despite accounting for only 4% of all skin cancers, about 80% of skin cancer related deaths are attributed to melanoma and the 5-year survival for advanced metastatic melanoma still remains low, ranging from 12-28% (76-79). According to the American Joint Committee on Cancer (AJCC), melanoma is classified in four clinical stages with some stages being further subdivided regarding the size of the primary tumor, involvement of local or distant lymph nodes, and the presence and location of distant metastasis (see Table 1&2). Patients with Stage IV melanoma are associated with a very poor prognosis and a mean survival of 8–10 months in large cohort analysis studies. A more accurate staging categorizes patients into stage IV sub-groups with only cutaneous metastases (M1a), lung metastases (M1b) or other visceral metastases (M1c), which yield associated 5-year survival rates of 18.8%, 6.7%, and 9.5%, respectively (77). When detected at early stage I, excision of the primary tumor results in an almost 100% cure rate. Therefore, self-examination and self-awareness can be lifesaving. Typical signs allowing melanoma detection by visual inspection are summarized in the "ABCDE"-rule: Asymmetry, border irregularity, color variation, diameter greater than 6mm, and evolving over time (78, 80) (Fig. 3). As mentioned above, the prognosis is much worse if the cancer has already spread and the 5-year OS correlates directly with the stage of the primary tumor and the presence of nodal and/or distant metastasis.

Today's treatment options in this stage are mainly immuno-based treatments or targeted therapies, which will be described later on. Other therapy options, like radiation or cryotherapy, merely play a minor role in the treatment of melanoma (81).

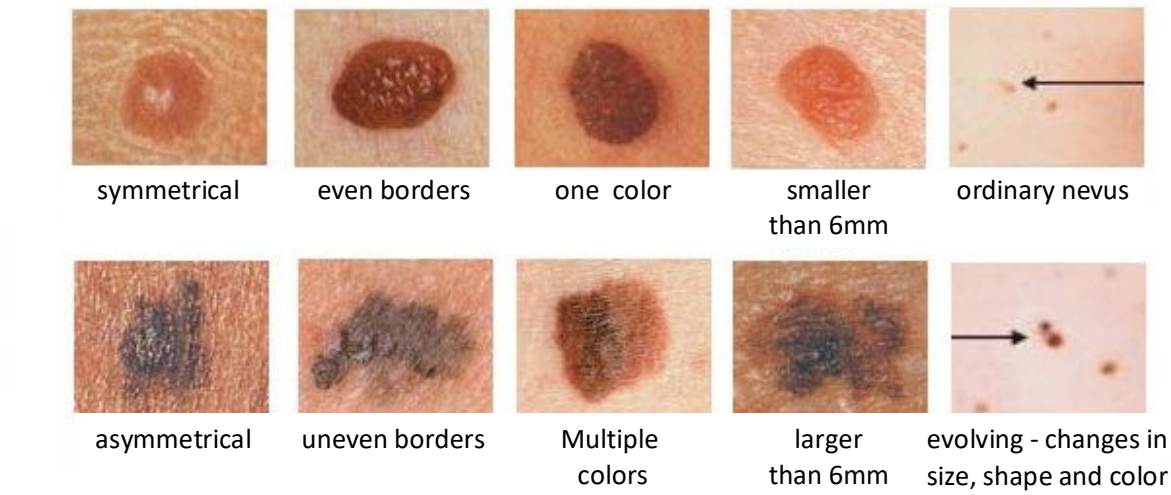

Fig. 3: "ABCDE" characteristics of melanoma.
ABCD characteristics help to distinguish between malignant melanoma and an ordinary mole (image adapted from (82)). Ordinary moles usually have a symmetrical form, even borders, one color, are smaller than 6mm and don't change or evolve over time. Malignant melanomas often present as asymmetrical lesions with uneven borders, have multiple colors varying from brown to black or blue, and grow larger than a 6mm diameter while changing over time (83).

Table 1: TNM staging categories for cutaneous melanoma.
Abbreviations: Tis, tumor in situ; NA, not applicable; LDH, lactate dehydrogenase. *Micrometastases are diagnosed after sentinel lymph node biopsy. #Macrometastases are defined as clinically detectable nodal metastases confirmed pathologically. Data obtained from (77).

	Primary Tumor	Thickness (mm)	Ulceration Status/Mitosis
T	Tis	NA	NA
	T1	≤ 1.00	a: Without ulceration and mitosis < 1/mm^2
			b: With ulceration or mitosis ≥ 1/mm^2
	T2	1.01-2.00	a: Without ulceration
			b: With ulceration
	T3	2.01-4.00	a: Without ulceration
			b: With ulceration
	T4	>4.00	a: Without ulceration
			b: With ulceration
	Nodal Involvement	No. of Metastatic Nodes	Nodal Metastatic Burden
N	N0	0	NA
	N1	1	a: Micrometastasis*
			b: Macrometastasis#
	N2	2-3	a: Micrometastasis*
			b: Macrometastasis#
			c: In tranist metastasis/satellites without metastatic nodes
	N3	4+ metastatic nodes, or matted nodes, or in Transit metastases/satellites with metastatic nodes	
	Distant Metastasis	Site	Serum LDH
M	M0	No distant metastasis	NA
	M1a	Distant skin, subcutaneous, or nodal metastases	Normal
	M1b	Lung metastases	Normal
	M1c	All other visceral metastases	Normal
		Any distant metastases	Elevated

Table 2: Anatomic stage groupings for cutaneous melanoma.
*Clinical staging includes microstaging of the primary melanoma and clinical/ radiologic evaluation for metastases. By convention, it should be used after complete excision of the primary melanoma with clinical assessment for regional and distant metastases. #Pathologic staging includes microstaging of the primary melanoma and pathologic information about the regional lymph nodes after partial (i.e., sentinel node biopsy) or complete lymphadenectomy. Pathologic stage 0 or stage IA patients are the exception; they do not require pathologic evaluation of their lymph nodes. Data obtained from (77).

Clinical Staging*				Pathologic Staging#			
	T	N	M		T	N	M
0	Tis	N0	M0	**0**	Tis	N0	M0
IA	T1a	N0	M0	**IA**	T1a	N0	M0
IB	T1b	N0	M0	**IB**	T1b	N0	M0
	T2a	N0	M0		T2a	N0	M0
IIA	T2b	N0	M0	**IIA**	T2b	N0	M0
	T3a	N0	M0		T3a	N0	M0
IIB	T3b	N0	M0	**IIB**	T3b	N0	M0
	T4a	N0	M0		T4a	N0	M0
IIC	T4b	N0	M0	**IIC**	T4b	N0	M0
III	Any T	N>0	M0	**IIIA**	T1-4a	N1a	M0
					T1-4a	N2a	M0
				IIIB	T1-4b	N1a	M0
					T1-4b	N2a	M0
					T1-4a	N1b	M0
					T1-4a	N2b	M0
					T1-4a	N2c	M0
				IIIC	T1-4b	N1b	M0
					T1-4b	N2b	M0
					T1-4b	N2c	M0
					Any T	N3	M0
IV	Any T	Any N	M1	**IV**	Any T	Any N	M1

Until recently, the standard first line treatment was dacarbazine, the only chemotherapeutic agent approved for the treatment of metastatic melanoma by the Food and Drug Administration (FDA) before 2011. The response rates of for dacabazine were rather low (7 to 12%) and the median OS of treated stage IV melanoma patients was only 5 to 8 months (84-87). In the last 15 years, however, major progress in understanding the molecular biological mechanisms underlying the process of developing melanoma has been made: a set of frequent molecular changes that occur during the transformation of a melanocyte to a malignant melanoma cell have been described, leading to the loss of cell cycle control. Growth stimulating mutations in the proto-oncogenes *NRAS* or *BRAF*, resulting in hyper-activation of the mitogen-activated protein kinase (MAPK) pathway, which is described later, have been reported in roughly 90% of melanomas (88, 89). However, these mutations do not suffice to evoke malignancy since proliferation is mostly interrupted by tumor-suppressor mechanisms that activate stress induced senescence (90); this is probably the situation in most benign nevi. Additional mutations occurring in the tumor-suppressor genes cyclin-dependent kinase inhibitor 2A (*CDKN2A)*, which encodes for 2 distinct tumor-suppressor proteins $p16^{INK4A}$ and $p14^{ARF}$, *PTEN* or *p53* are found with moderate frequencies in melanoma and may contribute to overcoming senescence (76). Furthermore, changes in genes or expression patterns of genes that are involved in melanocytic differentiation or cell adhesion have been described to play a role on the way towards malignancy. These are for example amplification of microphthalmia-associated transcription factor (*MITF*), decreased expression or loss of E-cadherin and melanocyte-specific gene melastatin1 (TRPM1) and aberrant or increased expression of N-cadherin, αVβ3 integrin, survivin and matrix metalloproteinase2 (MMP-2) (76). A more recent approach based on a large number of melanoma samples categorizes four different melanoma subtypes, regarding the most common driver oncogenes found: mutant *BRAF*, mutant *RAS*, mutant *NF1* or triple wild-type (89). All three named oncogenes are part of the MAPK pathway, highlighting its central role in melanoma. The following chapter takes a closer look at this pathway and describes several approaches provided by targeted therapies to exploit melanoma's dependency on it (oncogene addiction), what has become a pillar of modern day melanoma treatment.

4.3.1. The MAPK pathway as a therapeutic target in melanoma

Activation of the MAPK pathway occurs after binding of an extracellular growth stimulating signaling molecule, like epidermal growth factor (EGF), to a transmembrane receptor tyrosine kinase (RTK), such as the epidermal growth factor receptor (EGFR) (91). Receptor activation and phosphorylation of its tyrosine residues leads to the recruitment of docking proteins like GRB2, containing a SH2 domain that binds to the phosphor-tyrosine residues of the activated receptor. GRB2 additionally binds the guanine nucleotide exchange factor SOS with its two SH3 domains. When the GRB2-SOS complex docks to a phosphorylated RTK, SOS becomes activated and that promotes the removal of GDP from a RAS protein. RAS can now bind a GTP molecule and become active, resulting in initiation of RAS-RAF complex formation followed by phosphorylation of MEK1/2, which in turn catalyzes the phosphorylation of ERK1/2. ERKs translocate into the nucleus and regulate a multitude of cellular processes, like embryogenesis, cell differentiation, cell proliferation, and cell death by interaction with several transcription factors (92).

Some of the first oncogenes described in humans encode for the aforementioned RAS proteins with three main isotypes (HRAS, KRAS, and NRAS), and RAS mutations are also frequently found in melanoma, most of them being NRAS mutations (93). Unfortunately, direct inhibition of RAS with tipifarnib, a farnesyltransferase inhibitor (FTI), has been ineffective, making RAS elusive as a potential single target for effective treatment of metastatic melanoma (94). It is thought that the RAS proteins can escape that inhibition by prenylation through a geranylgeranyl transferase that transfers an alternate isoprenoid group to RAS and allows continued activity (95, 96). Nevertheless, targeting RAS in a multi-agent, multi-targeted approach may hold promise: a phase I clinical trial combining tipifarnib and sorafenib (a BRAF-inhibitor) showed stable disease in patients with different cancers, including one with metastatic melanoma (97). Additionally, an *in vitro* study revealed that the combination of lonafarnib (another FTI) and sorafenib led to improved sorafenib-induced apoptosis and suppression of melanoma cell invasion in raft culture assays (98).

The RTK c-kit is a transmembrane protein that transduces extracellular stimuli into the cytoplasm and universally expressed in mature human melanocytes, where it fosters

proliferation and survival trough signaling pathways like MAPK, PI3K/AKT, and JAK-STAT by receptor dimerization and auto-phosphorylation after ligand binding. Although rare in most cancers, relatively high numbers of c-kit-activating mutations and/or amplifications (28–39%) have been reported in melanomas of mucosal, acral, and sun-damaged skin (99, 100). Preclinical data demonstrated that melanoma cells harboring c-kit mutations show reduced proliferation and increased apoptosis, along with suppression of the MAPK, PI3K, JAK-STAT, and anti-apoptotic pathways, when treated with imatinib, an ATP-competitive inhibitor of several tyrosine kinases (101). Two clinical trials with selected melanoma patients that harbor c-kit mutations or amplifications displayed clinically significant results: one study reported a median progression-free survival (PFS) of 12 weeks and an OS of 46 weeks (102), while another study resulted in a median PFS of 3.5 months and an OS of 14 months (103). Other RTK inhibitors, like dasatinib and nilotinib, have also demonstrated responses in melanoma patients with c-kit mutations (104, 105), while lacking efficacy in unselected melanoma patients, similar to imatinib (106-108).

Further and essentially the most important targetable mutations in melanoma alter Valine 600 in the in the serine/threonine-protein kinase BRAF, rendering it constitutively active. Indeed, approximately 50% of melanomas harbor a mutation in this kinase, with the substitution of valine to the phosphorylation mimicking glutamic acid being the most common ($BRAF^{V600E}$), whereas lysine or arginine substitutions have also been reported (109, 110). Blocking specifically the mutated BRAF protein with a small molecule inhibitor leads to subsequent cell cycle arrest and apoptosis in melanoma cells (111). This has fundamentally changed the treatment options for metastatic and/or unresectable melanoma with BRAF mutation: in 2011, the FDA approved the first selective $BRAF^{V600E}$ inhibitor for melanoma called vemurafenib (PLX4032), which showed impressive clinical results (112, 113). In phase I and II clinical trials, significant tumor shrinkage and treatment-induced clinical responses were reported in more than 50% of the patients treated, and improved OS and PFS in patients with $BRAF^{V600E}$ mutant metastatic melanoma could be achieved (114, 115). Furthermore, a phase III study demonstrated superior outcome compared to cytostatic treatment: for patients with the $BRAF^{V600E}$ mutation, the estimated median PFS in the vemurafenib group was 6.9 months compared to 1.6 months for the dacarbazine group (116). Until now, new selective BRAF inhibitors are continuously under

development and subject to clinical trials, and some have also achieved FDA approval, like dabrafenib (117).

As BRAF-mutated cells frequently possess enhanced sensitivity towards MEK inhibition (118), MEK1/2 inhibitors like trametinib - which has gained FDA approval in 2013 - also yielded promising results in the treatment of melanoma (119). The combination of the $BRAF^{V600E}$ inhibitor dabrafenib and trametinib in inhibitor-treatment naive patients showed a significant improvement in PFS/OS, and a reduction of serious side effects like the appearance of cutaneous squamous cell carcinomas was observed as well (120-122). Therefore, combined targeting of mutant BRAF and the downstream kinase MEK has become today's standard of care for patients with advanced $BRAF^{V600}$ mutated melanoma (123, 124). An overview of the MAPK pathway and established or developmental drugs to inhibit key kinases are depicted in Fig. 4.

Despite this exciting progress, most patients with BRAF or MEK inhibitor-responsive melanoma show - due to outgrowth of treatment resistant cells - tumor progression or relapse within less than a year , which can only be delayed by combinatory treatment (BRAF + MEK inhibitor) (125). Hence, uncovering the molecular mechanisms of intrinsic and acquired resistances to BRAF/MEK inhibition has been a major duty in melanoma research over the last years. In this respect, it has been demonstrated that most resistances can be classified in one of the following three patterns: (I) Reactivation of ERK signaling, what can be caused by up-regulation of receptor tyrosine kinases like PDGFR-β, expression of mutant NRAS variants, alternatively spliced drug-insensitive $BRAF^{V600E}$ variants or $BRAF^{V600E}$ amplification (126, 127). (II) Activation of alternative pathways like the phosphoinositide 3-kinase/protein kinase B (PI3K/AKT) pathway, which is commonly linked to intrinsic and/or acquired resistance to MAPK inhibition in melanoma cells (128, 129). (III) Dysfunctional apoptotic signaling can be the cause of resistance (130-133). The latter was the major topic of this thesis and resulted in the first-author publication article IV. The next chapter focuses mainly on this issue.

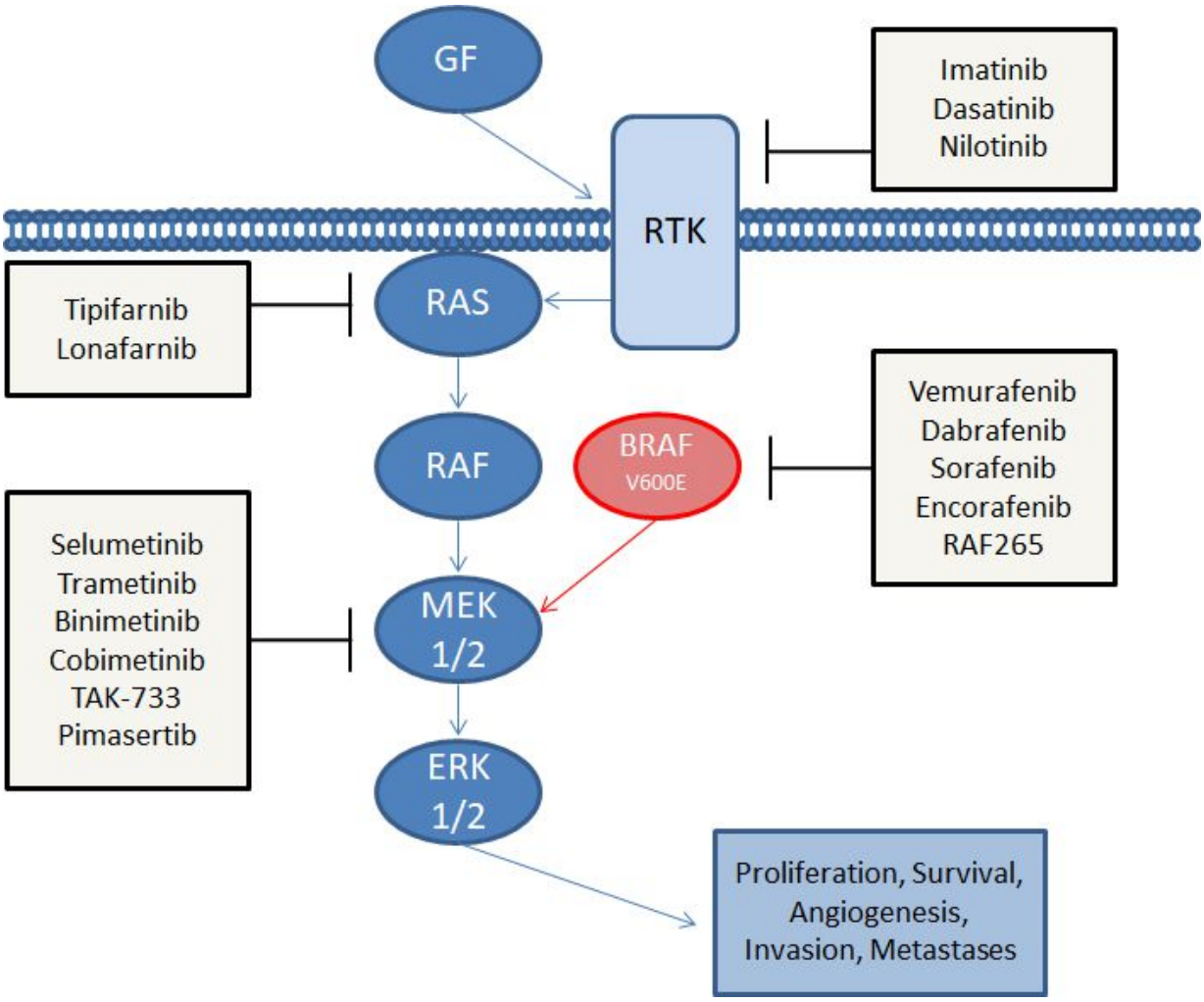

Fig. 4: Targeting the MAPK pathway with small molecule inhibitors.
Growth Factor (GF) binding to a trans-membrane receptor tyrosine kinase (RTK) transduces the proliferation signal into the cytoplasm. From there, a signaling cascade from RAS to RAF to MEK to ERK leads the stimulus into the nucleus, where gene expression is modified and promotes proliferation, survival, angiogenesis, and in case of cancer cells, invasion or metastases. V600E-mutant BRAF creates such intracellular signals without the binding of an extracellular stimulator. Different small molecule inhibitors can bind to key kinases of the MAPK signaling cascade to suppress growth stimulating signals, what results in cell death or cell cycle arrest.

4.3.2. MAPK inhibition & apoptosis in melanoma

Apoptosis, a caspase dependent form of programmed cell death, is a highly regulated and controlled process with pivotal importance in multicellular organisms and central roles in development and homeostasis (134). Two major apoptosis mediating pathways have been described: the extrinsic pathway is characterized by an extracellular ligand (e.g. TNFα/FAS), which binds to a specific death-receptor and activates caspase 8 or 10. Extrinsic mediated apoptosis has a crucial function in inflammation and the immune response to infected/aberrant cells. The intrinsic apoptosis pathway is triggered by intracellular stimuli, like irreparable DNA damage or cytotoxic stress, and is activated via cytochrome C release from the mitochondria and subsequent caspase 9 cleavage. After distinct signaling cascades, which are strictly regulated, both pathways finally result in effector caspase 3 cleavage and subsequent death substrate activation, leading to the execution of the cell death program (134, 135). Members of the B-cell lymphoma (Bcl)-2 protein family play a central role in initiation and regulation of intrinsic apoptosis, and can be divided into three sub-groups : the first group includes the pro-apoptotic Bcl-2 homology domain 3-only (BH3-only) proteins (BIM, BIK, BAD, BID, HRK, BMF, NOXA and PUMA), which sensitize for or trigger apoptotic signals. These BH3-only proteins can inhibit the second group, the anti-apoptotic Bcl-2 family members (BCL-2, BCL-xL, BCL-w, Bfl-1 and Mcl-1) that in turn bear the potential to functionally repress the third group, consisting of the pro-apoptotic effectors BAK and BAX, which finally induce cytochrome C release from the mitochondria (134, 136-138). Furthermore, it has been described that BH3-only protein induced BAX/BAK activation, which is necessary for the execution of intrinsic apoptosis, is not only indirectly achieved by blocking the anti-apoptotic Bcl-2 family members, but can also occur directly through BID and BIM (139, 140). A general overview of the intrinsic apoptosis pathway and the structural setup of the Bcl-2 family proteins is given in Fig. 5a&b.

The specificity of the BH3-only proteins is divergent: while BIM and PUMA appear to be less selective and have the potential to bind all anti-apoptotic Bcl-2 proteins, Noxa targets only Mcl-1 and Bfl-1, Bad has affinity for Bcl-2, Bcl-w and Bcl-X(L), while BIK/NBK inhibits specifically only Bcl-2 and Bcl-X(L) (141, 142).

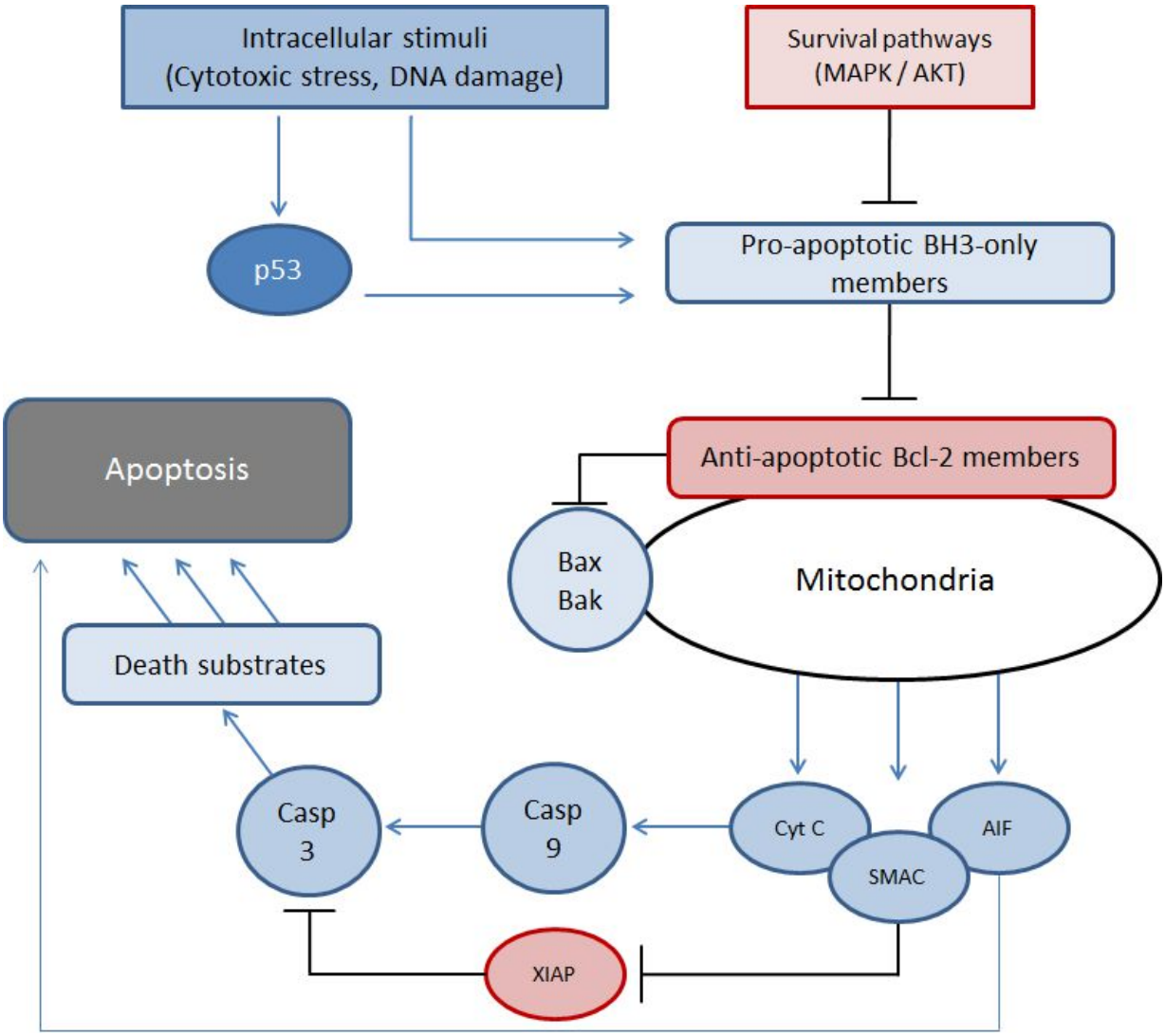

Fig. 5a: The intrinsic apoptosis pathway and its key proteins.
The decision between life and death of a cell is made at the mitochondria and determined by a shift in the balance between pro- and anti- apoptotic factors. Intracellular stimuli like cytotoxic stress, DNA damage or oncogene activation can trigger the pro-apoptotic BH3-only members of the Bcl-2 family in a p53 mediated or p53 independent manner, while survival pathways, like the MAPK or PI3K/AKT pathway, can counteract the BH3-only protein activation. Once activated, BH3-only proteins inhibit the anti-apoptotic Bcl-2 members, what in turn leads to Bax/Bak activation and subsequent changes of the outer mitochondrial membrane permeability, releasing several inter-membrane factors like cytochrome C, SMAC or AIF (apoptosis inducing factor) into the cytosol. Cytochrome C triggers the formation of the apoptosome, an Apaf-1 (apoptosis activating factor 1) multimer, which allows binding and activation of initiator caspase 9 followed by cleavage of effector caspase 3 that has several targets (death substrates) to activate or inactivate. The apoptotic potential of the released factors is dependent on IAP (inhibitor of apoptosis) proteins like XIAP, which are antagonized by SMAC (Diablo) and other released factors like HtrA2/Omi. In contrast, the apoptotic activity of AIF seems to take place after translocation to the nucleus, and is caspase-independent (135, 138).

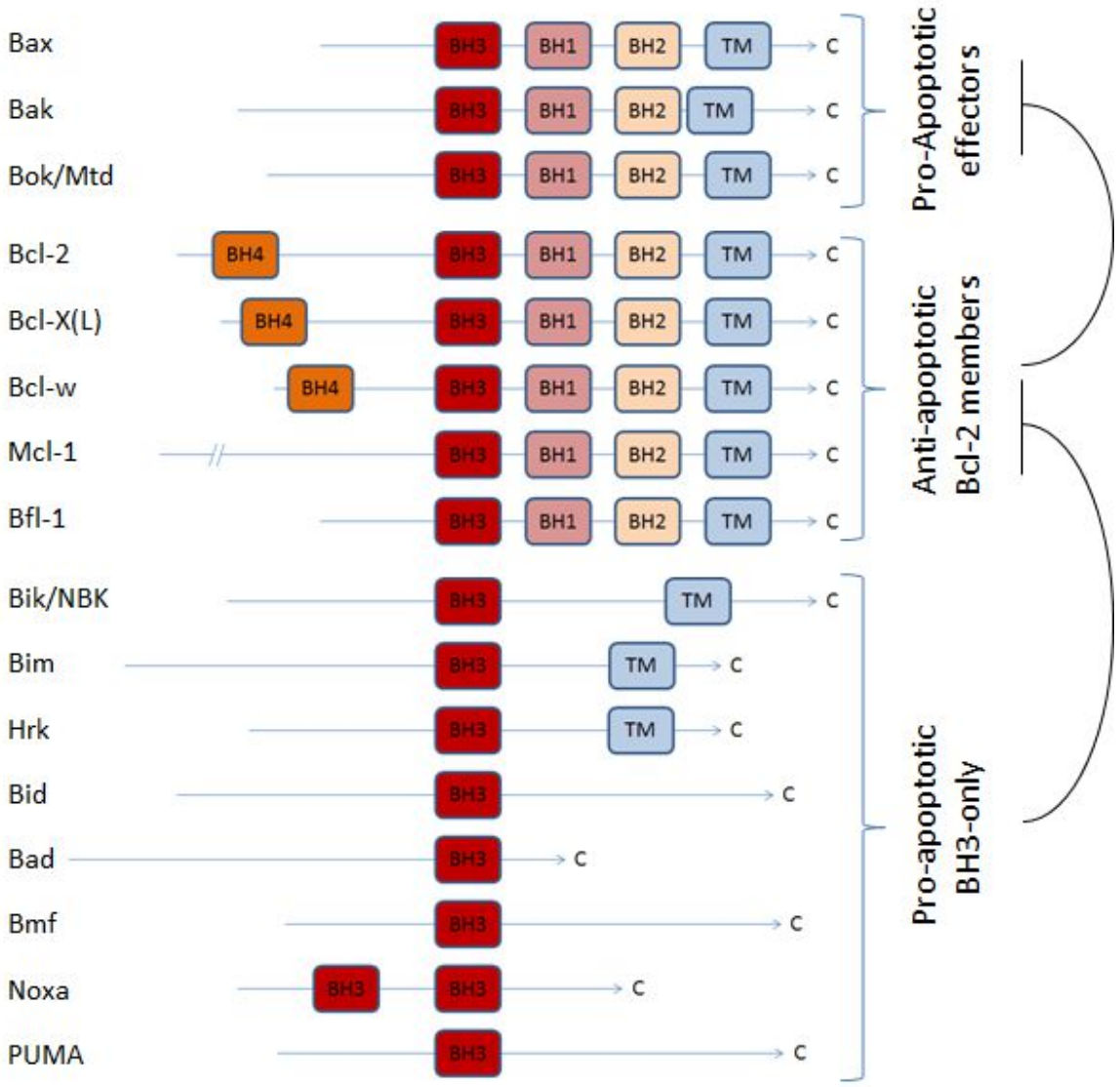

Fig. 5b: Members of the Bcl-2 protein family.
The Bcl-2 protein family consists of 3 sub-groups: anti-apoptotic factors like the name-giving Bcl-2, pro-apoptotic effectors like Bax and Bak, and BH3-only initiators of apoptosis. One to four so called Bcl-2 homology domains (BH1-4) are found in all, while a transmembrane domain (TM) at the C-terminal side is present only in some family members. The BH1 and BH2 domains function predominantly in pore formation and dimerization with pro-apoptotic BH3-only members, and the BH3 domain has a role in homo- and hetero- dimerization between the Bcl-2 family members. The BH4 domain is unique for the anti-apoptotic Bcl-2 members, and interacts with or regulates several other proteins involved in apoptosis (138, 143).

Several mechanisms involved in activation of BH3-only proteins have been reported (138, 144): phosphorylation, dephosphorylation, receptor triggered conformational changes or cleavage, and p53 mediated induction of transcription. Furthermore, proteasomal degradation and alternative splicing contribute to their diversity and regulation; for example, about 10 isoforms have been described for BIM, with BIM_S, BIM_L and BIM_{EL} being most prominent (138, 145-148). It has also been shown that transcriptional gene-silencing through epigenetic mechanisms, like DNA methylation or histone modification, can play a part in downregulation of BH3-only proteins, and this phenomenon is also associated with BRAF inhibitor resistance in melanoma (144, 149).

As mentioned above, defects or aberrations in the apoptotic signaling cascades are a central issue that can confer resistance to small molecule inhibitor treatment in melanoma. Indeed, evasion of cell-death is a common feature of tumor cells and also considered as one of the hallmarks of cancer (150). It has been reported that the intrinsic apoptosis pathway in melanoma is suppressed by active BRAF signaling, inhibiting expression of the BH3-only protein Bcl-2 interacting mediator of cell death (BIM) (147), whereas inhibition of the MAPK pathway triggers stress stimuli that induce upregulation of BIM and PUMA for subsequent apoptosis in melanoma cells (151-154). However, not all cells are killed, and the survivors may provide a source for relapse or a niche supporting tumor regrowth (155). Therefore, the major topic of this thesis and the two included publications dealing with melanoma, was to analyze the response of melanoma cells to the $BRAF^{V600}$ inhibitor vemurafenib and/or the MEK1/2 inhibitor trametinib treatment (article I), and to determine molecular characteristics, which affect the cell fate decision between death and survival (article IV).

4.3.3. Immunotherapy in melanoma

The immune system can recognize and target cancer cells, but is often held in check by inhibitory signals, which in healthy cells mediate self-tolerance and thereby avoid collateral tissue damage by an anti-microbial immune response (156). Avoiding immune destruction has also been added as a new emerging hallmark of some and perhaps all cancers by Hanahan & Weinberg in 2011, as the scientific community has got more aware of the important role of the

immune system - especially T and B lymphocytes, macrophages and natural killer cells - in destroying cancer cells (150). Modern cancer immunotherapy started with the FDA approval of the cytokines interleukin 2 (IL-2) and interferon alpha (INF-α) in 1995 for the treatment of melanoma. IL-2 is essential for central roles of the immune system, like tolerance and immunity, primarily due to its direct effect on T-cell differentiation. Furthermore, it also promotes the differentiation of T-cells when the initial T-cell is stimulated by an antigen, thus helping the body defend against infections (157). The interferons like INF-α are potent cytokines with anti-viral, anti-proliferative, and immunomodulatory capacities and are secreted by macrophages, fibroblasts, and endothelial cells. However, dendritic cells are considered the major producers of INF-α, in response to RNA or DNA viruses or nucleic acid-containing immune complexes (158). This first approach showed only mixed results, as high-dose Il-2 led to complete remissions in only 6% and to partial responses in 10% of patients (159, 160). Although durable remissions could be achieved in a minority of patients, this treatment was also associated with high toxicities. Indeed, adverse side effects killed 2% of the patients. Moreover, INF-α could only reduce the risk of recurrence by 10%, but did not have an effect on the OS (161). A new class of immunotherapeutic agents, the checkpoint inhibitors, was a big breakthrough several years later: ipilimumab, a cytotoxic T-lymphocyte-associated Protein 4 (CTLA-4) antibody, was approved by the FDA in 2011 for the treatment of advanced melanoma, after improved survival for late stage patients could be verified in clinical trials (162, 163). In Addition, the programmed cell death protein 1 (PD-1) antibodies pembrolizumab and nivolumab were FDA approved for melanoma in 2014, as these led also to durable remissions in some patients, but with considerably fewer toxic side effects than ipilimumab (164, 165). Both checkpoint-blocking strategies enable repressed tumor-specific T cells to fight cancer cells by suppressing surface molecule mediated signals that diminish T-cell activity: targeting CTLA-4 is believed to act primarily during the CD4+ T-helper cell priming phase, whereas the anti-PD-1 antibodies are thought to augment CD8+ T-killer cell activity directly in the tumor microenvironment (166).

At the moment, numerous new immunotherapeutic drugs are developed and tested alone or in combination in clinical trials, as further detailed in the discussion. Both treatment options - the immune based strategies as well as the targeted therapies - offer astonishing new possibilities in

the treatment of metastatic melanoma, and have massively improved the PFS and OS of patients (Table 3).

Table 3: Treatment specific average survival in metastatic melanoma.
Abbreviations: PFS, progression-free survival; OS, overall survival; n.d., not done. Data obtained from (167).

Therapeutic strategy			
First line therapy	**% PFS at 6 months**	**% OS at 12 months**	**% OS at 24 months**
Chemotherapy	22.1	42.2	22.6
BRAF inhibitors	55.4	63.4	37.6
BRAF + MEK inhibitors	72.3	76.9	53.5
CTLA-4 inhibitors	39.3	50.4	28.6
PD-1 inhibitors	51.1	72.2	59.3
CTLA-4 + PD-1 inhibitors	63.8	73.1	62.9
Second line or higher	**% PFS at 6 months**	**% OS at 12 months**	**% OS at 24 months**
Chemotherapy	20.7	45.8	27.3
BRAF inhibitors	55.9	56.9	n.d.
MEK inhibitors	21.3	42.3	n.d.
BRAF + MEK inhibitors	75.9	80.1	52.8
CTLA-4 inhibitors	21.8	48.6	29.1
PD-1 inhibitors	40.2	62.1	45.3
CTLA-4 + PD-1 inhibitors	73.2	86.9	n.d.

5. Discussion

Despite great advances in understanding the molecular pathogenesis of cancer in the last 50 years, cancer-related death rates in the western civilization have only marginally been reduced, leaving cancer the second most frequent cause of death after cardiovascular diseases in Germany (168). While today some malignancies like testicular cancer are curable in most cases, MCC and melanoma still present a challenge to treat, and in an advanced, metastatic stage the five-year OS remains very low and ranges between 0-18% for MCC and less than 30% for melanoma (79, 169, 170). Due to these yet unsatisfying numbers, basic and clinical research has been carried out, and has led not only to new insights in the pathogenic mechanisms of these tumor entities, but also yielded new treatment approaches, which are todays new standard of care for advanced melanoma and MCC (123, 171, 172). Indeed, for MCC as well as for melanoma, immunotherapeutic approaches have shown the capability to increase the survival of patients. These therapies act through inhibition of signals which suppress T cell function. The applied agents are antibodies targeting CTLA-4 (Ipilimumab), PD-1 (nivolumab or pembrolizumab) or PD-Ligand1 (PD-L1) (avelumab), and increase activity of cytotoxic CD8+ T cells, which are able to induce the extrinsic apoptosis pathway in the cancer cells. For melanoma, a second approach using small molecule kinase inhibitors specifically targeting activated oncogenic signaling pathways in the tumor cells is also applied, which induces the intrinsic apoptosis pathway. Here, these new therapies and further potential approaches for the treatment of MCC and melanoma will be discussed, with special emphasis on the topics addressed in the articles enclosed in this thesis.

5.1. Current state and outlook of immune-based therapies in melanoma & MCC

Immunotherapy with CTLA-4 and PD-1 antibodies is an established treatment for metastatic melanoma nowadays; however, not all patients do benefit from this approach and experience lasting responses. Furthermore, patients tend to react very differently to immunotherapy, and so far there are almost no predictive markers that identify those patients, who will potentially benefit from an immune-based therapy (173). According to the nature of the adaptive immune

system, presentation of antigenic peptides by major histocompatibility complex (MHC) class I molecules on the tumor cell surface is a prerequisite for the recognition by T-cells, and the response to an immunotherapy (174). Therefore, in particular tumors expressing viral antigens and many so called neoantigens, which correlate with a high burden of somatic mutations, are thought to be especially suited for immune-based approaches (175). MCC as well as melanoma fulfill these criteria, as MCV-negative MCC and cutaneous melanoma are the cancers with the highest load of somatic mutations, and MCV-positive MCC depends on the expression of the viral T antigens (47, 50, 89). Indeed, it has been shown that melanoma patients with a particularly high burden of clonal neoantigens have a greater benefit from immune-based therapies (175). Moreover, T cells recognizing clonal neoantigens were detectable in those patients, who experienced a durable clinical response (173, 175). This suggests the individual clonal neoantigen load as a possible predictive biomarker for the selection of patients indicated for immunotherapy.

It is expected that the combination of different drugs will be the key to improve the therapeutic success of immunotherapies in melanoma, since most malignancies seem to exploit multiple strategies to avoid the recognition and destruction through the immune system (immune escape mechanisms) at one. This includes loss of antigenicity, loss of immunogenicity or the establishment of an immunosuppressive microenvironment (176, 177). For example, the combination of ipilimumab and IL-2 led to complete response rates after a long follow-up in melanoma patients of 17%, compared to 7% in patients receiving ipilimumab with gp100 peptides (178). In 2015, a randomized phase III trial reported increased efficacy and safety for the use of combination-therapy of nivolumab and ipilimumab or nivolumab monotherapy, compared to ipilimumab monotherapy (179). Nevertheless, the search for more potential target-molecules besides the common targets CTLA-4, PD-1, and its ligand PD-L1 still is ongoing: recently, it has been reported that T-cell immunoreceptor with Ig and immunoreceptor tyrosine-based inhibition motif domains (TIGIT) is an immune checkpoint molecule that can limit CD8+ T-killer cell antitumor responses, in a comparable way to CTLA-4 and PD-1 (180, 181). Co-blockade of TIGIT and PD-1 has been proposed based on investigations, demonstrating that TIGIT-positive cells often co-express PD-1 (182). Another study suggests diphencyprone (DPCP), which has been used in melanoma patients as a sensitizing agent to induce tumor regression, as

a potential complementary agent to anti-PD-1 blockade, as PD-1 expression was significantly elevated in DPCP-applied regions (183).

Cytotoxic T-cells mediate cell death to the target tumor- or infected cell by the extrinsic, death receptor mediated apoptosis pathway, what results in initiator caspase 8 activation (184). As described in the introduction, BH3-only proteins of the Bcl-2 family play a pivotal role in intrinsic, mitochondria mediated apoptosis, and moreover, we outline the role of the BH3-only protein Bcl-2 interacting killer (BIK) for melanoma cell death after MAPK-pathway inhibition in article IV. These proteins, including BIK, could also play a role in extrinsic mediated apoptosis initiated by immunotherapy, as there is interaction between both pathways, for example through caspase 8 conducted cleavage and activation of the BH3-only protein Bid (135, 185). This truncated Bid protein (tBid) counteracts the anti-apoptotic Bcl-2 family members, outlining the importance of BH3-only proteins, also for the immune response. Furthermore, shared mechanisms of death induction by targeted and immunotherapy are also suggested by the observation that BRAF mutated patients, which were previously treated with BRAF inhibitors, demonstrate a reduced response rate in subsequent immunotherapy, compared to BRAF wild type patients treated solely with immunotherapy (186). To evaluate the relevance of BIK in melanoma treated with immune-stimulatory agents, co-culture of the M14-derived single cell clones described in article IV or patient derived BIK knockout melanoma cells with patient-derived cytotoxic T-cells, could elucidate the relevance of BIK expression under immunotherapy-conditions.

For MCC, there is a strong rationale that immune-based therapies could also be successful in the treatment of this cancer. Several clinical trials, applying immune checkpoint inhibitors as monotherapy or in combination with other agents for the treatment of advanced MCC, have recently been published or are still ongoing. Very promising results have been reported by two phase II trials in 2016: pembrolizumab, as first line treatment, was associated with a high response rate of 56% in 26 treatment-naive MCC patients, and avelumab, a PD-L1 antibody, as second line treatment for patients with chemo-refractory disease, could also reach a 32% response rate (14, 15). Both studies reported efficacy in MCV-positive and negative patients with a manageable safety profile. Further MCC-associated clinical trials are numerous and explore different immune-system associated strategies: these include, for example, the targeted

delivery of the Interleukin-12 (IL-12) gene - a pro-inflammatory cytokine, capable of stimulating the production of interferon gamma (IFN-γ) by natural killer and T-cells, which is also known to promote cell-mediated immunity and to activate anti-tumor responses (187) – by using intratumoral injection of a plasmid, followed by *in vivo* electroporation (NCT01440816). In addition, the use of IL-12 in combination with paclitaxel, a mitosis inhibiting toxin also known as taxol, is evaluated and compared to paclitaxel alone in an open-label, randomized phase II trial (NCT02054884). Furthermore, it has been demonstrated that MCV antigen-specific T cells are detectable in MCC patients, and these are capable of effectively kill MCV-positive MCC cell lines (188). Based on these findings, a phase I/II study (NCT02584829) evaluating safety and efficacy of avelumab in combination with MHC class I upregulation, mediated by interferon beta (IFN-β) administration and autologous T-cell transfer, is currently ongoing. Another phase I study is a proof-of-concept clinical trial, testing intratumoral injection of glucopyranosyl lipid adjuvant-stable emulsion (GLA-SE), a toll-like receptor-4 agonist, in patients with MCC (NCT02035657). Preliminary data has indicated that G100 (GLA-SE delivered intratumorally) is well tolerated and promotes inflammatory changes in the tumor microenvironment, thereby activating T-cells (189, 190). Taken together, this suggests the use of immunotherapies for both MCC variants. In March 2017, avelumab was the first treatment that gained FDA approval for metastatic MCC, and it will probably only be a matter of time until the next immune-based therapy for MCC achieves FDA approval.

The observed response towards immunotherapy does not depend on whether MCC is MCV associated or not. It is therefore likely that in MCV-negative cases a high neoepitope load – indeed virus-negative MCCs harbor more tumor neoantigens than melanomas or non-small cell lung cancers, due to their high frequency of somatic mutations (47) - provides targets for tumor-specific T cells, while in MCV-positive cases, which are characterized by a very low mutation load, viral epitopes serve as targets (191). In this respect, it is important that MCV-positive cells have been shown to be dependent on the expression of the viral proteins ST and LT (50, 52), not allowing MCC cells to evade the immune system by loss of expression of these antigens. In article III we were able to explain the LT dependency, as this protein is required to inactivate the tumor suppressor Rb, which in the absence of growth signals inhibits cellular proliferation (56). Thus, MCV TAs appear very viable as potential targets for immunotherapy; although the

dependency on LT may be lost in certain cases, for example, through a homozygous deletion of the Rb allele, as we demonstrated for the MCC cell line LoKe in article III, rendering this cell line independent of MCV-LT expression. However, MCV ST seems to fulfill a more complex and also indispensable role in virus-positive MCC (52, 53), and thus the loss of ST-dependency seems more unlikely, even though some data challenge its requirement for MCC proliferation (51). Expression levels of MCV ST and LT seem to differ substantially (51), most likely due to pre-mRNA or post-transcriptional protein processing, since both TA-variants are alternatively spliced viral proteins originating in one pre-mRNA (see Fig.2). Therefore it is at least questionable, if they could be expressed completely independent from each other. Importantly, in murine models using the B16 melanoma cell line expressing MCV LT or ST, DNA vaccines against both TAs generated antitumor effects mainly mediated by peptide-specific CD4+/CD8+ T-cells, and these mice experienced enhanced survival compared to those vaccinated with an empty vector (192, 193), further suggesting these structures as immunotherapeutic targets.

5.2. Current state and outlook of targeted therapies in melanoma

Small-molecule inhibitor based therapy for melanoma was developed after the $BRAF^{V600E}$ mutation was discovered in 2002, what finally resulted in FDA approval of vemurafenib, the first MAPK pathway targeting drug in 2011 (112, 113). Notably, the MAPK signaling pathway, which is strongly associated with proliferation and survival, still remains the most important to target. Soon after vemurafenib approval, the initial euphoria for small molecule inhibitors was abruptly lowered, as the awareness of resistances arose, which melanoma cells inevitably develop in the vast majority of patients after continuous therapy (125). Mechanisms of intrinsic or acquired resistance to BRAF or combined BRAF/MEK inhibition are many-sided, and vary between tumors and/or even within tumors. Lately, the most important mechanisms involved in intrinsic and acquired resistance have been reviewed by Amaral *et al.* in European Journal of Cancer. For intrinsic resistance, which is defined by the absence of response to BRAF/MEK inhibitor therapy (even despite the presence of a $BRAF^{V600}$ mutation), these include hepatocyte growth factor (HGF) stromal secretion, RTK signal alterations, COT expression, RAC1 gene mutations, neurofibromatosis 1 (NF1) dependent mechanisms, aberrations in cyclin and cyclin-dependent

kinase (CDK) expression or activity, and many more (194). Acquired resistance is described as an initial strong response to the inhibitor treatment, although a drug-tolerant sub-population of cells persists, what finally leads to progressive disease caused by proliferative resistant clones. Common sources of acquired resistances are RAS mutations, MAPK reactivation through a RAF isoform switch (ARAF,CRAF) or elevated CRAF levels, alternative BRAF splicing or amplification, activating mutations in the PI3K/AKT pathway, and so on (195). Many of these mechanisms identified overlap and fall into both categories; in fact, this classification is largely artificial, and some mechanisms are just incompletely understood, also putting a spotlight on the redundancy of some cellular pathways. Thus, it is believed that further improvements of the efficacy of targeted therapies can be achieved by a supplementary agent, targeting additionally those molecules involved in intrinsic resistance or acquired resistance to BRAF/MEK inhibition.

The tumor heterogeneity, characterized by the presence of different sub-populations that react differently to the BRAF/MEK inhibitor treatment, is a major issue to consider when we search for answers to resistance development. Cells with different cell cycle profiles, especially a slow cycling phenotype, appear to be refractory to cytotoxic and targeted therapy treatment (196-198). The importance of the cell cycle in intrinsic resistance to signaling inhibitors has also been emphasized by Beaumont *et al.*, who point out that a temporary G1 or G2 arrest confers resistance to specific treatment conditions (199). Cells in a growth-arrested state often exhibit increased mitochondrial metabolic activity, are high in autophagy, and may even show markers of senescence; a condition that can be induced by BRAF inhibition itself, as we demonstrated in the enclosed article I. Moreover, growth arrested cancer cells can still pose a threat for the organism: temporarily arrested (quiescent) cells can re-enter the cell cycle, and also permanently arrested (senescent) cells can be harmful by secreting factors that contribute to a pro-tumorigenic milieu. These changes in the secretome, paradoxically provoked by BRAF inhibitor treatment, can stimulate the outgrowth, dissemination, and metastasis of drug-resistant cancer cell clones or foster the survival of drug-sensitive cancer cells (200). Therefore, the ideal targeted therapy should aim at maximizing the eradication of cancer cells, rather than driving them into senescence or quiescence.

5.2.1. Bcl-2 family members as potential targets for melanoma therapy

Another condition in a sub-population of melanoma cells that mediates treatment resistance is apoptosis deficiency (130-133). A pivotal role in intrinsic, mitochondrial mediated apoptosis, which is induced by MAPK pathway inhibitor treatment in melanoma, plays the Bcl-2 protein family (136-138). The balance between pro-apoptotic and anti-apoptotic Bcl-2 proteins is of central importance for the induction of intrinsic apoptosis. Increased levels of anti-apoptotic Bcl-2 family members, like Bcl-X(L) and especially Mcl-1, which are commonly upregulated in progressing melanomas, have frequently been linked to resistance against small molecule inhibitors and cytotoxic agents (201-203); however, the role of Bcl-2 itself is still controversial (204-207). Targeting BCL-2 - either directly (for example by the use of inhibitors (208, 209)) or indirectly (for instance with BH3-mimetics that mimic the pro-apoptotic BH3-only proteins and thereby neutralize anti-apoptotic Bcl-2 family members (210, 211)) - has been demonstrated to effectively kill melanoma cells, and, even more important, melanoma cells with cancer stem cell-like characteristics, which are often made responsible for tumor persistence (212). Furthermore, the use of proteasomal inhibitors may in part exert its anti-tumorigenic effect by reducing proteasome dependent degradation of the BH3-only Proteins BIK, BIM, and NOXA (213-215). Additionally, epigenetic silencing of BH3-only proteins has been described in different cellular contexts, and can contribute to BRAF inhibitor resistance (144, 149). Indeed, we could identify epigenetic silencing of BIK as a potential mechanism to render melanoma cells refractory to BRAF/MEK inhibitor induced apoptosis, as demonstrated in article IV. We have shown that in melanoma cells lacking basal BIK expression, treatment with histone deacetylase inhibitors (HDACi) leads to increased Histone 3 Lysine 9 acetylation of the BIK promoter and de-repression of BIK expression. Moreover, the HDACi treatment made the previously refractory cells susceptible to apoptosis induction by BRAF/MEK inhibitors. This provides further pre-clinical prove for the therapeutic use of small molecules, upregulating or mimicking BH3-only proteins (210, 211), with special emphasis on BIK. Although some HDACi have been tested and approved for peripheral and cutaneous lymphoma and myeloma (216-218), in melanoma however, clinical trials with HDACi as monotherapy did not have the desired results (219, 220). Nevertheless some studies are still running, like the evaluation of vorinostat in resistant BRAF-

mutated advanced melanoma (NCT02836548). We and others provide a rationale for using HDACi in combination with BRAF/MEK inhibitor treatment or immunotherapy (221, 222). Some trials that combine immunotherapy with HDACi in melanoma, have already started as well: one study is recruiting patients for the treatment with panobinostat and ipilimumab (NCT02032810); another will evaluate the selective HDAC6 inhibitor ACY-241 in combination with ipilimumab and nivolumab (NCT02935790).

Similarly, first efforts at targeting Bcl-2 family members failed, most likely because of unfitting delivery systems and the unstable nature of the compounds, like antisense, single-chain antibodies, ribozymes, BH3 peptides and hydrocarbon stapling (223). Up-to-date approaches focus on more stable BH3-mimetics, like ABT-263 (navitoclax), an oral version of ABT-737 and ABT-199 (venetoclax). Both showed encouraging performance in hematologic tumors, and resulted in FDA approval of the latter for chronic lymphocytic leukemia (224-228). Unfortunately, none of these inhibit Mcl-1, what may be the reason for the inefficiency of ABT-737/ABT-263 single agent treatment in melanoma, as Mcl-1 is central for apoptosis-resistance in this cancer (229-232). However, it has been reported that ABT-737 sensitizes melanoma cells for BRAF inhibition mediated apoptosis (233), what is in line with our observation that upregulation of BIK via ectopic expression or HDACi has a similar effect, as both have the potential to inhibit Bcl-2 and Bcl-X(L) (234). At the moment, one phase I/II study is recruiting patients to explore the combination of dabrafenib with trametinib and navitoclax in BRAF-mutant melanoma and other solid tumors (NCT01989585). Currently, many inhibitors targeting Mcl-1 are developed that could complement BRAF/MEK inhibitor therapy: promising compounds for instance are maritoclax, WP1130, UMI-77, clitocine, and compound 11, which have shown efficacy in animal studies (235-239), but data from clinical trials are still missing. Figure 6 schematically summarizes the potential use of HDACi and BH3-mimetics as a complementary therapy to MAPK pathway inhibition.

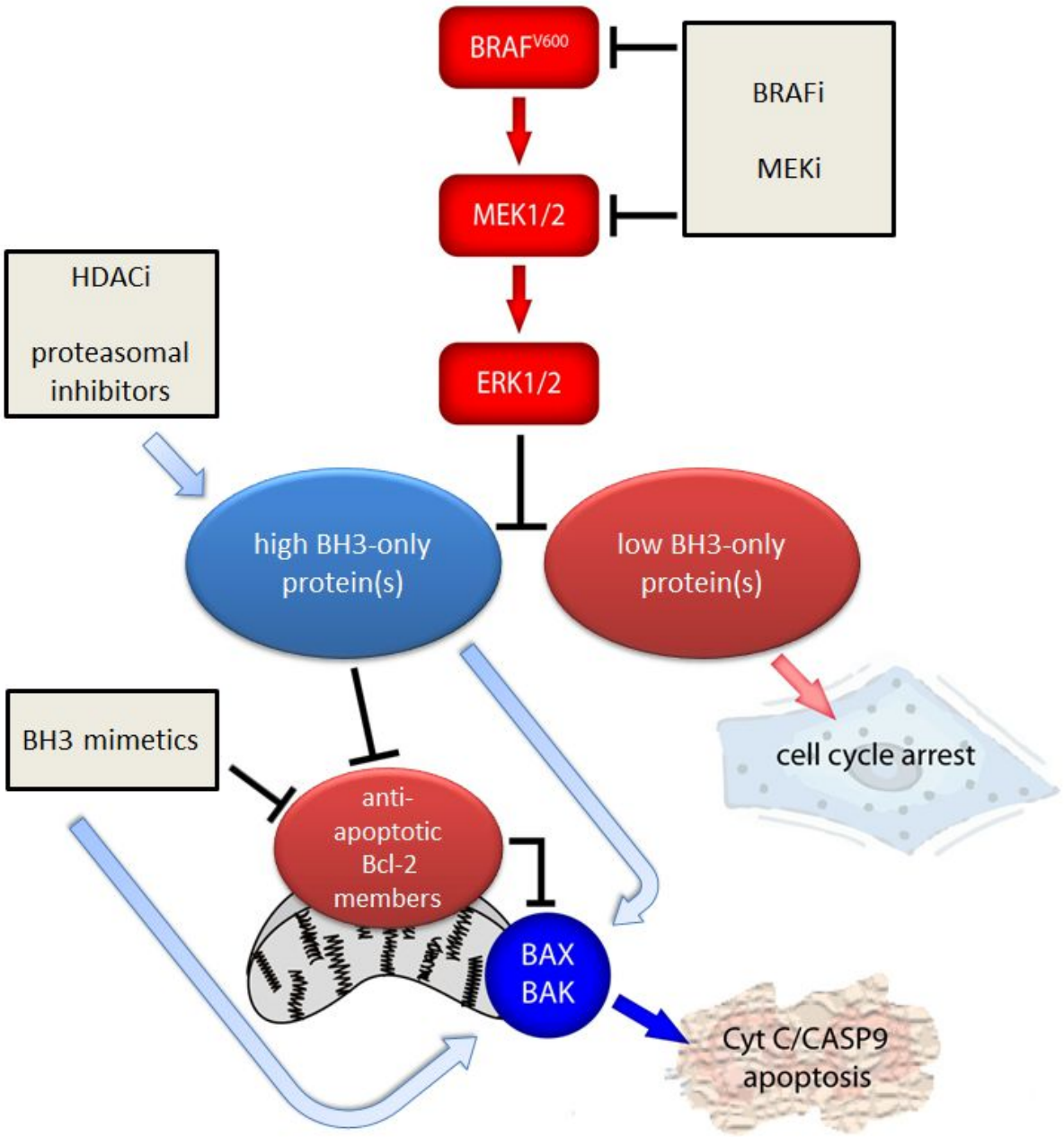

Fig. 6: HDACi and BH3-mimetics may help to overcome apoptosis defiance in MAPK pathway inhibition.
Apoptosis is the preferred outcome of MAPK pathway inhibition in melanoma cells. Factors that avoid apoptosis, like an active MAPK pathway, a low amount of BH3-only proteins or a high amount of anti-apoptotic Bcl-2 members are depicted in a red color, while factors that contribute to an apoptotic response, like a high amount of BH3-only proteins or activation of BAX/BAK are illustrated in blue. HDAC inhibition, proteasomal inhibition, and BH3-mimetics bear great potential to maximize the apoptotic response towards MAPK pathway inhibition. This is mediated by shifting the balance between anti-apoptotic Bcl-2 family members and pro-apoptotic BH3-only proteins in the direction of the latter.

5.3. Potential of targeted therapies in MCC

Unlike in melanoma, tumor-suppressors and especially oncogenes are not frequently mutated in virus-positive MCC, but numerous receptor kinases and ligands that may serve as therapeutic targets are expressed. These are PI3K/AKT, c-kit, platelet-derived growth factor A & B (PDGFA & PDGFB), vascular endothelial growth factors A and C as well as vascular endothelial growth factor receptor-2 (VEGF-A, VEGF-C, VEGFR-2) (240-243). One case reported a 92-year old woman with a complete resolution of a MCV and KIT positive tumor, after application of the tyrosine kinase inhibitor imatinib in combination with radiotherapy (244). Unfortunately, a phase II clinical trial of imatinib in MCC was canceled prematurely due to poor performance status, with the majority of patients progressing rapidly within one to two cycles of treatment (245). Multi-targeted kinase inhibitors could have better clinical effectivity in advanced MCC, and a clinical trial administering cabozantinib, a c-met and VEGFR-2 inhibitor, to MCC patients is running at the moment (NCT02036476). Activating mutations of the PI3K/AKT pathway have also been observed in MCC, suggesting the use of inhibitors of this pathway (241). In a case report, the PI3K inhibitor idelalisib was able to achieve a complete response in a patient with stage IV MCC (246). The mammalian target of rapamycin (mTOR) inhibitors MLN0128 and everolimus are investigated in ongoing trials for advanced MCC (NCT02514824 and NCT00655655), as mTOR is described as activated in MCC and a known regulator of the PI3K/AKT and MAPK pathway (247, 248).

Given that in many cancers tumor-suppressors are frequently mutated, deleted, silenced or dysfunctional by other reasons, restoring wild-type tumor suppressor activity appears to be a reasonable approach to eradicate cancer. This can be achieved either by direct virus-mediated and non-virus-mediated delivery methods, transporting functional tumor suppressor genes to their destination and ectopic expression of these (gene therapy), or by inhibitors that disrupt interactions between tumor suppressor genes and their negative regulators (249). This attempt may also be suitable for MCC, as reactivation of a single tumor-suppressor like Rb or p53 may be sufficient to stop MCC cell proliferation and/or induce apoptosis, how our data from the two enclosed MCC articles suggest (article II & article III).

The role of p53 in MCC is still not sufficiently elucidated: The majority of MCC lines show wild-type p53 expression with some transcriptional activity, which is not sufficient to restrict survival or proliferation in these cells, as we demonstrate in article II. It has been reported that despite the lack of the C-terminal p53-binding domain, SV40 LT is still able to inhibit p53-dependent transcription (250, 251), which may hint to a similar ability of MCV LT. However, our data from article II do not support this thesis, since knockdown of MCV TAs has no impact on p53 transcriptional activity in MCC cells. Additionally, according to these data, p53 reactivation through inhibition of its main negative regulator human double minute 2 (HDM2) with nutlin-3a is promising *in vitro*, and the application of a related agent (RG7112) has shown some clinical activity in liposarcoma and leukemia (252, 253). Moreover, local adenoviral delivery of a recombinant p53 gene with standard treatments showed good results in clinical studies (254, 255). A lot of clinical trials are going on exploring the effectivity and safety of the p53 gene therapy in various cancers and drug combinations (NCT02429037, NCT02435186, NCT02842125). Patients with still localized MCC could also benefit from a similar approach, and possibly experience a lower recurrence rate after tumor excision.

In contrast to p53, the role of Rb in MCC is clearer: inactivation of Rb either by mutations occurring frequently in virus-negative MCC, or by MCV LT in virus-positive MCC seems to be a crucial step in MCC carcinogenesis, and necessary for most MCC cells to proliferate (47, 73). Therefore, Rb reactivation is a logic effort to battle MCC. Blockade of Rb phosphorylation and maintenance of efficient E2F repression may be achieved by CDK-inhibitors, such as the highly selective CDK4/6 inhibitor PD-0332991 (palbociclib), which also yielded positive results in clinical trials (256-258). For MCC however, inhibition of CDKs appears not suitable, since Rb inactivation occurs downstream of CDKs. Because inactivation of Rb by MCV LT in MCV-positive MCC occurs by direct interaction of these two proteins (article III), development of small molecules interfering specifically with Rb/LT binding would be of great interest.

Taken together, targeted therapies that aim at reactivation of tumor-suppressors rather than oncogene blockade remain a viable strategy to fight cancer in the future, although a lot of considerable uncertainty remains. Many experiments and clinical trials to date are hindered by the lack of efficacy, specificity, and serious safety concerns by enhanced tumor suppressor activity in healthy cells. Furthermore, development of inhibitors for protein-protein interaction

rather than kinases with well-defined ATP-binding pockets is far more challenging, as these interfaces typically consist of large surface areas that display a lack of well-defined structures (249, 259).

5.4. Combining targeted and immune-based therapies: the future of melanoma treatment?

A possibility to achieve improved overall survival, which is increasingly explored in clinical melanoma research, is the combination of therapies: in particular, combining the high response rates of the targeted therapies with the longevity of the immunotherapies appears to be attractive. This approach may reduce the short-lived benefits of the BRAF/MEK inhibitors, and a broader number of patients could benefit than with CTLA-4/PD-1 blockade alone (260, 261). Furthermore, targeted therapy can affect antitumor immunity, and complications can be avoided or synergies may arise when applied together or sequential in a certain combination or order (186). In xenograft models, it has been shown that the effectivity of BRAF inhibition is at least partly dependent on the presence of CD8+ T-killer cells (262), and another study reported that BRAF inhibition and PD-1 blockade function in a synergistic manner (263). In contrast, MEK inhibition alone or in combination was associated with suppressed human T-lymphocyte proliferation, cytokine production, and antigen-specific expansion, whereas treatment with dabrafenib had no effect (264). In melanoma patients it has been shown that the MAPK pathway plays an important role in cancer immune evasion by secreting immune-suppressive cytokines like interleukin 6 & 10 (IL-6 & IL-10), while tumor samples after being exposed to vemurafenib had reduced levels of these cytokines (265, 266). Moreover, an increase in melanoma differentiation antigens, as well as a significant increase in clonal intra-tumoral CD8+ T-killer cells, has been reported after initiation of BRAF treatment. These findings were also associated with down regulated IL-6, IL-8, IL-1α and VEGF. Notably, increased immunomodulatory molecules, namely PD-1 and PD-L1, have been detected following BRAF inhibition, suggesting a potential immune-based mechanism of resistance, which might be overcome by applying the respective checkpoint antibodies (261, 266-269). Furthermore, BRAF inhibition in patients was associated with reduced immunosuppression mediated by myeloid derived suppressor cells (270).

Translation into clinical studies with large patient cohorts has already begun, and a first attempt of combining immune- with targeted therapy was the combination of the initial flagships of each treatment approach: ipilimumab and vemurafenib. This study was discontinued due to dose limiting toxicities and massive hepatotoxic adverse effects experienced by most patients (271). Recently, a clinical trial finished that utilizes dabrafenib with or without trametinib combined with ipilimumab in patients with BRAF-mutated metastatic melanoma (NCT01767454), where in the doublet arm administering dabrafenib with ipilimumab no dose limiting toxicities were observed, while the addition of trametinib was associated with severe gastrointestinal toxicity (272). These experiences teach us that there are a lot of challenges to overcome, until one day the two therapy approaches can finally be used successfully, as severe adverse events seem to occur frequently. However, myriads of clinical trials are currently conducted, evaluating different protocols of combining immunotherapeutics with MAPK pathway inhibitors in melanoma: one phase Ib study investigates the use of atezolizumab, an PD-L1 antibody, in combination with vemurafenib or vemurafenib plus cobimetinib in participants with BRAF-mutant melanoma (NCT01656642). Another trial scrutinizes the safety and efficacy of pembrolizumab in combination with trametinib and dabrafenib (NCT02130466). Further, not checkpoint antibody based approaches, try to use cytokines (NCT01603212, NCT01943422) or tumor infiltrating lymphocytes (NCT00338377, NCT01585415, NCT01659151) along with targeted therapies.

Taken together, metastatic melanoma treatment has undergone an astonishing development and faced many scientific breakthroughs in the past 10 years, but this progress also has added much complexity to the management of melanoma patients. The appropriate timing and/or sequencing of targeted therapy and immunotherapy remain to be elucidated, but synergies most likely exist between both treatment options. However, the potential benefits seem to be bought by a substantial increase in toxicity, and more studies are clearly needed for a better understanding of the responses to these types of therapy. The insights gained will eventually help identifying suitable patients for each of the established therapies, and further improve treatment outcome.

6. Reference list

(1) Proksch E, Brandner JM, Jensen JM. The skin: an indispensable barrier. Exp Dermatol 2008;17:1063-72.

(2) Munde PB, Khandekar SP, Dive AM, Sharma A. Pathophysiology of merkel cell. J Oral Maxillofac Pathol 2013;17:408-12.

(3) Tolleson WH. Human melanocyte biology, toxicology, and pathology. J Environ Sci Health C Environ Carcinog Ecotoxicol Rev 2005;23:105-61.

(4) headandneckcancerguide.org. http://headandneckcancerguide.org/adults/introduction-to-head-and-neck-cancer/skin-cancer/anatomy/. 2017.
Ref Type: Online Source

(5) Stakaityte G, Wood JJ, Knight LM, Abdul-Sada H, Adzahar NS, Nwogu N, et al. Merkel cell polyomavirus: molecular insights into the most recently discovered human tumour virus. Cancers (Basel) 2014;6:1267-97.

(6) NHS. http://www.nhs.uk/conditions/malignant-melanoma/pages/introduction.aspx. 2017.
Ref Type: Online Source

(7) Hughes MP, Hardee ME, Cornelius LA, Hutchins LF, Becker JC, Gao L. Merkel Cell Carcinoma: Epidemiology, Target, and Therapy. Curr Dermatol Rep 2014;3:46-53.

(8) Albores-Saavedra J, Batich K, Chable-Montero F, Sagy N, Schwartz AM, Henson DE. Merkel cell carcinoma demographics, morphology, and survival based on 3870 cases: a population based study. J Cutan Pathol 2010;37:20-7.

(9) Heath M, Jaimes N, Lemos B, Mostaghimi A, Wang LC, Penas PF, et al. Clinical characteristics of Merkel cell carcinoma at diagnosis in 195 patients: the AEIOU features. J Am Acad Dermatol 2008;58:375-81.

(10) Hanly AJ, Elgart GW, Jorda M, Smith J, Nadji M. Analysis of thyroid transcription factor-1 and cytokeratin 20 separates merkel cell carcinoma from small cell carcinoma of lung. J Cutan Pathol 2000;27:118-20.

(11) Tothill R, Estall V, Rischin D. Merkel cell carcinoma: emerging biology, current approaches, and future directions. Am Soc Clin Oncol Educ Book 2015;e519-e526.

(12) Becker J, Mauch C, Kortmann RD, Keilholz U, Bootz F, Garbe C, et al. Short German guidelines: Merkel cell carcinoma. J Dtsch Dermatol Ges 2008;6 Suppl 1:S15-S16.

(13) Becker JC. Merkel cell carcinoma. Ann Oncol 2010;21 Suppl 7:vii81-vii85.

(14) Kaufman HL, Russell J, Hamid O, Bhatia S, Terheyden P, D'Angelo SP, et al. Avelumab in patients with chemotherapy-refractory metastatic Merkel cell carcinoma: a multicentre, single-group, open-label, phase 2 trial. Lancet Oncol 2016;17:1374-85.

(15) Nghiem PT, Bhatia S, Lipson EJ, Kudchadkar RR, Miller NJ, Annamalai L, et al. PD-1 Blockade with Pembrolizumab in Advanced Merkel-Cell Carcinoma. N Engl J Med 2016;374:2542-52.

(16) Tang CK, Toker C. Trabecular carcinoma of the skin: further clinicopathologic and ultrastructural study. Mt Sinai J Med 1979;46:516-23.

(17) Tang CK, Toker C. Trabecular carcinoma of the skin: an ultrastructural study. Cancer 1978;42:2311-21.

(18) Tilling T, Moll I. Which are the cells of origin in merkel cell carcinoma? J Skin Cancer 2012;2012:680410.

(19) Zur HA, Rennspiess D, Winnepenninckx V, Speel EJ, Kurz AK. Early B-cell differentiation in Merkel cell carcinomas: clues to cellular ancestry. Cancer Res 2013;73:4982-7.

(20) Feng H, Shuda M, Chang Y, Moore PS. Clonal integration of a polyomavirus in human Merkel cell carcinoma. Science 2008;319:1096-100.

(21) Calvignac-Spencer S, Feltkamp MC, Daugherty MD, Moens U, Ramqvist T, Johne R, et al. A taxonomy update for the family Polyomaviridae. Arch Virol 2016;161:1739-50.

(22) zur HH. Novel human polyomaviruses--re-emergence of a well known virus family as possible human carcinogens. Int J Cancer 2008;123:247-50.

(23) Major EO, Mourrain P, Cummins C. JC virus-induced owl monkey glioblastoma cells in culture: biological properties associated with the viral early gene product. Virology 1984;136:359-67.

(24) Miller NR, McKeever PE, London W, Padgett BL, Walker DL, Wallen WC. Brain tumors of owl monkeys inoculated with JC virus contain the JC virus genome. J Virol 1984;49:848-56.

(25) Shah KV, Daniel RW, Strandberg JD. Sarcoma in a hamster inoculated with BK virus, a human papovavirus. J Natl Cancer Inst 1975;54:945-50.

(26) Foulongne V, Courgnaud V, Champeau W, Segondy M. Detection of Merkel cell polyomavirus on environmental surfaces. J Med Virol 2011;83:1435-9.

(27) Tolstov YL, Pastrana DV, Feng H, Becker JC, Jenkins FJ, Moschos S, et al. Human Merkel cell polyomavirus infection II. MCV is a common human infection that can be detected by conformational capsid epitope immunoassays. Int J Cancer 2009;125:1250-6.

(28) Viscidi RP, Rollison DE, Sondak VK, Silver B, Messina JL, Giuliano AR, et al. Age-specific seroprevalence of Merkel cell polyomavirus, BK virus, and JC virus. Clin Vaccine Immunol 2011;18:1737-43.

(29) DeCaprio JA. Merkel cell polyomavirus and Merkel cell carcinoma. Philos Trans R Soc Lond B Biol Sci 2017;372.

(30) Carter JJ, Daugherty MD, Qi X, Bheda-Malge A, Wipf GC, Robinson K, et al. Identification of an overprinting gene in Merkel cell polyomavirus provides evolutionary insight into the birth of viral genes. Proc Natl Acad Sci U S A 2013;110:12744-9.

(31) Moore PS, Chang Y. Why do viruses cause cancer? Highlights of the first century of human tumour virology. Nat Rev Cancer 2010;10:878-89.

(32) Adam C, Baeurle A, Brodsky JL, Wipf P, Schrama D, Becker JC, et al. The HSP70 modulator MAL3-101 inhibits Merkel cell carcinoma. PLoS One 2014;9:e92041.

(33) Topalis D, Andrei G, Snoeck R. The large tumor antigen: a "Swiss Army knife" protein possessing the functions required for the polyomavirus life cycle. Antiviral Res 2013;97:122-36.

(34) Nakamura T, Sato Y, Watanabe D, Ito H, Shimonohara N, Tsuji T, et al. Nuclear localization of Merkel cell polyomavirus large T antigen in Merkel cell carcinoma. Virology 2010;398:273-9.

(35) Lane DP, Simanis V, Bartsch R, Yewdell J, Gannon J, Mole S. Cellular targets for SV40 large T-antigen. Proc R Soc Lond B Biol Sci 1985;226:25-42.

(36) Poulin DL, Kung AL, DeCaprio JA. p53 targets simian virus 40 large T antigen for acetylation by CBP. J Virol 2004;78:8245-53.

(37) Cheng J, Rozenblatt-Rosen O, Paulson KG, Nghiem P, DeCaprio JA. Merkel cell polyomavirus large T antigen has growth-promoting and inhibitory activities. J Virol 2013;87:6118-26.

(38) Kassem A, Schopflin A, Diaz C, Weyers W, Stickeler E, Werner M, et al. Frequent detection of Merkel cell polyomavirus in human Merkel cell carcinomas and identification of a unique deletion in the VP1 gene. Cancer Res 2008;68:5009-13.

(39) Shuda M, Feng H, Kwun HJ, Rosen ST, Gjoerup O, Moore PS, et al. T antigen mutations are a human tumor-specific signature for Merkel cell polyomavirus. Proc Natl Acad Sci U S A 2008;105:16272-7.

(40) Moens U, Van GM, Johannessen M. Oncogenic potentials of the human polyomavirus regulatory proteins. Cell Mol Life Sci 2007;64:1656-78.

(41) Pallas DC, Shahrik LK, Martin BL, Jaspers S, Miller TB, Brautigan DL, et al. Polyoma small and middle T antigens and SV40 small t antigen form stable complexes with protein phosphatase 2A. Cell 1990;60:167-76.

(42) Kwun HJ, Shuda M, Feng H, Camacho CJ, Moore PS, Chang Y. Merkel cell polyomavirus small T antigen controls viral replication and oncoprotein expression by targeting the cellular ubiquitin ligase SCFFbw7. Cell Host Microbe 2013;14:125-35.

(43) Comerford SA, Schultz N, Hinnant EA, Klapproth S, Hammer RE. Comparative analysis of SV40 17kT and LT function in vivo demonstrates that LT's C-terminus re-programs hepatic gene expression and is necessary for tumorigenesis in the liver. Oncogenesis 2012;1:e28.

(44) Zerrahn J, Knippschild U, Winkler T, Deppert W. Independent expression of the transforming amino-terminal domain of SV40 large I antigen from an alternatively spliced third SV40 early mRNA. EMBO J 1993;12:4739-46.

(45) Seo GJ, Chen CJ, Sullivan CS. Merkel cell polyomavirus encodes a microRNA with the ability to autoregulate viral gene expression. Virology 2009;383:183-7.

(46) Shuda M, Arora R, Kwun HJ, Feng H, Sarid R, Fernandez-Figueras MT, et al. Human Merkel cell polyomavirus infection I. MCV T antigen expression in Merkel cell carcinoma, lymphoid tissues and lymphoid tumors. Int J Cancer 2009;125:1243-9.

(47) Goh G, Walradt T, Markarov V, Blom A, Riaz N, Doumani R, et al. Mutational landscape of MCPyV-positive and MCPyV-negative Merkel cell carcinomas with implications for immunotherapy. Oncotarget 2016;7:3403-15.

(48) Hahn WC, Dessain SK, Brooks MW, King JE, Elenbaas B, Sabatini DM, et al. Enumeration of the simian virus 40 early region elements necessary for human cell transformation. Mol Cell Biol 2002;22:2111-23.

(49) Bikel I, Montano X, Agha ME, Brown M, McCormack M, Boltax J, et al. SV40 small t antigen enhances the transformation activity of limiting concentrations of SV40 large T antigen. Cell 1987;48:321-30.

(50) Houben R, Shuda M, Weinkam R, Schrama D, Feng H, Chang Y, et al. Merkel cell polyomavirus-infected Merkel cell carcinoma cells require expression of viral T antigens. J Virol 2010;84:7064-72.

(51) Angermeyer S, Hesbacher S, Becker JC, Schrama D, Houben R. Merkel cell polyomavirus-positive Merkel cell carcinoma cells do not require expression of the viral small T antigen. J Invest Dermatol 2013;133:2059-64.

(52) Shuda M, Chang Y, Moore PS. Merkel cell polyomavirus-positive Merkel cell carcinoma requires viral small T-antigen for cell proliferation. J Invest Dermatol 2014;134:1479-81.

(53) Shuda M, Kwun HJ, Feng H, Chang Y, Moore PS. Human Merkel cell polyomavirus small T antigen is an oncoprotein targeting the 4E-BP1 translation regulator. J Clin Invest 2011;121:3623-34.

(54) Imai Y, Chumakov A, Miller C, Said J, Koeffler H. T-antigen of sv40 blocks p53 transactivation but not p53 specific binding to DNA. Int J Oncol 1994;5:945-53.

(55) Sullivan CS, Cantalupo P, Pipas JM. The molecular chaperone activity of simian virus 40 large T antigen is required to disrupt Rb-E2F family complexes by an ATP-dependent mechanism. Mol Cell Biol 2000;20:6233-43.

(56) Cobrinik D. Pocket proteins and cell cycle control. Oncogene 2005;24:2796-809.

(57) Wu CL, Zukerberg LR, Ngwu C, Harlow E, Lees JA. In vivo association of E2F and DP family proteins. Mol Cell Biol 1995;15:2536-46.

(58) Korenjak M, Brehm A. E2F-Rb complexes regulating transcription of genes important for differentiation and development. Curr Opin Genet Dev 2005;15:520-7.

(59) Munger K, Howley PM. Human papillomavirus immortalization and transformation functions. Virus Res 2002;89:213-28.

(60) Chen HZ, Tsai SY, Leone G. Emerging roles of E2Fs in cancer: an exit from cell cycle control. Nat Rev Cancer 2009;9:785-97.

(61) Maiti B, Li J, de BA, Gordon F, Timmers C, Opavsky R, et al. Cloning and characterization of mouse E2F8, a novel mammalian E2F family member capable of blocking cellular proliferation. J Biol Chem 2005;280:18211-20.

(62) Takahashi Y, Rayman JB, Dynlacht BD. Analysis of promoter binding by the E2F and pRB families in vivo: distinct E2F proteins mediate activation and repression. Genes Dev 2000;14:804-16.

(63) Balciunaite E, Spektor A, Lents NH, Cam H, Te RH, Scime A, et al. Pocket protein complexes are recruited to distinct targets in quiescent and proliferating cells. Mol Cell Biol 2005;25:8166-78.

(64) Cam H, Balciunaite E, Blais A, Spektor A, Scarpulla RC, Young R, et al. A common set of gene regulatory networks links metabolism and growth inhibition. Mol Cell 2004;16:399-411.

(65) Hollstein M, Sidransky D, Vogelstein B, Harris CC. p53 mutations in human cancers. Science 1991;253:49-53.

(66) Green DR, Chipuk JE. p53 and metabolism: Inside the TIGAR. Cell 2006;126:30-2.

(67) Han ES, Muller FL, Perez VI, Qi W, Liang H, Xi L, et al. The in vivo gene expression signature of oxidative stress. Physiol Genomics 2008;34:112-26.

(68) Vogelstein B, Lane D, Levine AJ. Surfing the p53 network. Nature 2000;408:307-10.

(69) Vousden KH. Activation of the p53 tumor suppressor protein. Biochim Biophys Acta 2002;1602:47-59.

(70) Blagosklonny MV. Loss of function and p53 protein stabilization. Oncogene 1997;15:1889-93.

(71) Mayo LD, Dixon JE, Durden DL, Tonks NK, Donner DB. PTEN protects p53 from Mdm2 and sensitizes cancer cells to chemotherapy. J Biol Chem 2002;277:5484-9.

(72) Sastre-Garau X, Peter M, Avril MF, Laude H, Couturier J, Rozenberg F, et al. Merkel cell carcinoma of the skin: pathological and molecular evidence for a causative role of MCV in oncogenesis. J Pathol 2009;218:48-56.

(73) Houben R, Adam C, Baeurle A, Hesbacher S, Grimm J, Angermeyer S, et al. An intact retinoblastoma protein-binding site in Merkel cell polyomavirus large T antigen is required for promoting growth of Merkel cell carcinoma cells. Int J Cancer 2012;130:847-56.

(74) Garibyan L, Fisher DE. How sunlight causes melanoma. Curr Oncol Rep 2010;12:319-26.

(75) Siegel R, Ma J, Zou Z, Jemal A. Cancer statistics, 2014. CA Cancer J Clin 2014;64:9-29.

(76) Miller AJ, Mihm MC, Jr. Melanoma. N Engl J Med 2006;355:51-65.

(77) Balch CM, Gershenwald JE, Soong SJ, Thompson JF, Atkins MB, Byrd DR, et al. Final version of 2009 AJCC melanoma staging and classification. J Clin Oncol 2009;27:6199-206.

(78) Jerant AF, Johnson JT, Sheridan CD, Caffrey TJ. Early detection and treatment of skin cancer. Am Fam Physician 2000;62:357-6, 381.

(79) Sandru A, Voinea S, Panaitescu E, Blidaru A. Survival rates of patients with metastatic malignant melanoma. J Med Life 2014;7:572-6.

(80) Friedman RJ, Rigel DS, Kopf AW. Early detection of malignant melanoma: the role of physician examination and self-examination of the skin. CA Cancer J Clin 1985;35:130-51.

(81) Maverakis E, Cornelius LA, Bowen GM, Phan T, Patel FB, Fitzmaurice S, et al. Metastatic melanoma - a review of current and future treatment options. Acta Derm Venereol 2015;95:516-24.

(82) consumerhealthdigest.com. https://www.consumerhealthdigest.com/health-conditions/melanoma.html. 2017.
Ref Type: Online Source

(83) melanoma.org. https://www.melanoma.org/understand-melanoma/diagnosing-melanoma/detection-screening/abcdes-melanoma. 2017.
Ref Type: Online Source

(84) Avril MF, Aamdal S, Grob JJ, Hauschild A, Mohr P, Bonerandi JJ, et al. Fotemustine compared with dacarbazine in patients with disseminated malignant melanoma: a phase III study. J Clin Oncol 2004;22:1118-25.

(85) Bedikian AY, Millward M, Pehamberger H, Conry R, Gore M, Trefzer U, et al. Bcl-2 antisense (oblimersen sodium) plus dacarbazine in patients with advanced melanoma: the Oblimersen Melanoma Study Group. J Clin Oncol 2006;24:4738-45.

(86) Chapman PB, Einhorn LH, Meyers ML, Saxman S, Destro AN, Panageas KS, et al. Phase III multicenter randomized trial of the Dartmouth regimen versus dacarbazine in patients with metastatic melanoma. J Clin Oncol 1999;17:2745-51.

(87) Middleton MR, Lorigan P, Owen J, Ashcroft L, Lee SM, Harper P, et al. A randomized phase III study comparing dacarbazine, BCNU, cisplatin and tamoxifen with dacarbazine and interferon in advanced melanoma. Br J Cancer 2000;82:1158-62.

(88) Nikolaou VA, Stratigos AJ, Flaherty KT, Tsao H. Melanoma: new insights and new therapies. J Invest Dermatol 2012;132:854-63.

(89) The Cancer Genome Atlas Network. Genomic Classification of Cutaneous Melanoma. Cell 2015;161:1681-96.

(90) Braig M, Schmitt CA. Oncogene-induced senescence: putting the brakes on tumor development. Cancer Res 2006;66:2881-4.

(91) Schulze WX, Deng L, Mann M. Phosphotyrosine interactome of the ErbB-receptor kinase family. Mol Syst Biol 2005;1:2005.

(92) Pearson G, Robinson F, Beers GT, Xu BE, Karandikar M, Berman K, et al. Mitogen-activated protein (MAP) kinase pathways: regulation and physiological functions. Endocr Rev 2001;22:153-83.

(93) Albino AP, Nanus DM, Mentle IR, Cordon-Cardo C, McNutt NS, Bressler J, et al. Analysis of ras oncogenes in malignant melanoma and precursor lesions: correlation of point mutations with differentiation phenotype. Oncogene 1989;4:1363-74.

(94) Gajewski TF, Salama AK, Niedzwiecki D, Johnson J, Linette G, Bucher C, et al. Phase II study of the farnesyltransferase inhibitor R115777 in advanced melanoma (CALGB 500104). J Transl Med 2012;10:246.

(95) Sebti SM, Der CJ. Opinion: Searching for the elusive targets of farnesyltransferase inhibitors. Nat Rev Cancer 2003;3:945-51.

(96) Whyte DB, Kirschmeier P, Hockenberry TN, Nunez-Oliva I, James L, Catino JJ, et al. K- and N-Ras are geranylgeranylated in cells treated with farnesyl protein transferase inhibitors. J Biol Chem 1997;272:14459-64.

(97) Hong DS, Sebti SM, Newman RA, Blaskovich MA, Ye L, Gagel RF, et al. Phase I trial of a combination of the multikinase inhibitor sorafenib and the farnesyltransferase inhibitor tipifarnib in advanced malignancies. Clin Cancer Res 2009;15:7061-8.

(98) Niessner H, Beck D, Sinnberg T, Lasithiotakis K, Maczey E, Gogel J, et al. The farnesyl transferase inhibitor lonafarnib inhibits mTOR signaling and enforces sorafenib-induced apoptosis in melanoma cells. J Invest Dermatol 2011;131:468-79.

(99) Curtin JA, Fridlyand J, Kageshita T, Patel HN, Busam KJ, Kutzner H, et al. Distinct sets of genetic alterations in melanoma. N Engl J Med 2005;353:2135-47.

(100) Curtin JA, Busam K, Pinkel D, Bastian BC. Somatic activation of KIT in distinct subtypes of melanoma. J Clin Oncol 2006;24:4340-6.

(101) Jiang X, Zhou J, Yuen NK, Corless CL, Heinrich MC, Fletcher JA, et al. Imatinib targeting of KIT-mutant oncoprotein in melanoma. Clin Cancer Res 2008;14:7726-32.

(102) Carvajal RD, Antonescu CR, Wolchok JD, Chapman PB, Roman RA, Teitcher J, et al. KIT as a therapeutic target in metastatic melanoma. JAMA 2011;305:2327-34.

(103) Guo J, Si L, Kong Y, Flaherty KT, Xu X, Zhu Y, et al. Phase II, open-label, single-arm trial of imatinib mesylate in patients with metastatic melanoma harboring c-Kit mutation or amplification. J Clin Oncol 2011;29:2904-9.

(104) Woodman SE, Trent JC, Stemke-Hale K, Lazar AJ, Pricl S, Pavan GM, et al. Activity of dasatinib against L576P KIT mutant melanoma: molecular, cellular, and clinical correlates. Mol Cancer Ther 2009;8:2079-85.

(105) Cho JH, Kim KM, Kwon M, Kim JH, Lee J. Nilotinib in patients with metastatic melanoma harboring KIT gene aberration. Invest New Drugs 2012;30:2008-14.

(106) Kluger HM, Dudek AZ, McCann C, Ritacco J, Southard N, Jilaveanu LB, et al. A phase 2 trial of dasatinib in advanced melanoma. Cancer 2011;117:2202-8.

(107) Wyman K, Atkins MB, Prieto V, Eton O, McDermott DF, Hubbard F, et al. Multicenter Phase II trial of high-dose imatinib mesylate in metastatic melanoma: significant toxicity with no clinical efficacy. Cancer 2006;106:2005-11.

(108) Ugurel S, Hildenbrand R, Zimpfer A, La RP, Paschka P, Sucker A, et al. Lack of clinical efficacy of imatinib in metastatic melanoma. Br J Cancer 2005;92:1398-405.

(109) Amaria RN, Lewis KD, Jimeno A. Vemurafenib: the road to personalized medicine in melanoma. Drugs Today (Barc) 2012;48:109-18.

(110) Houben R, Becker JC, Kappel A, Terheyden P, Brocker EB, Goetz R, et al. Constitutive activation of the Ras-Raf signaling pathway in metastatic melanoma is associated with poor prognosis. J Carcinog 2004;3:6.

(111) Yang H, Higgins B, Kolinsky K, Packman K, Go Z, Iyer R, et al. RG7204 (PLX4032), a selective BRAFV600E inhibitor, displays potent antitumor activity in preclinical melanoma models. Cancer Res 2010;70:5518-27.

(112) Chapman PB, Hauschild A, Robert C, Haanen JB, Ascierto P, Larkin J, et al. Improved survival with vemurafenib in melanoma with BRAF V600E mutation. N Engl J Med 2011;364:2507-16.

(113) Flaherty KT, Yasothan U, Kirkpatrick P. Vemurafenib. Nat Rev Drug Discov 2011;10:811-2.

(114) Sosman JA, Kim KB, Schuchter L, Gonzalez R, Pavlick AC, Weber JS, et al. Survival in BRAF V600-mutant advanced melanoma treated with vemurafenib. N Engl J Med 2012;366:707-14.

(115) Flaherty KT, Puzanov I, Kim KB, Ribas A, McArthur GA, Sosman JA, et al. Inhibition of mutated, activated BRAF in metastatic melanoma. N Engl J Med 2010;363:809-19.

(116) McArthur GA, Chapman PB, Robert C, Larkin J, Haanen JB, Dummer R, et al. Safety and efficacy of vemurafenib in BRAF(V600E) and BRAF(V600K) mutation-positive melanoma (BRIM-3): extended follow-up of a phase 3, randomised, open-label study. Lancet Oncol 2014;15:323-32.

(117) Hauschild A, Grob JJ, Demidov LV, Jouary T, Gutzmer R, Millward M, et al. Dabrafenib in BRAF-mutated metastatic melanoma: a multicentre, open-label, phase 3 randomised controlled trial. Lancet 2012;380:358-65.

(118) Solit DB, Garraway LA, Pratilas CA, Sawai A, Getz G, Basso A, et al. BRAF mutation predicts sensitivity to MEK inhibition. Nature 2006;439:358-62.

(119) Flaherty KT, Robert C, Hersey P, Nathan P, Garbe C, Milhem M, et al. Improved survival with MEK inhibition in BRAF-mutated melanoma. N Engl J Med 2012;367:107-14.

(120) Flaherty KT, Infante JR, Daud A, Gonzalez R, Kefford RF, Sosman J, et al. Combined BRAF and MEK inhibition in melanoma with BRAF V600 mutations. N Engl J Med 2012;367:1694-703.

(121) Long GV, Stroyakovskiy D, Gogas H, Levchenko E, De BF, Larkin J, et al. Combined BRAF and MEK inhibition versus BRAF inhibition alone in melanoma. N Engl J Med 2014;371:1877-88.

(122) Robert C, Karaszewska B, Schachter J, Rutkowski P, Mackiewicz A, Stroiakovski D, et al. Improved overall survival in melanoma with combined dabrafenib and trametinib. N Engl J Med 2015;372:30-9.

(123) Eroglu Z, Ribas A. Combination therapy with BRAF and MEK inhibitors for melanoma: latest evidence and place in therapy. Ther Adv Med Oncol 2016;8:48-56.

(124) Strickland LR, Pal HC, Elmets CA, Afaq F. Targeting drivers of melanoma with synthetic small molecules and phytochemicals. Cancer Lett 2015;359:20-35.

(125) Hartsough E, Shao Y, Aplin AE. Resistance to RAF inhibitors revisited. J Invest Dermatol 2014;134:319-25.

(126) Poulikakos PI, Persaud Y, Janakiraman M, Kong X, Ng C, Moriceau G, et al. RAF inhibitor resistance is mediated by dimerization of aberrantly spliced BRAF(V600E). Nature 2011;480:387-90.

(127) Shi H, Moriceau G, Kong X, Lee MK, Lee H, Koya RC, et al. Melanoma whole-exome sequencing identifies (V600E)B-RAF amplification-mediated acquired B-RAF inhibitor resistance. Nat Commun 2012;3:724.

(128) Gopal YN, Deng W, Woodman SE, Komurov K, Ram P, Smith PD, et al. Basal and treatment-induced activation of AKT mediates resistance to cell death by AZD6244 (ARRY-142886) in Braf-mutant human cutaneous melanoma cells. Cancer Res 2010;70:8736-47.

(129) Shao Y, Aplin AE. Akt3-mediated resistance to apoptosis in B-RAF-targeted melanoma cells. Cancer Res 2010;70:6670-81.

(130) Haq R, Yokoyama S, Hawryluk EB, Jonsson GB, Frederick DT, McHenry K, et al. BCL2A1 is a lineage-specific antiapoptotic melanoma oncogene that confers resistance to BRAF inhibition. Proc Natl Acad Sci U S A 2013;110:4321-6.

(131) Jazirehi AR, Nazarian R, Torres-Collado AX, Economou JS. Aberrant apoptotic machinery confers melanoma dual resistance to BRAF(V600E) inhibitor and immune effector cells: immunosensitization by a histone deacetylase inhibitor. Am J Clin Exp Immunol 2014;3:43-56.

(132) Shao Y, Le K, Cheng H, Aplin AE. NF-kappaB Regulation of c-FLIP Promotes TNFalpha-Mediated RAF Inhibitor Resistance in Melanoma. J Invest Dermatol 2015;135:1839-48.

(133) Serasinghe MN, Missert DJ, Asciolla JJ, Podgrabinska S, Wieder SY, Izadmehr S, et al. Anti-apoptotic BCL-2 proteins govern cellular outcome following B-RAF(V600E) inhibition and can be targeted to reduce resistance. Oncogene 2015;34:857-67.

(134) Green DR. Means to an end: apoptosis and other cell death mechanisms. Cold Spring Harbor, N.Y: Cold Spring Harbor Laboratory Press; 2011.

(135) Plotz M, Eberle J. BH3-only proteins: possible proapoptotic triggers for melanoma therapy. Exp Dermatol 2014;23:375-8.

(136) Baig S, Seevasant I, Mohamad J, Mukheem A, Huri HZ, Kamarul T. Potential of apoptotic pathway-targeted cancer therapeutic research: Where do we stand? Cell Death Dis 2016;7:e2058.

(137) Hata AN, Engelman JA, Faber AC. The BCL2 Family: Key Mediators of the Apoptotic Response to Targeted Anticancer Therapeutics. Cancer Discov 2015;5:475-87.

(138) Eberle J, Hossini AM. Expression and function of bcl-2 proteins in melanoma. Curr Genomics 2008;9:409-19.

(139) Letai A, Bassik MC, Walensky LD, Sorcinelli MD, Weiler S, Korsmeyer SJ. Distinct BH3 domains either sensitize or activate mitochondrial apoptosis, serving as prototype cancer therapeutics. Cancer Cell 2002;2:183-92.

(140) Czabotar PE, Lessene G, Strasser A, Adams JM. Control of apoptosis by the BCL-2 protein family: implications for physiology and therapy. Nat Rev Mol Cell Biol 2014;15:49-63.

(141) Chen L, Willis SN, Wei A, Smith BJ, Fletcher JI, Hinds MG, et al. Differential targeting of prosurvival Bcl-2 proteins by their BH3-only ligands allows complementary apoptotic function. Mol Cell 2005;17:393-403.

(142) Boyd JM, Gallo GJ, Elangovan B, Houghton AB, Malstrom S, Avery BJ, et al. Bik, a novel death-inducing protein shares a distinct sequence motif with Bcl-2 family proteins and interacts with viral and cellular survival-promoting proteins. Oncogene 1995;11:1921-8.

(143) Pistritto G, Trisciuoglio D, Ceci C, Garufi A, D'Orazi G. Apoptosis as anticancer mechanism: function and dysfunction of its modulators and targeted therapeutic strategies. Aging (Albany NY) 2016;8:603-19.

(144) Lomonosova E, Chinnadurai G. BH3-only proteins in apoptosis and beyond: an overview. Oncogene 2008;27 Suppl 1:S2-19.

(145) Akgul C, Moulding DA, Edwards SW. Alternative splicing of Bcl-2-related genes: functional consequences and potential therapeutic applications. Cell Mol Life Sci 2004;61:2189-99.

(146) Ewings KE, Wiggins CM, Cook SJ. Bim and the pro-survival Bcl-2 proteins: opposites attract, ERK repels. Cell Cycle 2007;6:2236-40.

(147) Cartlidge RA, Thomas GR, Cagnol S, Jong KA, Molton SA, Finch AJ, et al. Oncogenic BRAF(V600E) inhibits BIM expression to promote melanoma cell survival. Pigment Cell Melanoma Res 2008;21:534-44.

(148) Nikrad M, Johnson T, Puthalalath H, Coultas L, Adams J, Kraft AS. The proteasome inhibitor bortezomib sensitizes cells to killing by death receptor ligand TRAIL via BH3-only proteins Bik and Bim. Mol Cancer Ther 2005;4:443-9.

(149) Shao Y, Aplin AE. BH3-only protein silencing contributes to acquired resistance to PLX4720 in human melanoma. Cell Death Differ 2012;19:2029-39.

(150) Hanahan D, Weinberg RA. Hallmarks of cancer: the next generation. Cell 2011;144:646-74.

(151) Beck D, Niessner H, Smalley KS, Flaherty K, Paraiso KH, Busch C, et al. Vemurafenib potently induces endoplasmic reticulum stress-mediated apoptosis in BRAFV600E melanoma cells. Sci Signal 2013;6:ra7.

(152) Paraiso KH, Xiang Y, Rebecca VW, Abel EV, Chen YA, Munko AC, et al. PTEN loss confers BRAF inhibitor resistance to melanoma cells through the suppression of BIM expression. Cancer Res 2011;71:2750-60.

(153) Rohrbeck L, Gong JN, Lee EF, Kueh AJ, Behren A, Tai L, et al. Hepatocyte growth factor renders BRAF mutant human melanoma cell lines resistant to PLX4032 by downregulating the pro-apoptotic BH3-only proteins PUMA and BIM. Cell Death Differ 2016;23:2054-62.

(154) Wang YF, Jiang CC, Kiejda KA, Gillespie S, Zhang XD, Hersey P. Apoptosis induction in human melanoma cells by inhibition of MEK is caspase-independent and mediated by the Bcl-2 family members PUMA, Bim, and Mcl-1. Clin Cancer Res 2007;13:4934-42.

(155) Sondergaard JN, Nazarian R, Wang Q, Guo D, Hsueh T, Mok S, et al. Differential sensitivity of melanoma cell lines with BRAFV600E mutation to the specific Raf inhibitor PLX4032. J Transl Med 2010;8:39.

(156) Andersen MH, Schrama D, Thor SP, Becker JC. Cytotoxic T cells. J Invest Dermatol 2006;126:32-41.

(157) Liao W, Lin JX, Leonard WJ. IL-2 family cytokines: new insights into the complex roles of IL-2 as a broad regulator of T helper cell differentiation. Curr Opin Immunol 2011;23:598-604.

(158) Ronnblom L, Eloranta ML, Alm GV. Role of natural interferon-alpha producing cells (plasmacytoid dendritic cells) in autoimmunity. Autoimmunity 2003;36:463-72.

(159) Atkins MB, Kunkel L, Sznol M, Rosenberg SA. High-dose recombinant interleukin-2 therapy in patients with metastatic melanoma: long-term survival update. Cancer J Sci Am 2000;6 Suppl 1:S11-S14.

(160) Atkins MB, Lotze MT, Dutcher JP, Fisher RI, Weiss G, Margolin K, et al. High-dose recombinant interleukin 2 therapy for patients with metastatic melanoma: analysis of 270 patients treated between 1985 and 1993. J Clin Oncol 1999;17:2105-16.

(161) Lawson DH. Choices in adjuvant therapy of melanoma. Cancer Control 2005;12:236-41.

(162) Hodi FS, O'Day SJ, McDermott DF, Weber RW, Sosman JA, Haanen JB, et al. Improved survival with ipilimumab in patients with metastatic melanoma. N Engl J Med 2010;363:711-23.

(163) Lipson EJ, Drake CG. Ipilimumab: an anti-CTLA-4 antibody for metastatic melanoma. Clin Cancer Res 2011;17:6958-62.

(164) Philips GK, Atkins M. Therapeutic uses of anti-PD-1 and anti-PD-L1 antibodies. Int Immunol 2015;27:39-46.

(165) Sullivan RJ, Flaherty KT. Immunotherapy: Anti-PD-1 therapies-a new first-line option in advanced melanoma. Nat Rev Clin Oncol 2015;12:625-6.

(166) Topalian SL, Drake CG, Pardoll DM. Immune checkpoint blockade: a common denominator approach to cancer therapy. Cancer Cell 2015;27:450-61.

(167) Ugurel S, Rohmel J, Ascierto PA, Flaherty KT, Grob JJ, Hauschild A, et al. Survival of patients with advanced metastatic melanoma: the impact of novel therapies-update 2017. Eur J Cancer 2017;83:247-57.

(168) Statistisches Bundesamt Germany. https://www.destatis.de/DE/ZahlenFakten/GesellschaftStaat/Gesundheit/Todesursachen/Todesursachen.html. 2017. 7-9-2017.
Ref Type: Online Source

(169) Lemos BD, Storer BE, Iyer JG, Phillips JL, Bichakjian CK, Fang LC, et al. Pathologic nodal evaluation improves prognostic accuracy in Merkel cell carcinoma: analysis of 5823 cases as the basis of the first consensus staging system. J Am Acad Dermatol 2010;63:751-61.

(170) Santamaria-Barria JA, Boland GM, Yeap BY, Nardi V, Dias-Santagata D, Cusack JC, Jr. Merkel cell carcinoma: 30-year experience from a single institution. Ann Surg Oncol 2013;20:1365-73.

(171) Schadendorf D, Lebbe C, Zur HA, Avril MF, Hariharan S, Bharmal M, et al. Merkel cell carcinoma: Epidemiology, prognosis, therapy and unmet medical needs. Eur J Cancer 2017;71:53-69.

(172) Tsao H, Fukunaga-Kalabis M, Herlyn M. Recent Advances in Melanoma and Melanocyte Biology. J Invest Dermatol 2017;137:557-60.

(173) Van Allen EM, Miao D, Schilling B, Shukla SA, Blank C, Zimmer L, et al. Genomic correlates of response to CTLA-4 blockade in metastatic melanoma. Science 2015;350:207-11.

(174) Coulie PG, Van den Eynde BJ, van der Bruggen P, Boon T. Tumour antigens recognized by T lymphocytes: at the core of cancer immunotherapy. Nat Rev Cancer 2014;14:135-46.

(175) McGranahan N, Furness AJ, Rosenthal R, Ramskov S, Lyngaa R, Saini SK, et al. Clonal neoantigens elicit T cell immunoreactivity and sensitivity to immune checkpoint blockade. Science 2016;351:1463-9.

(176) Kim R, Emi M, Tanabe K. Cancer immunoediting from immune surveillance to immune escape. Immunology 2007;121:1-14.

(177) Beatty GL, Gladney WL. Immune escape mechanisms as a guide for cancer immunotherapy. Clin Cancer Res 2015;21:687-92.

(178) Prieto PA, Yang JC, Sherry RM, Hughes MS, Kammula US, White DE, et al. CTLA-4 blockade with ipilimumab: long-term follow-up of 177 patients with metastatic melanoma. Clin Cancer Res 2012;18:2039-47.

(179) Larkin J, Chiarion-Sileni V, Gonzalez R, Grob JJ, Cowey CL, Lao CD, et al. Combined Nivolumab and Ipilimumab or Monotherapy in Untreated Melanoma. N Engl J Med 2015;373:23-34.

(180) Johnston RJ, Yu X, Grogan JL. The checkpoint inhibitor TIGIT limits antitumor and antiviral CD8+ T cell responses. Oncoimmunology 2015;4:e1036214.

(181) Johnston RJ, Comps-Agrar L, Hackney J, Yu X, Huseni M, Yang Y, et al. The immunoreceptor TIGIT regulates antitumor and antiviral CD8(+) T cell effector function. Cancer Cell 2014;26:923-37.

(182) Inozume T, Yaguchi T, Furuta J, Harada K, Kawakami Y, Shimada S. Melanoma Cells Control Antimelanoma CTL Responses via Interaction between TIGIT and CD155 in the Effector Phase. J Invest Dermatol 2016;136:255-63.

(183) Gulati N, Garcet S, Fuentes-Duculan J, Gilleaudeau P, Sullivan-Whalen M, Li X, et al. Molecular Profiling of Immune Activation Associated with Regression of Melanoma Metastases Induced by Diphencyprone. J Invest Dermatol 2016;136:2101-3.

(184) Krammer PH, Arnold R, Lavrik IN. Life and death in peripheral T cells. Nat Rev Immunol 2007;7:532-42.

(185) Li H, Zhu H, Xu CJ, Yuan J. Cleavage of BID by caspase 8 mediates the mitochondrial damage in the Fas pathway of apoptosis. Cell 1998;94:491-501.

(186) Simeone E, Grimaldi AM, Festino L, Giannarelli D, Vanella V, Palla M, et al. Correlation between previous treatment with BRAF inhibitors and clinical response to pembrolizumab in patients with advanced melanoma. Oncoimmunology 2017;6:e1283462.

(187) Trinchieri G. Interleukin-12 and the regulation of innate resistance and adaptive immunity. Nat Rev Immunol 2003;3:133-46.

(188) Lyngaa R, Pedersen NW, Schrama D, Thrue CA, Ibrani D, Met O, et al. T-cell responses to oncogenic merkel cell polyomavirus proteins distinguish patients with merkel cell carcinoma from healthy donors. Clin Cancer Res 2014;20:1768-78.

(189) Iribarren K, Bloy N, Buque A, Cremer I, Eggermont A, Fridman WH, et al. Trial Watch: Immunostimulation with Toll-like receptor agonists in cancer therapy. Oncoimmunology 2016;5:e1088631.

(190) Schneider LP, Schoonderwoerd AJ, Moutaftsi M, Howard RF, Reed SG, de Jong EC, et al. Intradermally administered TLR4 agonist GLA-SE enhances the capacity of human skin DCs to activate T cells and promotes emigration of Langerhans cells. Vaccine 2012;30:4216-24.

(191) Iyer JG, Afanasiev OK, McClurkan C, Paulson K, Nagase K, Jing L, et al. Merkel cell polyomavirus-specific CD8(+) and CD4(+) T-cell responses identified in Merkel cell carcinomas and blood. Clin Cancer Res 2011;17:6671-80.

(192) Gomez B, He L, Tsai YC, Wu TC, Viscidi RP, Hung CF. Creation of a Merkel cell polyomavirus small T antigen-expressing murine tumor model and a DNA vaccine targeting small T antigen. Cell Biosci 2013;3:29.

(193) Zeng Q, Gomez BP, Viscidi RP, Peng S, He L, Ma B, et al. Development of a DNA vaccine targeting Merkel cell polyomavirus. Vaccine 2012;30:1322-9.

(194) Amaral T, Sinnberg T, Meier F, Krepler C, Levesque M, Niessner H, et al. The mitogen-activated protein kinase pathway in melanoma part I - Activation and primary resistance mechanisms to BRAF inhibition. Eur J Cancer 2017;73:85-92.

(195) Amaral T, Sinnberg T, Meier F, Krepler C, Levesque M, Niessner H, et al. MAPK pathway in melanoma part II-secondary and adaptive resistance mechanisms to BRAF inhibition. Eur J Cancer 2017;73:93-101.

(196) Zhang G, Herlyn M. Linking SOX10 to a slow-growth resistance phenotype. Cell Res 2014;24:906-7.

(197) Roesch A, Fukunaga-Kalabis M, Schmidt EC, Zabierowski SE, Brafford PA, Vultur A, et al. A temporarily distinct subpopulation of slow-cycling melanoma cells is required for continuous tumor growth. Cell 2010;141:583-94.

(198) Roesch A, Vultur A, Bogeski I, Wang H, Zimmermann KM, Speicher D, et al. Overcoming intrinsic multidrug resistance in melanoma by blocking the mitochondrial respiratory chain of slow-cycling JARID1B(high) cells. Cancer Cell 2013;23:811-25.

(199) Beaumont KA, Hill DS, Daignault SM, Lui GY, Sharp DM, Gabrielli B, et al. Cell Cycle Phase-Specific Drug Resistance as an Escape Mechanism of Melanoma Cells. J Invest Dermatol 2016;136:1479-89.

(200) Obenauf AC, Zou Y, Ji AL, Vanharanta S, Shu W, Shi H, et al. Therapy-induced tumour secretomes promote resistance and tumour progression. Nature 2015;520:368-72.

(201) Fofaria NM, Frederick DT, Sullivan RJ, Flaherty KT, Srivastava SK. Overexpression of Mcl-1 confers resistance to BRAFV600E inhibitors alone and in combination with MEK1/2 inhibitors in melanoma. Oncotarget 2015;6:40535-56.

(202) Hartman ML, Talar B, Gajos-Michniewicz A, Czyz M. MCL-1, BCL-XL and MITF Are Diversely Employed in Adaptive Response of Melanoma Cells to Changes in Microenvironment. PLoS One 2015;10:e0128796.

(203) Boisvert-Adamo K, Longmate W, Abel EV, Aplin AE. Mcl-1 is required for melanoma cell resistance to anoikis. Mol Cancer Res 2009;7:549-56.

(204) Zhuang L, Lee CS, Scolyer RA, McCarthy SW, Zhang XD, Thompson JF, et al. Mcl-1, Bcl-XL and Stat3 expression are associated with progression of melanoma whereas Bcl-2, AP-2 and MITF levels decrease during progression of melanoma. Mod Pathol 2007;20:416-26.

(205) Espindola MB, Corleta OC. Bcl-2 expression is not associated with survival in metastatic cutaneous melanoma: a historical cohort study. World J Surg Oncol 2008;6:65.

(206) Trisciuoglio D, Desideri M, Ciuffreda L, Mottolese M, Ribatti D, Vacca A, et al. Bcl-2 overexpression in melanoma cells increases tumor progression-associated properties and in vivo tumor growth. J Cell Physiol 2005;205:414-21.

(207) Benimetskaya L, Ayyanar K, Kornblum N, Castanotto D, Rossi J, Wu S, et al. Bcl-2 protein in 518A2 melanoma cells in vivo and in vitro. Clin Cancer Res 2006;12:4940-8.

(208) Mukherjee N, Lu Y, Almeida A, Lambert K, Shiau CW, Su JC, et al. Use of a MCL-1 inhibitor alone to de-bulk melanoma and in combination to kill melanoma initiating cells. Oncotarget 2016.

(209) Nemati F, de MC, Lang G, Kraus-Berthier L, Carita G, Sastre-Garau X, et al. Targeting Bcl-2/Bcl-XL induces antitumor activity in uveal melanoma patient-derived xenografts. PLoS One 2014;9:e80836.

(210) Liu Y, Xie M, Song T, Sheng H, Yu X, Zhang Z. A novel BH3 mimetic efficiently induces apoptosis in melanoma cells through direct binding to anti-apoptotic Bcl-2 family proteins, including phosphorylated Mcl-1. Pigment Cell Melanoma Res 2015;28:161-70.

(211) Jang GH, Lee M. BH3-mimetic gossypol-induced autophagic cell death in mutant BRAF melanoma cells with high expression of p21Cip(1).). Life Sci 2014;102:41-8.

(212) Mukherjee N, Schwan JV, Fujita M, Norris DA, Shellman YG. Alternative Treatments For Melanoma: Targeting BCL-2 Family Members to De-Bulk and Kill Cancer Stem Cells. J Invest Dermatol 2015;135:2155-61.

(213) Nikrad M, Johnson T, Puthalalath H, Coultas L, Adams J, Kraft AS. The proteasome inhibitor bortezomib sensitizes cells to killing by death receptor ligand TRAIL via BH3-only proteins Bik and Bim. Mol Cancer Ther 2005;4:443-9.

(214) Zhu H, Zhang L, Dong F, Guo W, Wu S, Teraishi F, et al. Bik/NBK accumulation correlates with apoptosis-induction by bortezomib (PS-341, Velcade) and other proteasome inhibitors. Oncogene 2005;24:4993-9.

(215) Fernandez Y, Verhaegen M, Miller TP, Rush JL, Steiner P, Opipari AW, Jr., et al. Differential regulation of noxa in normal melanocytes and melanoma cells by proteasome inhibition: therapeutic implications. Cancer Res 2005;65:6294-304.

(216) Lane AA, Chabner BA. Histone deacetylase inhibitors in cancer therapy. J Clin Oncol 2009;27:5459-68.

(217) Ververis K, Hiong A, Karagiannis TC, Licciardi PV. Histone deacetylase inhibitors (HDACIs): multitargeted anticancer agents. Biologics 2013;7:47-60.

(218) Harada T, Hideshima T, Anderson KC. Histone deacetylase inhibitors in multiple myeloma: from bench to bedside. Int J Hematol 2016.

(219) Haas NB, Quirt I, Hotte S, McWhirter E, Polintan R, Litwin S, et al. Phase II trial of vorinostat in advanced melanoma. Invest New Drugs 2014;32:526-34.

(220) Hauschild A, Trefzer U, Garbe C, Kaehler KC, Ugurel S, Kiecker F, et al. Multicenter phase II trial of the histone deacetylase inhibitor pyridylmethyl-N-{4-[(2-aminophenyl)-carbamoyl]-benzyl}-carbamate in pretreated metastatic melanoma. Melanoma Res 2008;18:274-8.

(221) Hornig E, Heppt MV, Graf SA, Ruzicka T, Berking C. Inhibition of histone deacetylases in melanoma-a perspective from bench to bedside. Exp Dermatol 2016;25:831-8.

(222) Lai F, Guo ST, Jin L, Jiang CC, Wang CY, Croft A, et al. Cotargeting histone deacetylases and oncogenic BRAF synergistically kills human melanoma cells by necrosis independently of RIPK1 and RIPK3. Cell Death Dis 2013;4:e655.

(223) Thomas S, Quinn BA, Das SK, Dash R, Emdad L, Dasgupta S, et al. Targeting the Bcl-2 family for cancer therapy. Expert Opin Ther Targets 2013;17:61-75.

(224) Gandhi L, Camidge DR, Ribeiro de OM, Bonomi P, Gandara D, Khaira D, et al. Phase I study of Navitoclax (ABT-263), a novel Bcl-2 family inhibitor, in patients with small-cell lung cancer and other solid tumors. J Clin Oncol 2011;29:909-16.

(225) Roberts AW, Seymour JF, Brown JR, Wierda WG, Kipps TJ, Khaw SL, et al. Substantial susceptibility of chronic lymphocytic leukemia to BCL2 inhibition: results of a phase I study of navitoclax in patients with relapsed or refractory disease. J Clin Oncol 2012;30:488-96.

(226) Wilson WH, O'Connor OA, Czuczman MS, LaCasce AS, Gerecitano JF, Leonard JP, et al. Navitoclax, a targeted high-affinity inhibitor of BCL-2, in lymphoid malignancies: a phase 1 dose-escalation study of safety, pharmacokinetics, pharmacodynamics, and antitumour activity. Lancet Oncol 2010;11:1149-59.

(227) Crombie J, Davids MS. Venetoclax for the treatment of patients with chronic lymphocytic leukemia. Future Oncol 2017.

(228) King AC, Peterson TJ, Horvat TZ, Rodriguez M, Tang LA. Venetoclax: A First-in-Class Oral BCL-2 Inhibitor for the Management of Lymphoid Malignancies. Ann Pharmacother 2017;51:410-6.

(229) Lucas KM, Mohana-Kumaran N, Lau D, Zhang XD, Hersey P, Huang DC, et al. Modulation of NOXA and MCL-1 as a strategy for sensitizing melanoma cells to the BH3-mimetic ABT-737. Clin Cancer Res 2012;18:783-95.

(230) Miller LA, Goldstein NB, Johannes WU, Walton CH, Fujita M, Norris DA, et al. BH3 mimetic ABT-737 and a proteasome inhibitor synergistically kill melanomas through Noxa-dependent apoptosis. J Invest Dermatol 2009;129:964-71.

(231) Keuling AM, Felton KE, Parker AA, Akbari M, Andrew SE, Tron VA. RNA silencing of Mcl-1 enhances ABT-737-mediated apoptosis in melanoma: role for a caspase-8-dependent pathway. PLoS One 2009;4:e6651.

(232) Chen S, Dai Y, Harada H, Dent P, Grant S. Mcl-1 down-regulation potentiates ABT-737 lethality by cooperatively inducing Bak activation and Bax translocation. Cancer Res 2007;67:782-91.

(233) Wroblewski D, Mijatov B, Mohana-Kumaran N, Lai F, Gallagher SJ, Haass NK, et al. The BH3-mimetic ABT-737 sensitizes human melanoma cells to apoptosis induced by selective BRAF inhibitors but does not reverse acquired resistance. Carcinogenesis 2013;34:237-47.

(234) van Delft MF, Wei AH, Mason KD, Vandenberg CJ, Chen L, Czabotar PE, et al. The BH3 mimetic ABT-737 targets selective Bcl-2 proteins and efficiently induces apoptosis via Bak/Bax if Mcl-1 is neutralized. Cancer Cell 2006;10:389-99.

(235) Belmar J, Fesik SW. Small molecule Mcl-1 inhibitors for the treatment of cancer. Pharmacol Ther 2015;145:76-84.

(236) Quinn BA, Dash R, Azab B, Sarkar S, Das SK, Kumar S, et al. Targeting Mcl-1 for the therapy of cancer. Expert Opin Investig Drugs 2011;20:1397-411.

(237) Sun JG, Li H, Li X, Zeng X, Wu P, Fung KP, et al. Clitocine targets Mcl-1 to induce drug-resistant human cancer cell apoptosis in vitro and tumor growth inhibition in vivo. Apoptosis 2014;19:871-82.

(238) Wei G, Margolin AA, Haery L, Brown E, Cucolo L, Julian B, et al. Chemical genomics identifies small-molecule MCL1 repressors and BCL-xL as a predictor of MCL1 dependency. Cancer Cell 2012;21:547-62.

(239) Abulwerdi F, Liao C, Liu M, Azmi AS, Aboukameel A, Mady AS, et al. A novel small-molecule inhibitor of mcl-1 blocks pancreatic cancer growth in vitro and in vivo. Mol Cancer Ther 2014;13:565-75.

(240) Brunner M, Thurnher D, Pammer J, Geleff S, Heiduschka G, Reinisch CM, et al. Expression of VEGF-A/C, VEGF-R2, PDGF-alpha/beta, c-kit, EGFR, Her-2/Neu, Mcl-1 and Bmi-1 in Merkel cell carcinoma. Mod Pathol 2008;21:876-84.

(241) Hafner C, Houben R, Baeurle A, Ritter C, Schrama D, Landthaler M, et al. Activation of the PI3K/AKT pathway in Merkel cell carcinoma. PLoS One 2012;7:e31255.

(242) Nardi V, Song Y, Santamaria-Barria JA, Cosper AK, Lam Q, Faber AC, et al. Activation of PI3K signaling in Merkel cell carcinoma. Clin Cancer Res 2012;18:1227-36.

(243) Su LD, Fullen DR, Lowe L, Uherova P, Schnitzer B, Valdez R. CD117 (KIT receptor) expression in Merkel cell carcinoma. Am J Dermatopathol 2002;24:289-93.

(244) Loader DE, Feldmann R, Baumgartner M, Breier F, Schrama D, Becker JC, et al. Clinical remission of Merkel cell carcinoma after treatment with imatinib. J Am Acad Dermatol 2013;69:e181-e183.

(245) Samlowski WE, Moon J, Tuthill RJ, Heinrich MC, Balzer-Haas NS, Merl SA, et al. A phase II trial of imatinib mesylate in merkel cell carcinoma (neuroendocrine carcinoma of the skin): A Southwest Oncology Group study (S0331). Am J Clin Oncol 2010;33:495-9.

(246) Shiver MB, Mahmoud F, Gao L. Response to Idelalisib in a Patient with Stage IV Merkel-Cell Carcinoma. N Engl J Med 2015;373:1580-2.

(247) Kannan A, Lin Z, Shao Q, Zhao S, Fang B, Moreno MA, et al. Dual mTOR inhibitor MLN0128 suppresses Merkel cell carcinoma (MCC) xenograft tumor growth. Oncotarget 2016;7:6576-92.

(248) Lin Z, McDermott A, Shao L, Kannan A, Morgan M, Stack BC, Jr., et al. Chronic mTOR activation promotes cell survival in Merkel cell carcinoma. Cancer Lett 2014;344:272-81.

(249) Guo XE, Ngo B, Modrek AS, Lee WH. Targeting tumor suppressor networks for cancer therapeutics. Curr Drug Targets 2014;15:2-16.

(250) Quartin RS, Cole CN, Pipas JM, Levine AJ. The amino-terminal functions of the simian virus 40 large T antigen are required to overcome wild-type p53-mediated growth arrest of cells. J Virol 1994;68:1334-41.

(251) Rushton JJ, Jiang D, Srinivasan A, Pipas JM, Robbins PD. Simian virus 40 T antigen can regulate p53-mediated transcription independent of binding p53. J Virol 1997;71:5620-3.

(252) Andreeff M, Kelly KR, Yee K, Assouline S, Strair R, Popplewell L, et al. Results of the Phase I Trial of RG7112, a Small-Molecule MDM2 Antagonist in Leukemia. Clin Cancer Res 2016;22:868-76.

(253) Ray-Coquard I, Blay JY, Italiano A, Le CA, Penel N, Zhi J, et al. Effect of the MDM2 antagonist RG7112 on the P53 pathway in patients with MDM2-amplified, well-differentiated or dedifferentiated liposarcoma: an exploratory proof-of-mechanism study. Lancet Oncol 2012;13:1133-40.

(254) Liu S, Chen P, Hu M, Tao Y, Chen L, Liu H, et al. Randomized, controlled phase II study of post-surgery radiotherapy combined with recombinant adenoviral human p53 gene therapy in treatment of oral cancer. Cancer Gene Ther 2013;20:375-8.

(255) Shen A, Liu S, Yu W, Deng H, Li Q. p53 gene therapy-based transarterial chemoembolization for unresectable hepatocellular carcinoma: A prospective cohort study. J Gastroenterol Hepatol 2015;30:1651-6.

(256) Bollard J, Miguela V, Ruiz de GM, Venkatesh A, Bian CB, Roberto MP, et al. Palbociclib (PD-0332991), a selective CDK4/6 inhibitor, restricts tumour growth in preclinical models of hepatocellular carcinoma. Gut 2017;66:1286-96.

(257) Flaherty KT, Lorusso PM, Demichele A, Abramson VG, Courtney R, Randolph SS, et al. Phase I, dose-escalation trial of the oral cyclin-dependent kinase 4/6 inhibitor PD 0332991, administered using a 21-day schedule in patients with advanced cancer. Clin Cancer Res 2012;18:568-76.

(258) Fry DW, Harvey PJ, Keller PR, Elliott WL, Meade M, Trachet E, et al. Specific inhibition of cyclin-dependent kinase 4/6 by PD 0332991 and associated antitumor activity in human tumor xenografts. Mol Cancer Ther 2004;3:1427-38.

(259) Knudsen ES, Wang JY. Targeting the RB-pathway in cancer therapy. Clin Cancer Res 2010;16:1094-9.

(260) Hermel DJ, Ott PA. Combining forces: the promise and peril of synergistic immune checkpoint blockade and targeted therapy in metastatic melanoma. Cancer Metastasis Rev 2017;36:43-50.

(261) Kim T, Amaria RN, Spencer C, Reuben A, Cooper ZA, Wargo JA. Combining targeted therapy and immune checkpoint inhibitors in the treatment of metastatic melanoma. Cancer Biol Med 2014;11:237-46.

(262) Knight DA, Ngiow SF, Li M, Parmenter T, Mok S, Cass A, et al. Host immunity contributes to the anti-melanoma activity of BRAF inhibitors. J Clin Invest 2013;123:1371-81.

(263) Cooper ZA, Juneja VR, Sage PT, Frederick DT, Piris A, Mitra D, et al. Response to BRAF inhibition in melanoma is enhanced when combined with immune checkpoint blockade. Cancer Immunol Res 2014;2:643-54.

(264) Vella LJ, Pasam A, Dimopoulos N, Andrews M, Knights A, Puaux AL, et al. MEK inhibition, alone or in combination with BRAF inhibition, affects multiple functions of isolated normal human lymphocytes and dendritic cells. Cancer Immunol Res 2014;2:351-60.

(265) Sumimoto H, Imabayashi F, Iwata T, Kawakami Y. The BRAF-MAPK signaling pathway is essential for cancer-immune evasion in human melanoma cells. J Exp Med 2006;203:1651-6.

(266) Frederick DT, Piris A, Cogdill AP, Cooper ZA, Lezcano C, Ferrone CR, et al. BRAF inhibition is associated with enhanced melanoma antigen expression and a more favorable tumor microenvironment in patients with metastatic melanoma. Clin Cancer Res 2013;19:1225-31.

(267) Cooper ZA, Frederick DT, Juneja VR, Sullivan RJ, Lawrence DP, Piris A, et al. BRAF inhibition is associated with increased clonality in tumor-infiltrating lymphocytes. Oncoimmunology 2013;2:e26615.

(268) Wilmott JS, Long GV, Howle JR, Haydu LE, Sharma RN, Thompson JF, et al. Selective BRAF inhibitors induce marked T-cell infiltration into human metastatic melanoma. Clin Cancer Res 2012;18:1386-94.

(269) Khalili JS, Liu S, Rodriguez-Cruz TG, Whittington M, Wardell S, Liu C, et al. Oncogenic BRAF(V600E) promotes stromal cell-mediated immunosuppression via induction of interleukin-1 in melanoma. Clin Cancer Res 2012;18:5329-40.

(270) Schilling B, Sucker A, Griewank K, Zhao F, Weide B, Gorgens A, et al. Vemurafenib reverses immunosuppression by myeloid derived suppressor cells. Int J Cancer 2013;133:1653-63.

(271) Ribas A, Hodi FS, Callahan M, Konto C, Wolchok J. Hepatotoxicity with combination of vemurafenib and ipilimumab. N Engl J Med 2013;368:1365-6.

(272) Minor DR, Puzanov I, Callahan MK, Hug BA, Hoos A. Severe gastrointestinal toxicity with administration of trametinib in combination with dabrafenib and ipilimumab. Pigment Cell Melanoma Res 2015;28:611-2.

ORIGINAL ARTICLE

Vemurafenib Induces Senescence Features in Melanoma Cells

Sebastian Haferkamp[1,4], Andreas Borst[1,4], Christian Adam[1], Therese M. Becker[2], Stephanie Motschenbacher[1], Simone Windhövel[1], Anita L. Hufnagel[3], Roland Houben[1,5] and Svenja Meierjohann[3,5]

A large proportion of human melanomas harbor a mutation leading to permanent activation of the serine/threonine kinase BRAF, and as a consequence, they have developed dependence on BRAF/mitogen-activated protein kinase signaling. Accordingly, BRAF inhibitors such as Vemurafenib show a good anti-tumorigenic effect on metastases with the $BRAF^{V600E}$ mutation. Although an initial period of sustained tumor regression is usually observed after Vemurafenib treatment, tumors often relapse at the same site, and apoptosis induction of melanoma cells *in vitro* is incomplete. Here, we demonstrate, using a large panel of melanoma cell lines, that Vemurafenib induces features of stress-induced senescence in addition to apoptosis. This senescence phenotype is characterized by heterochromatin formation, changes in cell shape, and increased senescence-associated β-galactosidase activity. Importantly, senescence features induced by $BRAF^{V600E}$ inhibition was also detected in human melanoma cells xenografted into nude mice. Our observations provide a possible explanation for the lack of complete and durable pro-apoptotic effect of Vemurafenib in patients.

Journal of Investigative Dermatology advance online publication, 14 February 2013; doi:10.1038/jid.2013.6

INTRODUCTION

Patients with metastatic melanoma have a poor prognosis and only limited therapeutic options are available (Miller and Mihm, Jr, 2006; Garbe *et al.*, 2011). However, the identification of oncogenic *BRAF* in the majority of melanomas and the demonstration that *BRAF* mutant melanoma cells are largely dependent on BRAF/mitogen-activated protein kinase (MAPK) signaling have been important findings with high pharmacological impact (Puzanov and Flaherty, 2010). More than 80% of these *BRAF* mutations lead to a valine to glutamate exchange at position 600, rendering the protein permanently active by releasing an intra-molecular inhibitory interaction (Davies *et al.*, 2002). Therefore, specific $BRAF^{V600E}$ inhibitors such as Vemurafenib (PLX4032) are beneficial to a large proportion of melanoma patients (Puzanov and Flaherty, 2010). The overall response rate of patients with $BRAF^{V600E}$-positive melanomas to Vemurafenib is roughly 50% and responsive patients display significant tumor regression and prolonged survival (Chapman *et al.*, 2011). Although the strategy of inhibiting mutant BRAF is the most successful melanoma treatment option so far, in most cases, the initial phase of tumor regression is followed by Vemurafenib resistance, disease relapse, and death of the patients (Aplin *et al.*, 2011; Chapman *et al.*, 2011). Consequently, the elucidation of resistance mechanisms is a highly investigated area and has revealed the involvement of CRAF, AKT, receptor tyrosine kinases, and *BRAF* amplifications or splice variants in BRAF inhibitor resistance (Fedorenko *et al.*, 2011). To better understand and improve BRAF inhibitor therapy, it is also crucial to evaluate the phenotypic cellular responses and thereby the extent of apoptosis versus cell cycle arrest initiated by Vemurafenib.

BRAF signaling can have different effects on cells of melanocyte origin. On the one hand, BRAF activation in primary melanocytes *in vitro* induces an irreversible growth arrest termed senescence, which is regarded as a major tumor suppressor mechanism (Michaloglou *et al.*, 2005). Senescence is triggered by a variety of cellular stresses, such as telomere attrition, UV exposure, reactive oxygen stress or—as in case of $BRAF^{V600E}$ expression—oncogene activation (oncogene-induced senescence; Ogrunc and d'Adda di Fagagna, 2011). In contrast to quiescent cells, senescent cells can be arrested in G0/G1 or G2/M and develop a characteristic flat and/or multinuclear phenotype. Benign melanocytic nevi, which frequently harbor oncogenic *BRAF* mutations, remain stably growth arrested for decades and display markers of oncogene-induced senescence, such as an increased activity of the acidic β-galactosidase and induction of the tumor suppressor

[1]*Department of Dermatology, Venereology and Allergology, University Hospital Würzburg, Würzburg, Germany;* [2]*Westmead Institute for Cancer Research, The University of Sydney at Westmead Millennium Institute, Westmead Hospital, Westmead, Australia and* [3]*Department of Physiological Chemistry I, Biocenter, University of Würzburg, Würzburg, Germany*

[4]*The first two authors contributed equally to this work.*

[5]*The last two authors contributed equally to this work.*

Correspondence: Roland Houben, Department of Dermatology, Venereology and Allergology, University Hospital Würzburg, Josef-Schneider-Street 2, Wurzburg 97080, Germany. E-mail: Houben_R@klinik.uni-wuerzburg.de or Svenja Meierjohann, Department of Physiological Chemistry I, University of Wurzburg, Biocenter, Am Hubland, 97074 Wurzburg, Germany. E-mail: svenja.meierjohann@biozentrum.uni-wuerzburg.de

Abbreviations: ERK, extracellular signal–regulated kinase; MAPK, mitogen-activated protein kinase; SA-β-Gal, senescence-associated β-galactosidase; Vem, Vemurafenib

Received 16 December 2011; revised 31 August 2012; accepted 29 October 2012; accepted article preview online 15 January 2013

p16 (Michaloglou *et al.*, 2005). Therefore, it has been suggested that benign nevi are an *in vivo* example of oncogene-induced senescence, and overcoming senescence is regarded as a key step in the progression to melanoma. However, the presence of senescent nevus cells remains controversial (Cotter *et al.*, 2007; Gray-Schopfer *et al.*, 2008; Michaloglou *et al.*, 2008; Tran *et al.*, 2012).

On the other hand, in *BRAF*-mutant melanoma, BRAF is essential for tumor survival and proliferation. BRAF signaling is involved in preventing apoptosis—e.g., by shifting the balance between pro- and anti-apoptotic proteins in the direction of the latter—and in cell cycle progression—e.g., by inducing the transcription of cyclin D and by suppressing cell cycle-inhibitory proteins, which are also relevant for mediating senescence (Balmanno and Cook, 2009). Vemurafenib treatment of melanoma cell lines was associated with a pro-apoptotic response (Lee *et al.*, 2010; Sondergaard *et al.*, 2010; Tap *et al.*, 2010), the preferred outcome of tumor therapy. However, in other tumor types, the inhibition of the driver oncogene also promoted senescence. For instance, non-small-cell lung cancer cells treated with EGFR or MAPK/extracellular signal–regulated (ERK) kinase inhibitors (Hotta *et al.*, 2007; Wang *et al.*, 2011) and colorectal cancer cells treated with vascular endothelial growth factor receptor 2 inhibitors underwent cellular senescence (Hasan *et al.*, 2011).

Here, we investigated the effect of Vemurafenib on apoptosis and senescence in a series of human melanoma cell lines.

RESULTS

To determine the response of melanoma cells to BRAF inhibition, we used a panel of 14 melanoma cell lines: 10 carried the $BRAF^{V600E}$ mutation, 1 harbored the $BRAF^{V600K}$ mutation, and 3 expressed wild-type BRAF. Seven of the $BRAF^{V600E}$ mutant cell lines are well-characterized lines from the NCI-60 panel (http://discover.nci.nih.gov/cellminer/mutationGeneLoad.do). The cells were treated with 0.5 μM Vemurafenib, a concentration previously demonstrated to effectively inhibit ERK1/2 signaling in $BRAF^{V600E}$-mutant cells (Joseph *et al.*, 2010), and cell cycle distribution was analyzed by flow cytometry. After 2 days of treatment, the M14 cell line responded by undergoing cell death in 15% of the cell population, but the proportion of dead cells decreased after prolonged Vemurafenib exposure (Figure 1a). In the *BRAF*-mutant Malme 3M cell line, cell death was induced in a delayed manner and did not start before 4 days of Vemurafenib exposure (Supplementary Figure S1a online). However, in M14 and Malme 3M cells, an increased proportion of the surviving cells was found in G0/G1 after 7 days of Vemurafenib treatment (Figure 1a and Supplementary Figure S1a online). Most cell lines showed a clear increase in the proportion of G0/G1 cells in response to Vemurafenib, but no evidence of cell death (Supplementary Figure 1b online). As a control, we included the melanoma cell line WMM1175, which expresses inducible p16 and can be triggered into senescence by addition of isopropyl-β-D-thiogalactopyranoside (Haferkamp *et al.*, 2008). Again, p16 expression caused accumulation of cells in G0/G1 (Supplementary Figure S1b online). Unexpectedly, the two *BRAF*-mutant melanoma cell lines LOX IMVI and RPMI 7951 showed no alteration of cell cycle phases in response to Vemurafenib. We also examined the proliferation behavior of several melanoma cell lines by performing carboxyfluorescein diacetate retention analyses. Here, cells are labeled with carboxyfluorescein diacetate, which is diluted out of proliferating cells over time but largely retained in non-proliferating cells. Figure 1c shows that the degree of label retention of the melanoma cell lines in response to Vemurafenib is comparable with the label retention in WMM1175 cells after 5 days of isopropyl-β-D-thiogalactopyranoside-induced p16 expression, which drives the cells into the senescence program.

As expected, all *BRAF*-mutant melanoma cell lines that responded to Vemurafenib showed diminished MAPK activity, as detected by reduced P-ERK1/2 levels (Figure 2). In addition, they also displayed diminished the accumulation of P-Rb, a marker of cell cycle arrest (Figure 2). LOX IMVI cells, which showed no reduction of P-ERK1/2 in response to Vemurafenib, displayed no reduction of P-Rb. In RPMI 7951 cells, reduction of P-ERK1/2 as well as P-Rb was noted in response to Vemurafenib, despite a lacking effect on the cell cycle.

To investigate the long-term effects of Vemurafenib, we treated the cell lines with the drug for 7 days. In many of the cell lines that previously showed an increase in G0/G1, namely M19-Mel, SK-MEL-28, UACC-62, UACC-257, and FM88, we observed a characteristic change in cell shape to an enlarged and flattened phenotype, which is reminiscent of senescence (Supplementary Figure S2 online). Some of the enlarged cells were binucleated or multinucleated (Figure 3a, b). This phenotype was never observed in the cell lines expressing wild-type *BRAF*, but only in cell lines carrying mutated *BRAF*. All cells displaying an enlarged phenotype showed increased senescence-associated β-galactosidase (SA-β-Gal) activity, supporting the notion that Vemurafenib can induce senescence features in BRAF-dependent melanoma cell lines (Figure 3c). In addition, cell lines without obvious cell shape alterations such as M14, Malme 3M, and Mel2a also showed increased SA-β-Gal staining (Figure 3d). The accumulation of nuclear heterochromatin and promyelocytic leukemia (PML)-positive nuclear bodies often accompanies senescence (Narita *et al.*, 2003; Courtois-Cox *et al.*, 2008), and trimethylated H3K9 (H3K9me3) as well as PML are well-established markers for these structures (Krauss, 2008; Vernier *et al.*, 2011). We first analyzed the protein amount of PML and H3K9me3 in untreated and Vemurafenib-treated melanoma cells (Figure 4a). An increase of either one of these markers or both of them was observed in those cell lines that showed SA-β-Gal staining in more than 10% of the cell population in response to Vemurafenib (compare Figures 3d and 4a). We also performed immunofluorescence staining of PML in nine of the *BRAF* mutant cell lines and found that the results concurred with our western blot data (Figure 4b and Supplementary Figure S3 online). All these data gained from *in vitro* analyses of the melanoma cell lines are summarized in Supplementary Table S1 online.

The tumor suppressor protein p16 is an important regulator of senescence in response to different cellular stress signals.

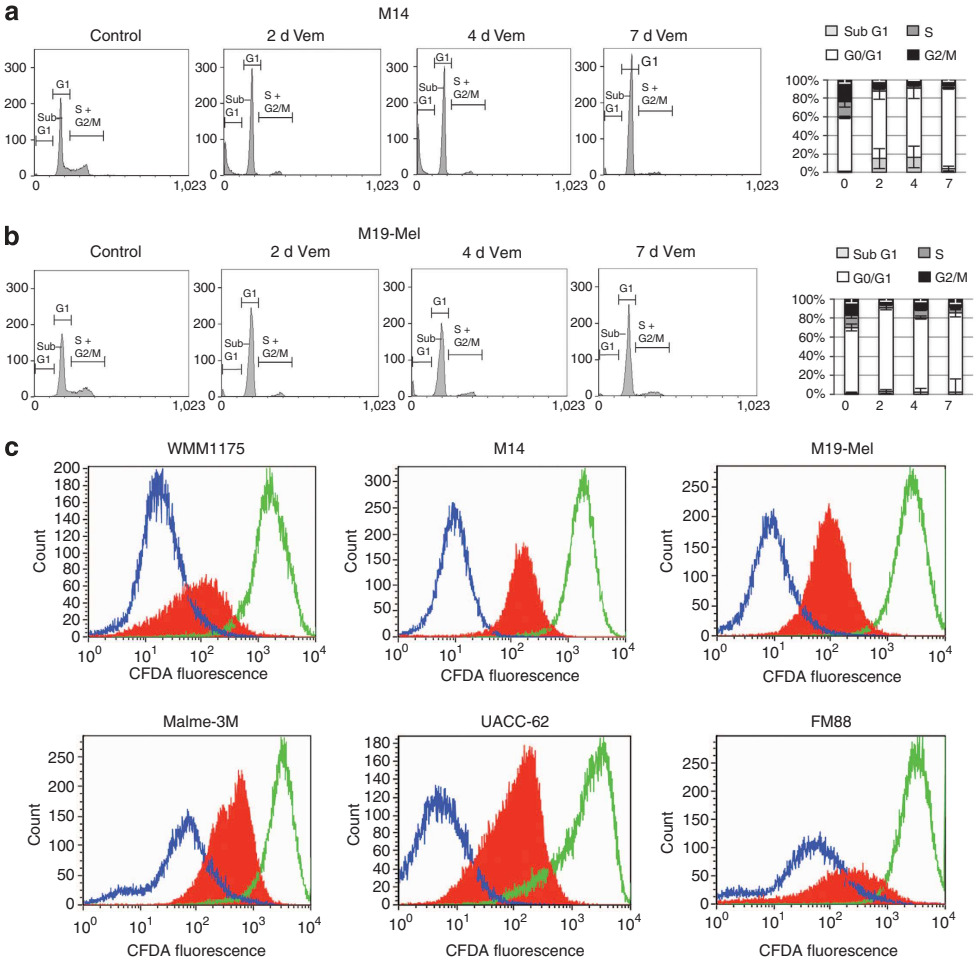

Figure 1. Apoptosis and G1 accumulation in response to BRAF^{V600E} inhibition. (**a**) Left: Cell cycle profile of M14 cells treated with the solvent DMSO or with 0.5 μM Vemurafenib (Vem) for 2, 4, and 7 days (d). Medium and inhibitor were changed every second day. Right: Bar graph representation, including standard deviations, of the cell cycle profiles of M14 cells after indicated times of Vem treatment. (**b**) Left: Cell cycle profile of M19-Mel cells under the same conditions as described in **a**. Right: Bar graph representation, including standard deviations, of the M19-Mel cell cycle profile after indicated times of Vem treatment. FACS analyses were repeated twice, and the presented profiles are representative. Data are mean values from three independent experiments. (**c**) Flow cytometry analysis of carboxyfluorescein diacetate (CFDA)-labeled cells. The histogram plot on day 0 is displayed in green. The blue and red lines represent the histogram plots of the CFDA fluorescence, following 6 days in the absence and presence of 0.5 μM Vem or 4 mM isopropyl-β-D-thiogalactopyranoside (WMM1175), respectively.

However, p16 is frequently inactivated in melanoma, and germline p16 mutations predispose to this cancer type (Castellano *et al.*, 1997; Sharpless and Chin, 2003). In line with these data, p16 expression was only detectable in two cell lines (SK-MEL-28 and Mel2a). Unexpectedly, it was even downregulated in the presence of Vemurafenib, suggesting that the observed decreased Rb phosphorylation is not mediated by p16 (Supplementary Figure S4 online).

To establish whether growth inhibition of Vemurafenib-treated cells was irreversible, as characteristic for senescent as opposed to quiescent cells, we investigated the colony formation capacity of those cells that display Vemurafenib-dependent senescence features and included control cells, which do not display senescence features (MDA-MB-435, RPMI 7951, Mel Juso). Following 5 days of Vemurafenib treatment, cells were washed to remove media with drug, and equal numbers of control- or Vemurafenib-treated cells were seeded at low density and cultivated for 8 and 9 days in the absence of the inhibitor. Colony formation was then monitored by crystal violet staining. Except M19-Mel and Mel2a, all cell lines that display Vemurafenib-dependent senescence features showed reduced capacity to form colonies, reaching significance in case of Malme 3M, SK-MEL-28, UACC-62, and FM88 (Figure 5a, b). In particular, the colony-forming capacity of SK-MEL-28 cells was reduced by >80% (Figure 5a, b). Here, the colonies formed by Vemurafenib pretreated SK-MEL-28 cells were much smaller than their counterparts from the control population. In addition, many enlarged single cells, having obviously not undergone cell division after removal of Vemurafenib, were detectable (Figure 5a). The colony-forming capacity of the control cells RPMI 7951 and Mel Juso were not affected by Vemurafenib pretreatment (Figure 5b). Curiously, in M19 Mel and MD-MBA 435 cells, Vemurafenib pretreatment even led to enhanced colony formation, although this did not reach statistical significance (Figure 5b).

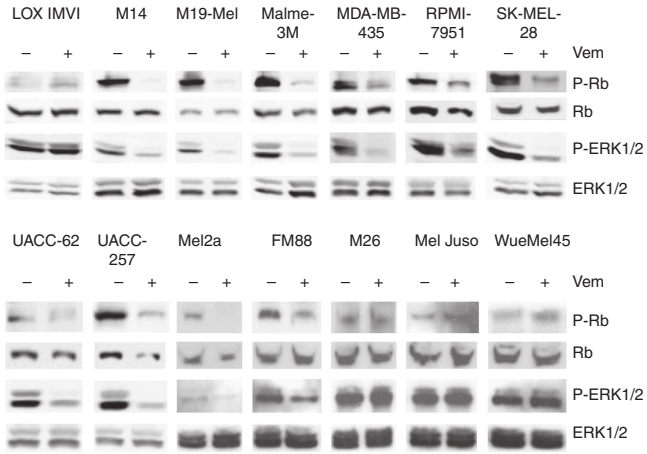

Figure 2. ERK1/2 inhibition and Rb dephosphorylation by Vemurafenib (Vem). Western blot analysis of the indicated melanoma cell lines after 48 h of treatment with the solvent DMSO (—) or 0.5 μM Vem. Cell lysates were analyzed for the expression of phospho-Rb (Ser 780), total Rb, phospho-ERK1/2 (Thr 202/Tyr 204), and total ERK1/2.

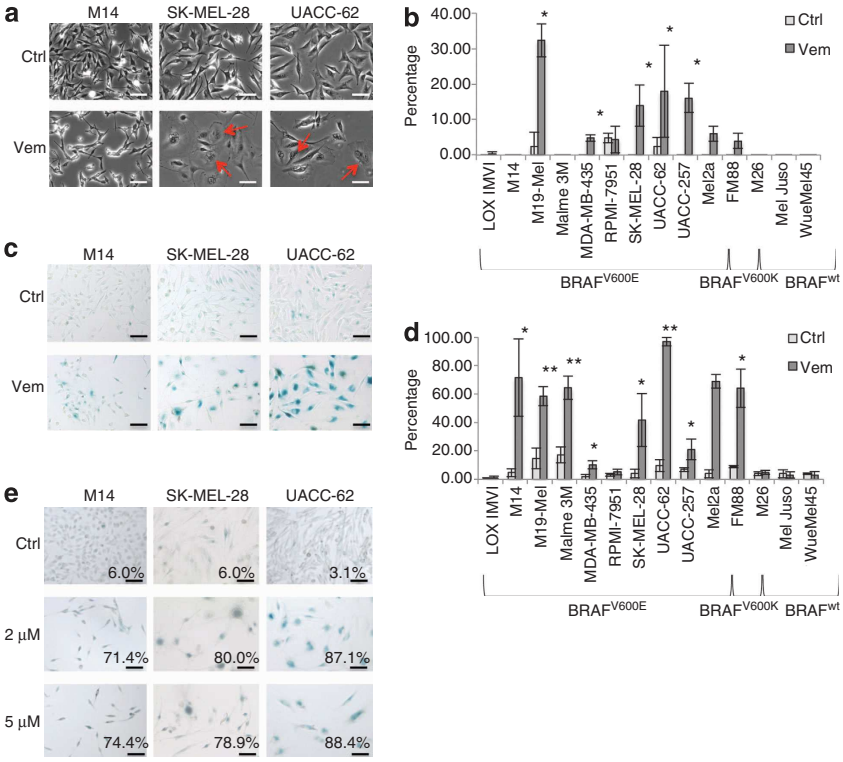

Figure 3. Appearance of senescent cells in response to BRAF^{V600E} inhibition. (**a**) Phase contrast images of indicated cell lines after 7 days of control (Ctrl; DMSO) or Vemurafenib (Vem) treatment (0.5 μM). Red arrows indicate binucleated or multinucleated cells, bars = 20 μm. (**b**) Quantification of binucleated and multinuclead cells after Vem treatment in percent. (**c**) Senescence-associated β-galactosidase (SA-β-Gal) staining of indicated cell lines after 7 days of control (DMSO) or Vem treatment (0.5 μM), bars = 20 μm. (**d**) Quantification of SA-β-Gal-positive cells after Vem treatment in percent. (**e**) SA-β-Gal staining of M14, SK-MEL-28, and UACC-62 cells after 7 days of control (DMSO) or Vem treatment with indicated concentrations. The percentage of SA-β-Gal-positive cells in each cell population is indicated, bar = 20 μm. Data shown are derived from three independent experiments. Standard deviations are indicated. *$P<0.05$, **$P<0.001$ (Student's *t*-test, two-tailed, paired).

To confirm these data in an independent assay, we performed SA-β-Gal staining of those cell lines that displayed significantly reduced colony formation in Figure 5b as well as MDA-MB-435 cells as control. Nine days after withdrawal of Vemurafenib, the percentage of SA-β-Gal-positive cells was still increased compared with control cells in SK-MEL-28, UACC-62, and FM88 cells (Figure 5c). Owing to the high SA-β-Gal background staining of Malme 3M cells, a difference could not be detected here. Altogether, we could show that the senescence-inducing effect of Vemurafenib is sustainable

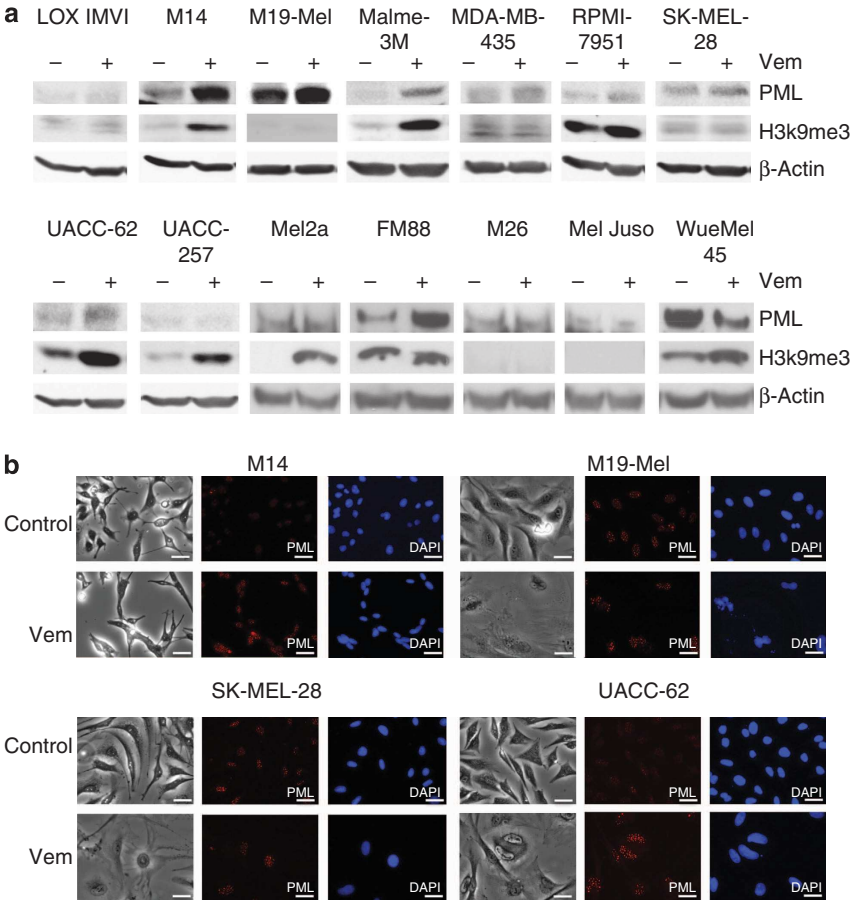

Figure 4. Vemurafenib causes the generation of heterochromatin and promyelocytic leukemia (PML) bodies in some melanoma cell lines. (**a**) Western blot analysis of the indicated melanoma cell lines after 48 h of treatment with the solvent DMSO (control) or 0.5 μM Vemurafenib (Vem). Cell lysates were analyzed for the expression of PML and trimethylated histone H3 (H3K9me3). β-Actin served as loading control. (**b**) Immunofluorescence showing focal nuclear accumulation of PML in indicated melanoma cell lines. Whole cells are depicted in phase contrast images, and the nuclei are visualized by 4′,6-diamidino-2-phenylindole (DAPI) staining, bar = 20 μm.

in some cell lines even after drug release. As only a fraction of the cell population (between 20% and 85%, see Figure 3d) becomes senescent because of the Vemurafenib treatment, the percentage of terminally arrested senescent cells in a cell population naturally decreases with time, dependent on the cell cycle duration of the unaffected cells. It is possible that the consequential expansion and colony formation of unaffected cells leads to the underestimation of the fraction of terminally arrested and senescent cells at the beginning of drug withdrawal.

To determine whether an increase in Vemurafenib concentration affects the degree of apoptosis and senescence induction, we selected nine $BRAF^{V600E}$-positive cell lines and treated them with 2 and 5 μM of the inhibitor in addition to the previously used 0.5 μM. Compared with 0.5 μM, 2 and 5 μM Vemurafenib led to a slightly stronger inhibition of P-ERK1/2 in some, but not all cell lines (Supplementary Figure S5 online). In concordance with the data shown above, LOX IMVI cells were irresponsive to Vemurafenib irrespective of the applied concentration. To analyze the effect of the increased Vemurafenib concentration on cell growth and death, we monitored cellular density in the absence or presence of the inhibitor over a 5-day period using the X-celligence system (Roche; Supplementary Figure S6a). This assay allows detection of the impedance or electric resistance of the cell population, which usually correlates with cell density: while cell growth leads to an increasing cell index, cell death is represented by a decreasing cell index. Because of their round cell shape, LOX IMVI cells are not suitable for this kind of analysis and were therefore omitted. In most cell lines, 2 and 5 μM Vemurafenib decreased cell density compared with 0.5 μM, indicating that the inhibitor is capable of inducing predominantly cell death instead of senescence at higher concentrations. In case of M19-Mel and UACC-62, addition of Vemurafenib first led to an increase of cell index, which can be attributed to the strongly increased cell shape that also influences impedance (see Supplementary Figures S2 and S6 online). Thus, we complemented these data with a BrdU incorporation analysis, showing the extent of viable and proliferating cells, as well as detection of dead cells by flow cytometry (Supplementary Figure S6b and S7a online). Both assays also demonstrated that increased Vemurafenib concentrations had an enhanced effect on the cells. In most cell lines, induction of cell death went along with increases in

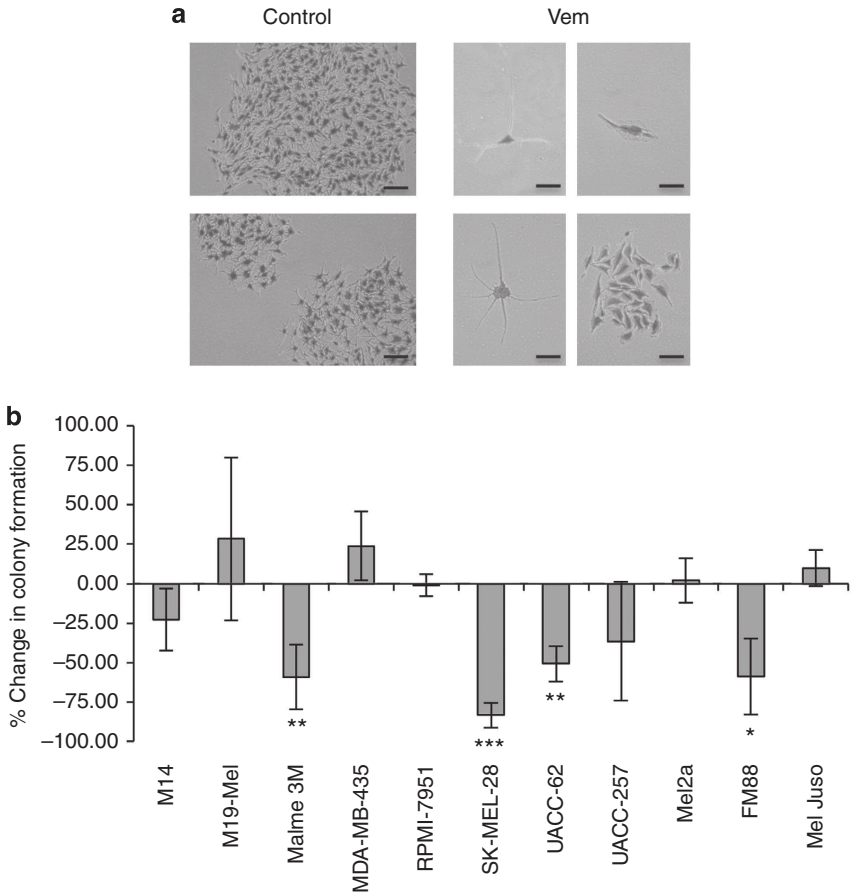

c

% SA-β Gal	Malme 3M	SK-MEL-28	UACC-62	FM88	MDA-MB-435
Control	17.3 ± 5.7	4.0 ± 3.0	7.0 ± 1.4	8.5 ± 0.7	1.8 ± 1.7
Vem release	20.9 ± 1.2	13.6 ± 3.2	15.3 ± 0.4	12.0 ± 0.2	0.9 ± 0.1

Figure 5. Detection of senescence features after release from Vemurafenib (Vem). (**a**, **b**) Indicated cell lines were treated for 5 days with 0.5 μM Vem. After extensive washing, cells were seeded at very low density to allow monitoring of colony formation by single cells (10.000 cells per T75 cell culture flasks) and were cultivated in the absence of Vem. After 8 and 9 days, cell colonies were stained with crystal violet. (**a**) Photomicrographs of colonies and single cells of the cell line SK-MEL-28, bar (control) = 100 μm, bar (Vem) = 20 μm. (**b**) Change of colony number in Vemurafenib-treated compared with untreated cells. Standard deviations are indicated. *$P<0.05$, **$P<0.001$, ***$P<0.0001$ (Student's *t*-test, two-tailed, paired). (**c**) Percentage of senescence-associated β-galactosidase (SA-β-Gal)-positive cells after control treatment or 5-day Vem treatment (0.5 μM), followed by an 8-day release.

the pro-apoptotic protein PUMA, thus indicating cell death by apoptosis (Supplementary Figure S7b online).

However, even though 2 and 5 μM Vemurafenib concentrations led to a stronger apoptosis response compared with 0.5 μM, we found that many of the surviving cells displayed senescence features such as flattened cell shape and positive SA-β-Gal staining, which was visible in up to 80% of the cell population (Figure 3e and Supplementary Figure S8 online).

To exclude that senescence induction upon BRAF inhibition is an *in vitro* artifact, we analyzed the effect of Vemurafenib in a mouse model. Tumors were induced in Nude mice (Hsd:Athymic Nude-*Foxn1*^{nu}) by subcutaneous injection of SK-MEL-28 cells. After the tumors had reached a size of approximately 150 mm^3, the animals were treated by daily intraperitoneal administration of 25 mg Vemurafenib per kg body weight. This led to initial tumor regression (Figure 6a). Control animals received the same volume of the solvent Miglyol 812, and here tumors continued growing. Tumors were excised following 7 days of treatment when tumor regression was evident in all Vemurafenib-treated mice (day 25 after start of the experiment). In accordance with the *in vitro* data, the tumor cells of inhibitor-treated mice displayed increased SA-β-Gal activity compared with the control tumors (Figure 6b). In addition, we could observe a decrease of the proliferation marker Ki67, a slight, but nonsignificant increase of PML and H3K9me3, and the occasional appearance of multinucleated cells in tumors from Vemurafenib-treated mice. An increase of apoptosis, measured by cleaved caspase 3 and TUNEL, was not noted. However, as tumor regression was rather prominent immediately after the addition of Vemurafenib (Figure 6a), apoptosis

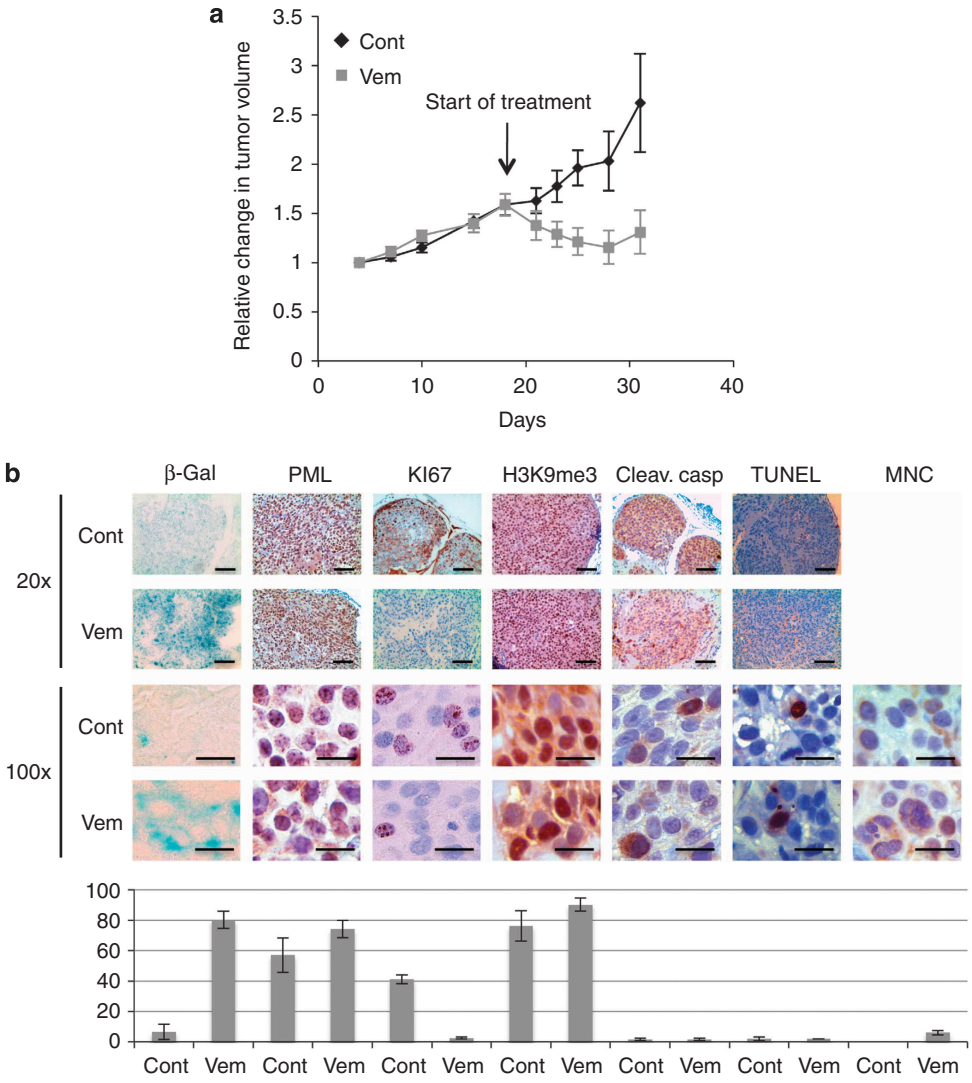

Figure 6. Shrinkage of xenotransplanted tumors in mice treated with Vemurafenib (Vem) is associated with the induction of senescence-associated β-galactosidase (SA-β-Gal) activity. In 12 nude mice, two tumors each were induced by subcutaneous injection of SK-MEL 28 cells. After 18 days, when the tumors reached a volume of around 150 mm^3 (indicated by arrow), the animals received intraperitoneal injections of either phosphate-buffered saline/DMSO or Vemurafenib (25 mg kg^{-1}). (**a**) Tumor growth curve of control (Cont)-treated and Vem-treated cells. Tumor size was measured and relative mean values (± standard deviation) are displayed. (**b**) Senescence and apoptosis markers in xenotransplanted tumors after 7 days of treatment (day 25 after tumor cell injection). Tumors were analyzed for the appearance of senescence markers, namely, multinucleated cells (MNCs), increased SA-β-Gal activity, and the expression of PML, trimethylated histone H3 (H3K9me3), and the proliferation marker Ki67. Apoptotic cells were detected using TUNEL assay and immunohistochemical staining of cleaved caspase 3 (Cleav. casp). Cell counts of each marker (including standard deviations) are shown in the histogram and correspond to the mean count number of three different tumors of each group (bar (20 ×) = 200 μm, bar (100 ×) = 10 μm). PML, promyelocytic leukemia.

has most likely taken place earlier and was not detectable anymore at the time of tumor excision.

DISCUSSION

Aberrant activation of BRAF in primary melanocytes and fibroblasts induces permanent cell cycle arrest through oncogene-induced senescence (Michaloglou *et al.*, 2005). Here we show that the induction of senescence is also an important response to BRAF inhibition in $BRAF^{V600E}$ and $BRAF^{V600K}$ -mutant melanoma cells. In this respect, we demonstrate that out of nine *BRAF* mutant cell lines that respond with cell cycle arrest to Vemurafenib treatment, eight display at least two markers of senescence-like typical changes in cell size and shape, increased SA-β-Gal activity, or H3K9me3-positive heterochromatic foci and PML bodies (see Supplementary Table S1 online). In the cell line LOX IMVI, Vemurafenib did not affect ERK1/2 phosphorylation at all, indicating that the reason for BRAF inhibitor resistance is likely found upstream of ERK1/2. Possible mechanisms for such a phenomenon include enhanced receptor tyrosine kinase signaling, the development of *BRAF* splice mutants, or mutations in the kinase COT1, all of which can overcome the inhibitory effect of Vemurafenib on ERK1/2 (Johannessen *et al.*, 2010; Villanueva *et al.*, 2010; Poulikakos *et al.*, 2011).

Most melanoma cells rely on an activated MAPK pathway, which is most often triggered by oncogenic $BRAF^{V600E}$. RAF

proteins phosphorylate and activate MAPK/ERK kinase, and MAPK/ERK kinase activates the ERK 1 and 2, which target more than 70 different substrates in different subcellular compartments (Chen *et al.*, 2001). ERK1/2 can exert their pro-tumorigenic function through different mechanisms. ERK1/2-dependent phosphorylation of the transcription factor FOXO3a leads to its proteasomal degradation, thus resulting in the reduced expression of the FOXO3a-dependent expression of pro-apoptotic Bcl-2-like protein 11 (Balmanno and Cook, 2009). Notably, pro-apoptotic PUMA is also induced by FOXO3a, and might therefore be indirectly regulated by ERK1/2 (You *et al.*, 2006). In addition, direct Bcl-2-like protein 11 and Bcl-2-associated death phosphorylation by ERK1/2 reduces protein stability or prevents binding of anti-apoptotic proteins, respectively, thereby shifting the balance between pro- and anti-apoptotic proteins in favor of cell survival. However, the cyclin-dependent kinase inhibitor gene *CDKN1B* (encoding $p27^{KIP1}$) is another target gene of FOXO3a, which is blocked by ERK1/2. In addition, cell cycle-promoting genes such as *CCND1* (cyclin D1) and *c-MYC* are induced by this pathway (Kerkhoff *et al.*, 1998; Ciuffreda *et al.*, 2009). Interestingly, small interfering RNA-mediated downregulation of the ERK1/2 target gene c-MYC in established melanoma cells results in senescence (Zhuang *et al.*, 2008). Thus, next to anti-apoptosis, proliferation is a major function of the ERK1/2 pathway in tumors.

The effect of Vemurafenib on melanoma cells expressing the $BRAF^{V600E}$ oncogene, the main activator of the ERK1/2 pathway in melanoma, is generally described as pro-apoptotic (Lee *et al.*, 2010; Tap *et al.*, 2010; Qin *et al.*, 2012). Although we could confirm this effect, in particular, when we used high concentrations of Vemurafenib, we found that a substantial proportion of surviving cells displays features of senescence. These data demonstrate that apoptosis and senescence response do not exclude each other in a cell population.

Although apoptosis induction is the preferred effect of drug treatment in cancer, senescence is also considered an eligible treatment objective (Acosta and Gil, 2012). It is known that senescence triggers a local immune response, which helps to clear the tumor mass (Chien *et al.*, 2011). As nude mice still possess natural killer cells, which reportedly display anti-melanoma activity, the observed tumor regression can be easily explained. However, senescent cells can also provide a microenvironment that increases the metastatic abilities of neighboring cells (Ohanna *et al.*, 2011), and might thereby contribute to resistance. Furthermore, cancer cells that were driven into senescence by chemotherapeutic agents can develop chemoresistant side populations with cancer stem cell-like properties (Achuthan *et al.*, 2011). BRAF has a role in regulating mitosis, and BRAF inhibition impairs spindle formation and leads to chromosomal missegregation in HeLa cells (Borysova *et al.*, 2008). Similar events might take place in Vemurafenib-treated melanoma cells, with the risk of causing increased genomic instability and selection for drug-resistant cells with more aggressive tumorigenic phenotypes. The involvement of senescence in melanoma regression and resistance in Vemurafenib-treated patients will be the subject of our future studies.

MATERIALS AND METHODS

Cell culture

Human melanoma cell lines LOX IMVI, M14, M19-Mel, Malme 3M, MDA-MB-435, RPMI 7951, SK-MEL-28, UACC-62, and UACC-257 were cultivated in DMEM and FM88, Mel2A, WüMel45, M26, and Mel Juso in RPMI-1640. For all cell lines, the medium was supplemented with 10% fetal calf serum, penicillin (100 U ml^{-1}, Gibco, Darmstadt, Germany), and streptomycin (100 µg ml^{-1}, Gibco). The WMM1175 cells have been described previously (Becker *et al.*, 2001). For induction of p16, 4 mM isopropyl-β-D-thiogalactopyranoside was added to the culture medium.

SA-β-Gal staining

Cells were either left untreated or were treated with indicated concentrations of Vemurafenib for 7 days, unless specified otherwise, before being washed with phosphate-buffered saline (PBS; pH 7.2) and fixed with 3.7% formaldehyde in PBS (pH 7.2) for 5 min at room temperature. After rinsing the cells with PBS (pH 7.2), they were subjected to β-Gal assay as described elsewhere (Dimri *et al.*, 1995) and then examined by light microscopy.

Cell lysis and immunoblot analysis

Attached and floating cells were harvested, rinsed twice with PBS, and were analyzed by western blot analysis as specified in the Supplemental information online.

Immunofluorescence

Cells were seeded on glass coverslips, treated for the indicated times with 0.5 µM Vemurafenib, and were fixed for 5 min at 4 °C in 100% methanol, followed by a permeabilization step in 100% acetone at 4 °C. Cells were then blocked with 1% bovine serum albumin and probed with anti-PML antibody (1:100; PG-M3; Santa Cruz Biotechnology, Santa Cruz, CA). Alexa Fluor 594 goat-anti-mouse (Invitrogen, Darmstadt, Germany) was used as secondary antibody. Nuclear counterstaining was performed with 4′,6-diamidino-2-phenylindole.

Flow cytometry

Cells were treated with 0.5, 2, and 5 µM Vemurafenib or the solvent DMSO alone. After indicated timespans, attached cells and floating cells in the medium supernatant were harvested and fixed in 70% ethanol. Details of the analysis are given in the Supplemental Material section.

Xenotransplantation

For tumor induction, SK-MEL-28 was injected subcutaneously into each lateral flank of 6-week-old female nude mice. When the tumors reached a volume of around 150 mm^3, mice were randomly divided into a vehicle control group and a Vemurafenib treatment group, as specifed in the Supplemental Materials section in detail. All the animal experiments were approved by the local authorities (government of Unterfranken) according to the legal requirements.

Immunohistochemistry

Three-micrometer sections of formalin-fixed and paraffin-embedded tumors were treated and stained as described previously (Houben *et al.*, 2012; see also Supplementary Materials online).

CONFLICT OF INTEREST

The authors state no conflict of interest.

ACKNOWLEDGMENTS

We thank Lena Völkert for excellent technical assistance and Helen Rizos for the critical review of the manuscript. This work was supported by grants from the Deutsche Krebshilfe (German Melanoma Research Network), the IZKF Würzburg, and the German Research Council (Transregio 17: RAS-dependent pathways in human cancers).

SUPPLEMENTARY MATERIAL

Supplementary material is linked to the online version of the paper at http://www.nature.com/jid

REFERENCES

Achuthan S, Santhoshkumar TR, Prabhakar J *et al.* (2011) Drug-induced senescence generates chemoresistant stemlike cells with low reactive oxygen species. *J Biol Chem* 286:37813–29

Acosta JC, Gil J (2012) Senescence: a new weapon for cancer therapy. *Trends Cell Biol* 22:211–9

Aplin AE, Kaplan FM, Shao Y (2011) Mechanisms of resistance to RAF inhibitors in melanoma. *J Invest Dermatol* 131:1817–20

Balmanno K, Cook SJ (2009) Tumour cell survival signalling by the ERK1/2 pathway. *Cell Death Differ* 16:368–77

Becker TM, Rizos H, Kefford RF *et al.* (2001) Functional impairment of melanoma-associated p16(INK4a) mutants in melanoma cells despite retention of cyclin-dependent kinase 4 binding. *Clin Cancer Res* 7:3282–8

Borysova MK, Cui Y, Snyder M *et al.* (2008) Knockdown of B-Raf impairs spindle formation and the mitotic checkpoint in human somatic cells. *Cell Cycle* 7:2894–901

Castellano M, Pollock PM, Walters MK *et al.* (1997) CDKN2A/p16 is inactivated in most melanoma cell lines. *Cancer Res* 57:4868–75

Chapman PB, Hauschild A, Robert C *et al.* (2011) Improved survival with vemurafenib in melanoma with BRAF V600E mutation. *N Engl J Med* 364:2507–16

Chen Z, Gibson TB, Robinson F *et al.* (2001) MAP kinases. *Chem Rev* 101:2449–76

Chien Y, Scuoppo C, Wang X *et al.* (2011) Control of the senescence-associated secretory phenotype by NF-kappaB promotes senescence and enhances chemosensitivity. *Genes Dev* 25:2125–36

Ciuffreda L, Del BD, Desideri M *et al.* (2009) Growth-inhibitory and antiangiogenic activity of the MEK inhibitor PD0325901 in malignant melanoma with or without BRAF mutations. *Neoplasia* 11:720–31

Cotter MA, Florell SR, Leachman SA *et al.* (2007) Absence of senescence-associated beta-galactosidase activity in human melanocytic nevi *in vivo*. *J Invest Dermatol* 127:2469–71

Courtois-Cox S, Jones SL, Cichowski K (2008) Many roads lead to oncogene-induced senescence. *Oncogene* 27:2801–9

Davies H, Bignell GR, Cox C *et al.* (2002) Mutations of the *BRAF* gene in human cancer. *Nature* 417:949–54

Dimri GP, Lee X, Basile G *et al.* (1995) A biomarker that identifies senescent human cells in culture and in aging skin *in vivo*. *Proc Natl Acad Sci USA* 92:9363–7

Fedorenko IV, Paraiso KH, Smalley KS (2011) Acquired and intrinsic BRAF inhibitor resistance in BRAF V600E mutant melanoma. *Biochem Pharmacol* 82:201–9

Garbe C, Eigentler TK, Keilholz U *et al.* (2011) Systematic review of medical treatment in melanoma: current status and future prospects. *Oncologist* 16:5–24

Gray-Schopfer VC, Soo JK, Bennett DC (2008) Comment on ''Absence of senescence-associated beta-galactosidase activity in human melanocytic nevi *in vivo*''. *J Invest Dermatol* 128:1581–4

Haferkamp S, Becker TM, Scurr LL *et al.* (2008) p16INK4a-induced senescence is disabled by melanoma-associated mutations. *Aging Cell* 7:733–45

Hasan MR, Ho SH, Owen DA *et al.* (2011) Inhibition of VEGF induces cellular senescence in colorectal cancer cells. *Int J Cancer* 129:2115–23

Hotta K, Tabata M, Kiura K *et al.* (2007) Gefitinib induces premature senescence in non-small cell lung cancer cells with or without EGFR gene mutation. *Oncol Rep* 17:313–7

Houben R, Adam C, Baeurle A *et al.* (2012) An intact retinoblastoma protein-binding site in Merkel cell polyomavirus large T antigen is required for promoting growth of Merkel cell carcinoma cells. *Int J Cancer* 130:847–56

Johannessen CM, Boehm JS, Kim SY *et al.* (2010) COT drives resistance to RAF inhibition through MAP kinase pathway reactivation. *Nature* 468:968–72

Joseph EW, Pratilas CA, Poulikakos PI *et al.* (2010) The RAF inhibitor PLX4032 inhibits ERK signaling and tumor cell proliferation in a V600E BRAF-selective manner. *Proc Natl Acad Sci USA* 107:14903–8

Kerkhoff E, Houben R, Loffler S *et al.* (1998) Regulation of c-myc expression by Ras/Raf signalling. *Oncogene* 16:211–6

Krauss V (2008) Glimpses of evolution: heterochromatic histone H3K9 methyltransferases left its marks behind. *Genetica* 133:93–106

Lee JT, Li L, Brafford PA *et al.* (2010) PLX4032, a potent inhibitor of the B-Raf V600E oncogene, selectively inhibits V600E-positive melanomas. *Pigment Cell Melanoma Res* 23:820–7

Michaloglou C, Soengas MS, Mooi WJ *et al.* (2008) Comment on ''Absence of senescence-associated beta-galactosidase activity in human melanocytic nevi *in vivo*''. *J Invest Dermatol* 128:1582–3

Michaloglou C, Vredeveld LC, Soengas MS *et al.* (2005) BRAFE600-associated senescence-like cell cycle arrest of human naevi. *Nature* 436:720–4

Miller AJ, Mihm MC Jr (2006) Melanoma. *N Engl J Med* 355:51–65

Narita M, Nunez S, Heard E *et al.* (2003) Rb-mediated heterochromatin formation and silencing of E2F target genes during cellular senescence. *Cell* 113:703–16

Ogrunc M, d'Adda di Fagagna F (2011) Never-ageing cellular senescence. *Eur J Cancer* 47:1616–22

Ohanna M, Giuliano S, Bonet C *et al.* (2011) Senescent cells develop a PARP-1 and nuclear factor-{kappa}B-associated secretome (PNAS). *Genes Dev* 25:1245–61

Poulikakos PI, Persaud Y, Janakiraman M *et al.* (2011) RAF inhibitor resistance is mediated by dimerization of aberrantly spliced BRAF(V600E). *Nature* 480:387–90

Puzanov I, Flaherty KT (2010) Targeted molecular therapy in melanoma. *Semin Cutan Med Surg* 29:196–201

Qin J, Xin H, Nickoloff BJ (2012) Specifically targeting ERK1 or ERK2 kills melanoma cells. *J Transl Med* 10:15

Sharpless E, Chin L (2003) The INK4a/ARF locus and melanoma. *Oncogene* 22:3092–8

Sondergaard JN, Nazarian R, Wang Q *et al.* (2010) Differential sensitivity of melanoma cell lines with BRAFV600E mutation to the specific Raf inhibitor PLX4032. *J Transl Med* 8:39

Tap WD, Gong KW, Dering J *et al.* (2010) Pharmacodynamic characterization of the efficacy signals due to selective BRAF inhibition with PLX4032 in malignant melanoma. *Neoplasia* 12:637–49

Tran SL, Haferkamp S, Scurr LL *et al.* (2012) Absence of distinguishing senescence traits in human melanocytic nevi. *J Invest Dermatol* 132:2226–34

Vernier M, Bourdeau V, Gaumont-Leclerc MF *et al.* (2011) Regulation of E2Fs and senescence by PML nuclear bodies. *Genes Dev* 25:41–50

Villanueva J, Vultur A, Lee JT *et al.* (2010) Acquired resistance to BRAF inhibitors mediated by a RAF kinase switch in melanoma can be overcome by cotargeting MEK and IGF-1R/PI3K. *Cancer Cell* 18:683–95

Wang M, Morsbach F, Sander D *et al.* (2011) EGF receptor inhibition radiosensitizes NSCLC cells by inducing senescence in cells sustaining DNA double-strand breaks. *Cancer Res* 71:6261–9

You H, Pellegrini M, Tsuchihara K *et al.* (2006) FOXO3a-dependent regulation of Puma in response to cytokine/growth factor withdrawal. *J Exp Med* 203:1657–63

Zhuang D, Mannava S, Grachtchouk V *et al.* (2008) C-MYC overexpression is required for continuous suppression of oncogene-induced senescence in melanoma cells. *Oncogene* 27:6623–34

Supplemental Material

Supplementary Materials and Methods

X-celligence analysis – $1.5x10^3$ cells were seeded on wells of a gold-layered 96-well-plate (Roche) and were monitored for the indicated timespan using the X-celligence system (Roche), as instructed by the manufacturer. Every five hours, resistance of the cell population was measured and was recorded as "cell index". The assay was done in triplicate, and two independent biological experiments were performed.

BrdU incorporation assay – Cells were pretreated with 0, 0.5, 2 or 5 μM Vemurafenib for 5 days and then incubated with 10 μM BrdU for 12 h. BrdU incorporation was quantified using a colorimetric BrdU cell proliferation ELISA, as recommended by the manufacturer (Roche).

Flow cytometry - For flow cytometry analysis, DNA was stained with 69 mM propidium iodide in 38 mM sodium citrate and 100 mg/ml RNase A for 30 min at 37°C. Samples were analyzed in a Beckman Coulter Cytomics FC 500. To analyze altered proliferation by a second method we applied carboxyfluorescein diacetate (CFDA) which can be used to label cells. Prior to treatment with Vemurafenib, cells were labeled applying the Vybrant CFDA SE Cell Tracer Kit (Invitrogen) according to the manufacturer's instructions. Changes of the green fluorescence in control and Vemurafenib-treated cells were analyzed in a FACSCanto (BD Biosciences).

Cell lysis and immunoblot analysis – Cells were lysed in lysis buffer (20 mM HEPES (pH 7.8), 500 mM NaCl, 5 mM $MgCl_2$, 5 mM KCl, 0.1% deoxycholate, 0.5% Nonidet-P40, 10 μg/ml aprotinin, 10 μg/ml leupeptin, 200 μM Na_3VO_4, 1 mM PMSF and 100 mM NaF). Proteins were resolved by SDS/PAGE and analyzed by immunoblotting using the following primary antibodies: Anti-β-actin (C-4; Santa Cruz Biotechnology), anti p16 (N20; Santa Cruz Biotechnology) anti-PML (H238, PG-M3; Santa Cruz Biotechnology), anti-PUMA (Cell

Signaling), anti-ERK2 (C14; Santa Cruz Biotechnology), anti-ERK1/2 (Cell Signaling), anti-phospho-ERK1/2 (Thr202/Tyr204; Cell Signaling), anti-phospho Rb (Ser780; Cell Signaling), anti-H3K9me3 (Active Motif), anti-Retinoblastoma protein (C15, Santa Cruz Biotechnology) and anti-tubulin (Sigma-Aldrich). The secondary antibodies were conjugated with horseradish peroxidase and were directed against mouse (Pierce) or rabbit (Bio-Rad).

Immunohistochemistry - For the detection of senescence markers previously validated primary antibodies were used recognizing Ki-67 (clone SP6; Lab Vision Corp.), cleaved caspase 3 (Asp175, clone 5A1E; Cell Signaling), PML (H238, clone PG-M3; Santa Cruz Biotechnology), anti-H3K9me3 (07-442; Millipore) and biotinylated multispecies-specific secondary antibody (DAKO) (Tomita 2010, Tran et al 2012). TUNEL assays were performed using the *in situ* cell death detection kit (Roche) according to the manufacturer's instructions.

Xenotransplantation - Six-week-old female nude mice (Hsd:Athymic Nude-*Foxn1*^{nu}), were obtained from Harlan Laboratories (Eystrup, Germany). For tumor induction, $5*10^6$ SK-MEL-28 cells suspended in PBS supplemented with 50% BD Matrigel^{TM} Basement Membrane Matrix (BD Biosciences, Heidelberg, Germany) were injected s.c. into each lateral flank of the mice. The size of the tumor was measured twice weekly using a slide gauche. When the tumors reached a volume of around 150 mm^3 (day 18 after cell injection), the mice were randomly divided into two groups (n=6): vehicle control group (mice injected intraperitoneally with PBS/DMSO daily), Vemurafenib group (mice injected intraperitoneally with 25 mg/kg Vemurafenib daily). For further analysis subcutaneously grown tumors were surgically removed. Subsequently the tumors were divided and snap-frozen in liquid nitrogen and formalin-fixed, paraffin-embedded.

Supplemental references

Tomita T (2010). Cleaved caspase-3 immunocytochemical staining for pancreatic islets and pancreatic endocrine tumors: A potential marker for biological malignancy. *Islets* **2:** 82-88.

Tran SL, Haferkamp S, Scurr LL, Gowrishankar K, Becker TM, Desilva C *et al* (2012). Absence of distinguishing senescence traits in human melanocytic nevi. *J Invest Dermatol* **132:** 2226-2234.

Supplementary Table 1: Induction of a senescence type cell cycle arrest by Vemurafenib in melanoma cell lines

	BRAF	phospho -ERK1/2	phospho -Rb	G0/G1 arrest	ß-Gal	cell size	H3K9me3	PML
LOX IMVI	V600E	0	0	0	0	0	0	0
M14	V600E	-	-	+	+	0	+	+
M19-Mel	V600E	-	-	+	+	+	0	+
Malme 3M	V600E	-	-	+	+	0	+	+
MDA-MB-435	V600E	-	-	+	0	0	0	+/0
RPMI 7951	V600E	-	-	0	0	0	0	0
SK-MEL-28	V600E	-	-	+	+	+	0	+/0
UACC-62	V600E	-	-	+	+	+	+	+
UACC-257	V600E	-	-	+	+	+	+	0
Mel2a	V600E	-	-	+	+	0	+	0
FM88	V600K	-	-	+	+	+	0	+
M26	wt	0	0	0	0	0	0	0
Mel Juso	wt	0	0	0	0	0	0	0
WüMel45	wt	0	0	0	0	0	+	-

Summary of proliferation and senescence parameters described in this manuscript.
0: unchanged; +: increase; -: decrease; +/0: weak increase

Supplementary figure legends

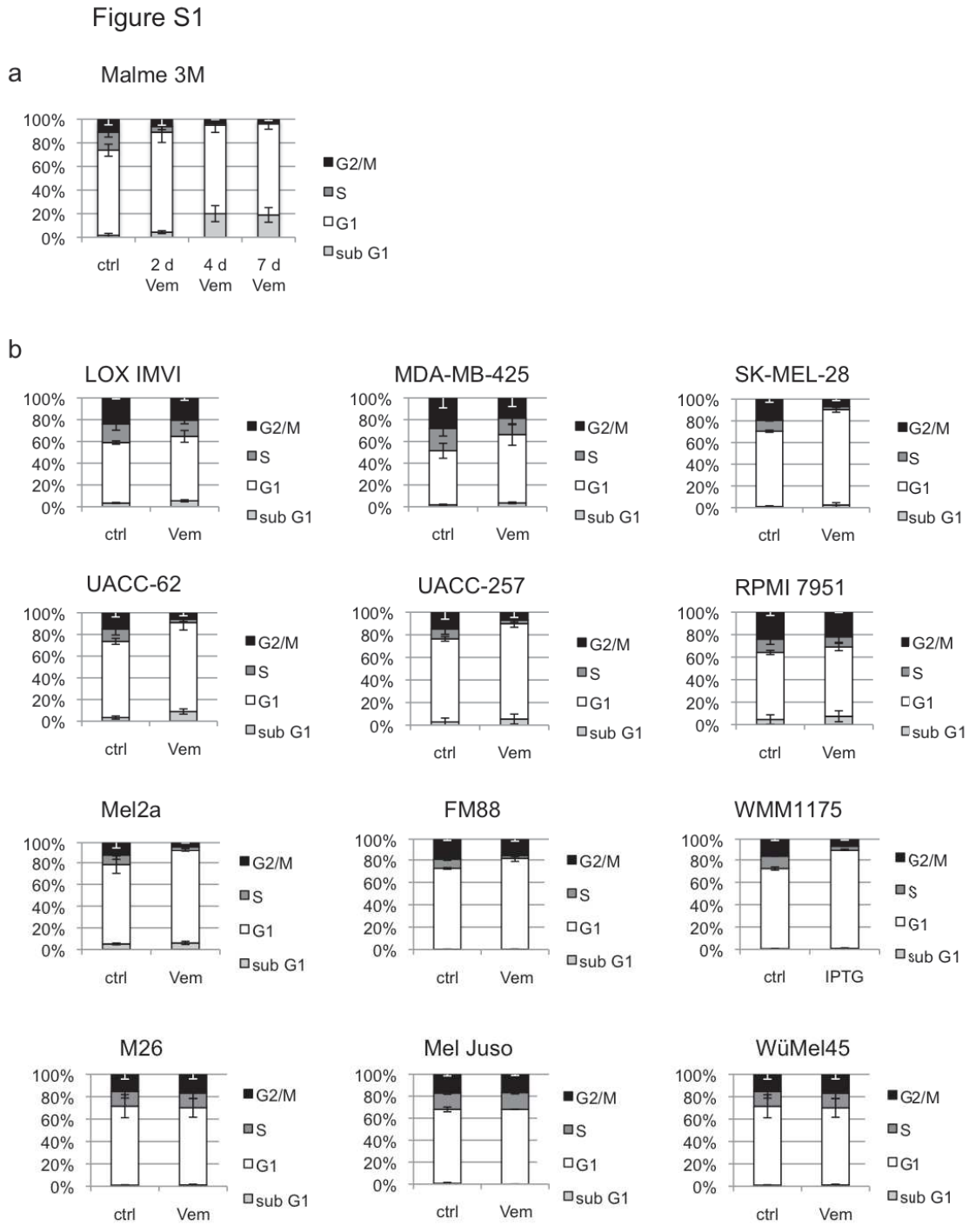

Figure S1: Effect of Vemurafenib on the cell cycle

Bar graph representation of the cell cycle profiles of melanoma cells after indicated times of Vemurafenib or IPTG (WMM1175) treatment. Data are mean values from three independent experiments. Standard deviations are indicated.

Figure S2

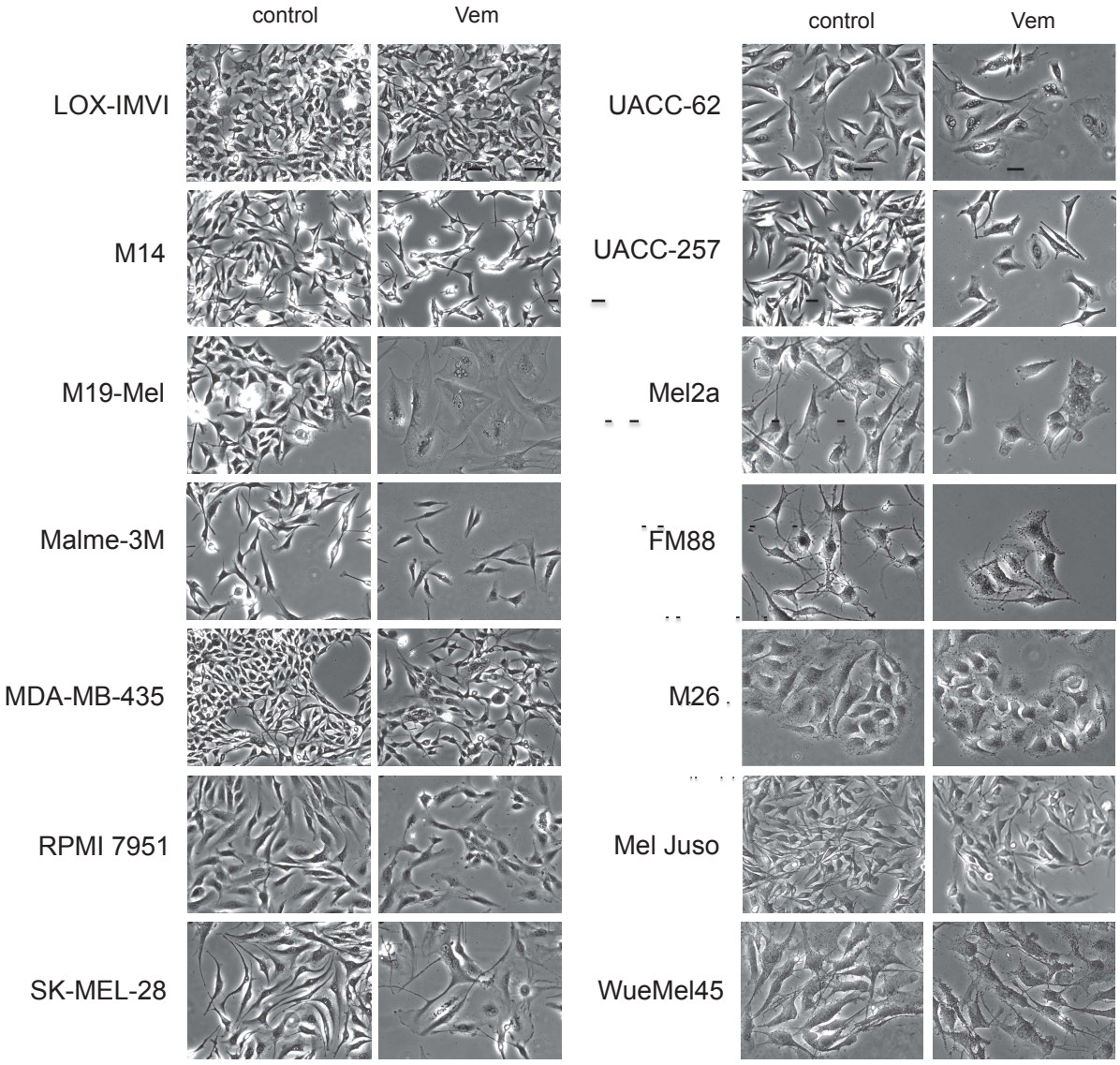

Figure S2: Effect of Vemurafenib on melanoma cell shape

Phase contrast images of indicated melanoma cell lines treated for 7 days with the solvent DMSO (control) or with 0.5 µM Vemurafenib (Vem), (bar=20µm).

Figure S3

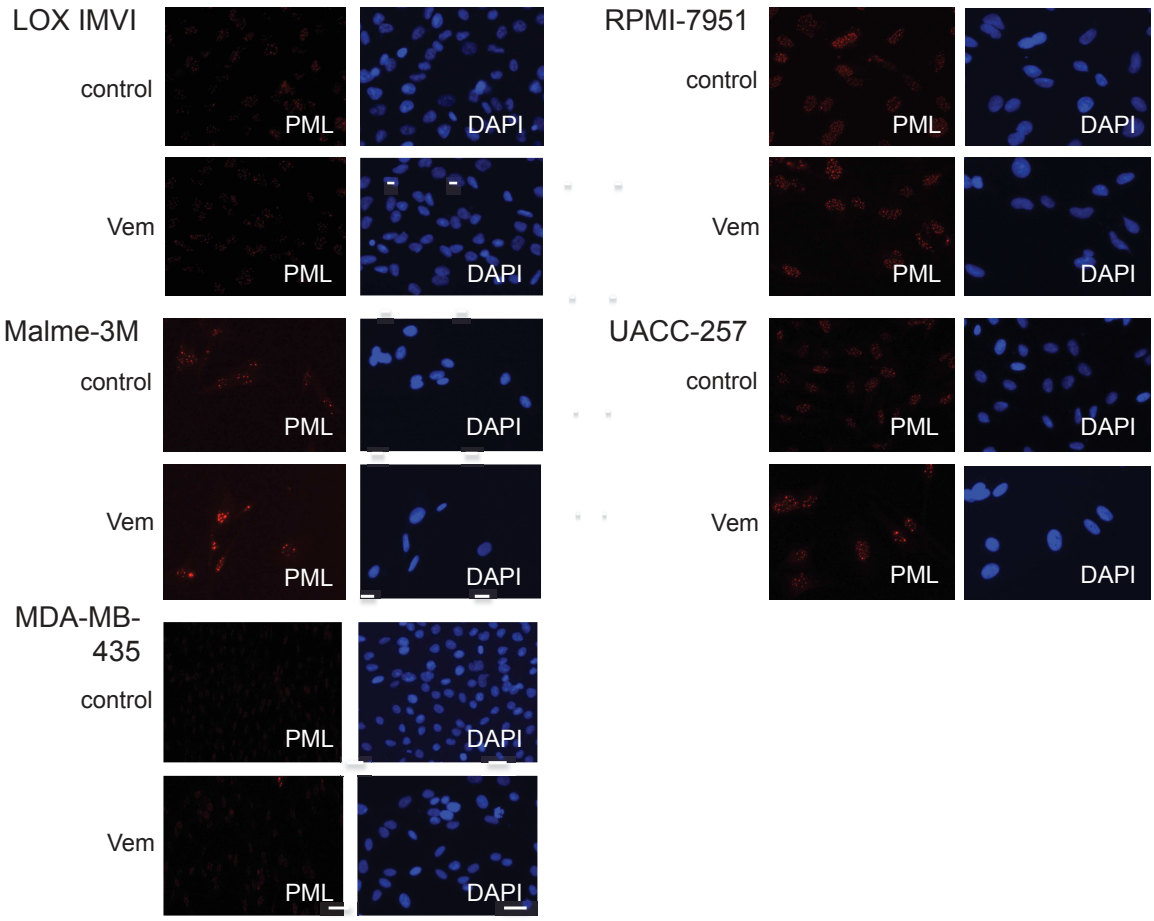

Figure S3: PML body formation by Vemurafenib

Immunofluorescence showing focal nuclear accumulation of PML in indicated melanoma cell lines. The nuclei are visualized by DAPI staining, (bar=20µm).

Figure S4

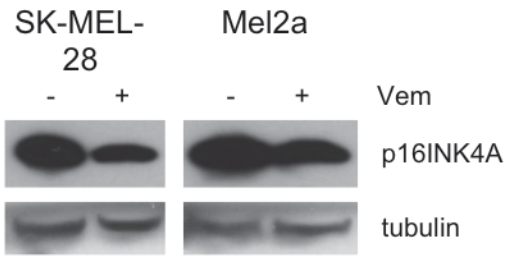

Figure S4: Effect of Vemurafenib on p16

Western blot of total cell lysates derived from the indicated cell lines after 2 days in the presence or absence of 0.5 μM Vemurafenib. Tubulin served as loading control.

Figure S5

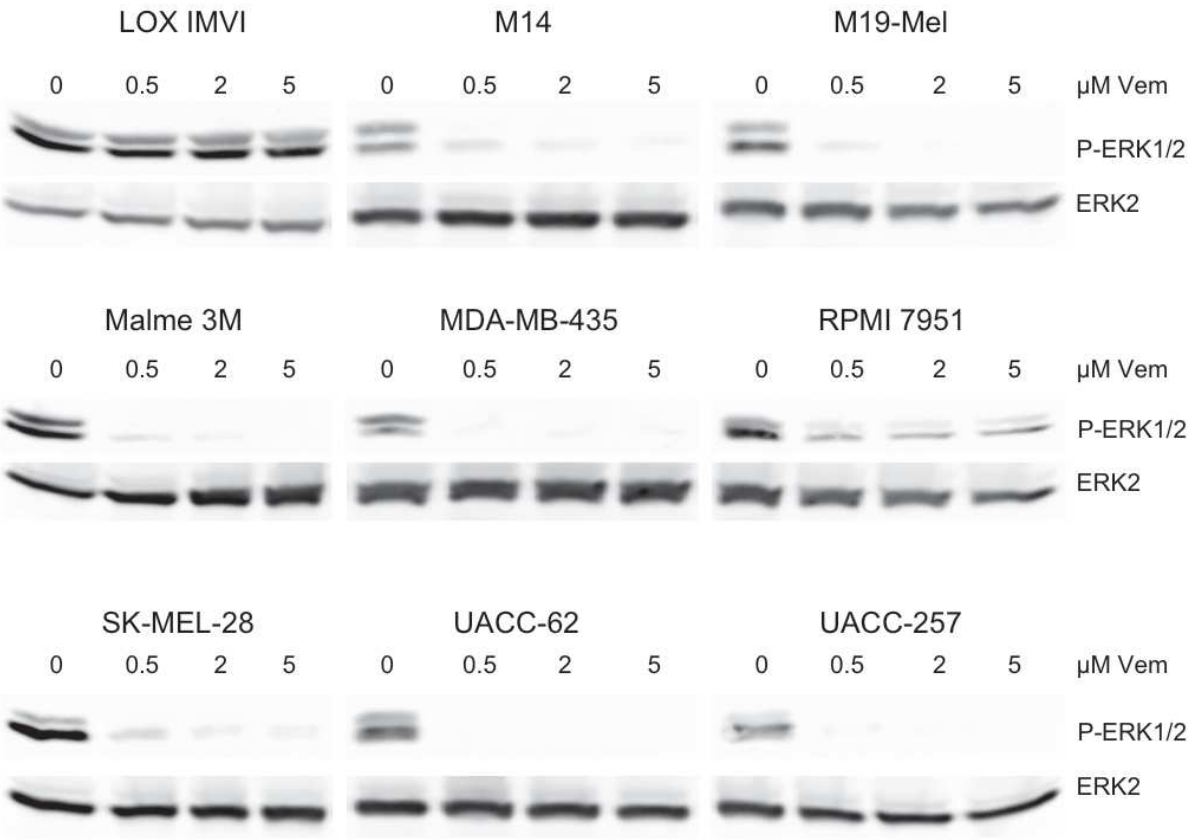

Figure S5: Inhibition of ERK1/2 by increasing concentrations of Vemurafenib

Western blot of the indicated melanoma cell lines after 48 h of treatment with the solvent DMSO (-) or with 0.5 µM, 2 µM and 5 µM Vemurafenib (Vem). Cell lysates were analyzed for the expression of phospho-ERK1/2 (Thr 202/ Tyr 204). Total ERK2 served as loading control.

Figure S6

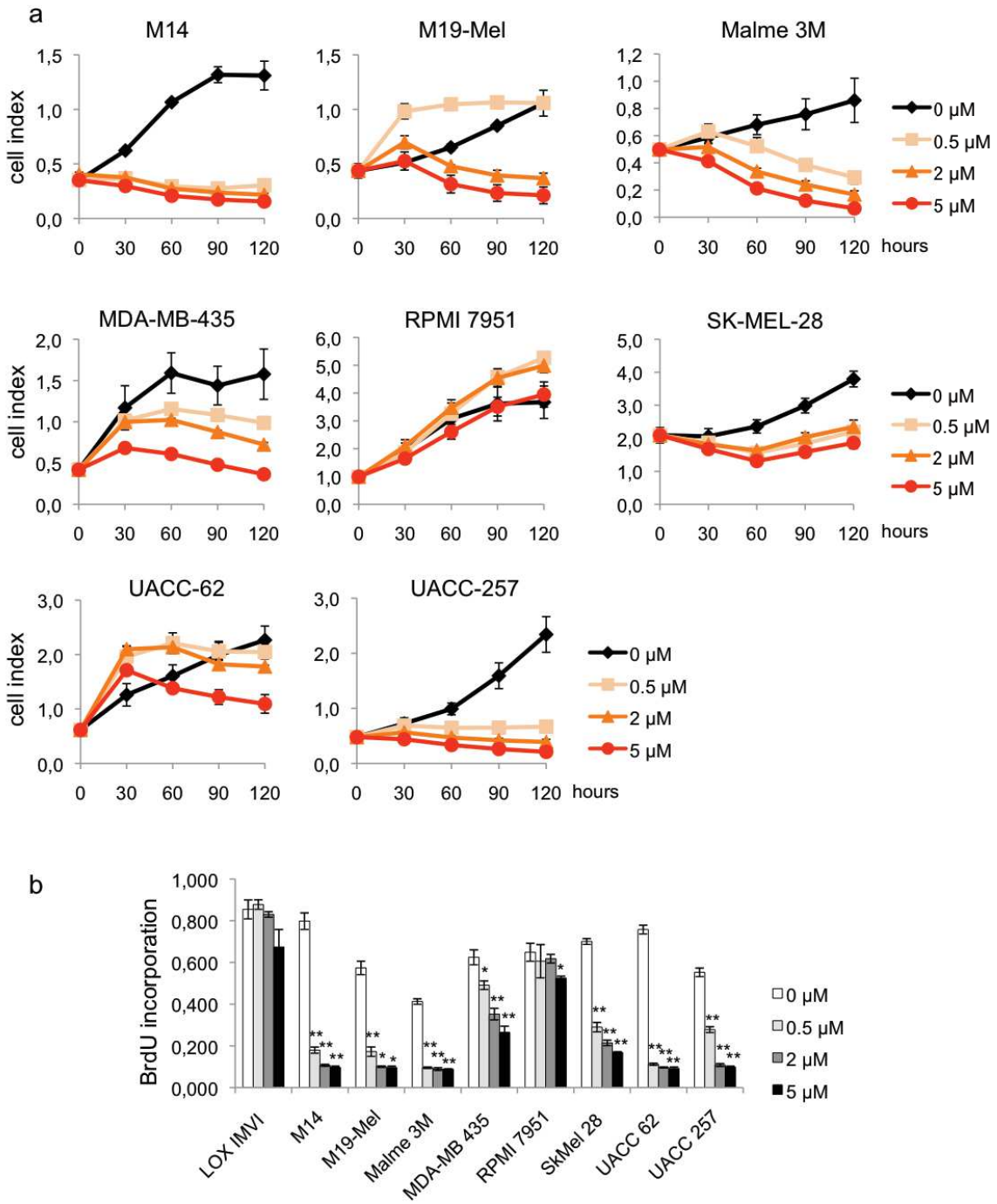

Figure S6: Effect of increasing concentration of Vemurafenib on cell growth and DNA synthesis

a: X-celligence measurement of indicated melanoma cells in presence of the indicated concentration of Vemurafenib up to 120 hours (5 days). The cell index represents the impedance of the cell population on a well of a 96-well dish. b: BrdU incorporation of indicated cell lines that were pretreated with the indicated concentrations of Vemurafenib for 5 days before incubation with BrdU for 12 h. The significance of differences between the DMSO control and the different Vemurafenib treatments are indicated. Standard deviations are indicated.*: $p<0.05$, **: $p<0.001$ (Student`s t-test, two-tailed, paired).

Figure S7

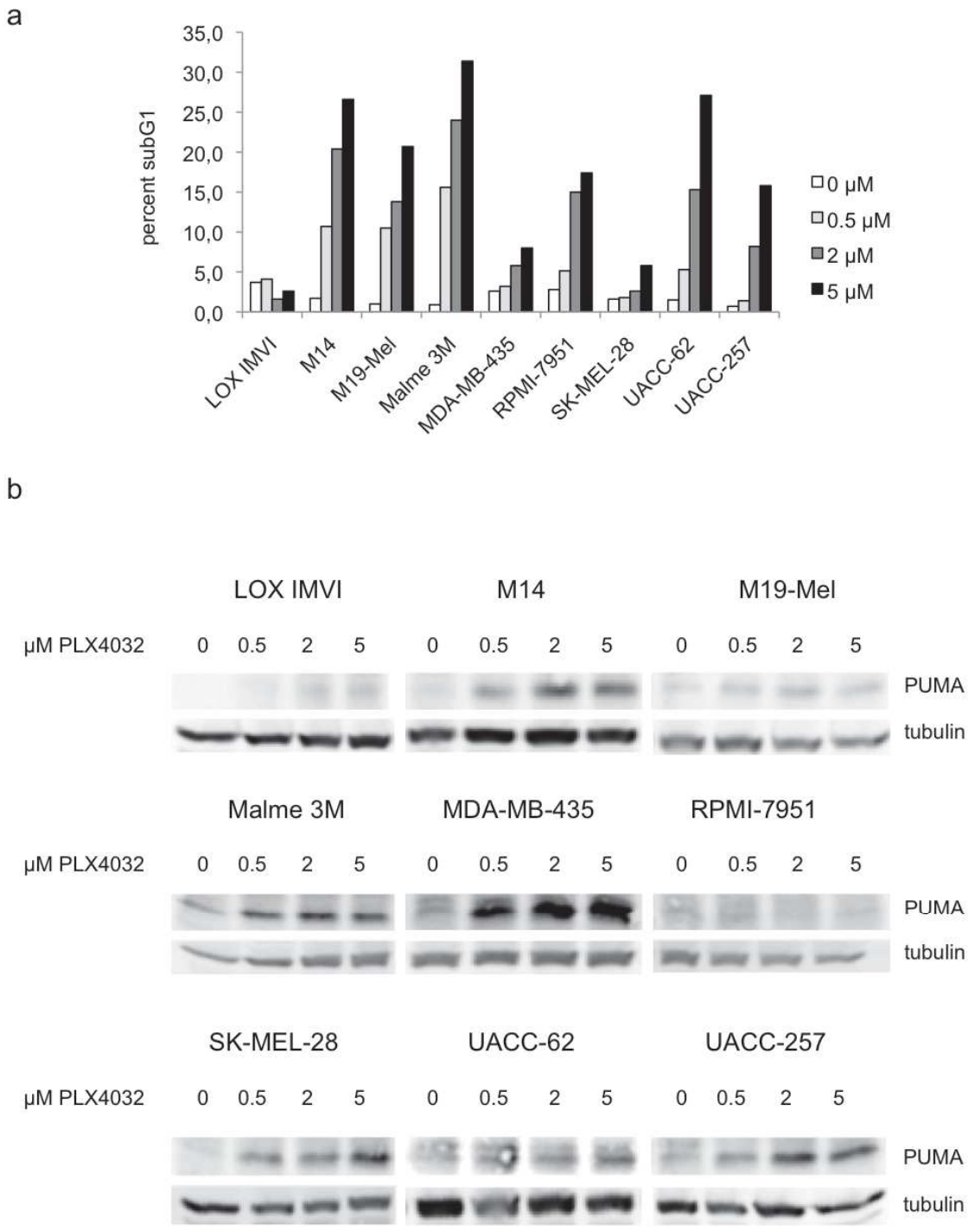

Figure S7: Apoptosis induction by Vemurafenib

Cells were treated for 5 days with the indicated concentrations of Vemurafenib, before cells and their supernatant were harvested and subjected to analyses. a: Cells were analyzed by flow cytometry, and the percentage of cells in subG1 are indicated. b: Western blot showing the induction of the pro-apoptotic protein PUMA in response to Vemurafenib treatment. Tubulin served as loading control.

Figure S8

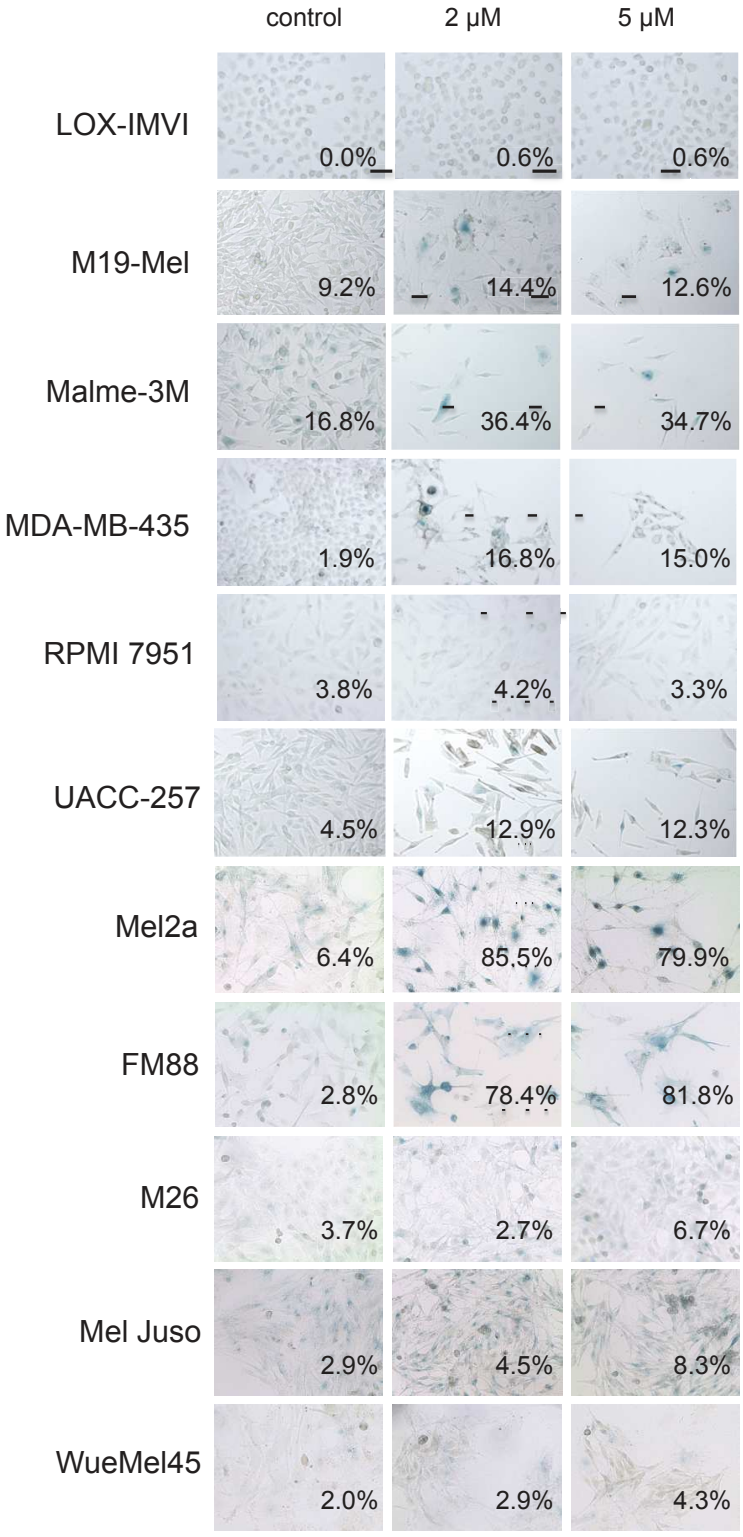

Figure S8: Induction of senescence in response to increased Vemurafenib concentration

SA-β-Gal staining of indicated cell lines after seven days of control (DMSO) or Vemurafenib treatment with the indicated concentrations. The percentage of SA-β-Gal-positive cells after Vemurafenib treatment is indicated.

Mechanisms of p53 Restriction in Merkel Cell Carcinoma Cells Are Independent of the Merkel Cell Polyoma Virus T Antigens

Roland Houben[1], Christina Dreher[1], Sabrina Angermeyer[1], Andreas Borst[1], Jochen Utikal[2,3], Sebastian Haferkamp[1], Wiebke K. Peitsch[3], David Schrama[1,4] and Sonja Hesbacher[1]

Merkel cell carcinoma (MCC) is a rare and very aggressive skin cancer with viral etiology. The tumor-associated Merkel cell polyoma virus (MCV) belongs to a group of viruses encoding T antigens (TAs) that can induce tumorigenesis by interfering with cellular tumor-suppressor proteins like p53. To explore possible modes of p53 inactivation in MCC p53 sequencing, expression analysis and reporter gene assays for functional analyses were performed in a set of MCC lines. In one MCV-negative and one MCV-positive cell line, p53 inactivating mutations were found. In the majority of MCC lines, however, wild-type p53 is expressed and displays some transcriptional activity, which is yet not sufficient to effectively restrict cellular survival or growth in these cell cultures. Interestingly, the MCV TAs are not responsible for this critical lack in p53 activity, as TA knockdown in MCV-positive MCC cells does not induce p53 activity. In contrast, inhibition of the ubiquitin ligase HDM-2 (human double minute 2) by Nutlin-3a leads to p53 activation and p53-dependent apoptosis or cell cycle arrest in five out of seven p53 wild-type MCC lines, highlighting p53 as a potential target for future therapies of this aggressive tumor.

Journal of Investigative Dermatology (2013) **133,** 2453–2460; doi:10.1038/jid.2013.169; published online 16 May 2013

INTRODUCTION

Merkel cell carcinoma (MCC) of the skin is a rare and very aggressive neuroendocrine tumor with more than 3-fold rise in incidence over the past decades (Hodgson, 2005). As MCC has a high tendency to metastasize, and there are no curative or life-prolonging therapies available for patients with distant metastases (Tai *et al.*, 2000; Becker, 2010), there is a great need to understand the molecular events driving this cancer.

Until recently, virtually nothing was known about oncogenes and tumor suppressors contributing to the pathogenesis of MCC (Lemos and Nghiem, 2007). However, an important step forward was the discovery of the Merkel cell polyoma virus (MCV) that is clonally integrated in the genome of the cancer cells in the majority of MCCs (Feng *et al.*, 2008; Sastre-Garau *et al.*, 2009). Integration of the virus before clonal expansion of the tumor cells as well as addiction of MCV-positive MCC cells to the expression of viral oncoproteins suggest that MCV is a major driver of MCC development and progression (Houben *et al.*, 2010, 2012a).

The polyomaviruses oncoproteins are the T antigens (TAs). All polyomaviruses encode alternatively spliced Large and small T antigen (LT and sT). Further splice variants are middle T antigen, 17 kT and 57 kT, that are encoded by murine polyomaviruses, simian virus 40 (SV40) and MCV, respectively (Shuda *et al.*, 2008; Cheng *et al.*, 2009; Gjoerup and Chang, 2010). Oncogenic transformation by the viral TAs is mediated by interaction with a multitude of cellular proteins. For example, protein phosphatase 2A is targeted by SV40 sT, whereas SV40 LT is capable of inactivating the tumor-suppressor proteins retinoblastoma protein and p53 (Gjoerup and Chang, 2010).

p53—also referred to as guardian of the genome—is a transcription factor that can modulate the expression of hundreds of genes (Song and Xu, 2007). In normal cells, p53 is frequently undetectable because of continuous ubiquitination by HDM-2 (human double minute 2) and subsequent proteasomal degradation (Blagosklonny, 1997). On several types of stresses including DNA damage or oncogene activation, p53 gets activated and induces cell cycle arrest, DNA repair, apoptosis, or senescence

[1]*Department of Dermatology, Venereology and Allergology, University Hospital Würzburg, Würzburg, Germany;* [2]*Skin Cancer Unit, German Cancer Research Center (DKFZ), Heidelberg, Germany;* [3]*Department of Dermatology, Venereology and Allergology, University Medical Center Mannheim, University of Heidelberg, Mannheim, Germany and* [4]*Department of General Dermatology, Medical University Graz, Graz, Austria*

Correspondence: Roland Houben, Department of Dermatology, Venereology and Allergology, University Hospital Würzburg, Josef-Schneider-Strasse 2, D-97080 Würzburg, Germany. E-mail: Houben_R@klinik.uni-wuerzburg.de

Abbreviations: GFP, green fluorescent protein; HDM-2, human double minute 2; LT, large T antigen; MCC, Merkel cell carcinoma; MCV, Merkel cell polyoma virus; shRNA, short hairpin RNA; sT, small T antigen; SV40, simian virus 40; TA, T antigen

Received 30 October 2012; revised 20 March 2013; accepted 21 March 2013; accepted article preview online 5 April 2013; published online 16 May 2013

(Green and Chipuk, 2006; Lavin and Gueven, 2006; Sherr, 2006). Thereby, p53 is central for the suppression of cancer, and its inactivation is one of the characteristics of cancer. Indeed, mutations of p53 are found in approximately half of all tumors (Roemer, 1999). Most of these aberrations are missense mutations in the central DNA-binding domain that abolish the transcriptional capacity and may render p53 dominant negative over coexpressed wild-type p53 (van Oijen and Slootweg, 2000). Beside mutations, further modes of p53 inactivation contributing to tumor development have been described, including the ability of certain viral proteins to impair p53 function. Indeed, p53 inactivation is a common feature of all DNA tumor viruses (Levine, 2009).

p53 inactivation by polyomaviruses was described mainly as a function of LT that binds to p53 and thereby abrogates its ability to act as a transcription factor (Bargonetti *et al.*, 1992; Jiang *et al.*, 1993; Pipas and Levine, 2001). MCV LTs in MCC cells, however, lack a putative p53-binding domain because of tumor-associated T-antigen deletion mutations generally present in MCC-associated MCV genomes (Shuda *et al.*, 2008; Sastre-Garau *et al.*, 2009). Nevertheless, recent reports suggested that mutations in p53 occur preferentially in MCC tumors that fail to express MCV LT (Sihto *et al.*, 2011; Rodig *et al.*, 2012). For example, p53 mutations were found in over 50% of MCCs lacking MCV LT expression but were not detectable in LT-positive MCCs (Sihto *et al.*, 2011). These observations suggest that even MCV with truncated LT is able to inactivate p53. In line with this notion, it has been reported that, on one hand, SV40 LT lacking the C-terminal p53-binding domain is still able to inhibit p53-dependent transcription (Quartin *et al.*, 1994; Rushton *et al.*, 1997) and, on the other hand, SV40 sT can repress p53 function (Gjoerup *et al.*, 2000).

Here we analyze the p53 signaling pathway in MCV-positive and MCV-negative MCC lines. Most of these cell lines harbor wild-type but insufficiently active p53 protein. We exclude the MCV TAs as relevant inhibitors of p53 activity in MCC and demonstrate that p53-dependent cell death or cell cycle arrest can be activated by a small-molecule inhibitor of HDM-2.

RESULTS AND DISCUSSION

p53 inactivating mutations in 2 of 14 MCC lines

The frequency of p53 inactivating mutations has been reported to be relatively low in MCC, i.e., 10% (1 in 10 tumors),14% (3 in 21 tumors) or 27% (11 in 40 tumors) (Van Gele *et al.*, 2000; Lassacher *et al.*, 2008; Sihto *et al.*, 2011). Thus, as a first step of a comprehensive p53 pathway analysis in MCC, we determined the p53 status in 14 MCC lines by sequencing exons 5–8 in a series of 14 MCC lines. We found that similar to the published tissue analyses only two MCC cell lines (14%) had p53 mutations, whereas the remaining 12 cell lines displayed wild-type sequences in the p53 mutation hot spot region (Table 1).

Table 1. MCV and p53 status of the MCC cell lines analyzed in this study

							Response to Nutlin-3a				
		MCV $^{+}$	p53 status (exons 5–8[1])	p53 mRNA	p53 protein	p53-specific reporter activity	p53 protein	Reporter activity	p53 targets	Cycle arrest	Apoptosis
1	BroLi	Yes	Wild type	+	+	+	+	+	+	–	+
2	WaGa	Yes	Wild type	+ +	+	+	+	+	+	–	+
3	Mkl-1	Yes	Wild type	+ +	+	+	+	+	+	–	+
4	MKL-2	Yes	Wild type	+ +	–	–	–	–	–	–	–
5	PeTa	Yes	Wild type	+ +	+	+	+	+	+	–	+
6	MS-1	Yes	Hemizygous deletion aa 251–253	+ + +	+ +	?	ND	ND	ND	ND	ND
7	AlDo	Yes	Wild type	+ +	+	ND	ND	ND	ND	ND	ND
8	WoWe	Yes	Wild type	ND	ND	ND	ND	ND	ND	ND	ND
9	HeRo	Yes	Wild type	ND	ND	ND	ND	ND	ND	ND	ND
10	KaRi	Yes	Wild type	ND	ND	ND	ND	ND	ND	ND	ND
11	LoKe	Yes	Wild type	ND	ND	ND	ND	ND	ND	ND	ND
12	MCC 26	No	Wild type	+	–	–	–	–	–	–	–
13	UISO	No	Wild type	+ +	+	+	+	+	+	+	–
14	MCC13	No	P278S and S241P both heterozygous	+ + +	+ +	?	–	–	–	–	–

Abbreviations: MCC, Merkel cell carcinoma; MCV, Merkel cell polyoma virus; ND, not done; ?, data difficult to interpret.
[1]Exons 5–8 harbor 95% of the known p53 mutations (Vousden and Lu, 2002).

The MCV-negative cell line MCC13 carried two different mutations in exon 7 and exon 8 (Table 1). As we cannot distinguish whether these two mutations affect the same or different alleles, it is unknown whether all the p53 molecules expressed in MCC13 are mutant or not. However, according to the IARC (International Agency for Research on Cancer) p53 mutation database, both loss-of-function and dominant-negative effects on wild-type p53 have been described for the P278S mutation in exon 8, suggesting that p53 is indeed inactivated in this cell line (Petitjean *et al.*, 2007). For the p53 deletion mutant lacking amino acids 251–253, which is present homo- or more likely hemizygously in the MCV-positive line MS-1, functional data are not available. Nevertheless, as several substitution mutants of the deleted amino acids have been characterized as inactive, this deletion mutant is likely to be inactivating (Petitjean *et al.*, 2007).

p53 expression and activity in MCC cell lines

Next we analyzed p53 mRNA and protein expression in nine MCC cell lines using real-time PCR and immunoblot. In the two p53 mutant cell lines (MCC13 and MS-1), the high mRNA expression level correlated with high p53 protein expression (Figure 1a). Accumulation of mutant p53 in tumor cells is a well-known, although not yet fully understood, phenomenon (Soussi, 2007). Among the seven p53 wild-type cell lines, however, p53 protein expression levels were diverging and did not correlate with mRNA expression. In two cell lines (MCC26 and MKL-2), p53 protein was not detectable despite p53 mRNA expression (Figure 1a), suggesting very strict posttranscriptional repression of p53 expression. In the remaining five p53 wild-type cell lines, p53 protein was expressed at levels sufficient for detection by western blot.

To estimate the transcriptional activity of p53 in the different MCC lines, we stably transduced the cells with a reporter gene construct (pGreenFire) expressing green fluorescent protein (GFP) under the control of a p53 response element. The mean GFP expression was measured by flow cytometry and normalized for the relative number of incorporated pGreenFire copies as determined by real-time PCR. Surprisingly, the normalized GFP expression from the pGreenFire construct did not correlate with p53 expression (Figure 1a). As it has been demonstrated that p53 reporter assays may sometimes yield unspecific responses (Wischhusen *et al.*, 2004), short hairpin RNA (shRNA) knockdown of p53 was performed to determine whether the observed GFP expression is p53 dependent. In the two p53 mutant cell lines (MS-1 and MCC13), GFP reporter expression was increased, and in MCC13, p21 was induced upon p53 knockdown (Figure 1b), suggesting that predominantly an inhibitory activity of mutant p53 was eliminated in these cells. In the two cell lines lacking detectable p53 expression (MCC26 and MKL-2), GFP expression remained

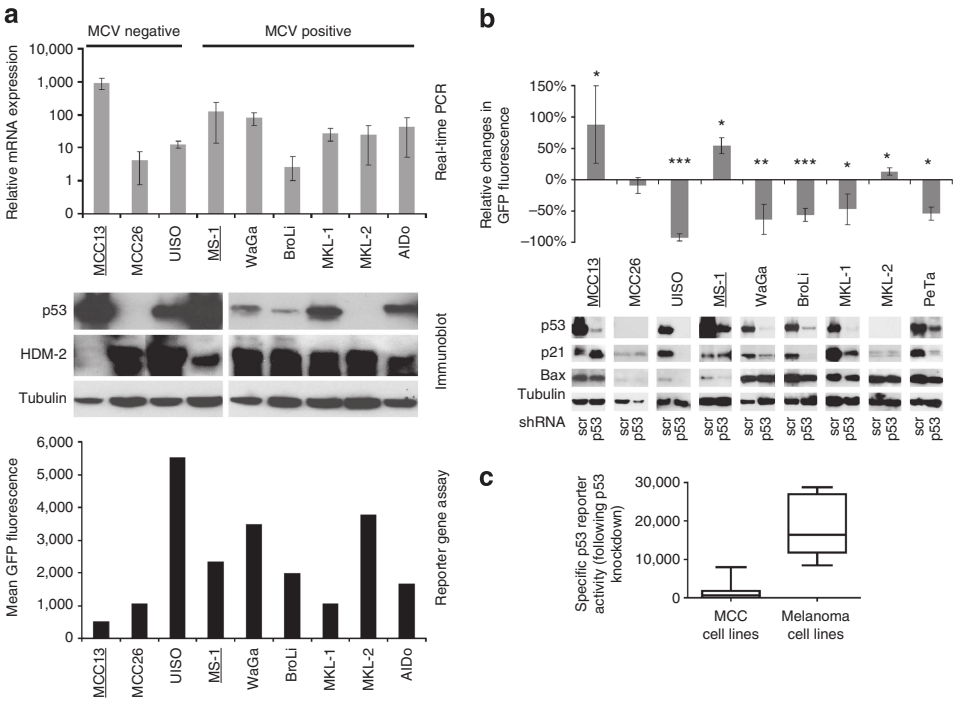

Figure 1. p53 expression and transcriptional activity in Merkel cell carcinoma (MCC) cell lines. (**a**) Upper bar graph: real-time PCR analysis of p53 mRNA relative to glyceraldehyde-3-phosphate dehydrogenase (GAPDH) depicted on a log scale. Immunoblot: p53 protein analysis. Lower bar graph: indicated MCC lines (p53 mutant lines underlined) were stably transduced with a p53 reporter construct expressing green fluorescent protein (GFP; pGreenFire). Mean GFP fluorescence was monitored by flow cytometry and normalized to the relative number of pGreenFire copies integrated into the cellular genome as determined by real-time PCR. (**b**) The cells were infected with short hairpin RNA (shRNA) expression constructs containing either a scrambled (scr) or a sequence targeting p53. Immunoblot: on day 4 after infection, total cell lysates were analyzed for the indicated proteins. Bar graph: mean GFP fluorescence of the scr control cells minus that of p53 knockdown cells (p53-specific GFP expression). Mean values (± SD) derived from at least three independent experiments are shown (statistics: one-sample *t*-test $*P<0.05$, $**P<0.005$, and $***P<0.0005$). (**c**) Box-and-whiskers plot: p53-specific GFP expression of seven p53 wild-type MCC cell lines compared with that of six p53 wild-type melanoma cell lines.

almost unchanged on application of the p53 shRNA, implying that in these cases GFP expression from the pGreenFire construct is not driven by p53. In contrast, in the remaining five p53 wild-type cell lines (UISO, WaGa, BroLi, MKL-1, and PeTa), GFP expression was at least partially p53 dependent. The p53-specific reporter gene activities in MCC lines, however, were low compared with the reporter gene activities found in p53 wild-type melanoma cell lines (Figure 1c). Nonetheless, p53 was observed to drive expression of its target gene p21 in all five p53 wild-type MCC lines, as p53 knockdown led to decreased p21 levels (Figure 1b). Obviously, however, p21 expression levels and p53 activity are not sufficient to effectively restrict growth of these proliferating tumor cells, evoking the question of what is limiting p53 activity in MCC.

MCC-derived MCV TAs do not repress p53 activity when overexpressed in cells with high endogenous p53 activity

Inhibition of p53 is a central feature of SV40 LT in transformation (Bargonetti *et al.*, 1992; Jiang *et al.*, 1993; Pipas and Levine, 2001). Truncated MCV LTs expressed in MCC cells, however, generally lack the C-terminal half of the protein and thereby the potential p53-binding domain (Shuda *et al.*, 2008; Sastre-Garau *et al.*, 2009). Nonetheless, the demonstration of p53 inhibiting activity for the N-terminus of SV40 LT (Quartin *et al.*, 1994; Rushton *et al.*, 1997) as well as for SV40 sT (Gjoerup *et al.*, 2000), and the recently published observation of p53 mutations only in LT-negative MCCs (Sihto *et al.*, 2011), argue for a role of the MCV TAs in repression of p53 in MCC.

To evaluate the capacity of the MCV TAs in inhibiting p53, we utilized two p53 wild-type melanoma cell lines with high p53-specific pGreenFire reporter gene activity (UACC-62 and Mel-U) as a model system. Importantly, GFP expression in these cells can almost completely be abrogated by p53 knockdown (data not shown). These cells were infected with a lentiviral expression vector encoding MCV TA^{LT279}* (sT and LT truncated at amino acid 279 resembling the stop codon position of the MCC line WaGa). An SV40 TA (sT and LT) expression construct encoding full-length SV40 LT was used for control purposes. Expression of the different LT proteins was confirmed by immunoblot (Figure 2a). The presence of SV40 TA as well as of MCC-derived MCV TA^{LT279}* stimulated cell cycle progression of the melanoma cell lines (data not shown). In SV40 TA–transduced cells, increased S-phase entry was accompanied by reduced p53 reporter gene activity, as expected. However, on expression of MCV TA^{LT279}*, the p53 reporter gene activity was elevated in both cell lines (Figure 2b). SV40 TA strongly increased p53 levels, as previously reported (Rushton *et al.*, 1997), whereas MCV TA^{LT279}* elevated p53 expression only moderately (Figure 2a and c). When p53 reporter gene activity is normalized to the p53 protein levels, it becomes clear that SV40 TA strongly suppresses p53 reporter gene activity, whereas MCC-derived MCV TA does not (Figure 2d). A major regulator of p53 expression and activity is human double minute (HDM-2 (Harris and Levine, 2005). Therefore, we analyzed whether ectopic TA expression would affect HDM-2 levels: HDM-2

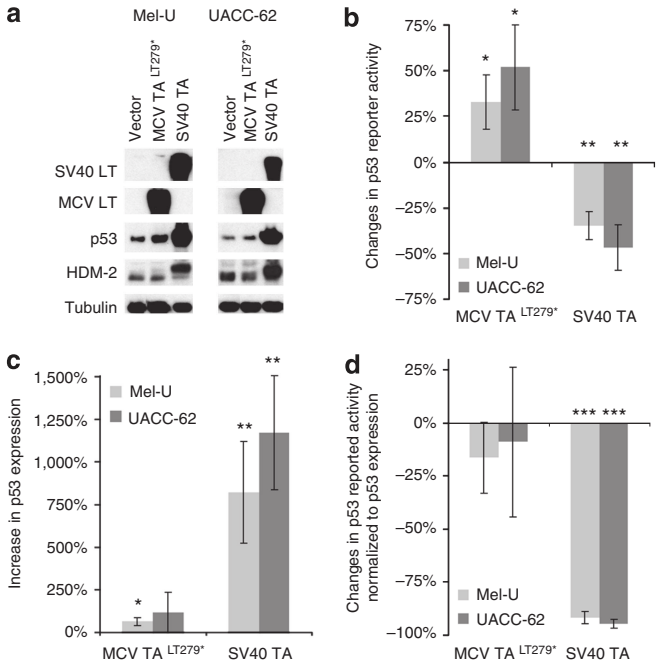

Figure 2. Overexpression of Merkel cell carcinoma (MCC)–derived Merkel cell polyoma virus (MCV) T antigens (TAs) does not repress p53. The indicated melanoma cell lines with high p53-specific green fluorescent protein (GFP) reporter gene expression were infected with the indicated lentiviral vectors containing simian virus 40 (SV40) or MCV TA gene, respectively. MCV TA^{LT279}* codes for MCV small T antigen (sT) and for MCV large T antigen (LT) truncated at amino acid 279, whereas SV40 TA contains wild-type sequences. (**a**) Immunoblot with cell lysates harvested 4 days after infection. (**b**) Changes in the mean GFP fluorescence measured on day 4. Mean values (±SD) from eight independent experiments are given. (**c**) Immunoblot signals for p53 relative to tubulin were quantified using the ImageJ software and data from five independent experiments. Mean values (±SD) are given. (**d**) Changes in p53 reporter expression normalized to p53 expression derived as described in **c**. *P<0.05, **P<0.005, and ***P<0.0005; one-sample t-test.

was strongly increased upon SV40 TA but was unaffected by MCV TA^{LT279}* expression (Figure 2a).

p53 transcriptional activity in MCC cells is not altered on knockdown of MCV TAs

To confirm the lack of impact of MCV TAs on p53, we analyzed p53 reporter gene activity following *knockdown* of the MCV TAs in five MCV-positive MCC lines. On application of an shRNA targeting LT and sT (Houben *et al.*, 2010), p53 reporter gene activity remained unchanged in three cell lines (WaGa, BroLi, and PeTa), whereas MKL-1 and MKL-2 displayed a small but statistically insignificant increase in GFP expression (Figure 3). Expression of p53 and—more importantly—expression of the p53 target genes p21, HDM-2, and Bax, however, was not elevated upon TA knockdown (Figure 3), suggesting that MCV sT and the truncated MCV LT do not repress p53 function in any of the five investigated cell lines. These findings together with the inability of overexpressed MCV TA^{LT279}* to suppress p53 activity (Figure 2) and the observation of a p53 mutation in the MCV-positive cell line MS-1 (Table 1) argue against an inhibition of the p53 pathway in MCV-positive MCCs by the MCV TAs.

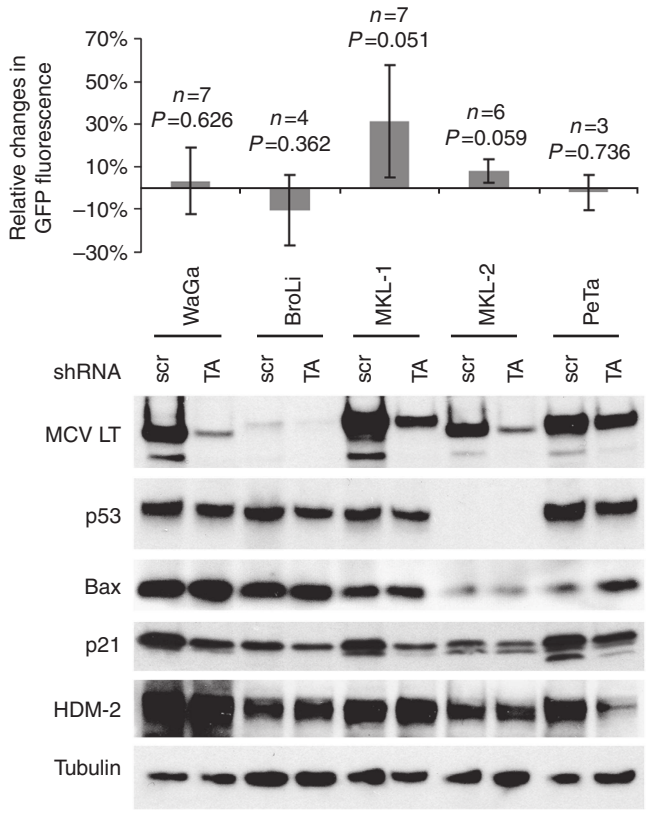

Figure 3. Knockdown of Merkel cell polyoma virus (MCV) T antigens (TAs) does not increase p53 activity in MCV-positive Merkel cell carcinoma (MCC) cells. The indicated MCC cell lines stably transduced with a p53 reporter construct (pGreenFire) were infected with a lentiviral short hairpin RNA (shRNA) vector targeting both T antigens (Houben *et al.*, 2010). On day 4 after infection, green fluorescent protein (GFP) total cell lysates were analyzed by immunoblot for the expression of the indicated proteins. Reporter gene expression was measured by flow cytometry. Mean values (±SD), number of independent experiments, and *P*-values of a one-sample *t*-test are annotated for all cell lines examined. HDM-2, human double minute 2; LT, large T antigen; scr, scrambled.

p53 is activated by Nutlin-3a in 5 out of 7 p53 wild-type MCC cell lines

Next we asked whether it is possible to reactivate p53 in MCC cells. In this respect we tested two compounds. Cisplatin is a DNA crosslinking antineoplastic agent frequently used for treatment of metastasized MCC that may activate p53 via the DNA damage response pathway (Tai *et al.*, 2000; Pectasides *et al.*, 2006; Pabla *et al.*, 2008). Nutlin-3a specifically inhibits the E3 ubiquitin ligase HDM-2 (Secchiero *et al.*, 2011) that is expressed in all analyzed MCC cell lines with the exception of MCC13 (Figure 1a). HDM-2 is the key player of several negative autoregulatory loops of p53 that, in the absence of p53-stabilizing signals, keep p53 levels low (Harris and Levine, 2005). HDM-2 promotes proteasomal degradation of the p53 protein through polyubiquitination of the C-terminus (Kubbutat *et al.*, 1997; Michael and Oren, 2003). Moreover, HDM-2 binding can affect p53 through direct repression of its transcriptional activity (Oliner *et al.*, 1993).

The p53 mutant cell line MCC13 was not affected by Nutlin3-a. In contrast, 5 out of 7 p53 wild-type cell lines (UISO, WaGa, BroLi, MKL-1, and PeTa) responded to Nutlin-3a treatment with increased GFP expression from the p53 reporter (Figure 4a), induction of p53 expression, and induction of at least two of the three p53 target proteins p21, Bax, and HDM-2 (Figure 4b). This corresponded with induction of cell cycle arrest in the MCV-negative cell line UISO and induction of apoptosis in the MCV-positive WaGa, BroLi, MKL-1, and PeTa, as indicated by an increased sub-G1 population in cell cycle analysis after 40 hours of Nutlin-3a treatment (Figure 4c, d and e). Induction of cell death by p53 reactivation distinguishes these MCC cell lines from many other p53 wild-type cancer cell lines that, although frequently responding with cell cycle arrest, are impaired in their apoptotic response to Nutlin-3a (Tovar *et al.*, 2006; Tseng *et al.*, 2010). The observed Nutlin-3a effects on MCC cells were mediated by p53, as p53 knockdown reverted Nutlin-3a-induced p53 reporter gene activity (data not shown) and prevented cell cycle arrest or apoptosis (Figure 4f). Therefore, repressed p53 activity due to HDM-2 activity might constitute a major factor for growth and survival of these MCC cells.

Cisplatin did not provoke a clearcut p53 response. Induction of p53 reporter gene activity was for most cell lines much less pronounced compared with Nutlin-3a (Figure 4a), there was no induction of the p53 target genes p21 and HDM-2 (Figure 4b), and—although the sub-G1 fraction was increased in all MCC cell lines (Figure 4e)—only in case of BroLi the induction of cell death was p53 dependent (Figure 4f). These results suggest that MCC cells have a general defect in activation of wild-type p53 by the DNA damage response pathway. This may be one of the reasons why this tumor entity frequently progresses without p53 mutations (Table 1 and see Van Gele *et al.*, 2000; Lassacher *et al.*, 2008) and it may contribute to the limited long-term efficacy of DNA-damaging agents and radiotherapy in advanced MCC (Voog *et al.*, 1999; Tai *et al.*, 2000; Poulsen *et al.*, 2003, 2006; Becker, 2010).

Neither Cisplatin nor Nutlin-3a treatment led to detectable p53 expression in MCC26 and MKL-2 cells (Figure 4b). Therefore, the strict repression of p53 expression in these two cell lines does not appear to be mediated by HDM-2. As p53 mRNA is expressed in both cell lines (Figure 1a and Table 1) either inhibition of p53 translation (e.g., by RNPC1; Zhang *et al.*, 2011) or HDM-2-independent degradation of p53 are possible mechanisms for its repression. The latter may play a role for MCC26 as incubation with the proteasome inhibitor bortezomib provoked a weak p53 band in immunoblot analysis and a 3-fold increase in GFP expression from the p53 reporter construct (data not shown).

Induction of p53 protein upon HDM-2 knockdown in four of five Nutlin-3a-sensitive MCC cell lines

Although Nutlin-3a is regarded to be a highly selective molecule targeting the HDM-2/p53 interaction (Patton *et al.*, 2006), inhibitor experiments always bear the risk to provoke unspecific effects not related to the targeted protein. Therefore, we aimed to complement the Nutlin-3a results by HDM-2 knockdown experiments. Application of an HDM-2 shRNA in the five cell lines responding with p53 activation to Nutlin-3a

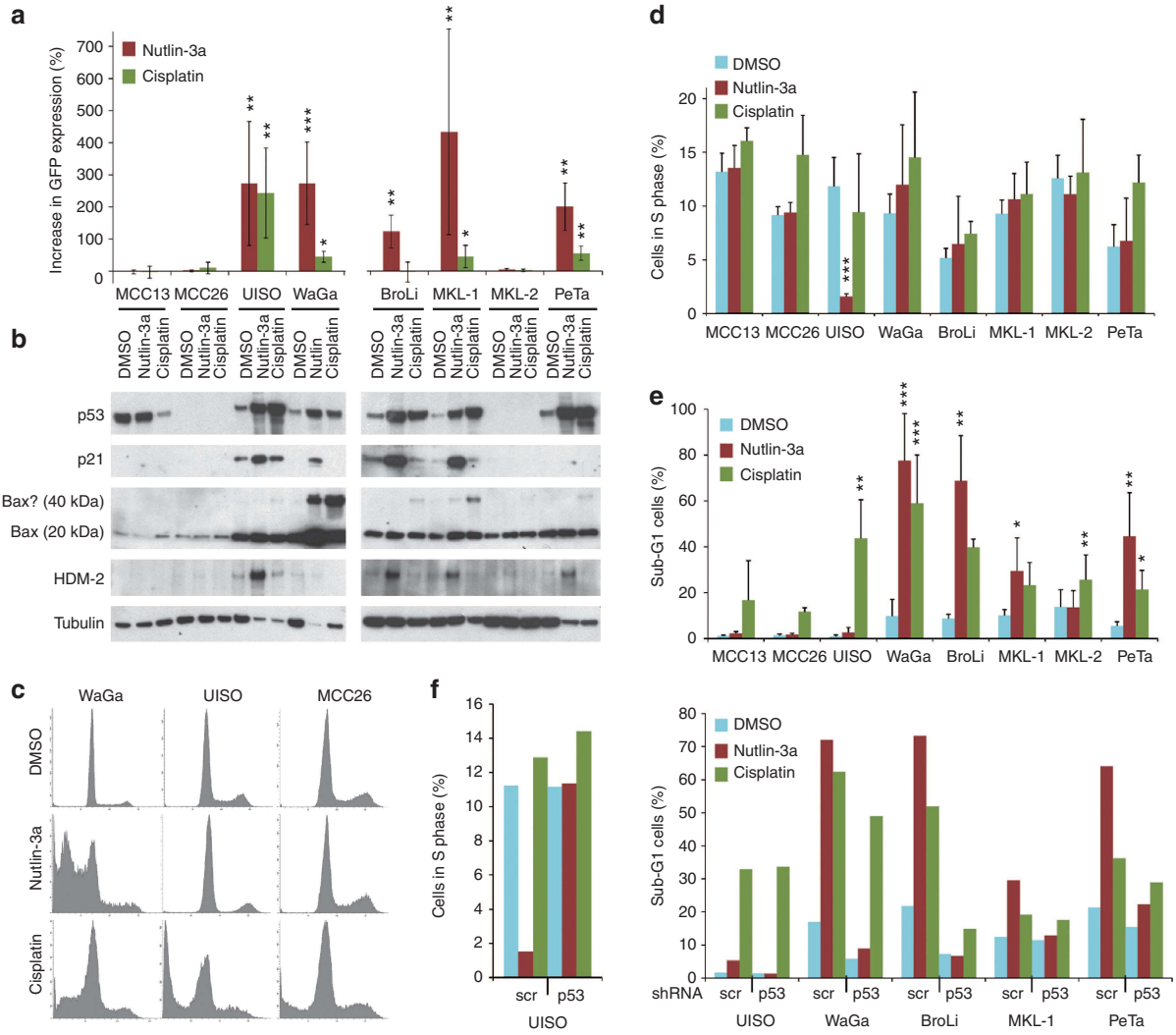

Figure 4. Induction of p53-dependent apoptosis or cell cycle arrest by Nutlin-3a. The indicated cells stably transduced with a green fluorescent protein (GFP) p53 reporter construct were treated with 10 μM Nutlin-3a or 10 μg ml^{-1} Cisplatin. After 24 hours, cells were analyzed by flow cytometry for GFP expression and cell lysates were subjected to immunoblot analysis. Cell cycle analysis was performed after 40 hours of treatment. (**a**) Changes in GFP expression relative to control cells are given (mean values (±SD) of at least five experiments). (**b**) Immunoblot analyzing of the indicated proteins. (**c**) Examples of histogram plots from the cell cycle analysis. (**d**, **e**) Mean values (±SD) of at least five experiments for cells in S or sub-G1, respectively. (**f**) Results of the cell cycle analysis of cells treated with Nutlin-3a or Cisplatin 4 days after infection with a lentiviral short hairpin RNA (shRNA) vector either targeting p53 or expressing a scrambled (scr) control shRNA. *P<0.05, **P<0.005, and ***P<0.0005. (**a**) One-sample t-test. (**d**, **e**) Repeated measures analysis of variance (ANOVA).

let to induction of p53 and the p53 target p21 in WaGa, PeTa, BroLi, and UISO (Figure 5), confirming that p53 in these cell lines is controlled by HDM-2. Moreover, HDM-2 knockdown like Nutlin-3a treatment provoked significant apoptosis in WaGa, BroLi, and PeTa cells (Figure 5). In contrast, in MKL-1 cells we could not induce any sign of p53 activation with the HDM-2 shRNA. This, as well as the fact that in the other cell lines induction of p53 expression is not as pronounced as on Nutlin-3a treatment, is likely due to less efficient and less synchronous repression of HDM-2 function by the shRNA compared with Nutlin-3a.

Conclusion

In summary, we demonstrate that expression and activity of p53—which is frequently wild type in MCC—is not repressed by the MCV TAs but can be restored by HDM-2 antagonism. This p53 reactivation induces cell cycle arrest or apoptosis in the majority of MCC cell lines. Therefore, p53 reactivation by inhibition of HDM-2 may be a possible future therapeutic approach. Phase-I clinical trials using the Nutlin-3a-related compound RG7112 for treatment of hematologic malignancies (nCT00623870) and solid tumors (nCT00559533) are currently ongoing (http://www.clinicaltrials.gov/). A clinically approved HDM-2 inhibitor will hopefully become available in the future.

MATERIALS AND METHODS

Ethics statement

This study was conducted according to the Declaration of Helsinki Principles and approved by the institutional review board of Würzburg University Hospital (Ethikkommission der Medizinischen Fakultät der Universität Würzburg; sequential study number 124/05).

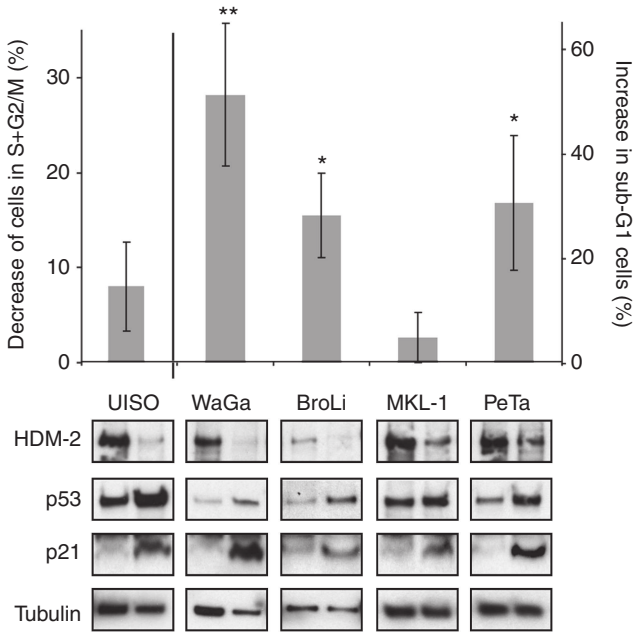

Figure 5. Induction of p53 and apoptosis by HDM-2 (human double minute 2) knockdown in WaGa, BroLi, and PeTa cells. The indicated Merkel cell carcinoma (MCC) cell lines were infected with a lentiviral short hairpin RNA (shRNA) vector targeting HDM-2. After 4 days, total cell lysates were harvested and subjected to immunoblot analysis. At the same time point, cell cycle analysis was performed; in the graphs the increase of cells in S + G2/M phase and sub-G1 cells are displayed for UISO or WaGa, BroLi, MKL-1, and PeTa, respectively. Mean values (± SD) of at least three independent experiments are given. *$P<0.05$ and **$P<0.005$; one-sample *t*-test.

Cell culture

A series of cell lines from patients with histologically confirmed MCC was established in our departments, including PeTa, AlDo, HeRo, KaRi, and WoWe, as well as BroLi, WaGa, and LoKe. Procedures for establishment of the three latter cell lines have been described previously (Houben *et al.*, 2010, 2012b). All cell lines mentioned as well as MKL-1 (Shuda *et al.*, 2008), MKL-2, and MS-1 (Houben *et al.*, 2010) harbor MCV DNA. In contrast, UISO (Ronan *et al.*, 1993), MCC13 (Leonard *et al.*, 1995), and MCC 26 (Van Gele *et al.*, 2002) are MCV negative. MCC lines were grown in RPMI-1640 supplemented with 10% fetal calf serum, 100 U ml^{-1} penicillin, and 0.1 mg ml^{-1} streptomycin.

Sequence analysis of p53 exons 5–8

Genomic DNA was extracted from the different MCC cell lines and subjected to seminested PCR using the primers previously reported (Houben *et al.*, 2011). The amplicons were sequenced by Sanger sequencing.

Lentiviral p53 reporter gene assay and shRNA transfer

To establish cells with an integrated p53 reporter gene, the lentiviral vector pGreenFire (System Biosciences, Mountain View, CA) was used that codes for puromycin resistance and GFP under the control of a p53-responsive element (4 × 5′-CGACATGCCCGGGCATGT-3′). Knockdown of p53 or MCV TA expression was achieved by lentiviral shRNA expression constructs described previously (Houben *et al.*, 2010, 2011). For overexpression of TAs in melanoma cell lines carrying a GFP p53 reporter, a wild-type SV40 TA gene (Lin and Simmons, 1991) or an MCV TA gene carrying a stop codon mutation at codon 279 (Houben *et al.*, 2012a) were cloned into the vector pCDHred. This was done to allow identification of the infected cells within a GFP-expressing population. pCDHred was derived from the vector pCDH-CMV-MCS-EF1-copGFP (System Biosciences) by replacing the copGFP sequence with a turboRFP. Infectious viruses were raised by transfecting HEK293T cells and target cells were infected as previously described (Houben *et al.*, 2012a). Pure populations carrying the pGreenFire reporter were selected by culturing the cells in the presence of puromycin. GFP expression from the reporter was analyzed by flow cytometry. The relative presence of the reporter constructs in the genomic DNA of the selected cells was analyzed by real-time PCR and calculated relative to the highly repetitive DNA elements LINE1 using the $\Delta\Delta C_t$ method.

Immunoblot

Cells were lysed in RIPA buffer, protein concentration was determined and equal amounts of protein were resolved by SDS-PAGE. Immunoblotting was performed as described previously (Houben *et al.*, 2012a). The following primary antibodies were applied: MCV LT (CM2B4), p53 (D-01), p21 (C-19), HDM-2 (SMP14; all from Santa Cruz Biotechnology, Santa Cruz, CA), Bax (2D2) (eBioscience, San Diego, CA), SV40 LT (Abcam, Cambridge, MA), and tubulin (Sigma-Aldrich, Taufkirchen, Germany).

Cell cycle analysis

DNA was stained with propidium iodide as described previously (Houben *et al.*, 2007). Analysis of the cellular DNA content was performed on a FACSCanto flow cytometer (Becton Dickinson, Heidelberg, Germany).

CONFLICT OF INTEREST

The authors state no conflict of interest.

ACKNOWLEDGMENTS

This study was funded by the Wilhelm-Sander-Stiftung (2007.057.3). We thank Johanna Kobler, Claudia Siedel, and Daria Lisicki for excellent technical assistance.

REFERENCES

Bargonetti J, Reynisdottir I, Friedman PN *et al.* (1992) Site-specific binding of wild-type p53 to cellular DNA is inhibited by SV40 T antigen and mutant p53. *Genes Dev* 6:1886–98

Becker JC (2010) Merkel cell carcinoma. *Ann Oncol* 21(Suppl 7):vii81–5, vii81-vii85

Blagosklonny MV (1997) Loss of function and p53 protein stabilization. *Oncogene* 15:1889–93

Cheng J, DeCaprio JA, Fluck MM *et al.* (2009) Cellular transformation by Simian Virus 40 and Murine Polyoma Virus T antigens. *Semin Cancer Biol* 19:218–28

Feng H, Shuda M, Chang Y *et al.* (2008) Clonal integration of a polyomavirus in human Merkel cell carcinoma. *Science* 319:1096–100

Gjoerup O, Chang Y (2010) Update on human polyomaviruses and cancer. *Adv Cancer Res* 106:1–51

Gjoerup O, Chao H, DeCaprio JA *et al.* (2000) pRB-dependent, J domain-independent function of simian virus 40 large T antigen in override of p53 growth suppression. *J Virol* 74:864–74

Green DR, Chipuk JE (2006) p53 and metabolism: Inside the TIGAR. *Cell* 126:30–2

Harris SL, Levine AJ (2005) The p53 pathway: positive and negative feedback loops. *Oncogene* 24:2899–908

Hodgson NC (2005) Merkel cell carcinoma: changing incidence trends. *J Surg Oncol* 89:1–4

Houben R, Adam C, Baeurle A *et al.* (2012a) An intact retinoblastoma protein-binding site in Merkel cell polyomavirus large T antigen is required for promoting growth of Merkel cell carcinoma cells. *Int J Cancer* 130:847–56

Houben R, Grimm J, Willmes C *et al.* (2012b) Merkel cell carcinoma and Merkel cell polyomavirus: evidence for hit-and-run oncogenesis. *J Invest Dermatol* 132:254–6

Houben R, Hesbacher S, Schmid CP *et al.* (2011) High-level expression of wild-type p53 in melanoma cells is frequently associated with inactivity in p53 reporter gene assays. *PLoS One* 6:e22096

Houben R, Ortmann S, Schrama D *et al.* (2007) Activation of the MAP kinase pathway induces apoptosis in the Merkel cell carcinoma cell line UISO. *J Invest Dermatol* 127:2116–22

Houben R, Shuda M, Weinkam R *et al.* (2010) Merkel cell polyomavirus-infected Merkel cell carcinoma cells require expression of viral T antigens. *J Virol* 84:7064–72

Jiang D, Srinivasan A, Lozano G *et al.* (1993) SV40 T antigen abrogates p53-mediated transcriptional activity. *Oncogene* 8:2805–12

Kubbutat MH, Jones SN, Vousden KH (1997) Regulation of p53 stability by Mdm2. *Nature* 387:299–303

Lassacher A, Heitzer E, Kerl H *et al.* (2008) p14ARF hypermethylation is common but INK4a-ARF locus or p53 mutations are rare in Merkel cell carcinoma. *J Invest Dermatol* 128:1788–96

Lavin MF, Gueven N (2006) The complexity of p53 stabilization and activation. *Cell Death Differ* 13:941–50

Lemos B, Nghiem P (2007) Merkel cell carcinoma: more deaths but still no pathway to blame. *J Invest Dermatol* 127:2100–3

Leonard JH, Dash P, Holland P *et al.* (1995) Characterisation of four Merkel cell carcinoma adherent cell lines. *Int J Cancer* 60:100–7

Levine AJ (2009) The common mechanisms of transformation by the small DNA tumor viruses: The inactivation of tumor suppressor gene products: p53. *Virology* 384:285–93

Lin JY, Simmons DT (1991) The ability of large T antigen to complex with p53 is necessary for the increased life span and partial transformation of human cells by simian virus 40. *J Virol* 65:6447–53

Michael D, Oren M (2003) The p53-Mdm2 module and the ubiquitin system. *Semin Cancer Biol* 13:49–58

Oliner JD, Pietenpol JA, Thiagalingam S *et al.* (1993) Oncoprotein MDM2 conceals the activation domain of tumour suppressor p53. *Nature* 362:857–60

Pabla N, Huang S, Mi QS *et al.* (2008) ATR-Chk2 signaling in p53 activation and DNA damage response during cisplatin-induced apoptosis. *J Biol Chem* 283:6572–83

Patton JT, Mayo LD, Singhi AD *et al.* (2006) Levels of HdmX expression dictate the sensitivity of normal and transformed cells to Nutlin-3. *Cancer Res* 66:3169–76

Pectasides D, Pectasides M, Psyrri A *et al.* (2006) Cisplatin-based chemotherapy for merkel cell carcinoma of the skin. *Cancer Invest* 24:780–5

Petitjean A, Mathe E, Kato S *et al.* (2007) Impact of mutant p53 functional properties on TP53 mutation patterns and tumor phenotype: lessons from recent developments in the IARC TP53 database. *Hum Mutat* 28:622–9

Pipas JM, Levine AJ (2001) Role of T antigen interactions with p53 in tumorigenesis. *Semin Cancer Biol* 11:23–30

Poulsen M, Rischin D, Walpole E *et al.* (2003) High-risk Merkel cell carcinoma of the skin treated with synchronous carboplatin/etoposide and radiation: a Trans-Tasman Radiation Oncology Group Study–TROG 96:07. *J Clin Oncol* 21:4371–6

Poulsen MG, Rischin D, Porter I *et al.* (2006) Does chemotherapy improve survival in high-risk stage I and II Merkel cell carcinoma of the skin? *Int J Radiat Oncol Biol Phys* 64:114–9

Quartin RS, Cole CN, Pipas JM *et al.* (1994) The amino-terminal functions of the simian virus 40 large T antigen are required to overcome wild-type p53-mediated growth arrest of cells. *J Virol* 68:1334–41

Rodig SJ, Cheng J, Wardzala J *et al.* (2012) Improved detection suggests all Merkel cell carcinomas harbor Merkel polyomavirus. *J Clin Invest* 122:4645–53

Roemer K (1999) Mutant p53: gain-of-function oncoproteins and wild-type p53 inactivators. *Biol Chem* 380:879–87

Ronan SG, Green AD, Shilkaitis A *et al.* (1993) Merkel cell carcinoma: in vitro and in vivo characteristics of a new cell line. *J Am Acad Dermatol* 29:715–22

Rushton JJ, Jiang D, Srinivasan A *et al.* (1997) Simian virus 40 T antigen can regulate p53-mediated transcription independent of binding p53. *J Virol* 71:5620–3

Sastre-Garau X, Peter M, Avril MF *et al.* (2009) Merkel cell carcinoma of the skin: pathological and molecular evidence for a causative role of MCV in oncogenesis. *J Pathol* 218:48–56

Secchiero P, Bosco R, Celeghini C *et al.* (2011) Recent advances in the therapeutic perspectives of Nutlin-3. *Curr Pharm Des* 17:569–77

Sherr CJ (2006) Divorcing ARF and p53: an unsettled case. *Nat Rev Cancer* 6:663–73

Shuda M, Feng H, Kwun HJ *et al.* (2008) T antigen mutations are a human tumor-specific signature for Merkel cell polyomavirus. *Proc Natl Acad Sci USA* 105:16272–7

Sihto H, Kukko H, Koljonen V *et al.* (2011) Merkel cell polyomavirus infection, large T antigen, retinoblastoma protein and outcome in Merkel cell carcinoma. *Clin Cancer Res* 17:4806–13

Song H, Xu Y (2007) Gain of function of p53 cancer mutants in disrupting critical DNA damage response pathways. *Cell Cycle* 6:1570–3

Soussi T (2007) p53 alterations in human cancer: more questions than answers. *Oncogene* 26:2145–56

Tai PT, Yu E, Winquist E *et al.* (2000) Chemotherapy in neuroendocrine/Merkel cell carcinoma of the skin: case series and review of 204 cases. *J Clin Oncol* 18:2493–9

Tovar C, Rosinski J, Filipovic Z *et al.* (2006) Small-molecule MDM2 antagonists reveal aberrant p53 signaling in cancer: implications for therapy. *Proc Natl Acad Sci USA* 103:1888–93

Tseng HY, Jiang CC, Croft A *et al.* (2010) Contrasting effects of nutlin-3 on TRAIL- and docetaxel-induced apoptosis due to upregulation of TRAIL-R2 and Mcl-1 in human melanoma cells. *Mol Cancer Ther* 9:3363–74

Van Gele M, Kaghad M, Leonard JH *et al.* (2000) Mutation analysis of P73 and TP53 in Merkel cell carcinoma. *Br J Cancer* 82:823–6

Van Gele M, Leonard JH, Van RN *et al.* (2002) Combined karyotyping, CGH and M-FISH analysis allows detailed characterization of unidentified chromosomal rearrangements in Merkel cell carcinoma. *Int J Cancer* 101:137–45

van Oijen MG, Slootweg PJ (2000) Gain-of-function mutations in the tumor suppressor gene p53. *Clin Cancer Res* 6:2138–45

Voog E, Biron P, Martin JP *et al.* (1999) Chemotherapy for patients with locally advanced or metastatic Merkel cell carcinoma. *Cancer* 85:2589–95

Vousden KH, Lu X (2002) Live or let die: the cell's response to p53. *Nat Rev Cancer* 2:594–604

Wischhusen J, Melino G, Weller M (2004) p53 and its family members – reporter genes may not see the difference. *Cell Death Differ* 11:1150–2

Zhang J, Cho SJ, Shu L *et al.* (2011) Translational repression of p53 by RNPC1, a p53 target overexpressed in lymphomas. *Genes Dev* 25:1528–43

RB1 is the crucial target of the Merkel cell polyomavirus Large T antigen in Merkel cell carcinoma cells

Sonja Hesbacher[1,*], Lisa Pfitzer[1,2,*], Katharina Wiedorfer[1], Sabrina Angermeyer[1], Andreas Borst[1], Sebastian Haferkamp[3], Claus-Jürgen Scholz[4], Marion Wobser[1], David Schrama[1], Roland Houben[1]

[1]Department of Dermatology, Venereology und Allergology, University Hospital Würzburg, Würzburg, Germany

[2]Department of Pharmacy, Center for Drug Research, University of Munich (Ludwigs-Maximilians-Universität), Munich, Germany

[3]Department of Dermatology, University of Regensburg, Regensburg, Germany

[4]Core Unit Systems Medicine, University of Würzburg, Würzburg, Germany

[*]These authors have contributed equally to this work

Correspondence to: *Roland Houben,* ***e-mail:*** *Houben_R@ukw.de*

Keywords: *Merkel cell carcinoma, polyomavirus, Large T antigen, retinoblastoma protein, viral carcinogenesis*

Received: *November 09, 2015* ***Accepted:*** *March 28, 2016* ***Published:*** *April 18, 2016*

ABSTRACT

The pocket protein (PP) family consists of the three members RB1, p107 and p130 all possessing tumor suppressive properties. Indeed, the PPs jointly control the G1/S transition mainly by inhibiting E2F transcription factors. Notably, several viral oncoproteins are capable of binding and inhibiting PPs. Merkel cell polyomavirus (MCPyV) is considered as etiological factor for Merkel cell carcinoma (MCC) with expression of the viral Large T antigen (LT) harboring an intact PP binding domain being required for proliferation of most MCC cells. Therefore, we analyzed the interaction of MCPyV-LT with the PPs. Co-IP experiments indicate that MCPyV-LT binds potently only to RB1. Moreover, MCPyV-LT knockdown-induced growth arrest in MCC cells can be rescued by knockdown of RB1, but not by p107 or p130 knockdown. Accordingly, cell cycle arrest and E2F target gene repression mediated by the single PPs can only in the case of RB1 be significantly reverted by MCPyV-LT expression. Moreover, data from an MCC patient indicate that loss of *RB1* rendered the MCPyV-positive MCC cells LT independent. Thus, our results suggest that RB1 is the dominant tumor suppressor PP in MCC, and that inactivation of RB1 by MCPyV-LT is largely sufficient for its growth supporting function in established MCPyV-positive MCC cells.

INTRODUCTION

Several members of the polyomaviridae family (e.g. Simian Virus 40 (SV-40)) are capable of inducing tumor formation in animal models [1, 2], and the potential of SV40 to transform their host cells has been ascribed to the expression of viral oncoproteins, i.e. the T antigens (TA) [3]. Up to date, however, the Merkel Cell Polyomavirus (MCPyV) described in 2008 is the polyomavirus that is widely accepted to be causal for a human malignancy, namely Merkel Cell Carcinoma (MCC) [4, 5].

MCC is a highly aggressive skin cancer, and although it is relatively rare its incidence is increasing considerably [6]. Notably, in the vast majority of MCCs the MCPyV genome can be detected [7-9], and the observed clonal integration of the virus in the genome of the tumor cells [5] implies the causal relationship between MCPyV and MCC. This is further sustained by the addiction of MCPyV-positive MCC cells to expression of the T antigens [10], particularly due to a dependence on Large T antigen (LT) for MCC cell growth [11]. Interestingly, MCC-associated LTs are, due to stop codon mutations or pre-mature integration break points, generally truncated deleting the C-terminus required for viral replication but always preserving the LxCxE motif found in many proteins which interact with pocket proteins (PPs) [12, 13].

The PP family comprises three members, i.e. the Retinoblastoma protein 1 (RB1) and the two RB-like proteins p107 (RBL1) and p130 (RBL2). The family name refers to their binding 'pockets' mediating interaction with

a multitude of other proteins [14]. All PPs bind to and thus regulate the activity of transcription factors of the E2F family. These interactions are regarded as central in controlling cell cycle progression from G1 to S phase [15]. Regulation of G1/S transition by PPs and E2Fs is a complex and at least partially redundant interplay of activator E2Fs (E2F-1, E2F-2, E2F-3a) preferentially binding RB1 and repressor E2Fs (E2F-3b, E2F-4, E2F-5) interacting with one or more of the PPs [16]. In normal quiescent cells, the PPs bound to E2Fs repress transcription of E2F-dependent promoters by different mechanisms; e.g. by recruiting histone deacetylases (HDACs) [17]. Upon phosphorylation by cyclin/cyclin-dependent kinase (CDK) complexes in late G1 PPs dissociate from their E2F partners, leading to transcription of S phase-specific genes [15].

Besides phosphorylation by CDKs, the suppressive function of the PPs can be halted by different viral proteins, such as HPV-E7, Ad-E1A and SV40-LT [18]. The binding of these oncoproteins via the conserved LxCxE motif results in disruption of repressive complexes of PPs with E2F family members leading to enhanced proliferation, and can thereby contribute to induction of cell transformation [18, 19].

Our previous finding, that the rescue of a TA knockdown-induced growth inhibition in MCC cells by ectopically expressed MCPyV-LT is dependent on an intact LxCxE motif suggested that PP inactivation is a critical function of MCPyV-LT in MCC [11]. Thus, here we address the questions which PPs are essential to be targeted by MCPyV-LT in MCC cells, and whether PP inactivation is sufficient for the growth promoting function of this viral protein in its natural tumor host cells. We provide evidence that inactivation of only RB1 by MCPyV-LT is essential and largely sufficient for supporting growth of MCC cells.

RESULTS

Homozygous deletion of the *RB1* gene in an MCPyV-positive cell line not depending on MCPyV-LT expression

In a first set of experiments we determined the expression of the pocket proteins in MCPyV-positive MCC cell lines. Real time quantitative PCR revealed that all PPs are expressed in almost all cell lines with generally higher mRNA levels for *p107* and *p130* than for *RB1* (Figure 1a). The only exception was the cell line LoKe for which no *RB1* expression could be detected. Notably, LoKe, although encoding a functional truncated MCPyV-LT [20], is up to date the only MCPyV-positive MCC cell line tested which is not dependent on LT expression for cell growth [21]. Immunoblot analysis confirmed the expression of all PPs in all other cell lines as well as the lack of RB1 expression in LoKe (Figure 1b).

Since real time PCR with genomic DNA suggested that lack of RB1 expression is due to a loss of the *RB1* gene (data not shown), we performed a comparative genomic hybridization for LoKe. This analysis revealed several genomic aberrations, with the relevant one being a very sharp homozygous deletion of the genomic region 13q14.2 (Figure 1c; basepairs 48.816.847 – 50.073.157 according to assembly GRCh37.p13) affecting only *RB1* and 10 additional genes (*CAB39L, CDADC1, CYSLTR2, FNDC3A, ITM2B, LPAR6, MLNR, PHF11, RCBTB2, SETDB2*).

The cell line LoKe was generated from a patient with metastatic MCC. Thus, to explore whether loss of RB1 had occurred after integration of MCPyV during tumor progression, we analyzed a metastasis excised at the time when the cell line LoKe was established and the primary tumor excised 3 years before. Real time PCR revealed largely reduced presence of the *RB1* gene in both tumors suggesting that at least the majority of tumor cells had lost both RB1 alleles. Immunohistochemistry on tissue sections revealed that in the metastasis all tumor cells were negative for RB1, in line with loss of both alleles of the *RB1* gene (Figure 1d). In contrast, in the primary tumor RB1 expression was heterogeneous with most parts lacking RB1 entirely (Figure 1d upper panel) while some minor areas demonstrated RB1 expression in a subset of tumor cells (Figure 1d middle panel). Sequencing of MCPyV-LT in genomic DNA derived from the primary tumor and several different metastases (including those analysed by immunohistochemistry) revealed that they all harboured the same unique stop codon present in the LoKe cell line (GenBank: KJ128381.1) implying that they are all clonally related.

MCPyV-LT knockdown can largely be rescued by RB1 knockdown

The LoKe cell line is characterized by loss of RB1 and independence of LT expression. In addition, analysis of the coding sequence of p107 and p130 demonstrated that both proteins are not affected by mutations (data not shown). These results suggest that inactivation of RB1 – but not the two other pocket proteins – is an essential function of MCPyV-LT in MCC cells. Consequently, to test whether RB1 inactivation might even be sufficient to substitute functionally for MCPyV-LT we performed shRNA knockdown experiments targeting MCPyV-LT and the different PP family members in MCC cells. To this end, we used the MCPyV-positive cell lines MKL-1, WaGa, BroLi and MKL-2 stably transduced with TA.shRNA.tet, a vector allowing Doxycycline (Dox)-inducible expression of an shRNA targeting all MCPyV-T antigen mRNAs [11]. We utilized the TA.shRNA instead of a LT-specific shRNA because the only effective LT-targeting shRNA exerts considerable off-target effects [11]. The TA.shRNA.tet cells were then stably transduced with a second shRNA

vector constitutively expressing either a scrambled (Scr) or a shRNA targeting RB1. In addition, in the cell lines MKL-1 and WaGa shRNAs targeting p107 or p130 were applied in combination with the TA.shRNA to specifically analyze the role of all PP family members. Reduced expression of the PPs in response to the respective shRNA as well as Dox-induced knockdown of LT in these cell lines was monitored by immunoblot (Figure 2).

The impact of the shRNAs on growth properties of MCC cell lines was then analyzed by flow cytometry in mixed cultures of double-infected, green fluorescent und uninfected parental cells on the basis of GFP expression driven by the TA.shRNA.tet vector. Dox-induced LT-knockdown was associated with growth inhibition of cells expressing additionally the control Scr shRNA, indicated by a gradual loss of GFP-positive cells over time (Figure 2). In all four tested cell lines additional knockdown of RB1, however, resulted in a partial (WaGa, MKL-2) or even an almost complete rescue (MKL-1, BroLi) of impaired cell growth (Figure 2). For the interpretation of these data two of our previous observations are of importance. First, the TA shRNA induced growth arrest can be rescued to the same extent by an LT cDNA as by a TA gene (coding for sT and LT) indicating that with this experimental system we evaluate only LT functions although the applied TA shRNA also targets sT [20, 22]. Second, in the cell line WaGa the rescue by TA or LT is incomplete demonstrating a similar

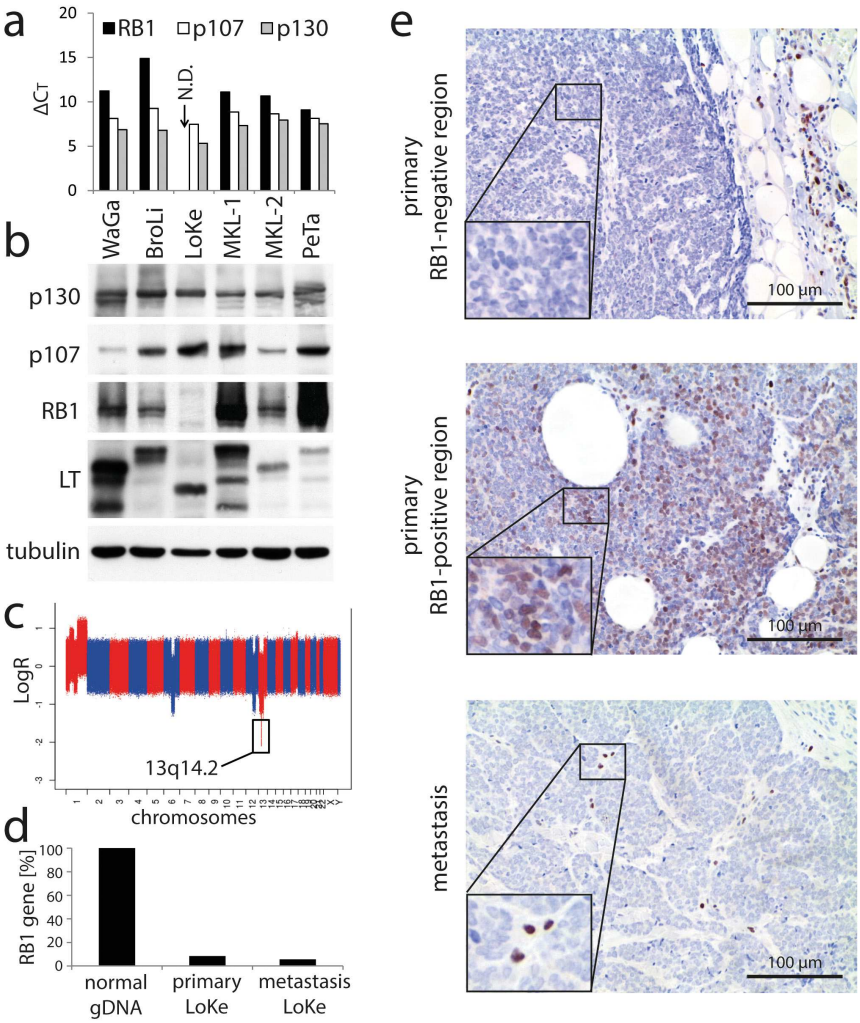

Figure 1: Loss of RB1 in the MCPyV-positive MCC cell line LoKe which is not depending on MCPyV-LT expression. a. mRNA expression levels of the three PP family members were determined in the indicated cell lines by real-time PCR. ΔC_T-values relative to the house keeping gene *RPLP0* (high values indicate low expression) are given. N.D.: not detectable. **b.** Immunoblot analysis of the PP protein expression levels in the indicated MCPyV-positive MCC cell lines. **c.** Microarray derived whole-genome copy number profile of the cell line LoKe, with x-axis coordinate representing positions along the genome. **d.** Relative quantification of the *RB1* gene by real time PCR in genomic DNA derived from the primary MCC tumor and in a subsequent metastasis of the respective patient excised 3 years later at the time when the LoKe cell line was derived from pleural effusion. Normal genomic DNA served as control. **e.** Immunohistochemical staining for RB1 in tissue sections of the two LoKe tumors described in d. Two different regions of the primary tumor are depicted.

rescue activity as achieved by RB1 knockdown (Figure 2; [20, 22]). Hence, it is likely that the TA shRNA exerts growth inhibiting off-target effects in WaGa. Interestingly, RB1 and p130 are induced upon TA shRNA induction (Figure 2) potentially contributing to the incomplete rescue. In summary, RB1 loss is almost sufficient to substitute for MCPyV-LT in the cell lines WaGa, MKL-1 and BroLi and at least partially capable to rescue the loss of LT in MKL-2 cells. In contrast, knockdown of p107 or p130 did not affect the growth inhibition induced by LT knockdown in WaGa and MKL-1 cells (Figure 2).

To further evaluate these findings, and to exclude the possibility that paracrine effects distort proliferation measurements in the mixed culture assay [23], cell cycle analyses were performed in MKL-1 and WaGa cells following TA and RB1 knockdown. In accordance with the results of the mixed culture assay, TA shRNA-induced reduction of cells in S and G2/M phase could significantly be reversed by additional knockdown of RB1 (Figure 3a and 3b). Moreover, quantitative RT-PCR experiments revealed that TA shRNA-induced cell cycle arrest was associated with reduced expression of cell cycle related

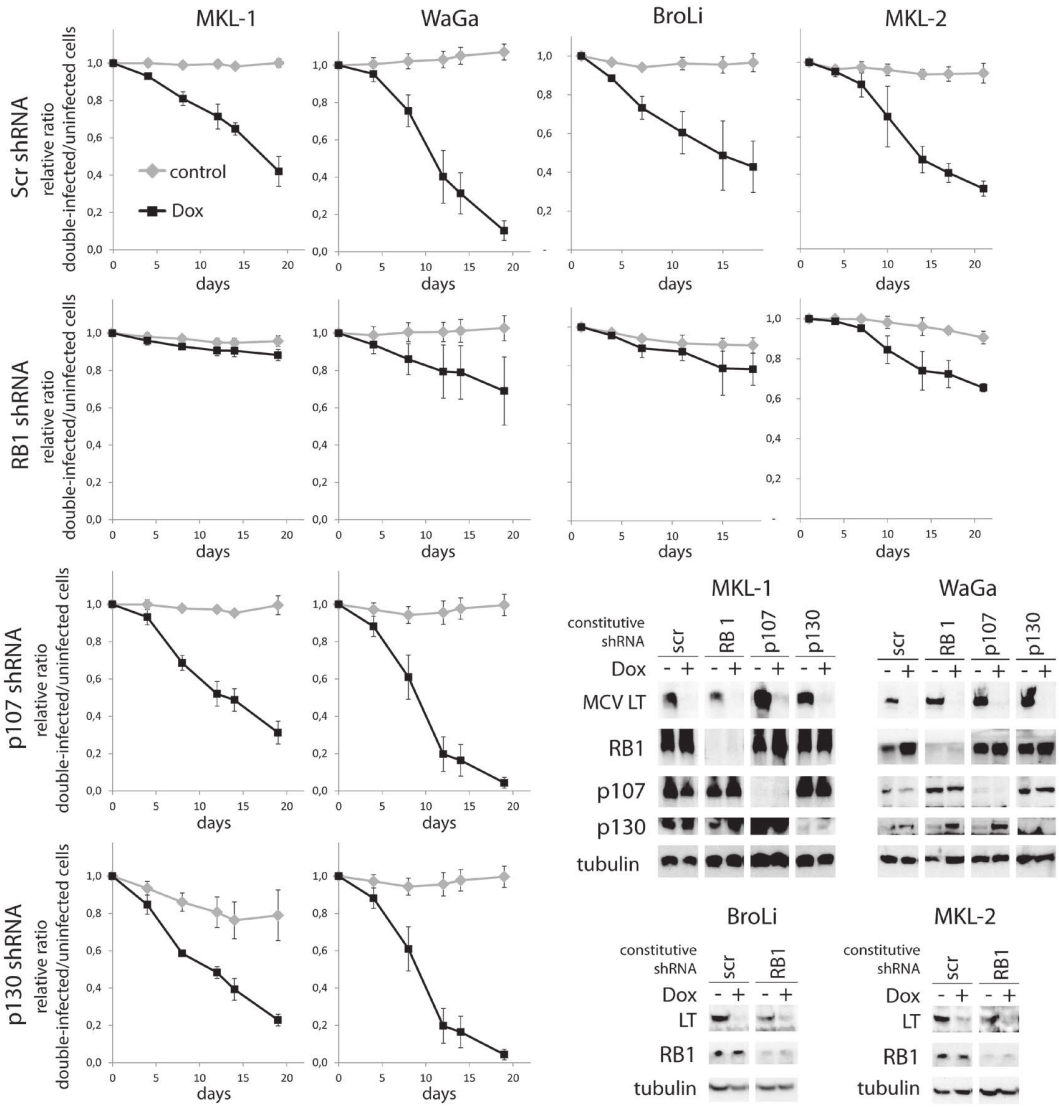

Figure 2: MCPyV-LT knockdown induced growth inhibition can be rescued by RB1 knockdown. MCPyV positive cell lines MKL-1, WaGa, BroLi and MKL-2 transduced with a Dox-inducible TA.shRNA.tet vector system were infected with lentiviral shRNA constructs targeting RB1 (all cell lines), p107 or p130 (MKL-1 and WaGa). A Scr shRNA served as control. Pure populations infected with the PP shRNA constructs were established by antibiotic selection. Following 5 days of Dox treatment total cell lysates were harvested and analyzed by immunoblot for expression of MCPyV-LT and the different PPs. To evaluate changes in cellular growth, mixed populations of double-shRNA-infected cells characterized by green fluorescent expression and parental cells were cultured in presence or absence of Dox and changes of ratios were measured over time by flow cytometry. Mean values (+/- SD) of at least 3 independent experiments are depicted.

RB1 target genes *CCNB1, MYB*, *PLK1* and *CDC6* while upon additional knockdown of RB1 expression levels were hardly affected (Figure 3c).

Strict overlap of genes regulated by MCPyV-LT and RB1 in MCC cells

To further scrutinize the extent RB1 inactivation can compensate for TA knockdown with respect to gene expression in MCC cells, we performed NanoString nCounter™ gene expression analyses [24]. To this end, the expression of 245 cancer related genes (+ 6 endogenous controls) was determined for mRNA derived from WaGa cells upon TA.shRNA expression. These cells were additionally stably transduced with either a construct coding for an shRNA-insensitive TA gene [11], with the RB1 shRNA or with the respective control vectors (cDNA vector; Scr shRNA). 90 genes demonstrating very low expression (less than 25 copies) were excluded from the analysis of differential expression upon TA.shRNA expression since for very rare mRNAs variability due to technical issues can be expected to be rather high [24]. From the remaining 155 cancer genes 21 gene demonstrated a more than 2-fold alteration in expression upon induced TA knock down, either downregulation (13 genes) or upregulation (8 genes), respectively (Figure 4). For all these 21 genes the TA.shRNA-induced changes were reversed by either TA re-expression or shRNA-mediated RB1 inactivation (Figure 4). Most of the genes downregulated following TA knockdown (e.g. *BIRC5 (survivin), BLM, CDC25a, BRCA 1 and 2, MYBL2, CCNA2, RAD54L, HHMR, TYMS*) have previously been described as E2F

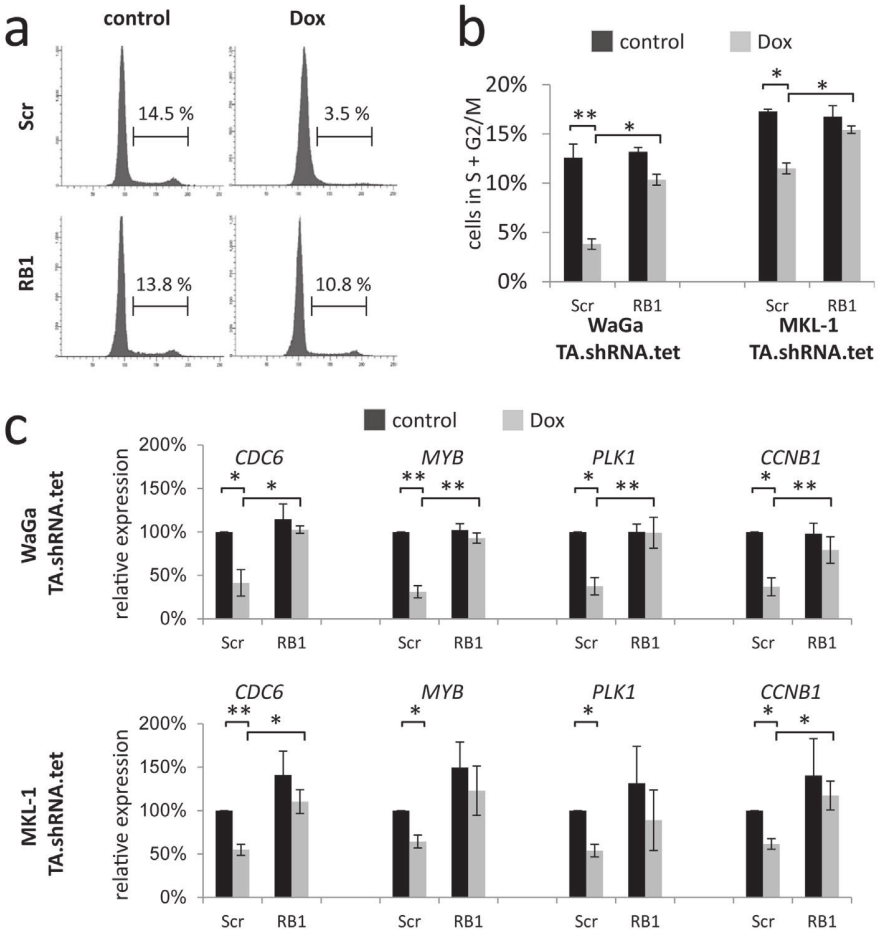

Figure 3: RB1 knockdown reverses TA knockdown-induced cell cycle arrest and E2F target gene repression. WaGa and MKL-1 cells double infected with inducible TA-shRNA and constitutive Scr- or RB1-shRNA expression constructs were cultured for 5 days in the absence or presence of Dox. **a** and **b.** Fixed cells were stained with propidium iodide and DNA content was determined by flow cytometry. a) Examples of cell cycle profiles for WaGa. b) Depiction of the percentage of cells with >2N DNA. Bars represent mean values (+/- SD) of at least 3 independent experiments. **c.** Relative expression levels of the indicated cell cycle-related RB target genes were determined by real-time PCR and the $\Delta\Delta C_T$ method. *RPLP0* served as endogenous control for normalization and Scr shRNA-infected cells without Dox treatment were used as calibrator. Mean values (+/- SD) of 3 independent experiments are depicted. Statistical analyses were performed using paired student's t-test. (**p<0.005; *p<0.05).

and/or RB1 target genes [25-28], a notion sustained by the observed re-expression upon RB1 knockdown (Figure 4). Others however, and in particular some of the genes upregulated upon TA.shRNA application (e.g. *PLAUR, FGFR3, TIMP3*) do not belong to the well established RB1 target genes. Nevertheless, re-expression upon RB1 knockdown suggests that these genes are at least indirectly regulated by RB1 in WaGa. Importantly, the observation that expression of every gene differentially expressed upon TA knockdown could be reversed by RB1 knockdown further supports that RB1 inactivation is the predominant function of truncated MCPyV-LT in MCC cells.

MCPyV-LT preferentially interacts with RB1

Our finding that RB1 inactivation is sufficient to rescue MCPyV-TA knockdown induced growth inhibition of MCPyV-positive MCC cells is surprising for two reasons. First, redundant functions of the PPs have been shown in many aspects, (e.g. unrestricted growth of fibroblasts can only be achieved by inactivation of all three pocket proteins [29]) and second, the related SV40-LT has been demonstrated to be capable of binding and inhibiting all three pocket proteins [30, 31]. Since the binding capacity of MCPyV-LT to RB1 is established [12, 32], we wondered whether MCPyV-LT can also bind to p107 and p130. Hence, transient co-expression of His-tagged versions of the three pocket proteins and V5-tagged SV40-LT or MCPyV-LT^{278} in 293T cells was followed by immunoprecipitations with an anti-His-tag antibody. As expected, SV40-LT co-immunoprecipitated with all three pocket proteins. In contrast, MCPyV-LT^{278} demonstrated a selective binding to RB1 (Figure 5a).

MCPyV-LT fails to inhibit functionality of p107 and p130

A lack of co-immunoprecipitation cannot formally proof the absence of interaction between two proteins. We thus analyzed next whether MCPyV-LT is able to functionally interfere with the PPs. To address this question in a model system that allows unequivocal distinction of the different PPs, we utilized mouse embryonic fibroblasts derived from animals in which all

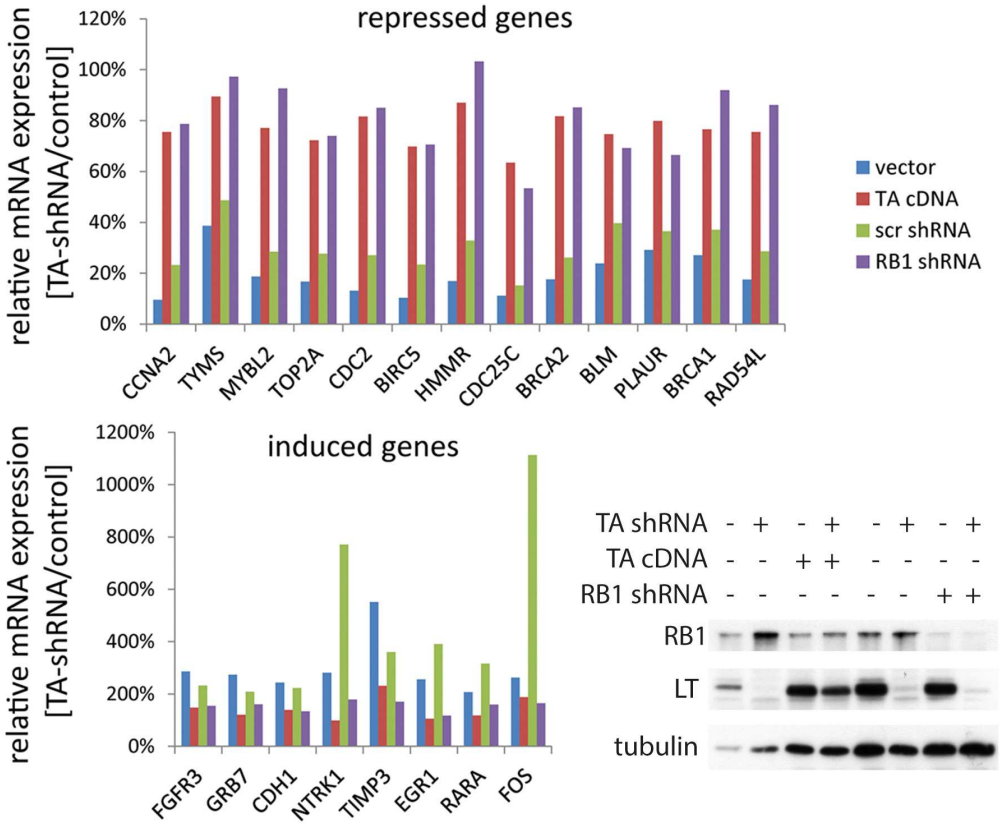

Figure 4: Overlap of genes regulated by MCPyV-TA and RB1 in MCC cells. TA-shRNA was expressed in WaGa cells stably transduced with either empty vector, vector coding for MCPyV-TA, a Scr-shRNA vector or an RB1-shRNA construct. After 5 days LT and RB1 protein levels were analyzed by immunoblot, and mRNA expression levels of 245 cancer related genes were analyzed using the NanoString nCounter™ gene expression system [24]. 90 genes were excluded from further analysis due to very low expression. The absolute expression values of the remaining 155 genes were normalized to the mean value of the 6 house keeping genes. Depicted are the relative mRNA expression levels, i.e. TA-shRNA expressing cells relative to their controls, of the 21 genes displaying a more than two fold change in the empty vector and the Scr-shRNA cells.

three PP genes have been knocked out (MEF-TKO) [29] engineered for Dox-inducible expression of MCPyV-LT[278] (Figure 5b). Ectopic expression of p107, p130 or RB1 in these cells (Figure 5b and Supplementary Figure S1) led to a partial cell cycle arrest (Figure 5c and 5d) as well as to reduced expression of the E2F target genes *MYBL2*, *CCNB1* and *MKI67* (Figure 5e). Upon induction of MCPyV-LT RB1-induced cell cycle arrest and gene repression were significantly reversed while MCPyV-LT did not affect the p107- and p130-induced effects (Figure 5c and 5d).

DISCUSSION

The causal relation between MCPyV and MCC is widely accepted [33]. In this regard, although one study suggested that MCPyV is present in all MCCs [9], several other investigations imply that the entity MCC – as diagnosed by classical criteria – can be stratified into MCPyV-positive and MCPyV-negative cases [34-38]. Due to discrepancies in some of these reports it is not yet clear if the presence of the viral genome impacts clinical outcome of the disease. However, concerning molecular

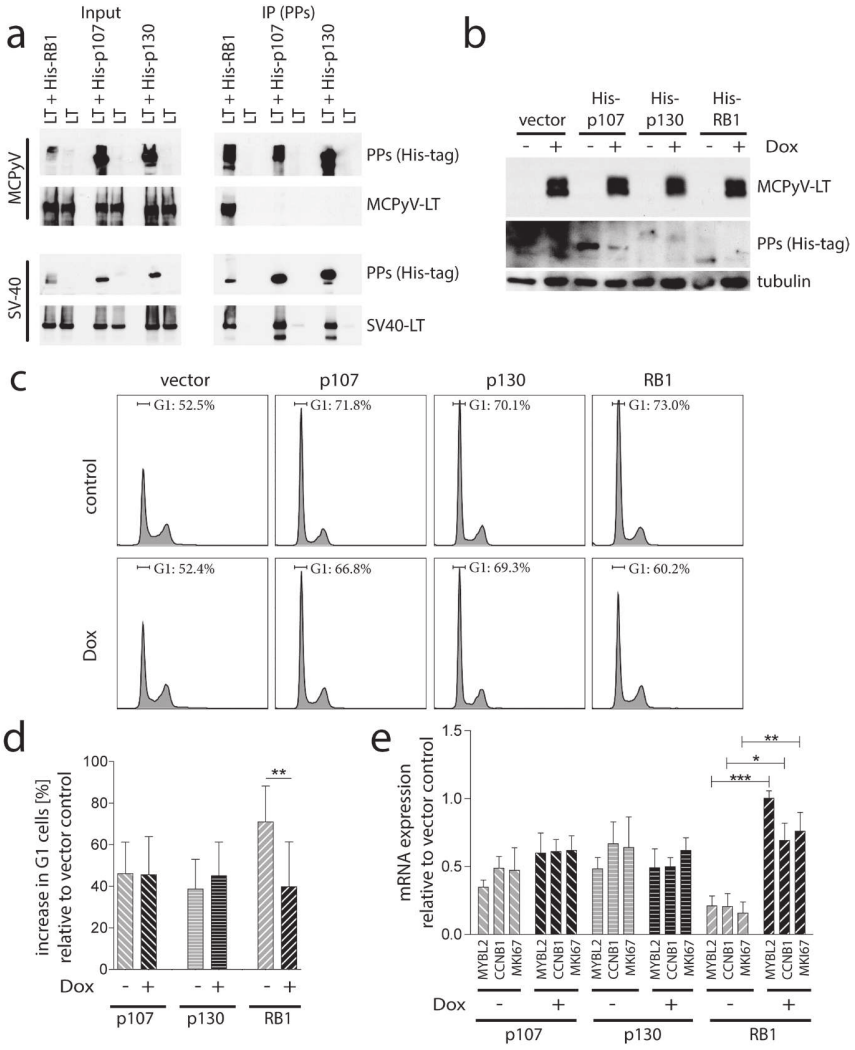

Figure 5: Preferential binding and inactivation of RB1 by MCPyV-LT a. Co-immunoprecipitation. His-tagged PPs were co-expressed with V5-tagged MCPyV-LT[278] or SV40-LT in 293T cells. After 24 hours RB1 was immunoprecipitated with a His-tag-antibody. Co-immunoprecipitation of the LT proteins was analyzed by immunoblot using a V5-antibody. **b, c** and **d.** PP triple knockout mouse embryonic fibroblasts (MEF-TKO) [29] were manipulated for Dox-inducible expression of V5-tagged MCPyV-LT[278]. His-tagged versions of the different PPs were lentivirally transferred and 14 h later Dox-treatment was started. 24 hours later cells were fixed or lysed. b) Total cell lysates were subjected to immunoblot analysis using an α-His-antibody for detection of the PPs and an α-V5-antibody for the LT proteins c and d) Fixed cells were stained with propidium iodide and the percentage of cells in G1 was determined by flow cytometry. c) Representative cell cycle profiles are depicted. d) Mean values (±SD; n=6) of the increase in G1 cells relative to the vector control are displayed. **e.** Relative expression levels of the indicated E2F target genes were determined by real-time PCR. *muRPL37* served as endogenous control. Mean values (±SD; n=3) of the expression level relative to the vector control cells are depicted. Statistical analyses were performed using paired student's t-test. (***p<0.0005; **p<0.005; *p<0.05).

differences, several recent sequencing studies consistently reported that MCPyV-negative MCCs in contrast to MCPyV-positive cases are characterized by frequent deletions/mutations of the *RB1* gene [39-41]. Thus, RB1 inactivation seems to be an essential step in MCC development with inactivation occurring either genetically or in MCPyV-positive tumors by expression of a truncated LT with a generally preserved RB binding site [12, 13]. In the related SV40-LT this binding site contributes to LT's capability to inactivate all three pocket protein members, i.e. RB1, p130 and p107 [42].

MCPyV-LT, however, seems to discriminate between the different PPs. This is supported by our co-IP experiments in 293T cells as well as our functional data derived from co-expression of PPs and MCPyV-LT in triple PP knockout cells. We observed preferential binding of MCPyV-LT to RB1 compared to the two other PP family members, and demonstrated also a differential capability to interfere functionally with the different PPs. Indeed, co-expression of truncated MCPyV-LT can reverse cell cycle arrest and E2F target gene expression induced by RB1, but not the effects induced by p107 or p130 in MEF-TKO cells. This restricted interaction capacity with PPs distinguishes MCPyV-LT from LTs encoded by other polyomaviruses. Indeed, SV40-LT has the potential to abrogate RB1- as well as p130- and p107-induced gene repression and cell cycle arrest in $RB1^{-/-}$ Saos cells [43]. Moreover, also LT proteins from the human JC and BK polyomaviruses have been demonstrated to bind to all three PPs [44, 45]. Interestingly JC-LT exhibits the highest affinity for p107 while RB1 binding is relatively weak [45].

The observed preferential binding of RB1 by MCPyV-LT further expands the list of described differences such as that i) LT from MCPyV does not possess transforming capacity in fibroblast assays in contrast to e.g. SV40 (Shuda *et al.*, 2011) and ii) MCPyV-LT lacks a CKII consensus sequence at an important phosphorylation site which is present in SV40 and all human polyomaviruses harbouring an RB1 binding site (Schrama *et al.*, 2015). Differences between LT from MCPyV and those of SV40, JC and BK might reflect their assignment to different phylogenetic clades with MCPyV grouping with polyomaviruses found in chimpanzee, gorilla and bats [46].

In contrast to the many cellular interaction partners described for the well-studied SV40-LT [42], the number of proteins identified to interact with MCPyV-LT, i.e. RB1, HSC-70, Brd4 and Vam6p, is limited [12, 47-49]. Importantly, our findings in the current study suggest that in the natural tumor host cells MCPyV inactivation of RB1 appears to be the predominant and in some MCC cell lines the only essential function of MCPyV-LT to support growth of these cells. Indeed, knockdown of RB1 led in the tested MCPyV-positive MCC cell lines to a rescue of LT-knockdown-induced E2F target gene repression and more importantly, to a reversion of LT-knockdown-induced cell growth inhibition. The importance of the RB1-LT interaction is further sustained by a recent report: revealing that the overwhelming majority of MCPyV-LT induced gene expression alterations require the intact LxCxE binding motif [50].

Our findings on cell culture level pointing to a restricted but important interaction of MCPyV-LT with RB1 is supported by clinical findings. For example, LoKe is up to now the only studied MCPyV-positive MCC cell line not depending on expression of the viral LT protein despite the presence of an MCC-typical LT mutation preserving the RB binding motif. This suggests that LT and the RB-binding domain were required at some point during carcinogenesis [21]. The observed homozygous loss of the *RB1* gene in LoKe cells seems to render them independent of MCPyV-LT expression. The expression of wild type p107 and p130 in LoKe thus implies that inactivation of RB1 – but not the two other PPs – is an essential function of MCPyV-LT in MCC cells. Assuming equivalent molecular mechanisms in all MCCs, this is in line with the fact that inactivation of p107 and p130 in MCPyV-negative MCCs has not been reported [39, 40, 51]. Indeed, neither homozygous deletion/mutation of p107 and p130 nor mutation/copy number variations of upstream factors like $p16^{INK4A}$, CDK4 or Cyclin D – which are common features of many tumor types [52] – have been described.

Regarding the molecular history of the MCPyV-LT-independent MCPyV-positive cell line LoKe co-presence of RB1 and MCPyV-LT in a portion of the neoplastic cells of the respective primary MCC tumor suggests that integration of MCPyV into the genome of the tumor cells preceded homozygous loss of RB1.

Although being essential for growth of established RB1 expressing MCC cells the role of MCPyV-LT in malignant transformation has not been finally established. In contrast to SV40-LT, MCPyV-LT is not transforming in fibroblast assays. Indeed, transforming capacity has been demonstrated only for MCPyV-sT so far, and could not be enhanced by MCPyV-LT [53]. In accordance, MCPyV-TA cannot induce a fully malignant phenotype in mouse models [54]. Fibroblast transformation *in vitro*, as well as induction of hyperproliferative lesions in mouse models by MCPyV-sT has been demonstrated to be dependent on a region called the LT stabilization domain, which is mediating the inhibition of different E3 ligases. Inactivation of protein phosphatase A the major function of SV40-sT seems not to be relevant [53, 55, 56]. Therefore, our observation that MCPyV-LT in contrast to SV40-LT - besides not binding p53 directly [32, 57] - discriminates between the different pocket proteins adds only one more piece to the puzzle of distinct features of these two oncogenic polyomaviruses.

These differences between SV40-LT and MCPyV-LT certainly contribute to their transforming capacity. In

this regard, in some cellular systems inactivation of all three PPs is required to allow unrestricted growth [29]. Accordingly, many tumors require a broad disruption of the PP/E2F pathway by e.g. activation of cyclin-dependent kinases or inactivation of cyclin dependent kinase inhibitors [14]. MCC, however, seems to belong to a group of tumors, like small cell lung cancer and retinoblastoma in which inactivation of only RB1 is sufficient to allow tumor formation [52, 58]. The limited ability of MCPyV-LT to interfere with p107 and p130 may, therefore, account for a limited subset of cell types being transformable by MCPyV. Besides other factors (e.g. virus tropism) this may contribute to the fact that only the rare MCC and some subsets of chronic lymphocytic leukemia [59, 60] have been reported to be associated with this omnipresent virus. Finally, our data suggest that inactivation of RB1 is the only crucial function of MCPyV-LT to support growth of MCC cells.

MATERIALS AND METHODS

Ethics statement

This study was conducted according to the principles of the Declaration of Helsinki and analysis of patient derived samples was approved by the Institutional Review Board of Würzburg University Hospital (Ethikkommission der Medizinischen Fakultät der Universität Würzburg; sequential study number 124/05).

Cell culture

The cell lines analyzed in this study include the MCPyV-positive MCC cell lines LoKe [21], PeTa [61], WaGa, BroLi, MKL-2 (all described in [10]) and MKL-1 [62] as well as the triple PP knock out mouse embryonic fibroblasts (MEF-TKO) [29]. HEK-293T cells were used for lentivirus production and for co-immunoprecipitation assays. All cell lines were grown in RPMI 1640 supplemented with 10% FCS, 100 U/ml penicillin and 0.1 mg/ml streptomycin. MEF-TKO cell were directly obtained from the lab were the cells were generated and characterized [29] and were not passaged for more than 6 months. All MCC cell lines as well as the HEK-293T cells were authenticated by STR profiling. Moreover, the MCC cell lines are routinely checked by sequencing for the presence of the characteristic Large T truncating mutations, which lead to a distinct molecular weight of the protein detectable by immune blotting (Figure 1).

Vectors

For inducible knockdown of MCPyV-LT, we used the lentiviral single vector TA.shRNA.tet allowing constitutive GFP expression and Doxycycline (Dox)-inducible expression of an shRNA targeting all transcripts derived from the MCPyV early region [11]. For constitutive knockdown shRNA sequences targeting RB1, p107 or p130 (see Supplementary Table S1) were cloned into the lentiviral vector pGreenPuro. For Dox-inducible LT expression we used the two vector system Lenti-X Tet-On-3G (Clontech) with the cloning vector pLVX-Tre3G-IRES allowing inducible expression of two cDNAs from an internal ribosomal entry site (IRES)-containing transcript. Truncated MCPyV-LT^{278} was cloned into the cloning site preceding the IRES and GFP was inserted downstream of the IRES.

Lentiviral infection

Lentiviral supernatants were produced in HEK293T cells using three (pRSV rev, pHCMV-G and pMDLg/pRRE) helper plasmids. Harvested virus supernatant was sterile filtered (0.45 µm) and polybrene was added (1 µg/ml) for infection. After 14-20 h incubation target cells were washed twice with medium and subjected to antibiotic selection.

Mixed cell culture assay

Constitutive GFP expression from the TA.shRNA.tet construct was used to compare the growth behavior of double-infected and uninfected cells: TA.shRNA.tet cells were mixed with approximately 20% of untransduced cells, and changes in the frequency of GFP-positive TA.shRNA cells were recorded by flow cytometry over time.

Cell cycle analysis

Cell were fixated in ice cold EtOH, treated with propidium iodide mix (PBS+ 1% FCS + 0.1 mg/ml propidium iodide + 0.1 mg/ml RNAse A) at 37°C for 1 h and analyzed by flow cytometry.

Real time PCR

Total RNA was isolated with peqGOLD Total RNA Kit (PeqLab) and reverse transcribed using the Superscript II RT First Strand Kit (Invitrogen). Real time PCR was conducted in the ABI 7500 Fast Real-Time PCR cycler (Applied Biosystems) using a SYBR Green I Low Rox Mastermix (Eurogentec GmbH) and the respective primers (Supplementary Table S2). Following a 10 min denaturing step at 95°C 40 cycles with 15 seconds 95°C and 1 min 60°C were applied. Primer sequences and PCR efficiencies are given in Supplementary Table S2.

Comparative genomic hybridization

DNA from MCC cell lines was hybridized to Affymetrix SNP 6.0 arrays, and data analysis was carried out with the Bioconductor package "copynumber". Microarray data has been deposited at Gene Expression Omnibus (GSE73879).

Immunohistochemistry

Three-micrometer sections of formalin fixed and paraffin embedded tumor tissues were stained as previously described [11] with an antibody targeting RB1 (G3-245; BD Pharmingen).

NanoString nCounter™ gene expression analysis

100 ng total RNA were subjected to hybridization with the Nanostring Cref Kit (Cancer-Kit) containing probes for 245 cancer related gene products and the mRNAs of 6 house keeping genes. Following nCounter digital reading the values were normalized to the mean value of the house keeping genes.

Immunoblotting

Immunoblotting was performed as previously described [11] The primary antibodies used in this study were directed against RB1 (G3-245; BD Pharmingen), p107 (sc-318; Santa Cruz), p130 (sc-317; Santa Cruz) MCPyV-LT (CM2B4; Santa Cruz), the V5 tag (SV5-Pk1; Abcam), His-tag (D3I1O; Cell Signaling) or β-tubulin (TUB 2.1; Sigma-Aldrich).

Co-immunoprecipitation

293T cells were co-transfected with expression constructs coding for 6xHis tagged PPs and V5-tagged MCPyV-LT^{278} or V5-tagged SV40-LT. 24 hours after transfection cell lysates were harvested and Co-Immunoprecipitation was performed as recently described [63].

Statistics

Student t test was performed with GraphPad Prism 5.03 software.

ACKNOWLEDGMENTS

We are grateful to Julien Sage for providing the MEF-TKO cells.

CONFLICTS OF INTEREST

The authors declare no conflicts of interest.

GRANT SUPPORT

The study was supported by the German Research Foundation (HO5280/2-1). CJS was supported by the Interdisziplinäres Zentrum für Klinische Forschung Würzburg (IZKF Z-6).

REFERENCES

1. Stewart SE, Eddy BE and Borgese N. Neoplasms in mice inoculated with a tumor agent carried in tissue culture. Journal of the National Cancer Institute. 1958; 20:1223-1243.
2. Eddy BE, Stewart SE, Young R and Mider GB. Neoplasms in hamsters induced by mouse tumor agent passed in tissue culture. Journal of the National Cancer Institute. 1958; 20:747-761.
3. Black PH, Rowe WP, Turner HC and Huebner RJ. A Specific Complement-Fixing Antigen Present in Sv40 Tumor and Transformed Cells. Proceedings of the National Academy of Sciences of the United States of America. 1963; 50:1148-1156.
4. Chang Y and Moore PS. Merkel cell carcinoma: a virus-induced human cancer. Annual review of pathology. 2012; 7:123-144.
5. Feng H, Shuda M, Chang Y and Moore PS. Clonal integration of a polyomavirus in human Merkel cell carcinoma. Science. 2008; 319:1096-1100.
6. Fitzgerald TL, Dennis S, Kachare SD, Vohra NA, Wong JH and Zervos EE. Dramatic Increase in the Incidence and Mortality from Merkel Cell Carcinoma in the United States. The American surgeon. 2015; 81:802-806.
7. Kassem A, Schopflin A, Diaz C, Weyers W, Stickeler E, Werner M and Zur HA. Frequent detection of Merkel cell polyomavirus in human Merkel cell carcinomas and identification of a unique deletion in the VP1 gene. Cancer Res. 2008; 68:5009-5013.
8. Becker JC, Houben R, Ugurel S, Trefzer U, Pfohler C and Schrama D. MC polyomavirus is frequently present in Merkel cell carcinoma of European patients. J Invest Dermatol. 2009; 129:248-250.
9. Rodig SJ, Cheng J, Wardzala J, Dorosario A, Scanlon JJ, Laga AC, Martinez-Fernandez A, Barletta JA, Bellizzi AM, Sadasivam S, Holloway DT, Cooper DJ, Kupper TS, Wang LC and DeCaprio JA. Improved detection suggests all Merkel cell carcinomas harbor Merkel polyomavirus. JClinInvest. 2012; 122:4645-4653.
10. Houben R, Shuda M, Weinkam R, Schrama D, Feng H, Chang Y, Moore PS and Becker JC. Merkel cell polyomavirus-infected Merkel cell carcinoma cells require expression of viral T antigens. J Virol. 2010; 84:7064-7072.
11. Houben R, Adam C, Baeurle A, Hesbacher S, Grimm J, Angermeyer S, Henzel K, Hauser S, Elling R, Brocker EB, Gaubatz S, Becker JC and Schrama D. An intact retinoblastoma protein-binding site in Merkel cell polyomavirus large T antigen is required for promoting growth of Merkel cell carcinoma cells. IntJ Cancer. 2012; 130:847-856.

12. Shuda M, Feng H, Kwun HJ, Rosen ST, Gjoerup O, Moore PS and Chang Y. T antigen mutations are a human tumor-specific signature for Merkel cell polyomavirus. ProcNatlAcadSciUSA. 2008; 105:16272-16277.
13. Schmitt M, Wieland U, Kreuter A and Pawlita M. C-terminal deletions of Merkel cell polyomavirus large T-antigen, a highly specific surrogate marker for virally induced malignancy. IntJCancer. 2012; 131:2863-2868.
14. Giacinti C and Giordano A. RB and cell cycle progression. Oncogene. 2006; 25:5220-5227.
15. Cobrinik D. Pocket proteins and cell cycle control. Oncogene. 2005; 24:2796-2809.
16. Chen HZ, Tsai SY and Leone G. Emerging roles of E2Fs in cancer: an exit from cell cycle control. Nat RevCancer. 2009; 9:785-797.
17. Harbour JW and Dean DC. Chromatin remodeling and Rb activity. Current opinion in cell biology. 2000; 12:685-689.
18. Felsani A, Mileo AM and Paggi MG. Retinoblastoma family proteins as key targets of the small DNA virus oncoproteins. Oncogene. 2006; 25:5277-5285.
19. An P, Saenz Robles MT and Pipas JM. Large T antigens of polyomaviruses: amazing molecular machines. Annual review of microbiology. 2012; 66:213-236.
20. Houben R, Angermeyer S, Haferkamp S, Aue A, Goebeler M, Schrama D and Hesbacher S. Characterization of functional domains in the Merkel cell polyoma virus Large T antigen. IntJCancer. 2015; 136:E290-E300.
21. Houben R, Grimm J, Willmes C, Weinkam R, Becker JC and Schrama D. Merkel cell carcinoma and Merkel cell polyomavirus: evidence for hit-and-run oncogenesis. J Invest Dermatol. 2012; 132:254-256.
22. Angermeyer S, Hesbacher S, Becker JC, Schrama D and Houben R. Merkel cell polyomavirus-positive Merkel cell carcinoma cells do not require expression of the viral small T antigen. JInvest Dermatol. 2013; 133:2059-2064.
23. Shuda M, Chang Y and Moore PS. Merkel Cell Polyomavirus Positive Merkel Cell Carcinoma Requires Viral Small T Antigen For Cell Proliferation. JInvest Dermatol. 2013:10.
24. Geiss GK, Bumgarner RE, Birditt B, Dahl T, Dowidar N, Dunaway DL, Fell HP, Ferree S, George RD, Grogan T, James JJ, Maysuria M, Mitton JD, Oliveri P, Osborn JL, Peng T, et al. Direct multiplexed measurement of gene expression with color-coded probe pairs. Nature biotechnology. 2008; 26:317-325.
25. Sharma A, Yeow WS, Ertel A, Coleman I, Clegg N, Davis PL, Miron A, Andersen LM, Iglehart JD and Marks JR. The retinoblastoma tumor suppressor controls androgen signaling and human prostate cancer progression Isolation and initial characterization of the BRCA2 promoter. Oncogene. 1999; 18:6000-6012.
26. Sharma A, Yeow WS, Ertel A, Coleman I, Clegg N, Thangavel C, Morrissey C, Zhang X, Comstock CE, Witkiewicz AK, Gomella L, Knudsen ES, Nelson PS and Knudsen KE. The retinoblastoma tumor suppressor controls androgen signaling and human prostate cancer progression. JClinInvest. 2010; 120:4478-4492.
27. Eckerle I, Muth D, Batzler J, Henrich KO, Lutz W, Fischer M, Witt O, Schwab M and Westermann F. Regulation of BIRC5 and its isoform BIRC5-2B in neuroblastoma. Cancer Letters. 2009; 28:99-107.
28. Karstensen B, Poppelreuther S, Bonin M, Walter M, Iftner T and Stubenrauch F. Gene expression profiles reveal an upregulation of E2F and downregulation of interferon targets by HPV18 but no changes between keratinocytes with integrated or episomal viral genomes. Virology. 2006; 353:200-209.
29. Sage J, Mulligan GJ, Attardi LD, Miller A, Chen S, Williams B, Theodorou E and Jacks T. Targeted disruption of the three Rb-related genes leads to loss of G(1) control and immortalization. Genes Dev. 2000; 14:3037-3050.
30. Stubdal H, Zalvide J, Campbell KS, Schweitzer C, Roberts TM and DeCaprio JA. Inactivation of pRB-related proteins p130 and p107 mediated by the J domain of simian virus 40 large T antigen. MolCell Biol. 1997; 17:4979-4990.
31. Zalvide J and DeCaprio JA. Role of pRb-related proteins in simian virus 40 large-T-antigen-mediated transformation. MolCell Biol. 1995; 15:5800-5810.
32. Borchert S, Czech-Sioli M, Neumann F, Schmidt C, Wimmer P, Dobner T, Grundhoff A and Fischer N. High-Affinity Rb Binding, p53 Inhibition, Subcellular Localization, and Transformation by Wild-Type or Tumor-Derived Shortened Merkel Cell Polyomavirus Large T Antigens. JVirol. 2014; 88:3144-3160.
33. Samimi M, Gardair C, Nicol JT, Arnold F, Touze A and Coursaget P. Merkel cell polyomavirus in merkel cell carcinoma: clinical and therapeutic perspectives. Seminars in oncology. 2015; 42:347-358.
34. Bhatia K, Goedert JJ, Modali R, Preiss L and Ayers LW. Immunological detection of viral large T antigen identifies a subset of Merkel cell carcinoma tumors with higher viral abundance and better clinical outcome. IntJ Cancer. 2010; 127:1493-1496.
35. Schrama D, Peitsch WK, Zapatka M, Kneitz H, Houben R, Eib S, Haferkamp S, Moore PS, Shuda M, Thompson JF, Trefzer U, Pfohler C, Scolyer RA and Becker JC. Merkel cell polyomavirus status is not associated with clinical course of Merkel cell carcinoma. J Invest Dermatol. 2011; 131:1631-1638.
36. Sihto H, Kukko H, Koljonen V, Sankila R, Bohling T and Joensuu H. Clinical factors associated with Merkel cell polyomavirus infection in Merkel cell carcinoma. J NatlCancer Inst. 2009; 101:938-945.
37. Sastre-Garau X, Peter M, Avril MF, Laude H, Couturier J, Rozenberg F, Almeida A, Boitier F, Carlotti A, Couturaud B and Dupin N. Merkel cell carcinoma of the skin: pathological and molecular evidence for a causative role of MCV in oncogenesis. J Pathol. 2009; 218:48-56.

38. Handschel J, Muller D, Depprich RA, Ommerborn MA, Kubler NR, Naujoks C, Reifenberger J, Schafer KL and Braunstein S. The new polyomavirus (MCPyV) does not affect the clinical course in MCCs. IntJ Oral MaxillofacSurg. 2010; 39:1086-1090.

39. Harms PW, Vats P, Verhaegen ME, Robinson DR, Wu YM, Dhanasekaran SM, Palanisamy N, Siddiqui J, Cao X, Su F, Wang R, Xiao H, Kunju LP, Mehra R, Tomlins SA, Fullen DR, et al. The Distinctive Mutational Spectra of Polyomavirus-Negative Merkel Cell Carcinoma. Cancer Res. 2015; 75:3720-3727.

40. Cimino PJ, Robirds DH, Tripp SR, Pfeifer JD, Abel HJ and Duncavage EJ. Retinoblastoma gene mutations detected by whole exome sequencing of Merkel cell carcinoma. Modern pathology. 2014; 27:1073-1087.

41. Sahi H, Savola S, Sihto H, Koljonen V, Bohling T and Knuutila S. RB1 gene in Merkel cell carcinoma: hypermethylation in all tumors and concurrent heterozygous deletions in the polyomavirus-negative subgroup. APMIS. 2014; 122:1157-1166.

42. Ahuja D, Saenz-Robles MT and Pipas JM. SV40 large T antigen targets multiple cellular pathways to elicit cellular transformation. Oncogene. 2005; 24:7729-7745.

43. Zalvide J, Stubdal H and DeCaprio JA. The J domain of simian virus 40 large T antigen is required to functionally inactivate RB family proteins. Mol Cell Biol. 1998; 18:1408-1415.

44. Harris KF, Christensen JB and Imperiale MJ. BK virus large T antigen: interactions with the retinoblastoma family of tumor suppressor proteins and effects on cellular growth control. J Virol. 1996; 70:2378-2386.

45. Bollag B, Prins C, Snyder EL and Frisque RJ. Purified JC virus T and T' proteins differentially interact with the retinoblastoma family of tumor suppressor proteins. Virology. 2000; 274:165-178.

46. Carter JJ, Daugherty MD, Qi X, Bheda-Malge A, Wipf GC, Robinson K, Roman A, Malik HS and Galloway DA. Identification of an overprinting gene in Merkel cell polyomavirus provides evolutionary insight into the birth of viral genes. ProcNatlAcadSciUSA. 2013; 110:12744-12749.

47. Kwun HJ, Guastafierro A, Shuda M, Meinke G, Bohm A, Moore PS and Chang Y. The minimum replication origin of merkel cell polyomavirus has a unique large T-antigen loading architecture and requires small T-antigen expression for optimal replication. JVirol. 2009; 83:12118-12128.

48. Liu X, Hein J, Richardson SC, Basse PH, Toptan T, Moore PS, Gjoerup OV and Chang Y. Merkel cell polyomavirus large T antigen disrupts lysosome clustering by translocating human Vam6p from the cytoplasm to the nucleus. J Biol Chem. 2011; 286:17079-17090.

49. Wang X, Li J, Schowalter RM, Jiao J, Buck CB and You J. Bromodomain protein Brd4 plays a key role in Merkel cell polyomavirus DNA replication. PLoS Pathog. 2012; 8:e1003021.

50. Richards KF, Guastafierro A, Shuda M, Toptan T, Moore PS and Chang Y. Merkel Cell Polyomavirus T Antigens Promote Cell Proliferation and Inflammatory Cytokine Gene Expression. The Journal of general virology. 2015.

51. Sihto H, Kukko H, Koljonen V, Sankila R, Bohling T and Joensuu H. Merkel cell polyomavirus infection, large T antigen, retinoblastoma protein and outcome in Merkel cell carcinoma. ClinCancer Res. 2011; 17:4806-4813.

52. Wikenheiser-Brokamp KA. Retinoblastoma family proteins: insights gained through genetic manipulation of mice. Cell Mol Life Sci. 2006; 63:767-780.

53. Shuda M, Kwun HJ, Feng H, Chang Y and Moore PS. Human Merkel cell polyomavirus small T antigen is an oncoprotein targeting the 4E-BP1 translation regulator. J ClinInvest. 2011; 121:3623-3634.

54. Spurgeon ME, Cheng J, Bronson RT, Lambert PF and DeCaprio JA. Tumorigenic activity of merkel cell polyomavirus T antigens expressed in the stratified epithelium of mice. Cancer Res. 2015; 75:1068-1079.

55. Kwun H-J, Shuda M, Feng H, Camacho C-J, Moore P-S and Chang Y. Merkel Cell Polyomavirus Small T Antigen Controls Viral Replication and Oncoprotein Expression by Targeting the Cellular Ubiquitin Ligase SCFFbw7. Cell Host & Microbe. 2013; 14:125-135.

56. Verhaegen ME, Mangelberger D, Harms PW, Vozheiko TD, Weick JW, Wilbert DM, Saunders TL, Ermilov AN, Bichakjian CK, Johnson TM, Imperiale MJ and Dlugosz AA. Merkel cell polyomavirus small T antigen is oncogenic in transgenic mice. J Invest Dermatol. 2015; 135:1415-1424.

57. Cheng J, Rozenblatt-Rosen O, Paulson KG, Nghiem P and DeCaprio JA. Merkel cell polyomavirus large T antigen has growth-promoting and inhibitory activities. JVirol. 2013; 87:6118-6126.

58. Xu XL, Singh HP, Wang L, Qi DL, Poulos BK, Abramson DH, Jhanwar SC and Cobrinik D. Rb suppresses human cone-precursor-derived retinoblastoma tumours. Nature. 2014; 514:385-388.

59. Pantulu ND, Pallasch CP, Kurz AK, Kassem A, Frenzel L, Sodenkamp S, Kvasnicka HM, Wendtner CM and Zur Hausen A. Detection of a novel truncating Merkel cell polyomavirus large T antigen deletion in chronic lymphocytic leukemia cells. Blood. 2010; 116:5280-5284.

60. Cimino PJ, Jr., Bahler DW and Duncavage EJ. Detection of Merkel cell polyomavirus in chronic lymphocytic leukemia T-cells. Experimental and molecular pathology. 2013; 94:40-44.

61. Houben R, Dreher C, Angermeyer S, Borst A, Utikal J, Haferkamp S, Peitsch WK, Schrama D and Hesbacher S. Mechanisms of p53 restriction in Merkel cell carcinoma

cells are independent of the Merkel cell polyoma virus T antigens. J Invest Dermatol. 2013:10.

62. Rosen ST, Gould VE, Salwen HR, Herst CV, Le Beau MM, Lee I, Bauer K, Marder RJ, Andersen R and Kies MS. Establishment and characterization of a neuroendocrine skin carcinoma cell line. Lab Invest. 1987; 56:302-312.

63. Schrama D, Hesbacher S, Angermeyer S, Schlosser A, Haferkamp S, Aue A, Adam C, Weber A, Schmidt M and Houben R. Serine 220 phosphorylation of the Merkel cell polyomavirus large T antigen crucially supports growth of Merkel cell carcinoma cells. International journal of cancer. 2016; 138:1153-1162.

Cancer Letters 404 (2017) 70–78

Contents lists available at ScienceDirect

Cancer Letters

journal homepage: www.elsevier.com/locate/canlet

Original Article

BIK is involved in BRAF/MEK inhibitor induced apoptosis in melanoma cell lines

Andreas Borst [a], Sebastian Haferkamp [b], Johannes Grimm [c], Manuel Rösch [a], Guannan Zhu [d], Sen Guo [d], Chunying Li [d], Tianwen Gao [d], Svenja Meierjohann [c], David Schrama [a], Roland Houben [a, *]

[a] Department of Dermatology, Venereology and Allergology, University Hospital Wuerzburg, Wuerzburg, Germany
[b] Department of Dermatology, University Hospital Regensburg, Regensburg, Germany
[c] Department of Physiological Chemistry I, Biocenter, Wuerzburg, Germany
[d] Department of Dermatology, Xijing Hospital, Fourth Military Medical University, Xi'an, China

ARTICLE INFO

Article history:
Received 14 December 2016
Received in revised form
4 July 2017
Accepted 7 July 2017

Keywords:
Melanoma
Vemurafenib
Trametinib
BIK/NBK
Apoptosis

ABSTRACT

In patients with BRAF-mutated melanoma specific inhibitors of $BRAF^{V600E}$ and MEK1/2 frequently induce initial tumor reduction, frequently followed by relapse. As demonstrated previously, $BRAF^{V600E}$-inhibition induces apoptosis only in a fraction of treated cells, while the remaining arrest and survive providing a source or a niche for relapse. To identify factors contributing to the differential initial response towards BRAF/MEK inhibition, we established M14 melanoma cell line-derived single cell clones responding to treatment with BRAF inhibitor vemurafenib and MEK inhibitor trametinib predominantly with either cell cycle arrest (CCA-cells) or apoptosis (A-cells). Screening for differentially expressed apoptosis-related genes revealed loss of BCL2-Interacting Killer (*BIK*) mRNA in CCA-cells. Importantly, ectopic expression of BIK in CCA-cells resulted in increased apoptosis rates following vemurafenib/trametinib treatment, while knockdown/knockout of BIK in A-cells attenuated the apoptotic response. Furthermore, we demonstrate reversible epigenetic silencing of *BIK* mRNA expression in CCA-cells. Importantly, HDAC inhibitor treatment associated with re-expression of BIK augmented sensitivity of CCA-cells towards vemurafenib/trametinib treatment both *in vitro* and *in vivo*. In conclusion, our results suggest that BIK can be a critical mediator of melanoma cell fate determination in response to MAPK pathway inhibition.

Introduction

Somatic mutations in the *BRAF* gene rendering the protein constitutively active occur in approximately 50% of cutaneous malignant melanoma [1]. In this regard, targeting mutant BRAF and the downstream kinase MEK has become one pillar of today's standard of care for patients with advanced $BRAF^{V600}$ mutated melanoma [2]. However, although most patients initially respond with rapid and significant tumor regression, not all tumor cells are eliminated and residual tumors frequently relapse [3]. In accordance, preclinical models demonstrated that BRAF inhibition induces cell death in only a subset of tumor cells while others persist in a growth-arrested state [4,5]. These surviving tumor cells provide a potential threat for the organism, as they can cause tumor relapse either by acquiring resistance [6,7] or by contributing to a pro-tumorigenic milieu through therapy-induced alterations of the secretome [8]. Therefore, incomplete melanoma cell death in response to inhibition of BRAF/MEK signaling is a key factor limiting therapeutic success.

Persistent tumor cell survival is frequently associated with aberrant apoptosis signaling [9]. In this respect, two major apoptosis mediating pathways have been described: the extrinsic death receptor and the intrinsic mitochondria mediated pathway regulated by members of the B-cell lymphoma (BCL)2 protein family [10]. The BCL2 family can be subdivided into three groups: i) the pro-apoptotic "activator or sensitizer" BCL2 homology domain 3-only (BH3-only) proteins (BIM, BIK, BAD, BID, HRK, BMF, NOXA and PUMA), which interact with and inhibit the ii) anti-apoptotic family members (BCL2, BCL-xL, BCL-w, BFL-1 and MCL-1) that in

* Corresponding author. Department of Dermatology, Venereology und Allergology, University Hospital Wuerzburg, Josef-Schneider-Str. 2, 97080 Wuerzburg, Germany.
E-mail address: houben_r@ukw.de (R. Houben).

http://dx.doi.org/10.1016/j.canlet.2017.07.005
0304-3835/

turn functionally repress the iii) pro-apoptotic effectors BAK and BAX. The latter initiate apoptosis by mediating cytochrome C release from the mitochondria [10,11].

For $BRAF^{V600}$ mutant melanomas it has been proposed that the intrinsic apoptosis pathway is suppressed by active BRAF signaling, which inhibits the expression of the BH3-only protein BCL2 interacting mediator of cell death (BIM) [12]. Consequently, inhibition of $BRAF^{V600}$ mutant signaling induces upregulation of BIM and thereby melanoma cell apoptosis [13,14].

The current study addresses the question which factor determines pro-apoptotic cell fate in the melanoma cells upon $BRAF^{V600}$ inhibition. To this end, we analyzed single cell clones responding to BRAF or combined BRAF/MEK inhibition either predominantly with apoptosis (A-cells/clones) or with cell cycle arrest (CCA-cells/clones). We identify BCL2 Interacting Killer (BIK) as differentially expressed in apoptotic versus arresting responders, and provide evidence that epigenetic silencing of the *BIK* gene can contribute to failed cell death induction upon inhibition of BRAF signaling in $BRAF^{V600}$ mutant melanoma. Indeed, HDAC inhibition triggers re-expression of BIK and sensitizes CCA-cells to BRAF/MEK inhibition *in vitro* and *in vivo*.

Material & methods

Cell culture

All cell lines [4,15] used in this study were derived from ATCC and routinely tested for mycoplasma. Cells were cultivated in RPMI 1640 supplemented with 10% FCS, 100 U/ml penicillin and 0.1 mg/ml streptomycin. For colony formation analysis the cells were washed with PBS and fixed using ice-cold methanol for 10 min on ice, washed again and stained for 10 min with Gram's crystal violet solution (Merck).

Cell cycle analysis

Cells were fixed for 24 h using ice-cold ethanol, treated with a propidium iodide solution (PBS + 1% FCS + 0.1 mg/ml propidium iodide + 0.1 mg/ml RNAse A) at 37 °C for 1 h and immediately analyzed by flow cytometry.

MTS assay

The CellTiter 96®Aqueous One Solution Cell Proliferation Assay Kit (Promega) was used according to manufacturer's instructions.

Real time PCR

Total RNA was isolated using the peqGOLD Total RNA Kit (PeqLab) and reverse transcribed with the Superscript II RT First Strand Kit (Invitrogen). Real time PCR was performed in the ABI 7500 Fast Real-Time PCR cycler (Applied Biosystems) by using a SybrGreen I Low Rox Mastermix (Eurogentec GmbH) and the respective primers for *BIK* (fw: 5-TCT TGA TGG AGA CCC TCC TGT-3 and rv: 5- CAA GAA CCT CCA TGG TCG GG-3) and *GAPDH* (fw: 5-GCC CAA TAC GAC CAA ATC C-3 and rv: 5-AGC CAC ATC GCT CAG ACA C-3). Relative expression was calculated using the $\Delta\Delta$-C_T method. The RT^2 Profiler PCR-Array (PAHS-012Z, Qiagen) was used according to manufacturer's instructions.

Immunoblotting

Analysis of protein expression by immunoblots was performed as previously described [16], and the primary antibodies used in this study are listed in supplementary table 1.

Ectopic BIK expression

A *BIK* cDNA amplified from pTRE-Nbk [17] was cloned into the lentiviral pcDH Vector (SBI) coding also for GFP. Lentiviral infection was carried out as described previously [16], and stably transduced cell lines were selected by fluorescence activated cell sorting (FACS).

BIK knockdown/knockout

BIK (s1989) and control siRNA were purchased from Ambion®/Life Technologies™ and transfected at 50 nM using TurboFect™ Transfection Reagent (Thermo Fisher). Plasmids sc-401751 (coding for Cas9 and the BIK guide RNA) and sc-401751-HDR (allowing homology directed repair mediated introduction of a red fluorescence protein (RFP) and a puromycin resistance into the BIK gene), were purchased from Santa Cruz and double transfected with UltraCruz™ Transfection reagent (sc-395739) according to manufacturer's instructions. Following puromycin selection, FACS was used additionally to select for RFP^{high} cells.

Mixed cell culture assay

GFP or RFP expression in pCDH or sc-401751-HDR-infected cells was used to determine changes in the ratio of infected and parental uninfected cells in mixed cell cultures by flow cytometry.

Chromatin-immunoprecipitation (ChIP)

Acetylation of the BIK promoter was analyzed by ChIP followed by real time PCR. To this end, we used the SimpleChIP Plus Enzymatic Chromatin IP Kit (Cell Signaling) according to the manufacturer's instructions. The antibodies applied for IP were targeting Histone H3 (clone D2B12; Rabbit mAb; Cell Signaling) and Histone H3 acetylated on Lysine 9 (H3K9Ac) (clone 1B10; mouse mAB; Active Motif). The primer sets used to quantify the co-precipitated BIK promoter are given in supplementary figure S5.

Xenotransplantation

For tumor induction, 5×10^6 M14 cells (clone #1 and #4) suspended in PBS supplemented with 50% BD Matrigel™ Basement Membrane Matrix (BD Biosciences, Heidelberg, Germany) were injected s.c. into each lateral flank of 6 weeks old Balb/C Nu mice (one clone on the left, one on the right). The size of the tumor was measured every three days. When the tumors reached a volume of around 100 mm^3 (day 30 after cell injection), the mice were randomly divided into two groups (n = 5): Vem/Tra group (mice injected intraperitoneally with Vem/Tra daily), Vem/Tra/FK228 group (mice injected intraperitoneally with Vem/Tra/FK228 daily). For further analysis subcutaneously grown tumors were surgically removed. Animal experiments were performed in compliance with Fourth Military Medical University animal protection guidelines and were approved by local government authorities.

Results

Single cell melanoma sub-lines with differential response to MAPK pathway targeting

This study was based on the concept that molecular differences determining the cell death or cell cycle arrest response of $BRAF^{V600\ E/K}$ melanoma cells upon MAPK pathway inhibition can be identified by analyzing differentially responding single cell clones from a heterogeneously responding cell line. For this approach we chose M14 as a $BRAF^{V600E}$ mutated melanoma cell line because cell cycle analysis of 11 different melanoma cell lines revealed both, a G1 arrest as well as a substantial increase in sub-G1 for M14 cells after 4 days treatment with the $BRAF^{V600E}$ inhibitor vemurafenib (Vem) or the MEK inhibitor trametinib (Tra) (supplementary Fig. S1). Following establishment of M14 single cell sub-lines, two clones were identified (#2 and #4, marked by red boxes in the figures) which responded with cell cycle arrest (Fig. 1A) rather than cell death upon treatment with Vem or combined treatment with Vem/Tra (Fig. 1B and C). The reduced inhibitor induced cell death of clones #2 and #4 was further confirmed by lactate dehydrogenase release assay (supplementary Fig. S2A). In comparison to these arresting clones, we included in further analyses two single cell clones (#1 and #3) with relatively high sub-G1 fractions after four days of Vem or Vem/Tra treatment (Fig. 1A–C). These early differences between arresting and apoptotic clones were not transient but translated into increased long term survival of clones #2 and #4 evident in MTS assays performed after 8 weeks of Vem treatment (Fig. 1D). Moreover, while the surviving cells of the arresting clones #2 and #4 bore the potential to form colonies after Vem removal, the surviving cells of the apoptotic clones lacked colony formation capability (supplementary Fig. S2D).

Drug resistance of melanoma cells can be associated with a slow cycling phenotype [18,19]. Comparison of the proliferation rates of the four single cell clones and the parental M14 cells did, however, not reveal any significant differences (supplementary Fig. S2B). To evaluate whether lack of cell death following MAPK pathway inhibition of the arresting clones is due to a general apoptotic defect, we determined death rates after puromycin treatment. The observed similar sensitivity of all clones (supplementary Fig. S2C)

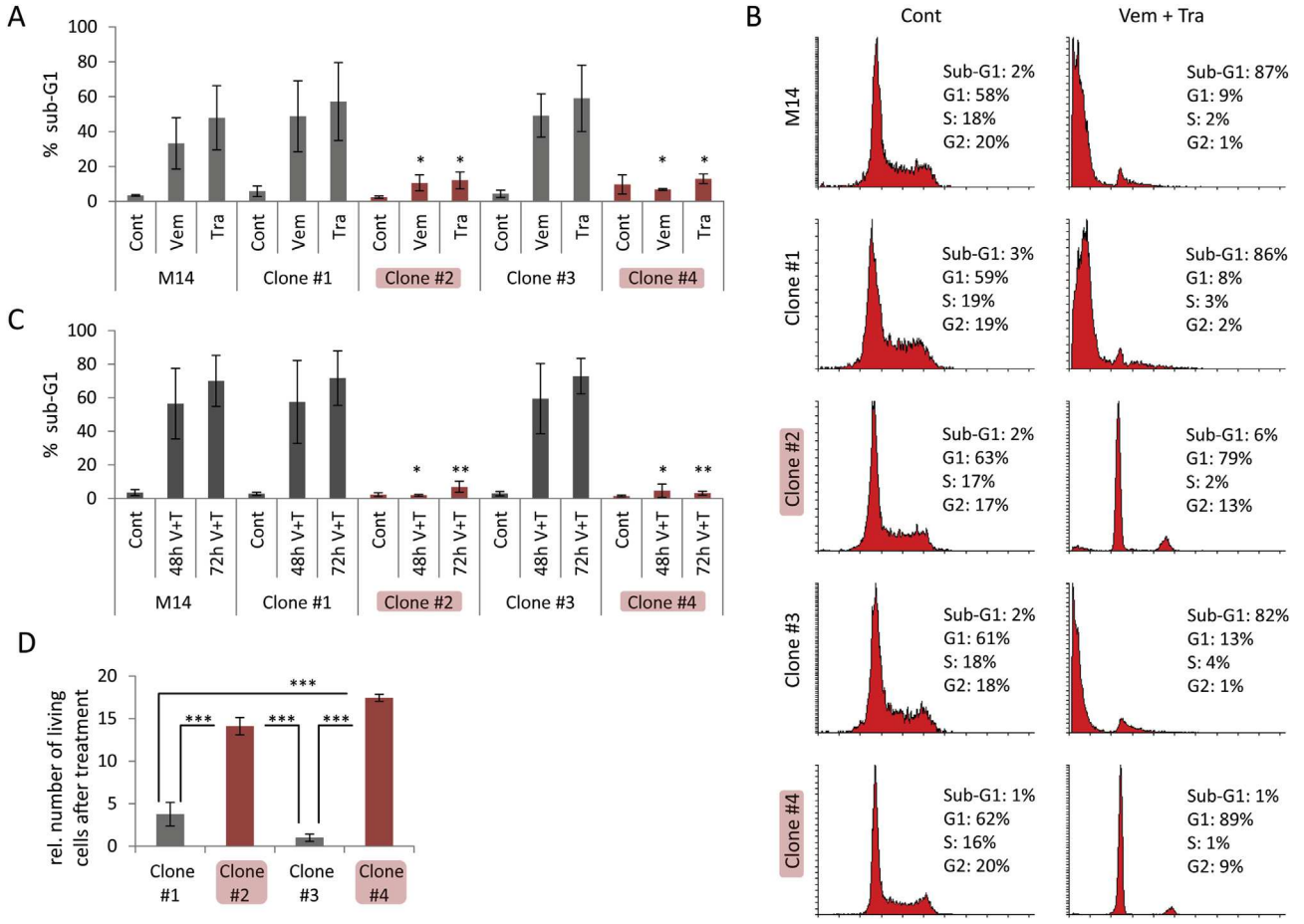

Fig. 1. M14 derived single-cell clones preferentially responding with either apoptosis or cell cycle arrest to MAPK-pathway inhibition. A: After four days of treatment with vemurafenib (5 μM) or trametinib (10 nM) parental M14 cells or selected single-cell clones were subjected to cell cycle analysis. **B:** Exemplary cell cycle profiles of at least 3 independent experiments after 72 h of combined Vem/Tra treatment. **C:** The cells were treated for the indicated time with the Vem/Tra combination and DNA content was determined by flow cytometry. **D:** Following eight weeks of Vem-treatment, the relative number of the surviving cells was analyzed in MTS assays after one week of standard cultivation (normalized to Clone #3; 96-wells with 20.000 cells at start). **A, C and D:** ($n \geq 3$, mean ± SD, Students t-test, unpaired, A and C compared to parental M14, two-tailed, $^{*}p < 0.05$; $^{**}p < 0.01$; $^{***}p < 0.001$).

indicates that the differential apoptotic response of the M14 sub-lines upon MAPK pathway inhibition is specific.

Low BIK mRNA expression in M14 sub-lines arresting upon MAPK pathway inhibition

To identify molecules involved in the hampered cell death response of the arresting clones, we analyzed gene expression using a qPCR array covering 84 apoptosis related genes. While most of the analyzed genes and in particular most BCL2 family members were equally expressed, *BIK/NBK* RNA levels in the CCA-clones #2 and #4 were clearly lower than in the A-clones #1 and #3 (Fig. 2A). This observation was confirmed by quantitative real-time PCR (Fig. 2B).

The discrepancy of *BIK* expression translated also to the protein level: Immunoblot analysis revealed the presence of BIK protein in the A-clones #1 and #3 and the parental M14 cells, and almost no expression in the CCA-clones #2 and #4. Surprisingly, however, long film exposure was necessary to detect BIK expression suggesting low protein levels (Fig. 2C). This may be due to BIK being downregulated through proteasomal degradation [20,21]. Indeed, BIK levels were highly elevated in apoptotic clones and the parental M14 cells by a 24 h treatment with the proteasome inhibitor bortezomib, indicating a fast BIK turnover in these cell lines (Fig. 2D). In contrast, BIK expression could not be induced by bortezomib in the CCA-clones #2 and #4, further demonstrating BIK protein deficiency in these cells (Fig. 2D). Furthermore, immunoblot analysis revealed that reduced pERK levels upon BRAF/MEK inhibition were associated with decrease of procaspase 9 levels and subsequent cleavage of effector caspase 3 only in the A-clones #1 and #3 and the parental M14 (Fig. 2B). Largely treatment-independent expression of the anti-apoptotic BIK targets BCL2 and BCL-X(L) [22] and of the executor Bcl-2 family pro-apoptotic proteins Bax and Bak was observed in all clones. In contrast, BIM^{EL} and PUMAα/β which have been demonstrated to be essential for apoptosis upon MAPK pathway inhibition in melanoma [12,23,24], demonstrated increased protein expression upon Vem/Tra treatment (Fig. 2C). However, given the comparable induction of BIM^{EL} and PUMAα/β in all clones, this mere induction is not sufficient to induce apoptosis in CCA-clones #2 and #4.

MAPK pathway inhibition selects for BIK^{low} cells in different $BRAF^{V600\ E/K}$ melanoma cell lines

To explore whether BIK expression contributing to the decision between arrest and death upon MAPK pathway inhibition is limited to M14 cells or generally observable in BRAF mutant melanoma cell lines, we extended our analyses to nine $BRAF^{V600E}$ and one $BRAF^{V600K}$ (FM88) melanoma cell lines. *BIK* mRNA expression was detectable in all ten analyzed melanoma cell lines. BIK protein

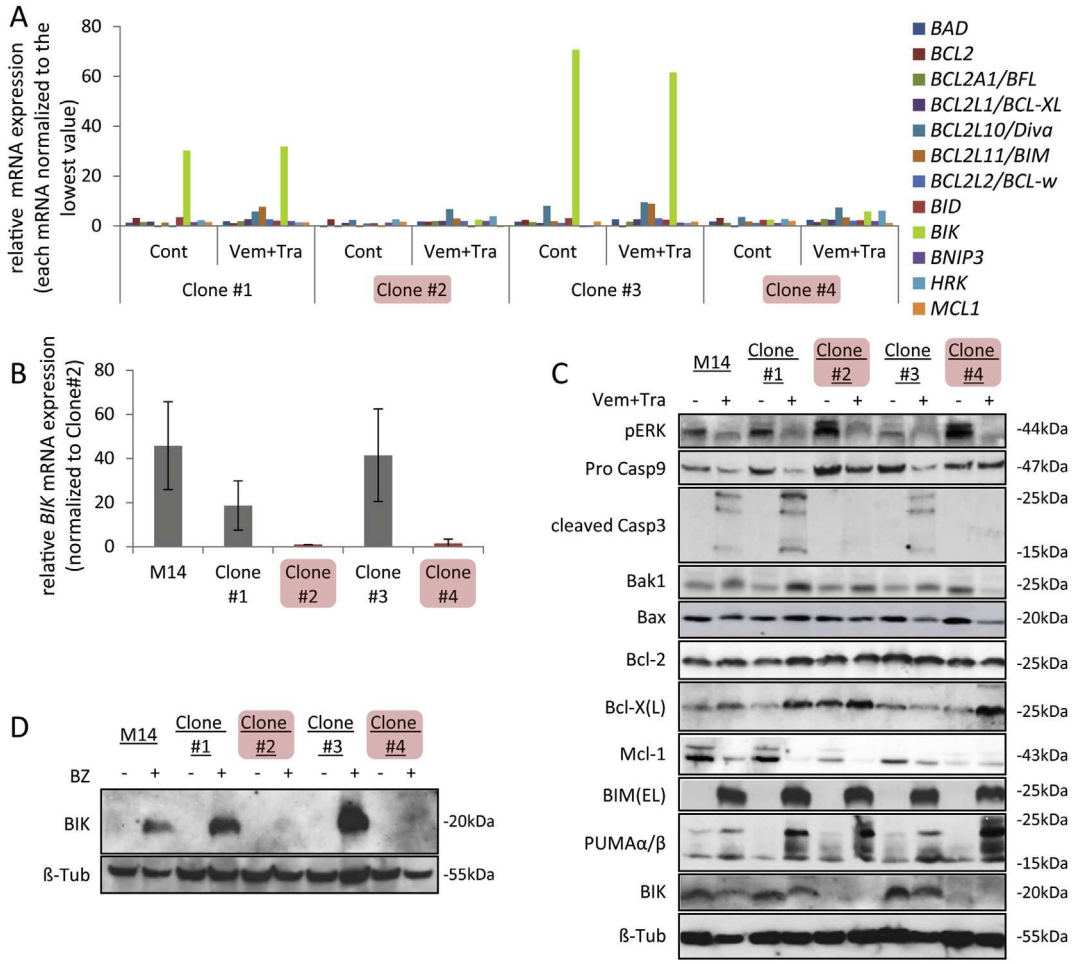

Fig. 2. Lack of BIK expression in M14 single cell clones with diminished apoptosis upon MAPK pathway inhibition. A: Relative mRNA expression (each mRNA normalized to the lowest value) of BCL2 family members after 24 h with and without Vem/Tra (5 μM/10 nM) using the RT^2 Profiler PCR-Array. **B:** relative *BIK* mRNA expression analyzed by qRT-PCR ($n \geq 3$, mean ± SD). Clone #2 served as calibrator and GAPDH as housekeeping gene. **C:** Immunoblot analysis probing the indicated apoptosis-associated proteins in whole cell lysates derived from cells cultured for 72 h in the absence or presence of Vem/Tra (long exposure of the film in case of BIK). **D:** Analysis of BIK expression by immunoblot in bortezomib (24 h; 2.5 μM) treated cells (short film exposure).

levels, however, were low, but inducible by proteasomal inhibition in eight lines and the level of induced protein correlated with mRNA expression (Fig. 3A and B). Next, we analyzed the induction of sub-G1 cells upon Vem/Tra in the ten melanoma cell lines (Fig. 3C), and statistical analysis revealed a significant correlation between *BIK* mRNA expression and apoptosis rates ($p = 0.041$; $R^2 = 0.4235$; Fig. 3D). To further confirm involvement of BIK in cell fate decision upon MAPK pathway inhibition, we analyzed the surviving cells after separation from dead cells following four days of Vem/Tra treatment. We hypothesized that in a heterogeneous cell population BIK^{high} cells would be preferentially killed, and indeed, we observed moderate to near complete reduction of BIK protein in all eight BIK expressing melanoma cell lines after Vem/Tra treatment (Fig. 3E and supplementary Fig. S3).

Ectopic BIK expression increases while BIK knockdown/knockout reduces the apoptotic response towards MAPK pathway inhibition

In order to formally prove the impact of BIK expression on cell fate decision, BIK was ectopically expressed in the CCA-clones #2 and #4 as well as in the MDA-MB 435 cell line by lentiviral transduction. MDA-MB 435 also lacks endogenous BIK expression and demonstrates only a minor cell death response upon Vem/Tra treatment (Fig. 3A–C). Immunoblot analysis confirmed effective BIK expression in the transduced and GFP-sorted cells (Fig. 4A) which, under standard cultivation conditions, had very little or no effect on apoptosis or proliferation rate (supplementary Fig. S4A and B). In the presence of Vem/Tra, however, the BIK overexpressing cells demonstrated elevated fractions of apoptotic sub-G1 cells (Fig. 4B). Moreover, relative loss of BIK overexpressing cells in mixed cell cultures with the corresponding parental cells indicates increased sensitivity towards MAPK pathway inhibition (Fig. 4C).

Vice versa, we performed siRNA knockdown of BIK in the BIK^{high} A-clones #1 and #3 as well as in the parental M14 cells and in FM88 cells (Fig. 5A). BIK knockdown in these cells resulted in reduced induction of sub-G1 cells compared to cells transfected with a control scrambled siRNA upon Vem or Vem/Tra treatment (Fig. 5B).

As a separate control, we also performed CRISPR/CAS9 mediated *BIK* gene knockout in all cell lines with predominant apoptotic response towards Vem/Tra treatment, according to our previous results (Fig. 3C). The resulting loss of bortezomib inducible BIK protein expression was associated with reduced induction of apoptosis upon Vem or Vem/Tra treatment in 5 out of 7 investigated cell lines (Fig. 5C and D). Furthermore, most of BIK knockout A-cells accumulated relative to the BIK-positive parental cells upon Vem/Tra treatment (Fig. 5E left). In contrast, BIK knockout in CCA-cell lines lacking intrinsic BIK expression (Clone #2, #4 and MDA-

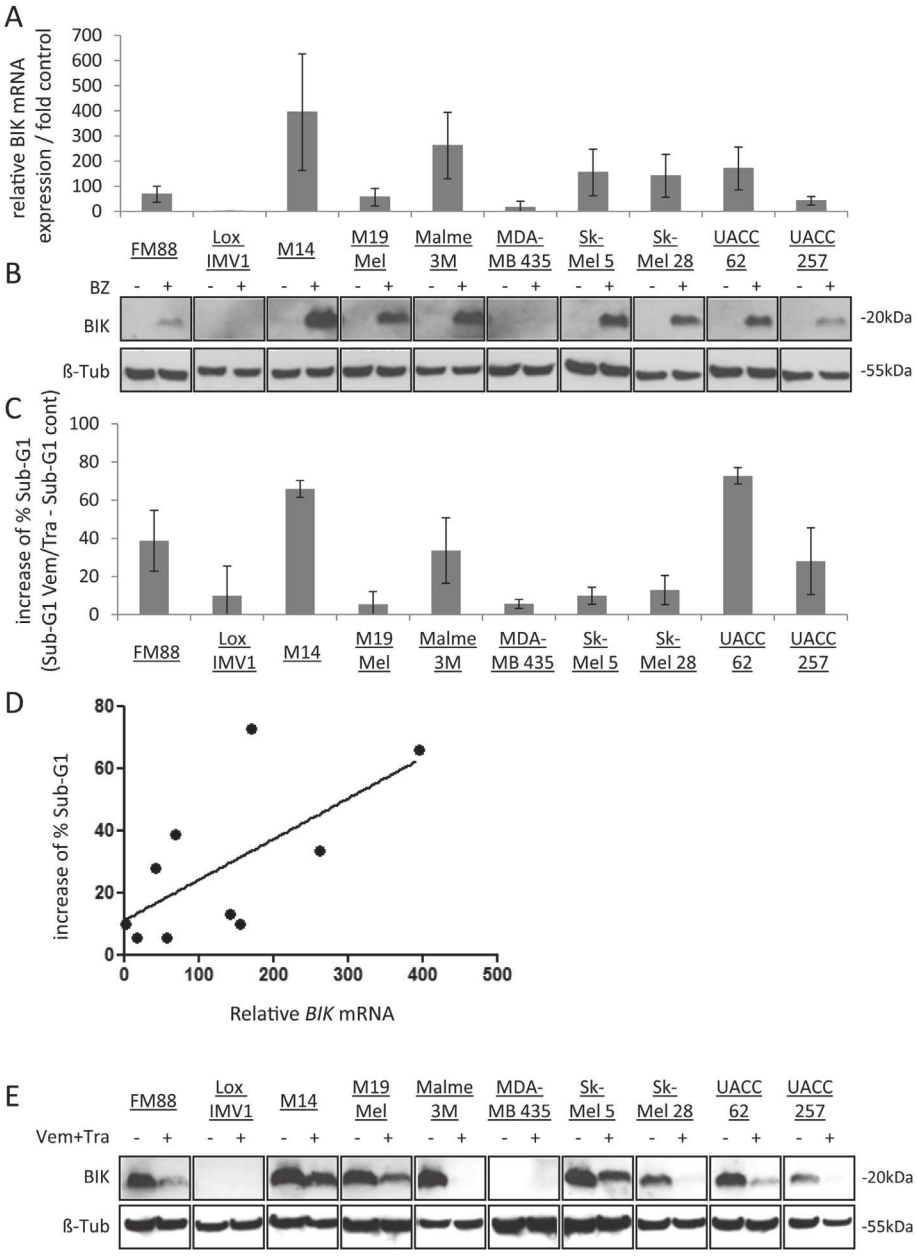

Fig. 3. MAPK pathway inhibition of BRAF mutant melanoma cells selects for reduced BIK expression. A: qRT-PCR: relative *BIK* mRNA expression in the indicated BRAF-mutant melanoma cell lines with LoxIMV1 as calibrator and GAPDH as housekeeping gene. Mean values (+/− SD) of six independent experiments. **B:** Immunoblot analysis of cell lysates harvested after 24 h in the presence or absence of bortezomib (2.5 μM). **C:** Following 48 h of Vem/Tra (5 μM/10 nM) treatment the DNA content was measured by flow cytometry. Depicted is the increase of the sub-G1 population (%sub-G1 Vem/Tra - %sub-G1 control) ($n \geq 3$, mean ± SD). **D:** Linear regression of *BIK* expression and Vem/Tra induced sub-G1 fraction (based on data presented in A and C) ($p = 0.041$; $R^2 = 0.4235$). **E:** Following four days in the presence or absence of Vem/Tra, the surviving cells were collected and treated with bortezomib for 24 h and then analyzed by immunoblot for BIK expression.

MB 435) did not affect sensitivity towards MAPK pathway inhibition (Fig. 5E right). In summary, BIK overexpression and knockdown/knockout experiments suggest a substantial contribution of BIK in mediating MAPK pathway inhibition induced cell death in several BRAF mutated melanoma cell lines with loss of BIK expression shifting the response towards survival.

De-repression of BIK expression by HDAC inhibition

Since sequencing analysis did not reveal any reason for suppressed BIK expression in M14 Clones #2 and #4 (data not shown), we hypothesized that this was due to epigenetic modifications. In this regard, silencing of gene expression can be mediated by histone deacetylases (HDACs) as acetylation of lysine residues in histones is an important mechanism stimulating expression of the respective genes [25]. Hence, we performed experiments applying the HDAC inhibitor Romidepsin (FK228) to explore whether HDACs are involved in BIK repression in the BIK^{low} CCA-cell lines. Chromatin Immunoprecipitation followed by real time PCR demonstrated elevated H3K9 acetylation in the BIK promotor region upon treatment with FK228 (Fig. 6A and supplementary Fig. 4). In line with increased promoter acetylation we observed FK228-induced elevated *BIK* mRNA levels - in particular in the BIK^{low} CCA-cell lines (M14 Clones #2 and #4 as well as MDA-MB 435) (Fig. 6B) - which resulted in increased BIK protein levels in all analyzed cell lines (Fig. 6C). Moreover, FK228 was not only cytotoxic as single

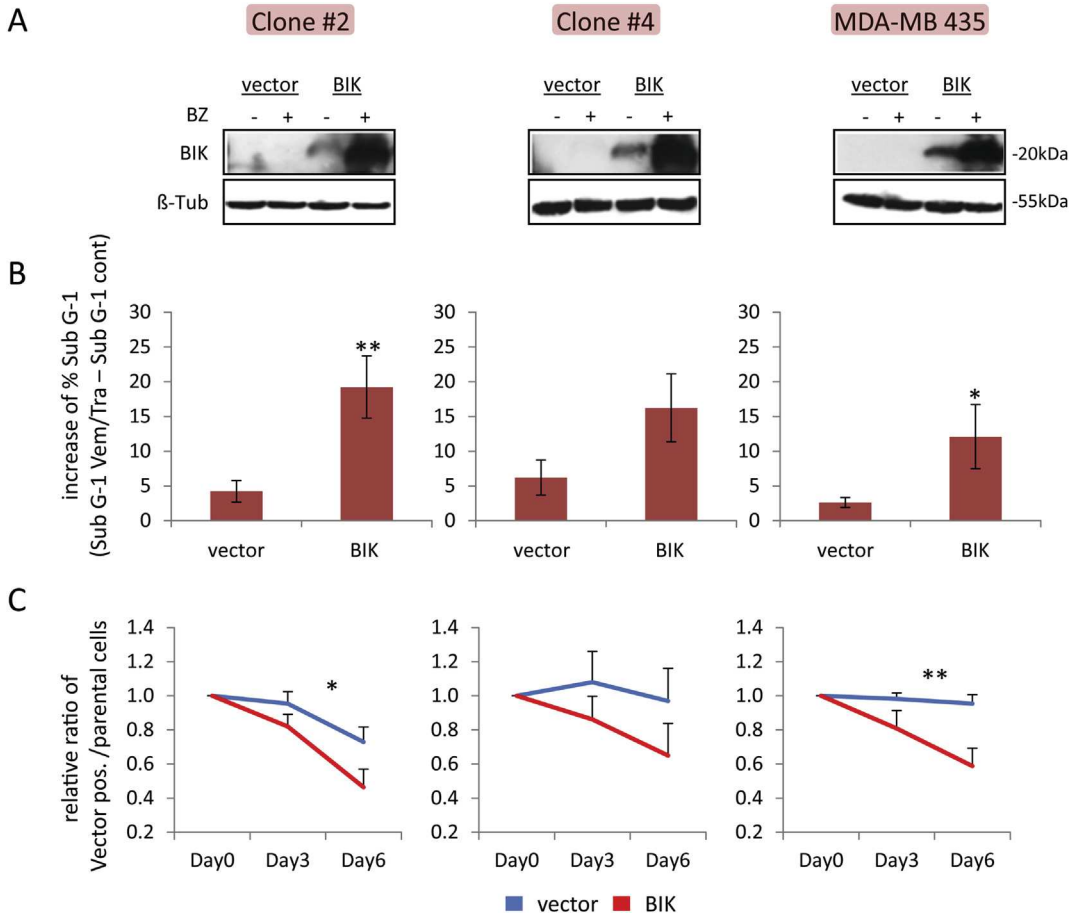

Fig. 4. Ectopic BIK expression increases the apoptotic response upon MAPK pathway inhibition. The indicated cell-lines were stably transduced with a vector coding either for GFP or for BIK and GFP. **A:** BIK protein levels analyzed by immunoblot after 24 h with and without bortezomib (2.5 μM). **B:** Increase in sub-G1 cells following 72 h of Vem/Tra treatment as determined by flow cytometry of PI-stained cells (%sub-G1 Vem/Tra - %sub-G1 control) (n = 5). **C:** GFP expression was used to monitor the response to Vem/Tra (5 μM/10 nM) in mixed cell cultures with parental cells over time. Relative ratios based in each case on the measurement of the first time point were calculated, and mean values (±SD) of four independent experiments are depicted. (Students t-test, paired, two-tailed, *p < 0.05; **p < 0.01; in **C** the areas under the curve were compared).

agent treatment, but also increased the apoptotic response of CCA-cells upon Vem/Tra treatment (Fig. 6D), indicating that FK228 sensitized BIK-negative cells for Vem/Tra therapy.

HDAC inhibition increases efficacy of BRAF/MEK inhibition against BIK^{low} xeno-transplanted tumors

Next, we performed xeno-transplantation experiments to test if our *in vitro* observations can be confirmed in the *in vivo* setting. To this end, BIK^{low} and BIK^{high} tumors were induced in nude mice by simultaneously injecting M14 clone #4 and clone #1 cells, in the right and left flank, respectively. Upon treatment with Vem/Tra, the BIK^{high} tumor clone #1 shrank significantly faster than the of BIK^{low} tumor clone #4 (Fig. 6E). When mice were additionally treated with the HDAC inhibitor FK228, however, tumor burden of BIK^{low} tumors was significantly decreased compared to Vem/Tra only treatment. Indeed, therapeutic efficacy as determined by tumor volume decrease of Vem/Tra/FK228-treated BIK^{low} tumors was in the same range as for Vem/Tra or Vem/Tra/FK228 treated BIK^{high} tumors (Fig. 6E).

Discussion

The major problem of current targeted therapy for patients with BRAF^{V600} mutant melanoma is the occurrence of inhibitor resistant tumors after an initial, distinct reduction in tumor mass [26,27]. In this respect, several molecular mechanisms rendering BRAF mutant melanoma cells insensitive towards BRAF and/or MEK inhibition have been uncovered [6,7,28]. However, not only acquired or pre-existing resistance contributes to relapse, but also incomplete killing of the inhibitor sensitive tumor cells has been demonstrated to support outgrowth, dissemination and metastasis of drug-resistant cancer cell clones [8]. Indeed, often a fraction of inhibitor-sensitive BRAF mutant melanoma cells survive inhibition of MAPK pathway signaling in a cell cycle-arrested, senescence-like state, while the remaining cells undergo apoptosis [4,5,8,27]. Here we identified the pro-apoptotic BCL2 family member BIK as a protein involved in this cell fate decision with epigenetic silencing of BIK supporting survival of RAF/MEK inhibitor treated melanoma cells.

BIK is a protein predominantly found at the ER where it can bind and inhibit anti-apoptotic BCL2 and BCL-X(L), leading to subsequent activation of BAX, triggering Ca^{2+} release from the ER that enhances cytochrome *c* liberation from the mitochondria and subsequent caspase 9 cleavage [29–33]. Furthermore, inhibition of anti-apoptotic MCL-1- a protein implicated in apoptosis deficiency in melanoma [34] - has been described [35]. A study in IFNγ-treated airway epithelial cells attributed the role of BIK in cell death to its ability to inhibit nuclear translocation of ERK1/2 through BH3 mediated interaction with the activated ERK proteins [36].

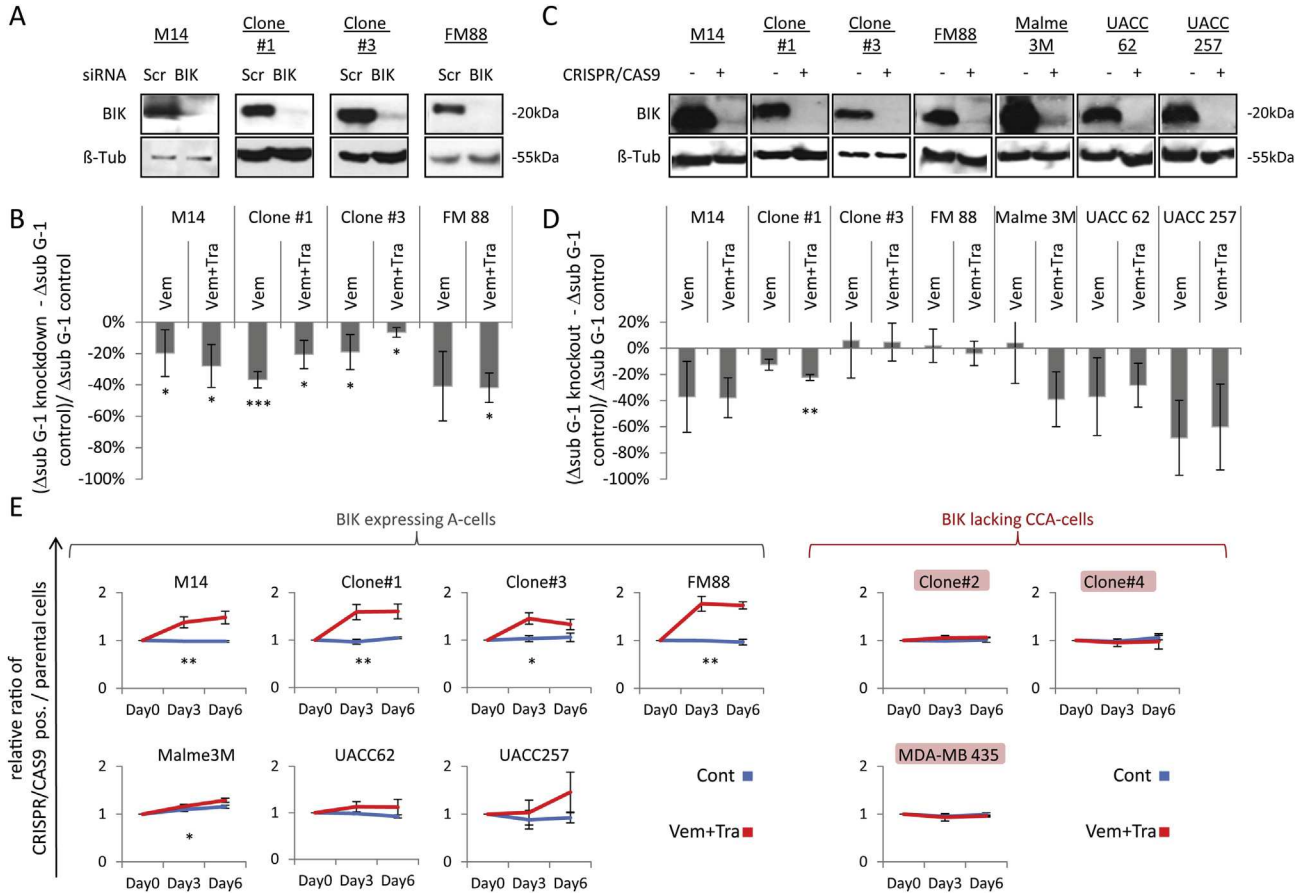

Fig. 5. BIK knockdown/knockout reduces the apoptotic response towards MAPK pathway inhibition. A and B: 24 h before subsequent inhibitor treatment the indicated cell lines were transfected with a *BIK* or scr siRNA. **C and D:** *BIK* knockout in the indicated cell-lines was achieved using CRISPR/CAS9 technology and a selectable donor integrating into the *BIK* locus. **A and C:** BIK knockdown/knockout evaluated by immunoblot analysis of cell lysates harvested following bortezomib treatment (24 h; 2.5 μM). **B and D:** Reduction of sub-G1 cells relative to control cells after 48 h Vem (5 μM) or Vem/Tra (5 μM/10 nM) treatment of BIK knockdown (**B**) or knockout cells (**D**). Depicted is the mean relative difference [(Δsub G-1 knockout - Δsub G-1 control)/Δsub G-1 control] of at least three independent experiments. **E:** RFP expression of the BIK-knockout cells was used to monitor the response to Vem/Tra in mixed cell cultures with parental cells over time. Relative ratios based in each case on the measurement of the first time point were calculated, and mean values (±SD) of at least three independent experiments are depicted ($n \geq 3$, Students t-test, paired, two-tailed, $^{*}p < 0.05$; $^{**}p < 0.01$; $^{***}p < 0.001$; in **E** the areas under the curve were compared).

Several results obtained in our present study support an important function of BIK in cell death induced by ERK1/2 inactivation in $BRAF^{V600}$ mutant melanoma cells treated with RAF/MEK inhibitor: (i) correlation of *BIK* expression with the apoptotic response towards RAF/MEK inhibition in different $BRAF^{V600}$ mutant melanoma cell lines and in particular in M14 derived single cell clones, (ii) preferred survival of BIK^{low} melanoma cells upon treatment with RAF/MEK inhibitors, (iii) increased inhibitor induced apoptosis and reduced proliferation/cell death rate in cells ectopically expressing BIK and (iv) reduced apoptotic response and increased proliferation/cell-death rate of BIK knockdown/knockout melanoma cells. In line with our findings it has been demonstrated that suppression of BIK can mediate apoptosis resistance in B-cells, as well as in lymphoblastoid, renal cell carcinoma and breast cancer cells [37–41].

Although, our data clearly demonstrate a possible role of BIK loss for reduced apoptotic response upon BRAF/MEK inhibition in melanoma cells we would like to point out that this does not exclude that other molecular mechanisms may mediate such an effect as well. Similarly, several different mechanisms have been described for adaptive resistance to MAPK pathway inhibition [42].

In contrast to several other cancer cell types where BIK expression is increased upon death inducing stimuli [43–45], we did not observe distinct changes of *BIK* mRNA or protein expression upon Vem or Vem/Tra treatment in BRAF mutant melanoma cells. Even flow cytometry analyses of BIK-GFP fusion protein expressing cells did not reveal an increase in BIK protein expression preceding inhibitor induced death (data not shown). Therefore, BIK may either be functionally activated by MAPK pathway inhibition or basal level expression of BIK is an essential prerequisite for other induced/repressed factors to trigger apoptosis. Regarding the first possibility it has been proposed that due to its exposed BH3 domain BIK is, in contrast to BID, a constitutively active protein [46] while another study suggested that phosphorylation of BIK is required for full apoptotic activity, however, without providing evidence that phosphorylation increases in response to death inducing stimuli [47]. Furthermore, subcellular localization influencing BIK activity has been reported [48], and last but not least glucose-regulated protein 78 (GRP78) has been described to negatively regulate BIK function through direct interaction [38,49]. Interestingly, GRP78 expression is repressed in BRAF mutant melanoma cells in response to vemurafenib [13], which also suggests BIK as a MAPK pathway inhibition triggered mediator of apoptosis in melanoma.

Regarding the second possibility, i.e. that basal BIK expression is required for other induced factors to promote apoptosis, the BCL2 family members BIM and PUMA are promising candidates potentially cooperating with BIK in cell death induction, similar to what is reported for BIK and NOXA [31]. Indeed, BIM and PUMA have been demonstrated to be both elevated and required for apoptosis upon MAPK pathway inhibition in melanoma cells [12–14,23,24]. Moreover, we observed induction of BIM and PUMA also in those

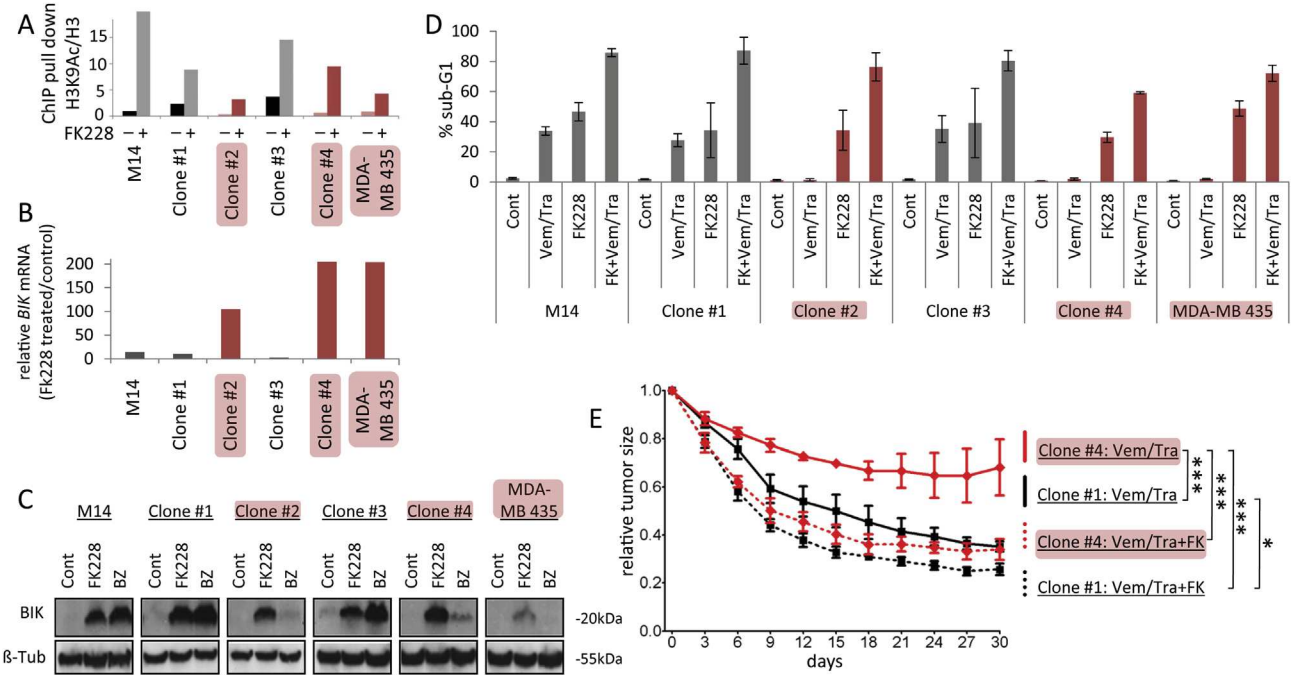

Fig. 6. HDAC inhibition leads to increased BIK expression and sensitization of BIK^{low} cells towards MAPK pathway inhibition induced apoptosis. A: Following 24 h of FK228 treatment (100 nM) the indicated cells were fixed, and digested chromatin was pulled down with antibodies targeting Histone H3 and H3K9Ac, respectively. Purified DNA was analyzed for the presence of the BIK promoter by real-time PCR using primer set A (supplementary figure S5). Values for H3K9Ac relative to H3 are depicted. **B:** Relative *BIK* mRNA induction (treated/untreated) determined by qRT-PCR after 24 h of FK228 treatment. **C:** Immunoblot of indicated cell lines treated for 24 h with bortezomib (2.5 μM) or FK228 (100 nM). **D:** The number of sub-G1 cells following 48 h of treatment with the indicated inhibitors was determined by flow cytometry of PI-stained cells ($n \geq 3$). **E:** In 10 nude mice, two tumors were induced in each flank of the mice by subcutaneous injection of M14 clone#1 or #4 cells. When the tumors reached a volume of around 100 mm^3, the animals were divided into two groups and received intraperitoneal injections of either Vem (25 mg/kg) + Tra (0.05 mg/kg) or as third component FK228 (0.5 mg/kg). Tumor size was measured in the course of time and mean values relative to the start of the treatment (±standard error) are displayed. For statistical evaluation the area under the curve (AUC) for each individual tumor was calculated and then the AUCs of the different groups were compared by one-way-ANOVA followed by Newman-Keuls multiple comparison post hoc testing (*$p < 0.05$; ***$p < 0.001$).

cell lines largely lacking inhibitor induced apoptosis as well as BIK expression (Fig. 2C). Upon ectopic BIK expression, however, Vem/Tra treatment leads to elevated killing of these cells (Fig. 4) suggesting BIK as a critical co-factor for BIM/PUMA mediated apoptosis and, *vice versa*, lack of BIK expression in BRAF mutant melanoma cells limiting the desired apoptotic response upon MAPK pathway inhibition (Fig. 5).

De-repression of BIK expression was achievable in our BIK^{low} melanoma cell lines by applying an HDAC inhibitor (Fig. 6), suggesting transcriptional repression of BIK due to lack of histone acetylation. Similarly, epigenetic silencing of BH3-only proteins and its contribution to acquired resistance has been described for several tumor entities [50,51] providing part of the rationale for the potential use of HDAC inhibitors to treat cancer patients. Indeed, several HDAC inhibitors are tested in clinical trials and some have already been approved for peripheral and cutaneous lymphoma as well as for myeloma [52–54]. However, in melanoma, clinical trials with HDAC inhibitors as monotherapy have failed so far [55,56]. Supporting other pre-clinical studies suggesting combination of HDAC and MAPK pathway inhibitors for the treatment of BRAF mutant cancer [57,58] our results presented here suggest that combination of HDAC inhibitors with MAPK pathway inhibitors may result in an increased initial apoptosis response possibly leading to improved long term efficacy.

Acknowledgements

The study was supported by the Interdisziplinäres Zentrum für Klinische Forschung Würzburg (IZKF B-193 and B-323) and the Hiege Foundation against Skin Cancer. We are very thankful to Jürgen Eberle for providing the BIK expression construct. Furthermore, we thank Lena Völkert, Kristina Vogtmann, Luis Zanon Rodriguez and Sarah Schuster for excellent technical assistance.

Conflict of interest

The authors have no conflict of interest to declare.

Appendix A. Supplementary data

Supplementary data related to this article can be found at http://dx.doi.org/10.1016/j.canlet.2017.07.005.

References

[1] Genomic classification of cutaneous melanoma, Cell 161 (2015) 1681–1696.
[2] Z. Eroglu, A. Ribas, Combination therapy with BRAF and MEK inhibitors for melanoma: latest evidence and place in therapy, Ther. Adv. Med. Oncol. 8 (2016) 48–56.
[3] B.P. Singh, A.K. Salama, Updates in therapy for advanced melanoma, Cancers 8 (2016).
[4] S. Haferkamp, A. Borst, C. Adam, T.M. Becker, S. Motschenbacher, S. Windhovel, et al., Vemurafenib induces senescence features in melanoma cells, J. Invest Dermatol 133 (2013) 1601–1609.
[5] H. Yang, B. Higgins, K. Kolinsky, K. Packman, Z. Go, R. Iyer, et al., RG7204 (PLX4032), a selective BRAFV600E inhibitor, displays potent antitumor activity in preclinical melanoma models, Cancer Res. 70 (2010) 5518–5527.
[6] E. Hartsough, Y. Shao, A.E. Aplin, Resistance to RAF inhibitors revisited, J. Invest Dermatol 134 (2014) 319–325.
[7] M. Holderfield, M.M. Deuker, F. McCormick, M. McMahon, Targeting RAF kinases for cancer therapy: BRAF-mutated melanoma and beyond, Nat. Rev. Cancer 14 (2014) 455–467.
[8] A.C. Obenauf, Y. Zou, A.L. Ji, S. Vanharanta, W. Shu, H. Shi, et al., Therapy-induced tumour secretomes promote resistance and tumour progression, Nature 520 (2015) 368–372.

[9] A.R. Jazirehi, R. Nazarian, A.X. Torres-Collado, J.S. Economou, Aberrant apoptotic machinery confers melanoma dual resistance to BRAF(V600E) inhibitor and immune effector cells: immunosensitization by a histone deacetylase inhibitor, Am. J. Clin. Exp. Immunol. 3 (2014) 43–56.
[10] S. Baig, I. Seevasant, J. Mohamad, A. Mukheem, H.Z. Huri, T. Kamarul, Potential of apoptotic pathway-targeted cancer therapeutic research: where do we stand? Cell death Dis. 7 (2016) e2058.
[11] A.N. Hata, J.A. Engelman, A.C. Faber, The BCL2 family: key mediators of the apoptotic response to targeted anticancer therapeutics, Cancer Discov. 5 (2015) 475–487.
[12] R.A. Cartlidge, G.R. Thomas, S. Cagnol, K.A. Jong, S.A. Molton, A.J. Finch, et al., Oncogenic BRAF(V600E) inhibits BIM expression to promote melanoma cell survival, Pigment. Cell Melanoma Res. 21 (2008) 534–544.
[13] D. Beck, H. Niessner, K.S. Smalley, K. Flaherty, K.H. Paraiso, C. Busch, et al., Vemurafenib potently induces endoplasmic reticulum stress-mediated apoptosis in BRAFV600E melanoma cells, Sci. Signal. 6 (2013) ra7.
[14] K.H. Paraiso, Y. Xiang, V.W. Rebecca, E.V. Abel, Y.A. Chen, A.C. Munko, et al., PTEN loss confers BRAF inhibitor resistance to melanoma cells through the suppression of BIM expression, Cancer Res. 71 (2011) 2750–2760.
[15] O.N. Ikediobi, H. Davies, G. Bignell, S. Edkins, C. Stevens, S. O'Meara, et al., Mutation analysis of 24 known cancer genes in the NCI-60 cell line set, Mol. cancer Ther. 5 (2006) 2606–2612.
[16] R. Houben, C. Adam, A. Baeurle, S. Hesbacher, J. Grimm, S. Angermeyer, et al., An intact retinoblastoma protein-binding site in Merkel cell polyomavirus large T antigen is required for promoting growth of Merkel cell carcinoma cells, Int.J Cancer 130 (2012) 847–856.
[17] M. Oppermann, C.C. Geilen, L.F. Fecker, B. Gillissen, P.T. Daniel, J. Eberle, Caspase-independent induction of apoptosis in human melanoma cells by the proapoptotic Bcl-2-related protein Nbk/Bik, Oncogene 24 (2005) 7369–7380.
[18] A. Roesch, A. Vultur, I. Bogeski, H. Wang, K.M. Zimmermann, D. Speicher, et al., Overcoming intrinsic multidrug resistance in melanoma by blocking the mitochondrial respiratory chain of slow-cycling JARID1B(high) cells, Cancer Cell 23 (2013) 811–825.
[19] G. Zhang, M. Herlyn, Linking SOX10 to a slow-growth resistance phenotype, Cell Res. 24 (2014) 906–907.
[20] M. Nikrad, T. Johnson, H. Puthalalath, L. Coultas, J. Adams, A.S. Kraft, The proteasome inhibitor bortezomib sensitizes cells to killing by death receptor ligand TRAIL via BH3-only proteins Bik and Bim, Mol. cancer Ther. 4 (2005) 443–449.
[21] H. Zhu, L. Zhang, F. Dong, W. Guo, S. Wu, F. Teraishi, et al., Bik/NBK accumulation correlates with apoptosis-induction by bortezomib (PS-341, Velcade) and other proteasome inhibitors, Oncogene 24 (2005) 4993–4999.
[22] J.M. Boyd, G.J. Gallo, B. Elangovan, A.B. Houghton, S. Malstrom, B.J. Avery, et al., Bik, a novel death-inducing protein shares a distinct sequence motif with Bcl-2 family proteins and interacts with viral and cellular survival-promoting proteins, Oncogene 11 (1995) 1921–1928.
[23] Y.F. Wang, C.C. Jiang, K.A. Kiejda, S. Gillespie, X.D. Zhang, P. Hersey, Apoptosis induction in human melanoma cells by inhibition of MEK is caspase-independent and mediated by the Bcl-2 family members PUMA, Bim, and Mcl-1, Clin. Cancer Res. 13 (2007) 4934–4942.
[24] L. Rohrbeck, J.N. Gong, E.F. Lee, A.J. Kueh, A. Behren, L. Tai, et al., Hepatocyte growth factor renders BRAF mutant human melanoma cell lines resistant to PLX4032 by downregulating the pro-apoptotic BH3-only proteins PUMA and BIM, Cell Death Differ. 23 (2016) 2054–2062.
[25] M. Yoshida, R. Furumai, M. Nishiyama, Y. Komatsu, N. Nishino, S. Horinouchi, Histone deacetylase as a new target for cancer chemotherapy, Cancer Chemother. Pharmacol. 48 (Suppl 1) (2001) S20–S26.
[26] R. Fisher, J. Larkin, Vemurafenib: a new treatment for BRAF-V600 mutated advanced melanoma, Cancer Manag. Res. 4 (2012) 243–252.
[27] A. Swaika, J.A. Crozier, R.W. Joseph, Vemurafenib: an evidence-based review of its clinical utility in the treatment of metastatic melanoma, Drug Des. Dev. Ther. 8 (2014) 775–787.
[28] N. Wagle, C. Emery, M.F. Berger, M.J. Davis, A. Sawyer, P. Pochanard, et al., Dissecting therapeutic resistance to RAF inhibition in melanoma by tumor genomic profiling, J. Clin. Oncol. official J. Am. Soc. Clin. Oncol. 29 (2011) 3085–3096.
[29] G. Chinnadurai, S. Vijayalingam, R. Rashmi, BIK, the founding member of the BH3-only family proteins: mechanisms of cell death and role in cancer and pathogenic processes, Oncogene 27 (Suppl 1) (2008) S20–S29.
[30] M. Germain, J.P. Mathai, G.C. Shore, BH-3-only BIK functions at the endoplasmic reticulum to stimulate cytochrome c release from mitochondria, J. Biol. Chem. 277 (2002) 18053–18060.
[31] M. Germain, J.P. Mathai, H.M. McBride, G.C. Shore, Endoplasmic reticulum BIK initiates DRP1-regulated remodelling of mitochondrial cristae during apoptosis, EMBO J. 24 (2005) 1546–1556.
[32] B. Gillissen, F. Essmann, V. Graupner, L. Starck, S. Radetzki, B. Dorken, et al., Induction of cell death by the BH3-only Bcl-2 homolog Nbk/Bik is mediated by an entirely Bax-dependent mitochondrial pathway, EMBO J. 22 (2003) 3580–3590.
[33] Y. Tong, Q. Yang, C. Vater, L.K. Venkatesh, D. Custeau, T. Chittenden, et al., The pro-apoptotic protein, Bik, exhibits potent antitumor activity that is dependent on its BH3 domain, Mol. cancer Ther. 1 (2001) 95–102.
[34] D. Senft, C. Berking, S.A. Graf, C. Kammerbauer, T. Ruzicka, R. Besch, Selective induction of cell death in melanoma cell lines through targeting of Mcl-1 and A1, PLOS one 7 (2012) e30821.
[35] T. Shimazu, K. Degenhardt, E.K.A. Nur, J. Zhang, T. Yoshida, Y. Zhang, et al., NBK/BIK antagonizes MCL-1 and BCL-XL and activates BAK-mediated apoptosis in response to protein synthesis inhibition, Genes Dev. 21 (2007) 929–941.
[36] Y.A. Mebratu, B.F. Dickey, C. Evans, Y. Tesfaigzi, The BH3-only protein Bik/Blk/Nbk inhibits nuclear translocation of activated ERK1/2 to mediate IFNgamma-induced cell death, J. Cell Biol. 183 (2008) 429–439.
[37] R. Viedma-Rodriguez, L.A. Baiza-Gutman, A. Garcia-Carranca, L. Moreno-Fierros, F. Salamanca-Gomez, D. Arenas-Aranda, Suppression of the death gene BIK is a critical factor for resistance to tamoxifen in MCF-7 breast cancer cells, Int. J. Oncol. 43 (2013) 1777–1786.
[38] H. Zhou, Y. Zhang, Y. Fu, L. Chan, A.S. Lee, Novel mechanism of anti-apoptotic function of 78-kDa glucose-regulated protein (GRP78): endocrine resistance factor in breast cancer, through release of B-cell lymphoma 2 (BCL-2) from BCL-2-interacting killer (BIK), J. Biol. Chem. 286 (2011) 25687–25696.
[39] E.M. Campion, R. Hakimjavadi, S.T. Loughran, S. Phelan, S.M. Smith, B.N. D'Souza, et al., Repression of the proapoptotic cellular BIK/NBK gene by Epstein-Barr virus antagonizes transforming growth factor beta1-induced B-cell apoptosis, J. Virol. 88 (2014) 5001–5013.
[40] I. Prieto-Remon, D. Sanchez-Carrera, M. Lopez-Duarte, C. Richard, C. Pipaon, BIK (NBK) is a mediator of the sensitivity of Fanconi anaemia group C lymphoblastoid cell lines to interstrand DNA cross-linking agents, Biochem. J. 448 (2012) 153–163.
[41] I. Sturm, C. Stephan, B. Gillissen, R. Siebert, M. Janz, S. Radetzki, et al., Loss of the tissue-specific proapoptotic BH3-only protein Nbk/Bik is a unifying feature of renal cell carcinoma, Cell Death Differ. 13 (2006) 619–627.
[42] S.J. Welsh, H. Rizos, R.A. Scolyer, G.V. Long, Resistance to combination BRAF and MEK inhibition in metastatic melanoma: where to next? Eur. J. Cancer 62 (2016) 76–85.
[43] J. Hur, J. Chesnes, K.R. Coser, R.S. Lee, P. Geck, K.J. Isselbacher, et al., The Bik BH3-only protein is induced in estrogen-starved and antiestrogen-exposed breast cancer cells and provokes apoptosis, Proc. Natl. Acad. Sci. U. S. A. 101 (2004) 2351–2356.
[44] J.P. Mathai, M. Germain, G.C. Shore, BH3-only BIK regulates BAX,BAK-dependent release of Ca2+ from endoplasmic reticulum stores and mitochondrial apoptosis during stress-induced cell death, J. Biol. Chem. 280 (2005) 23829–23836.
[45] L.C. Spender, D.I. O'Brien, D. Simpson, D. Dutt, C.D. Gregory, M.J. Allday, et al., TGF-beta induces apoptosis in human B cells by transcriptional regulation of BIK and BCL-XL, Cell Death Differ. 16 (2009) 593–602.
[46] J.M. McDonnell, D. Fushman, C.L. Milliman, S.J. Korsmeyer, D. Cowburn, Solution structure of the proapoptotic molecule BID: a structural basis for apoptotic agonists and antagonists, Cell 96 (1999) 625–634.
[47] S. Verma, L.J. Zhao, G. Chinnadurai, Phosphorylation of the pro-apoptotic protein BIK: mapping of phosphorylation sites and effect on apoptosis, J. Biol. Chem. 276 (2001) 4671–4676.
[48] C. Paquet, E. Schmitt, M. Beauchemin, R. Bertrand, Activation of multidomain and BH3-only pro-apoptotic Bcl-2 family members in p53-defective cells, Apoptosis Int. J. Program. cell death 9 (2004) 815–831.
[49] Y. Fu, J. Li, A.S. Lee, GRP78/BiP inhibits endoplasmic reticulum BIK and protects human breast cancer cells against estrogen starvation-induced apoptosis, Cancer Res. 67 (2007) 3734–3740.
[50] Y. Shao, A.E. Aplin, BH3-only protein silencing contributes to acquired resistance to PLX4720 in human melanoma, Cell Death Differ. 19 (2012) 2029–2039.
[51] C. Pompeia, D.R. Hodge, C. Plass, Y.Z. Wu, V.E. Marquez, J.A. Kelley, et al., Microarray analysis of epigenetic silencing of gene expression in the KAS-6/1 multiple myeloma cell line, Cancer Res. 64 (2004) 3465–3473.
[52] A.A. Lane, B.A. Chabner, Histone deacetylase inhibitors in cancer therapy, J. Clin. Oncol. official J. Am. Soc. Clin. Oncol. 27 (2009) 5459–5468.
[53] K. Ververis, A. Hiong, T.C. Karagiannis, P.V. Licciardi, Histone deacetylase inhibitors (HDACIs): multitargeted anticancer agents, Biol. targets Ther. 7 (2013) 47–60.
[54] T. Harada, T. Hideshima, K.C. Anderson, Histone deacetylase inhibitors in multiple myeloma: from bench to bedside, Int. J. Hematol. 104 (2016) 300–309.
[55] N.B. Haas, I. Quirt, S. Hotte, E. McWhirter, R. Polintan, S. Litwin, et al., Phase II trial of vorinostat in advanced melanoma, Investig. new drugs 32 (2014) 526–534.
[56] A. Hauschild, U. Trefzer, C. Garbe, K.C. Kaehler, S. Ugurel, F. Kiecker, et al., Multicenter phase II trial of the histone deacetylase inhibitor pyridylmethyl-N-{4-[(2-aminophenyl)-carbamoyl]-benzyl}-carbamate in pretreated metastatic melanoma, Melanoma Res. 18 (2008) 274–278.
[57] R. Carson, B. Celtikci, C. Fenning, A. Javadi, N. Crawford, L. Perez-Carbonell, et al., HDAC inhibition overcomes acute resistance to MEK inhibition in BRAF-mutant colorectal cancer by downregulation of c-FLIPL, Clin. Cancer Res. 21 (2015) 3230–3240.
[58] F. Lai, S.T. Guo, L. Jin, C.C. Jiang, C.Y. Wang, A. Croft, et al., Cotargeting histone deacetylases and oncogenic BRAF synergistically kills human melanoma cells by necrosis independently of RIPK1 and RIPK3, Cell death Dis. 4 (2013) e655.

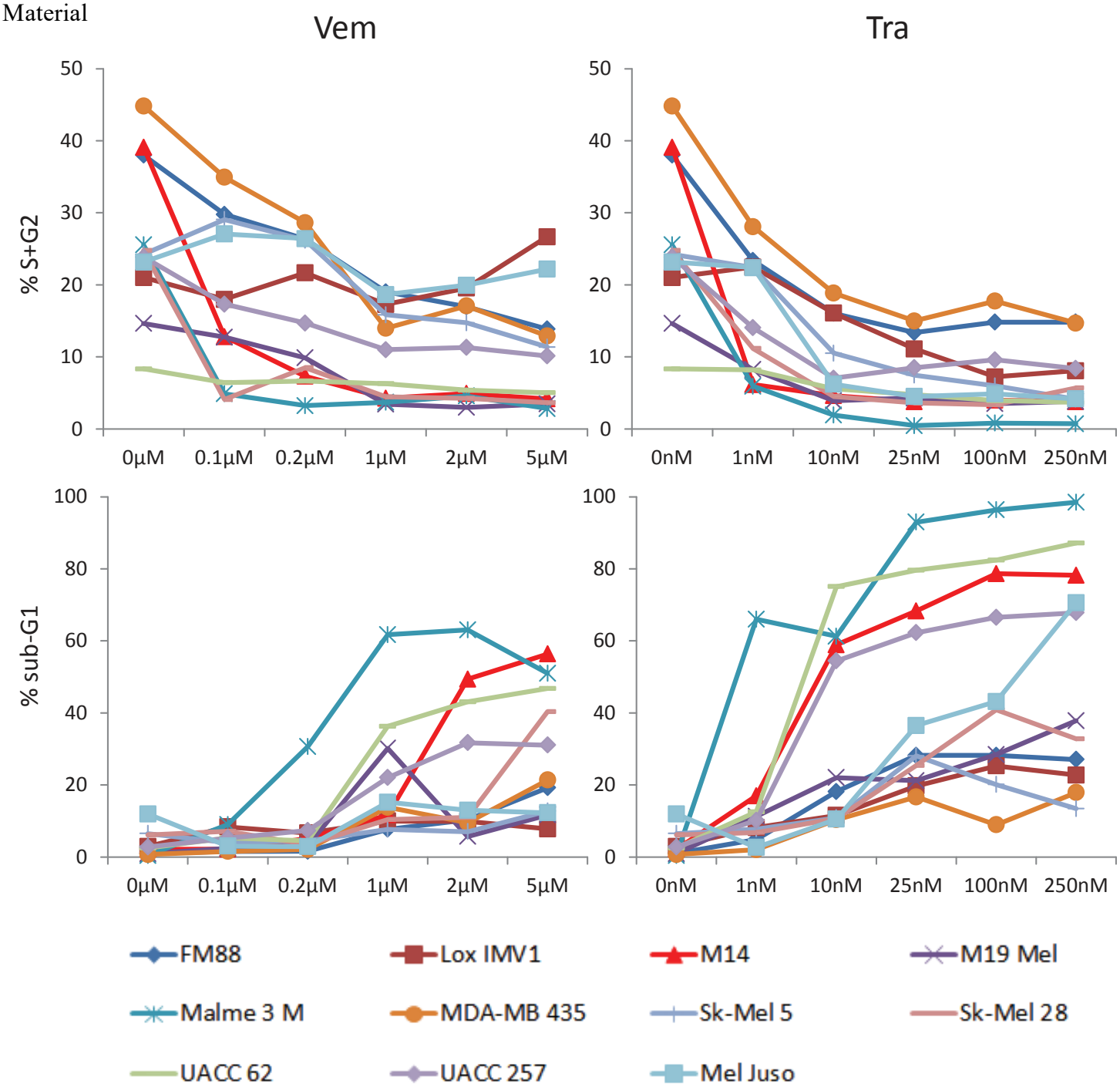

Figure S1: Apoptosis and cell cycle arrest induced by Vem or Tra in different melanoma cell lines. The indicated BRAF mutant cell lines were treated with increasing concentrations of Vem or Tra. After 4 days, cells were stained with propidium iodide and analysed by flow cytometry. Decreasing percentages of cells in S and G2 phase relative to (G1+S+G2) indicate a G1 arrest. The percentage of sub-G1 cells serves as a measure of cell death. Mel Juso was used as BRAF wild-type control.

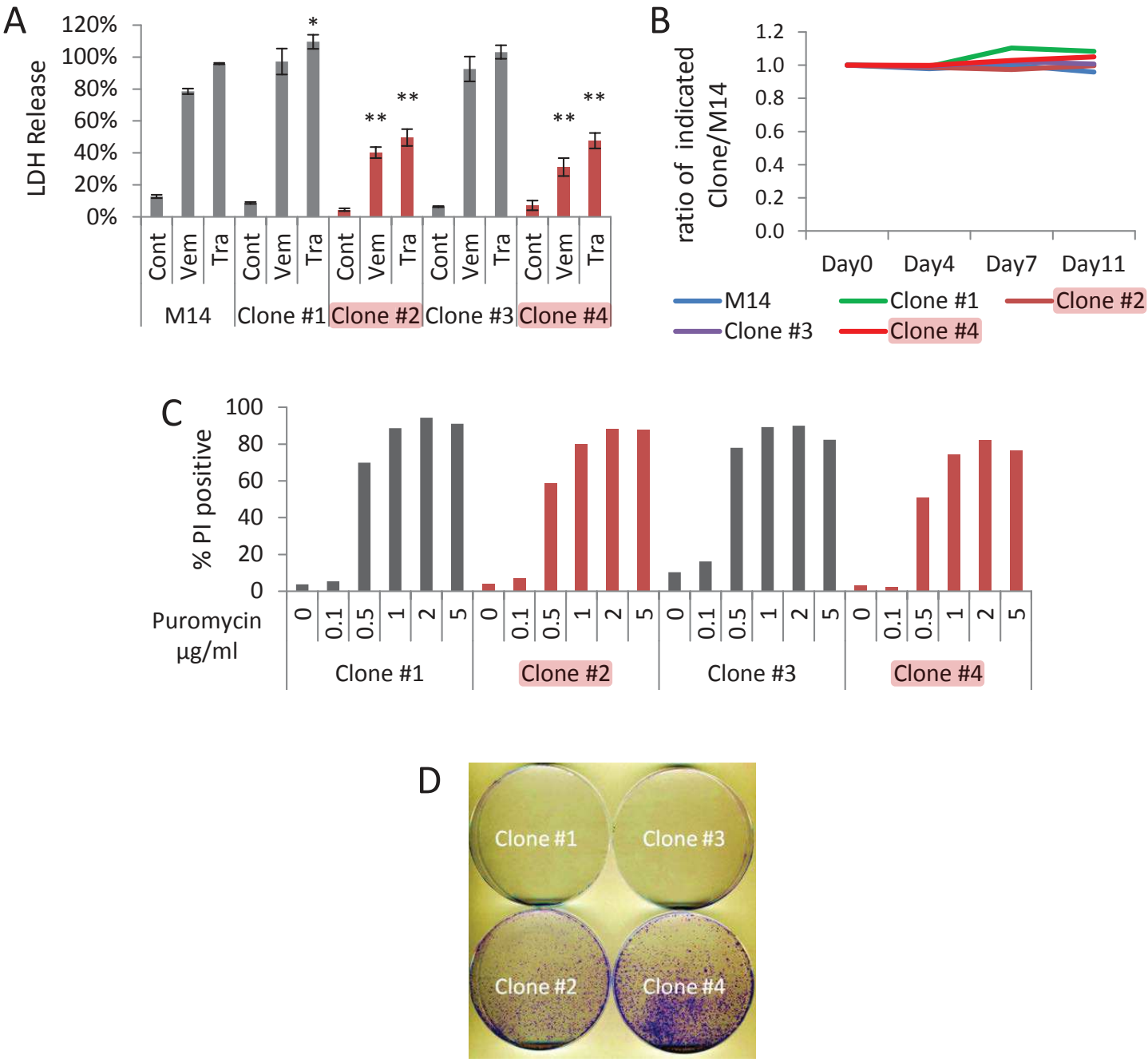

Figure S2: Further characterization of apoptotic and arresting M14 single cell clones. A: Vem or Tra mediated apoptosis after 4 days measured with the CytoTox 96® Non- radioactive Cytotoxicity Assay (Promega) according to manufacturers instructions (n=3, mean +/- SD, Students t-test, paired, two-tailed, *p<0.05; **p<0.01. Each clone compared to correspondingly treated parental M14 cells). **B:** Growth rates compared in mixed cell culture assay. Cells were mixed with stably GFP expressing parental M14 cells and altered growth characteristics of the single cell clones were excluded by determining the ratio of GFP^+/GFP^- cells over time. **C:** Sensitivity to varying concentrations of puromycin was measured by determining the percentage of propidium-iodide permeable cells after a 72 h treatment by flow cytometry. **D:** Surviving cells after eight weeks of Vem treatment (from Fig. 1D) of one 96-well were reseeded and cultivated under standard conditions. Crystal Violet staining was performed after 13 days to analyze the ability to form colonies. Photograph is representative for three experiments.

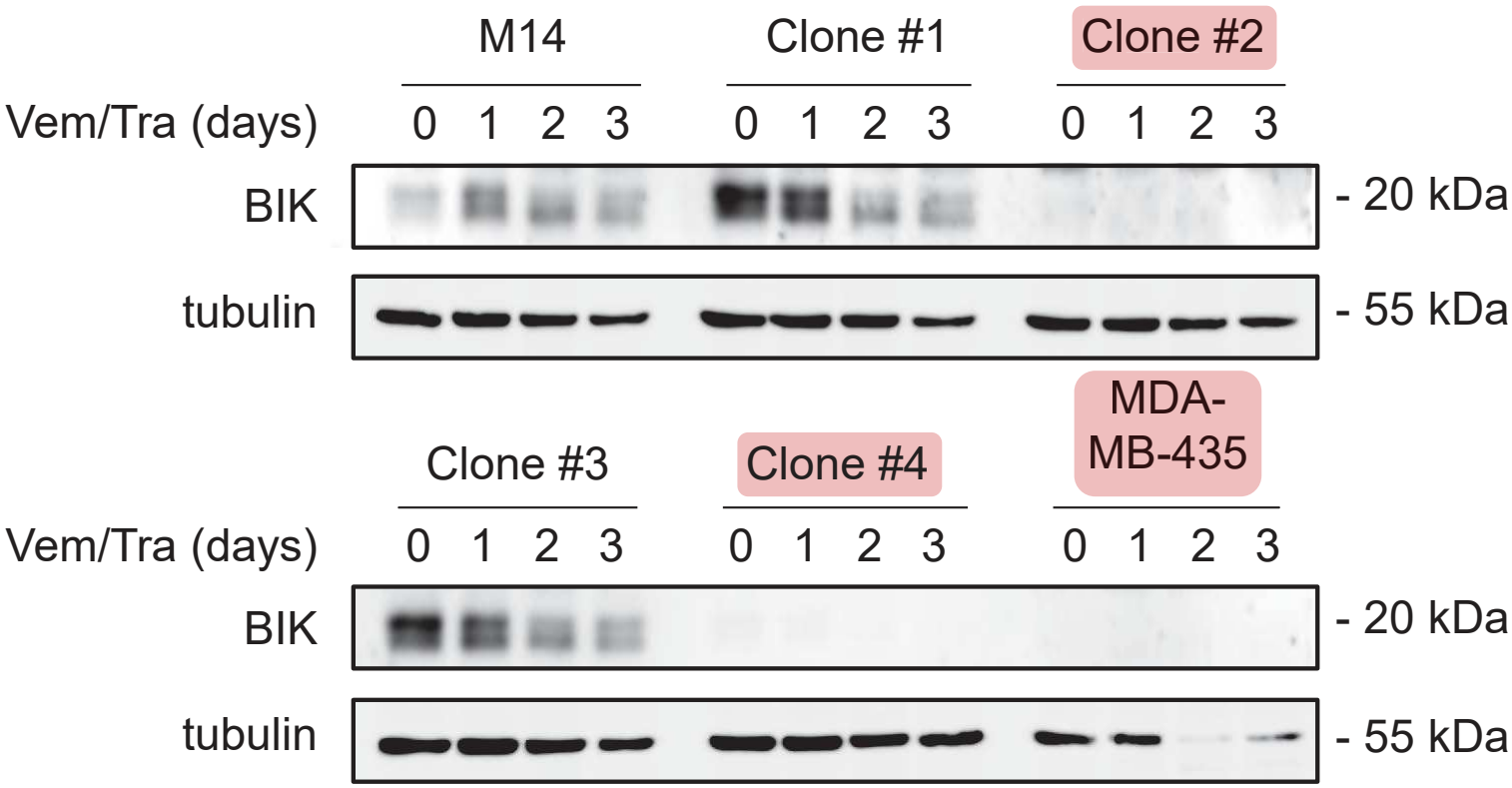

Fig. S3: BIK levels in apoptotic and arresting cells in the course of Vemurafenib/Trametinib treatment. Immunoblot analysis was performed with whole cell lysates derived from the indicated cell lines or M14 single cell clones treated with Vem/Tra (5 µM/10 nM) for 0, 1, 2 or 3 days. Prior to harvesting cells were treated with bortezomib (24 h; 2.5 µM).

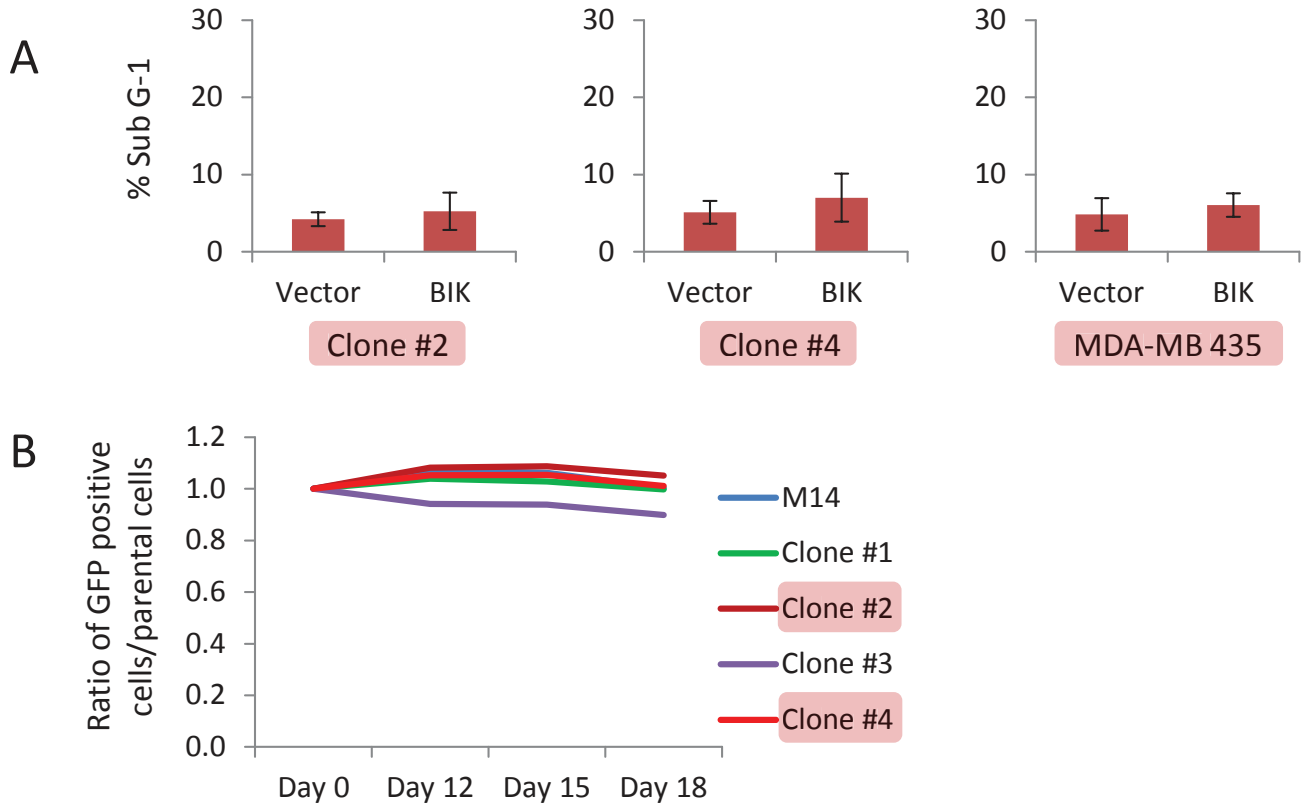

Figure S4: Ectopic BIK expression in the arresting M14 clones and MDA-MB 435 does not affect growth or background apoptosis under standard conditions: A: The indicated cells either transduced with empty vector or with a BIK expression vector were fixed and stained by propidium-iodide and analyzed by flow cytometry for the proportion of sub-G1 cells. **B:** Ectopically BIK expressing single cell-lines were mixed with GFP expressing parental cells and altered growth was excluded by analyzing the ratio of GFP^+/GFP^- cells over time.

A

Real time PCR primers (CHIP)

	forward	reverse
BIK ChIP A	GAGGGGATCAAGACAGAAGTAAA	AGCGCTCCTGGAATAACAAAGTAA
BIK ChIP B	CCTGGCTTCGGGTATGGAT	CTGGCAGCTTTGGGATTTAGG
BIK ChIP C	GCAGAACAGCAGGGGGCAGAGA	GGCATTGGCAACAGAACCGCTACA

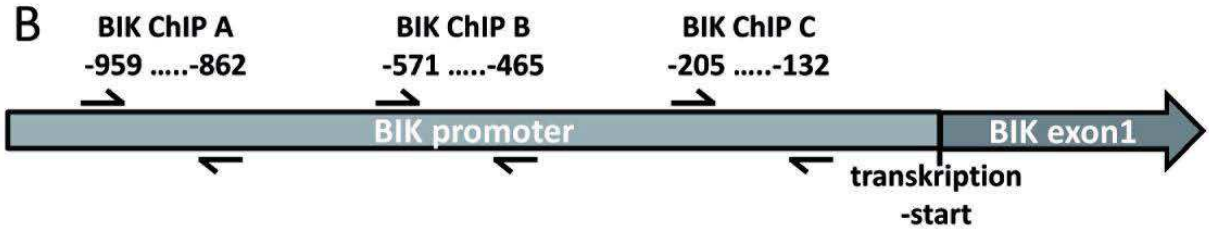

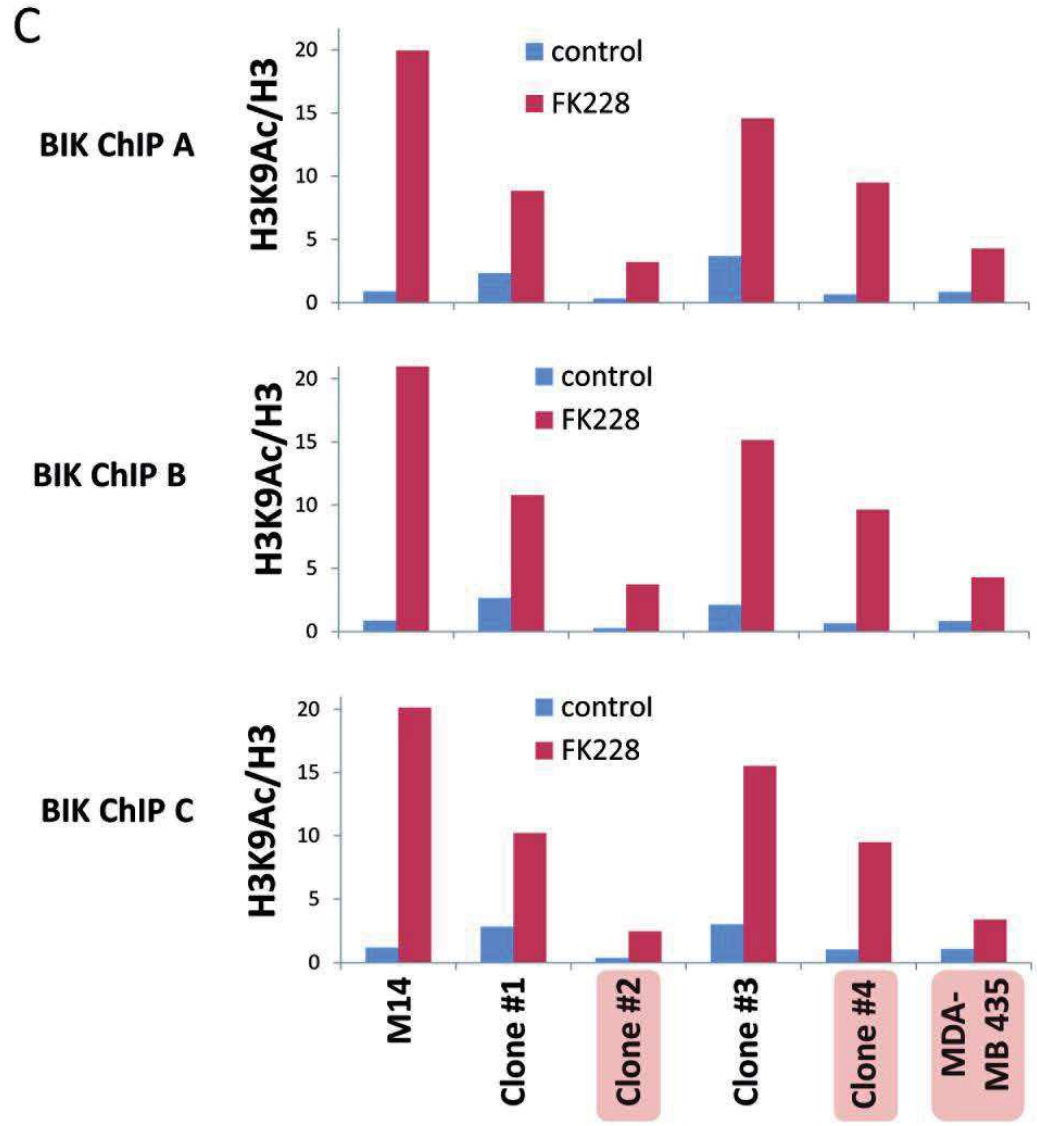

Figure S5: Chromatin-Immunoprecipitation (ChiP) followed by real-time PCR to demonstrate that HDAC inhibition leads to increased BIK promoter acetylation. A and B: Sequence of the different real time PCR primers pairs and their location in the BIK-promoter region **C:** Following 24 h of FK228 treatment (100 nM) of the indicated cells**,** fixed and digested chromatin was pulled down with antibodies targeting Histone H3 and H3K9Ac, respectively. Purified DNA was analyzed for the presence of the BIK promoter by real-time PCR using the three different primer sets. Values for H3K9Ac relative to H3 pull down are depicted.

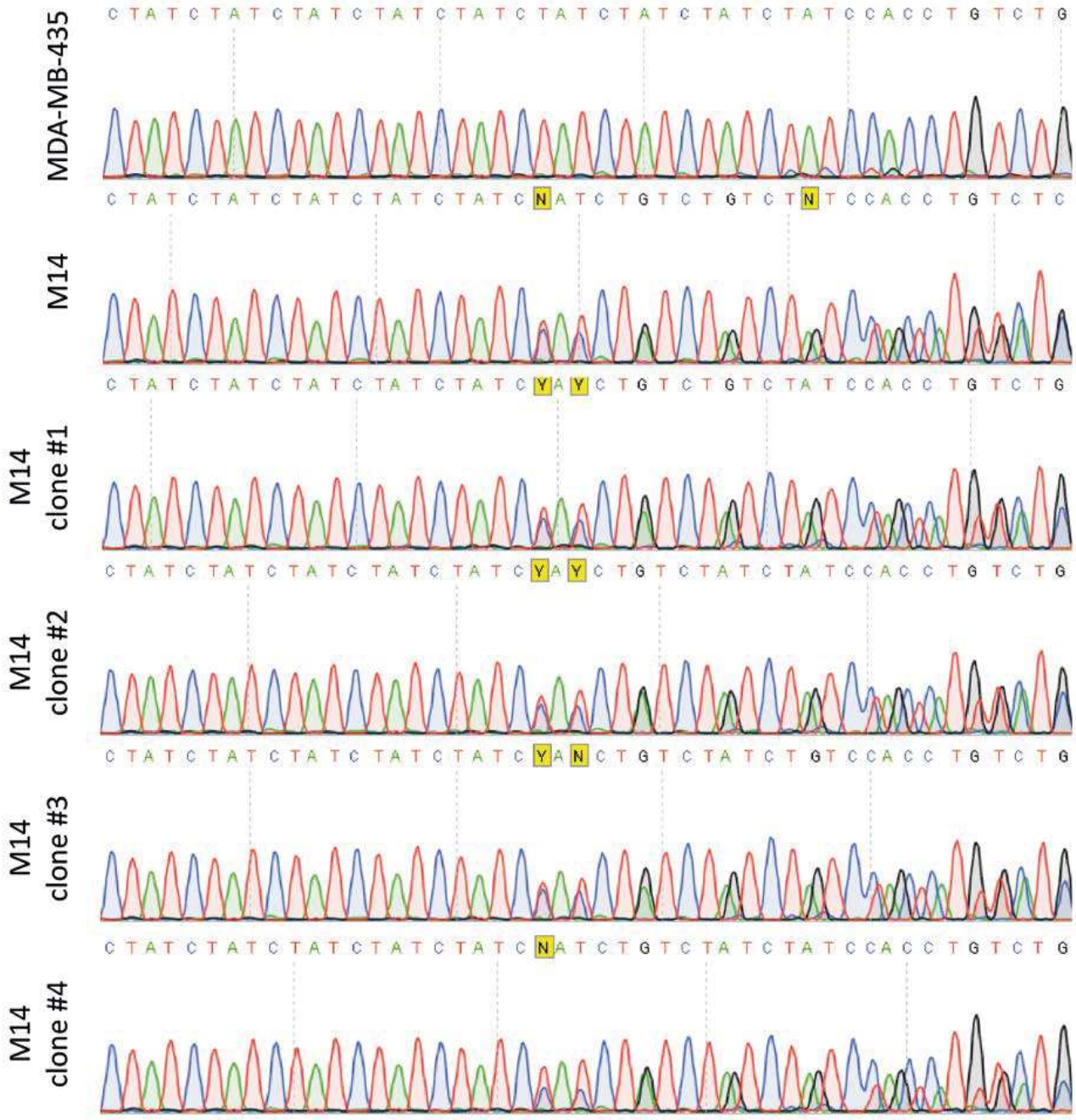

Figure S6: **Demonstration that the different M14 single cell clones were directly derived from M14 and not mixed-up with the M14 derivative MDA-MB-435.** First, exon 8 of the p53 gene of was sequenced and indeed, we could detect in all single cell clones as well as in M14 and MDA-MB-435 derived DNA the G797A (G266E) mutation (data not shown) which is characteristic for M14 and MDA-MB-435 (Ikediobi *et al.*, 2006). Since MDA-MB-435 and M14 differ in respect to their STR profile only in one locus namely D16S539 (Fang *et al.*, 2001; Rae *et al.*, 2007) we amplified this locus by PCR (primers: 5'-tatgggagcaaacaaaggcagat-3' rev: 5'-cagcctacagagtgattccatt-3')) and sequenced the product. Thereby, we could confirm that the parental M14 as well as the 4 clones carry the two different alleles as indicated by double peaks showing up from a distinct position for M14 and the M14 single cell clones while the MDA-MB-435 sequence is clean until the end of the amplicon. This is in line with MDA-MB-435 carrying only one allele with 13 4-bp repeats while M14 has two alleles with either 13 or 9 repeats leading to a 16 nucleotide difference between the two alleles (Fang *et al.*, 2001; Rae *et al.*, 2007).

Fang R, et al. (2001) STR Profiling of Human Cell Lines: Challenges and Possible Solutions to the Growing Problem. J Forensic Res S2:005.

Ikediobi ON et al. (2006) Mutation analysis of 24 known cancer genes in the NCI-60 cell line set. Molecular cancer therapeutics 5:2606-12.

Rae JM, Cet al. (2007) MDA-MB-435 cells are derived from M14 melanoma cells--a loss for breast cancer, but a boon for melanoma research. Breast cancer research and treatment 104:13-9.

Supplementary Materials and Methods

Supplementary Table 1: Table of primary antibodies used in this study.

Target	Company	ID
Bak1	BD Pharmingen	#556382
Bax	eBioscience	#14-6996
Bcl-2	Dako	Clone 124
BCL-X(L)	BD Pharmingen	#556361
BIK/NBK	Santa Cruz	sc-1710
BIM	Sigma Aldrich	B7929
Caspase9	Cell Signaling	#9502
Cleaved Caspase3	Cell Signaling	#9661
Mcl-1	Santa Cruz	#sc-12756
Phospho-p44/42 MAPK (Erk1/2)	Cell Signaling	#9106
PUMA	Santa Cruz	sc-374223
ß-Tubulin	Sigma Aldrich	T4026

Borst, Andreas
Frankenstr. 2
97277 Neubrunn
Tel: 0151 68 140 724
E-Mail: andreas_borst@web.de

Erklärungen nach §4 Abs. 3 Satz 3, 5, 8 der Promotionsordnung der Fakultät für Biologie

Affidavit

I hereby declare that my thesis entitled: „ **Apoptosis & senescence: cell fate determination in inhibitor-treated melanoma cells**" is the result of my own work.

I did not receive any help or support from commercial consultants. All sources and / or materials applied are listed and specified in the thesis.

Furthermore I verify that the thesis has not been submitted as part of another examination process neither in identical nor in similar form.

Eidesstattliche Erklärung

Hiermit erkläre ich an Eides statt, die Dissertation: „**Apoptosis & senescence: cell fate determination in inhibitor-treated melanoma cells**", eigenständig, d. h. insbesondere selbständig und ohne Hilfe eines kommerziellen Promotionsberaters, angefertigt und keine anderen, als die von mir angegebenen Quellen und Hilfsmittel verwendet zu haben.

Ich erkläre außerdem, dass die Dissertation weder in gleicher noch in ähnlicher Form bereits in einem anderen Prüfungsverfahren vorgelegen hat.

Würzburg , den 12.10.2017

Unterschrift

9. Danksagung

Als erstes möchte ich Roland dafür danken, mir im Tumorbiologischen Forschungslabor der Hautklinik die Möglichkeit gegeben zu haben, meine Promotion zu machen. Dabei konnte ich immer selbstständig und ohne Druck an meinen Projekten arbeiten; und sollte ich mich mal in eine Sackgasse manövriert haben, immer Rat und Ideen bei dir abholen.

An David Schrama ebenfalls vielen Dank für den Ideeninput, meistens zu Uhrzeiten zu denen kein „normaler“ Mensch mehr im Labor war außer uns beiden. Natürlich auch an die AG Schmidt, von euch habe ich mir öfters dringen benötigte Antikörper “borgen“ können. Ebenfalls ein Danke an Sebastian Haferkamp & Svenja Meierjohann, aufgrund der Finanzierung eures IZKF Projekts hatte ich genügen Geld während meiner Doktorandenzeit, um nicht verhungern zu müssen.

An das ganze Laborteam (Sonja, Claudia, Eva, Lena, Alex), ehemalige Laborteam (Sabrina, Christian, Rainee) und fleißige Praktikanten (Luis, Manu, Sahra, Maria & Antje) ein dickes Dankeschön für durchgeführte Versuche, (vor allem als ich bewegungsunfähig im Krankenhaus lag!), jede Menge Spaß, einen angenehmen, kollegialen und kreativen Laboralltag, Spiele Abende und das wichtigste zuletzt, tonnenweise Kuchen!

Ich denke immer gerne an die schöne Zeit in der Hautklinik zurück!

Zuletzt möchte ich natürlich vor allem meinen Eltern & Bruder, Tanten & Onkels, Oma, dem Rest der Family und allen Freunden für die Unterstützung jedweder Art danken. Sei es finanzieller oder menschlicher Art, vor allem während der schwierigen Zeit nach der Krebsdiagnose, den Operationen und der Genesungsphase! Dank euch konnte ich das vorliegende Werk beenden.